Author:
Zambrano, Damaris E

Title:
Synthesis, coordination chemistry and hydroformylation catalysis with new trioxa-phospha-adamantane ligands

Synthesis, coordination chemistry and hydroformylation catalysis with new trioxa-phospha-adamantane ligands

by

Damaris E. Zambrano

A thesis submitted to the University of Bristol in accordance with the requirements for the degree of Doctor of Philosophy in the School of Chemistry, Faculty of Science.

October 2003

Abstract

Attempts to separate *meso/rac*-1,3-bis(^{Me}adamphosphino)propane diastereoisomers by recrystallization and selective complexation are described. Recrystallization from methanol was found to be the best option.

The cage diphosphines *meso/rac*-1,4-bis(^{Me}adamphosphino)butane and *meso/rac*-1,4-bis(^{CF3}adamphosphino)butane have been synthesised. These ligands were prepared *via* hydrophosphination of $RC(O)CH_2C(O)R$ (R = CH_3, CF_3) with the diprimary phosphine $H_2P(CH_2)_4PH_2$. Platinum(II) and palladium(II) complexes of these new ligands are reported. The cone angle of the *meso*-1,4-bis(^{Me}adamphosphino)butane was measured from the *X*-ray crystal structure of its dichloroplatinum(II) complex and found to be 167°. The cage diphosphines *meso/rac*-1,5-bis(^{Me}adamphosphino)pentane and *meso/rac*-1,5-bis(^{CF3}adamphosphino)pentane have been synthesised by hydrophosphination of $RC(O)CH_2C(O)R$ (R = CH_3, CF_3) with the diprimary phosphine $H_2P(CH_2)_5PH_2$. The dichloroplatinum(II) complex of *meso/rac*-1,5-bis(^{Me}adamphosphino)pentane was synthesised, but the palladium(II) complexation produced oligomeric products.

The monodentate cages 1,3,5,7-tetraethyl-2,4,8-trioxa-6-phospha-adamantane (^{Et}CgPH) and 1,3,5,7-tetraethyl-6-phenyl-2,4,8-trioxa-6-phospha-adamantane (^{Et}CgPPh) have been synthesised. The palladium(II) and platinum(II) complexes for each of these ligands are reported and the *X*-ray crystal structure of *trans*-[$PdCl_2$(^{Et}CgPPh)] was determined which gave an estimated cone angle of 157° for ^{Et}CgPPh. The bidentate cages *meso/rac*-1,3-bis(^{Et}adamphosphino)propane, *meso/rac*-1,4-bis(^{Et}adamphosphino)-butane and *meso/rac*-1,5-bis(^{Et}adamphosphino)pentane were prepared. The palladium complex of *meso/rac*-1,3-bis(^{Et}adamphosphino)propane was synthesised, [$PdCl_2$(P-P)], whose *X*-ray crystal structure gave an estimated cone angle of 155° for this ligand. The ligands *meso/rac*-1,4-bis(^{Et}adamphosphino)butane and *meso/rac*-1,5-bis(^{Et}adamphosphino)pentane gave a mixture of oligomeric species when complexation with palladium(II) was attempted. The ligand *meso/rac*-1,4-bis(^{Et}adamphosphino)butane formed a chelate with platinum(II).

The catalytic activity of the monodentate and bidentate cages *meso/rac*-1,4-bis(^{Me}adamphosphino)butane, *meso/rac*-1,4-bis(^{Et}adamphosphino)butane, *meso/rac*-1,3-bis(^{Me}adamphosphino)propane and ^{Et}CgPPh in the Rh-catalyzed hydroformylation of hex-1-ene is described. The best result was obtained with ^{Et}CgPPh, which was faster than the commercial rhodium catalyst [$RhH(CO)(PPh_3)_3$].

Para mis muy queridos Mamá, Papá, mi Hermano
y mi adorado Esposo, mi triunfo es el de ustedes.

"Según sea tu fé, asi serán las cosas que te sucedan."- Mateo 8-13.

"Dios concede la Victoria a la constancia."- Simon Bolivar

Acknowledgements

I am indebted to my supervisor Prof. Paul Pringle for all his wise advice, encouragement and enthusiasm. Paul you are always right, the thing is because I have been a good student I think you are now 95% right. Thank you for being a great supervisor and a marvellous mate. There have been many occasions where we have shared really good times and they are great memories for me.

Thank you to Dr. Katie Heslop, Miss Angharad Baber and Dr. Jon Charmant for carrying out the crystal structure determinations included in this thesis.

Many thanks to Adrian and Tony for their advice and help handling the phosphines in the cold laboratory in the old building.

I would like to thank La Fundacion Gran Mariscal de Ayacucho for their economical support, and for promoting the preparation of professionals for a better country.

Many thanks to the School of Chemistry and Shell (specially Eite Drent and Rob Pugh) for their financial contributions.

Thanks also to my fantastic lab-mates and friends for being so lovely, and making my time in Bristol so enjoyable:

Matt Clarke, his good humour, patience, willingness to help, and readiness to dance. Thank you for helping me with the hydroformylation catalysis experiments.

Andy I really enjoyed my time with you in the lab. You were a fantastic project student, always very enthusiastic in the lab and in the Lizard Lounge for dancing.

Rich, the king of surprising last minute enthusiasm for dancing. Thank you for your advice in the lab.

Lee with his copper and elastic-band technique, always very friendly.

Emma and Aina I will always be grateful to them for putting the fire out, was it really a big flame?

Matt Wilkinson I never understood his jokes, thank you for trying to cheer me up in my downs in chemistry.

Asli thank you for being a great supportive friend in and out of the lab, and for encouraging me in my singing career.

Paul Marsh it was nice to share with you this time in the lab, I will always remember your blue trendy shoes (very nice!).

Joëlle thank you for the nice days in the lab.

Annie, Karl and Cass; sausage, strawberry pudding and a dancing sandwich with some wine makes a good combination for a great time. Thank you for the good times.

I am very graceful to Asli, Rich, Karl and Annie for the patient proof reading.

Thank you to Annabel, Andres and Silvia for their friendship and support. Silvia a special thank you for your help to sort out the troublesome final printing.

Thank you to all the members of the Inorganic section, Sarah, Cheryl and especially to Dr. Nick Norman for his supportive questions such as "have you finished your thesis!" which have been appreciated.

Memorandum

The work described in this thesis was carried out in the School of Chemistry at the University of Bristol between February 2000 and February 2003. Unless otherwise acknowledged in the text, it is the original work of the author and has not been submitted previously for a degree. In addition, any views expressed in this thesis are those of the author, and not of the University.

Damaris E. Zambrano

University of Bristol

October 2003

Contents

Table of Contents

Abbreviations

BINAP	1,1'-bis(diphenylphosphino)binaphthalene
Bu^t	*tertiary*-Butyl
Cod	*cis,cis*-1,5-cyclooctadiene
Cy	cyclohexyl
d	day(s)
dba	*trans,trans*-dibenzylideneacetone
d^tbpe	1,2-bis(di-t-butylphosphino)ethane
d^tbpp	1,3-bis(di-t-butylphosphino)propane
dbpf	1,1'-bis(di-t-butylphosphino)ferrocene
dppf	1,1'-bis(diphenylphosphino)ferrocene
dppp	1,3-bis(diphenylphosphino)propane
d^tbpx	1,2-bis(di-t-butylphosphinomethyl)benzene
equiv.	equivalents
Et	ethyl
FAB	fast atom bombardment
h	hour(s)
IR	infrared
cm^{-1}	wavenumbers
υ	stretching frequency
L	ligand
L_2	bidentate ligand
M	metal
m/z	mass/charge
min	minute(s)
nb	norbornene
Ph	phenyl
Pr^i	*iso*-propyl
R	alkyl (or aryl)
TFA	trifluoroacetyl
thf	tetrahydrofuran
TPPTS	meta-sulfonated triphenylphosphine sodium salt

NMR data

NMR	nuclear magnetic resonance
δ	chemical shift (in ppm)
Δδ	coordination chemical shift
ppm	parts per million
s	singlet
d	doublet
dd	doublet of doublets
dt	doublet of triplets
t	triplet
q	quartet
sept	septet
m	multiplet
bm	broad multiplet
bs	broad singlet
Hz	hertz
MHz	megahertz
J	coupling constant
$\{^1H\}$	proton decoupled

Chapter 1

Introduction

1.1 Introduction

The chemistry of tertiary phosphines is a very large and currently highly active field, partly due to their widespread application in many industrial processes.[1-3] One of the earliest metal-phosphine complexes to find commercial use (in 1938) was the Reppe compound $[Ni(CO)_2(PPh_3)_2]$,[4] which was used to catalyse the polymerisation of alkenes and acetylenes.[5] Triphenylphosphine is also the ligand in Wilkinson's catalyst $[RhCl(PPh_3)_3]$ for the homogeneous hydrogenation of alkenes,[6,7] and $[RhH(CO)(PPh_3)_3]$ is a catalyst for the hydroformylation of alkenes.[8]

In this thesis, we will describe the synthesis and coordination chemistry of bulky cage-phosphine and cage-diphosphine ligands of type **1.1** and **1.2**.

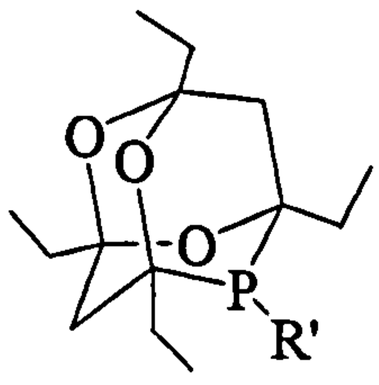

R' = H, Ph

1.1

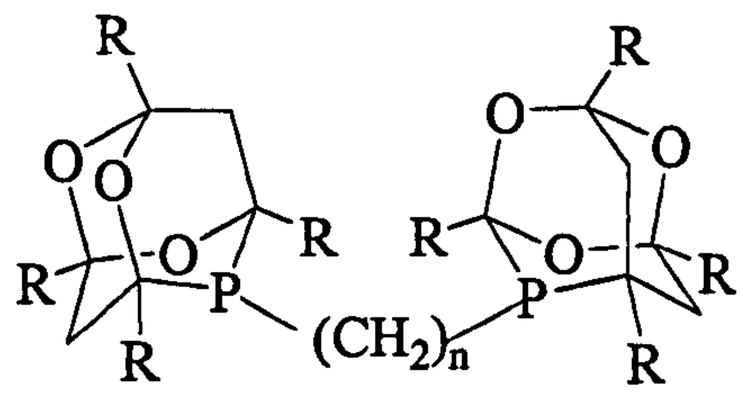

R = Me, Et, CF_3
n = 4, 5

1.2

To put this work in context, in this Chapter the key features of bulky phosphines are discussed such as phosphorus-metal bonding, stereoelectronic properties, and the significance of sterically demanding alkyl phosphines and their importance in transition metal chemistry and homogeneous catalysis.

1.2 Bonding in phosphorus(III) ligand metal complexes

The nature of the bonding of phosphorus ligands makes them able to stabilise a wide range of oxidation states, due to the varying degrees of σ-donation and π-acceptance in the M-P bond. Phosphine ligands can be strong σ–donors (e.g. PMe_3) or

strong π–acceptors (e.g. PF_3), and can be very small (e.g. PH_3) or very large (e.g. PBu^t_3).

The classical picture of metal-phosphorus bonding involves σ–donation from an sp^3 orbital on P into a suitable metal orbital (e.g. d_z^2) and the π-acceptor properties are attributed to the use of empty phosphorus *3d* orbitals (Figure 1.1).[9]

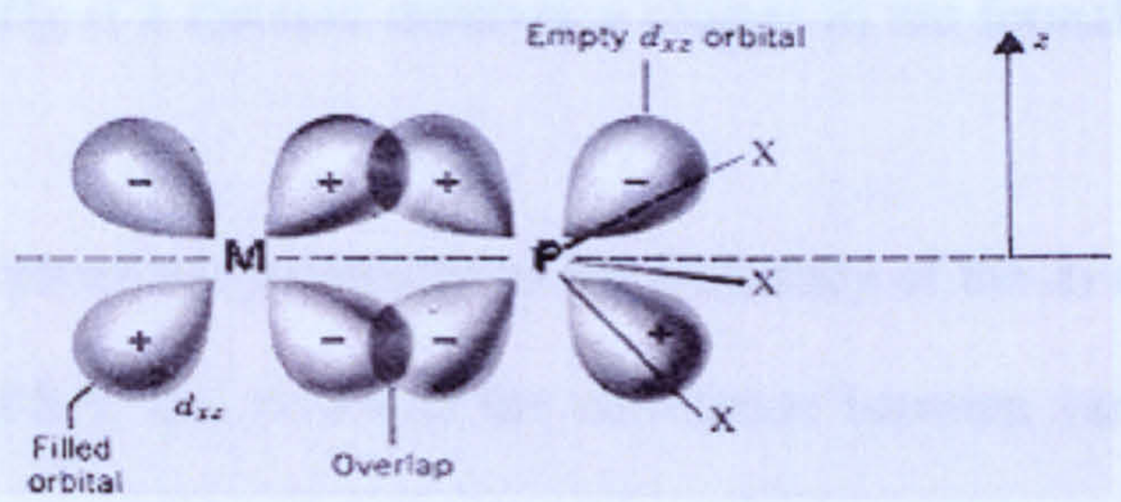

Figure 1.1

A more recent model for the π-bonding, based on quantum mechanical calculations,[10] uses hybridisation of the *3d* orbitals and P-X σ* orbitals to give the hybrid π-acceptor orbital shown in Figure 1.2. This rationalises why an increase in π-donation from the metal to the phosphorus results in an increase in the P-X bond length (due to the participation of P-X σ*orbitals) and a decrease in M-P distances.

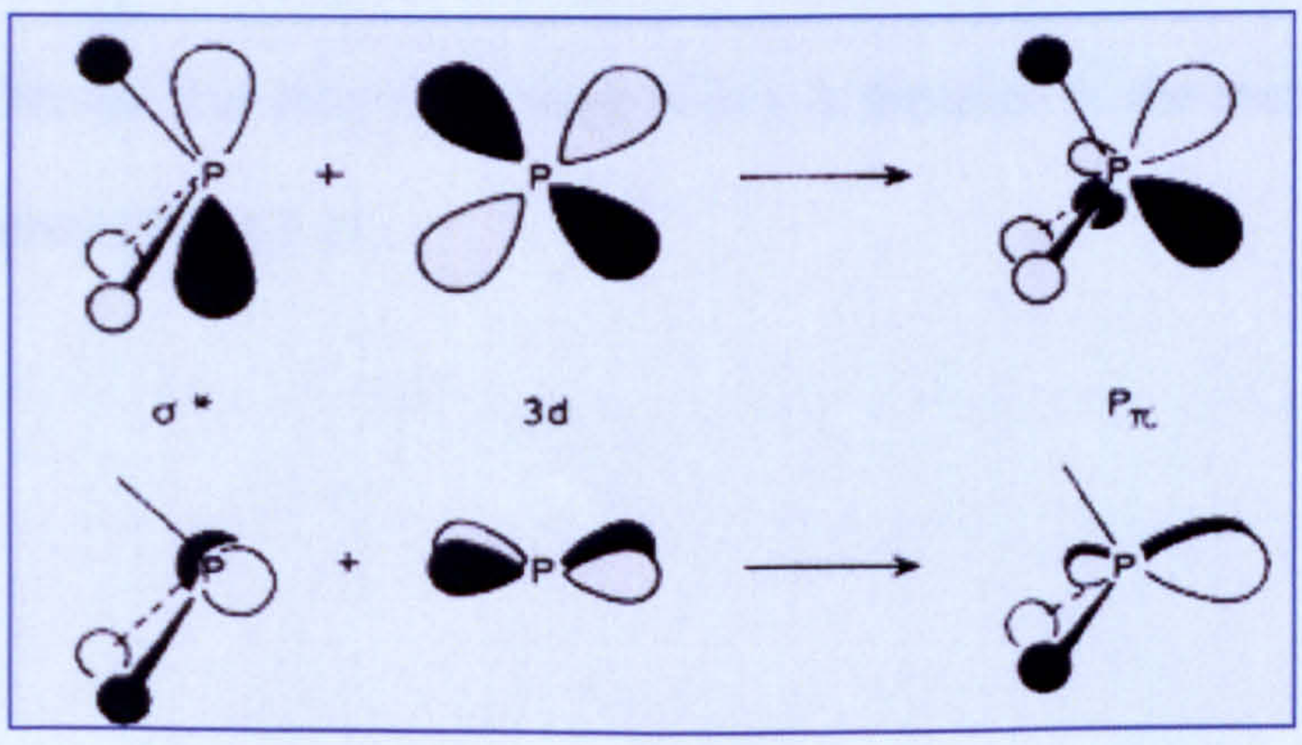

Figure 1.2

1.3 Stereoelectronic effects of ditertiary phosphine ligands

Ligand stereoelectronic effects control the thermodynamics and kinetics of reactions of metal complexes and are therefore of critical importance in catalysis.

1.3.1 Electronic effects

Electronic effects in which ligands affect the electron density on the metal are important, particularly if a reaction involves a change in the formal oxidation state of the metal.

Tolman[11] based his electronic parameter on the frequency of the A_1 carbonyl stretching mode in $[Ni(CO)_3(PR_3)]$ and reviewed the correlation between various spectroscopic properties and the phosphine-metal bonding in transition metal complexes (e.g. NMR chemical shifts and coupling constants). A convenient way to quantify electronic effects of phosphorus ligands (π-accepting capacity) is by comparing the frequency of the A_1 stretching vibration of $[Ni(CO)_3L]$ complexes in CH_2Cl_2.[11] The carbonyl complexes form rapidly on mixing L with solutions of $[Ni(CO)_4]$, and the A_1 band is strong and sharp. Higher frequencies mean reduced electron density on the metal (reduced π-backbonding to the carbonyl ligands). As the electronegativity of the phosphorus substituents increases, the π-acceptor properties of the phosphine also increase and so the CO ligands accept less electron density which is detected in the increase in the CO stretching frequency (Table 1.1).

Table 1.1 IR frequencies of ν_{CO} in the $[Ni(CO)_3L]$ complexes in CH_2Cl_2

L	$Ni(CO)_3L$ $\nu_{CO}(A_1)^c$
PCl_3	2097.0
$P(OMe)_3$	2079.5
PMe_3	2064.1
PEt_3	2061.7
$P(Pr^i)_3$	2059.2
$P(Bu^t)_3$	2056.1

Tolman's electronic parameter (ν_{CO} (A_1) in (Table 1.1) can be useful in explaining equilibrium data. For example Table 1.2 shows $\nu_{CO}(A_1)$ for three ligands and the K values for the equilibrium (Equation 1.1)

$$HCN + NiL_4 \xrightarrow{K} HNiL_3CN + L$$

Equation 1.1

The 300 fold decrease in K on going from electron-rich (poor π-acceptor) $PPh(OEt)_2$ to electron-poor (good π-acceptor) $P(OCH_2CH_2Cl)_3$ is reflected by ν_{CO}. Lower frequencies mean greater electron density on the metal and therefore the greater propensity to undergo oxidative addition of HCN.

Table 1.2 Equilibrium constants[13] for Equation 1.1 and IR frequencies of ν_{CO} (A_1) in $[Ni(CO)_3L]$

L	K	$[Ni(CO)_3L]$ $\nu_{CO}(A_1)^c$
$PPh(OEt)_2$	0.03	2074.2
$P(OEt)_3$	0.005	2076.3
$P(OCH_2CH_2Cl)_3$	0.0001	2084.0

[a] At 25 °C in CH_2Cl_2, [b] in cm^{-1}, in toluene, [c] in cm^{-1}, in CH_2Cl_2

1.3.2 Size Effects

1.3.2.1 Cone angle

The steric bulk of the ligands can be quantified using the Tolman Cone Angle θ.[11] The magnitude of θ is a measure of the space occupied by the ligand in the coordination sphere of the metal (Figure 1.3). For symmetrical ligands, the cone angle is measured for the largest extension of the ligand, and all cone angles are measured with a constant M-P bond distance (2.28 Å).

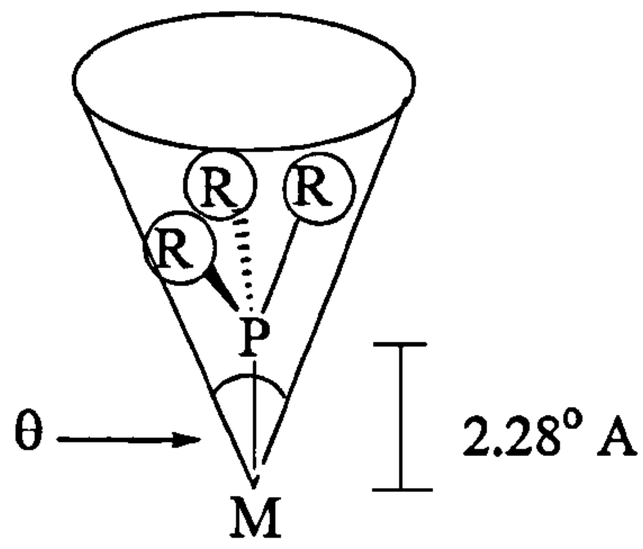

Figure 1.3 Measurement of a Tolman Cone Angle θ.[11]

For unsymmetrical ligands $PX_1X_2X_3$, an effective ligand cone angle θ is defined as the average of the sum of the semivertex angles for each PX_i by reference to Figure 1.4. The *ith* substituent will have a half angle $\theta_i/2$ defined by the metal-phosphorus axis and an outermost van der Waals contact.

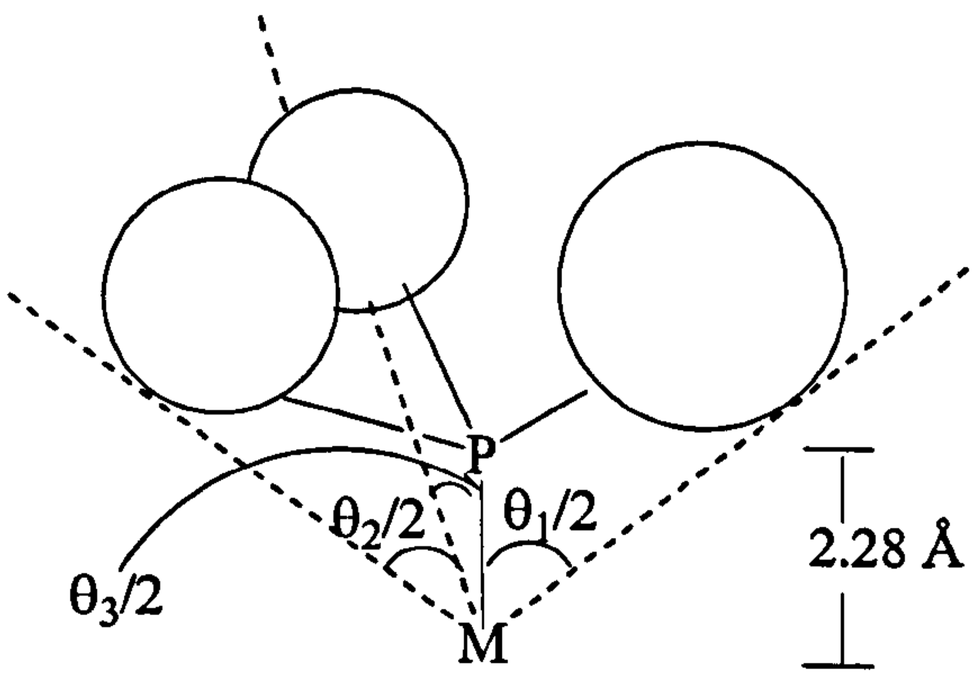

$$\text{Cone angle, } \theta = (2/3) \sum_{i=1}^{3} \theta i/2$$

Figure 1.4

In Table 1.3 are shown some examples of how the cone angle increases with the increase in bulkiness of the substituents.

Table 1.3 Cone angles for some monophosphine and diphosphine ligands

Ligand	Cone Angle (θ)/°
PH_3	87
PMe_3	118
$P(Bu^n)_3$	132
$P(Bu^t)_3$	182
$Et_2PCH_2CH_2PEt_2$	115
$Ph_2PCH_2CH_2PPh_2$	125

The influence of the ligand size is dramatically exemplified by the increase in dissociation constant K_1 for Equation 1.2 by a factor of 10^8 on going from L = P(O-*p*-tolyl)$_3$ (θ = 128) to P(O-*o*-tolyl)$_3$, (θ = 141).

$$NiL_4 \xrightarrow{K_1} NiL_3 + L$$

Equation 1.2

1.3.2.2 Bite angle

The "natural" preference of a ligand for a certain coordination mode can influence a catalytic cycle in several ways; by the stabilization or destabilization of the initial, transition, or final state. In addition, the flexibility of a bidentate ligand may be important in order to accelerate certain reactions. Casey and Whiteker[14] introduced the concepts of natural bite angle (β) and flexibility range (α) for diphosphine ligands as explained below.

The "metal-preferred" ligand bite angle β (Figure 1.5) for octahedral and square-planar complexes (Figure 1.5) is 90°, for tetrahedral complexes 109°, and for bis-equatorial trigonal bipyramidal complexes 120°.

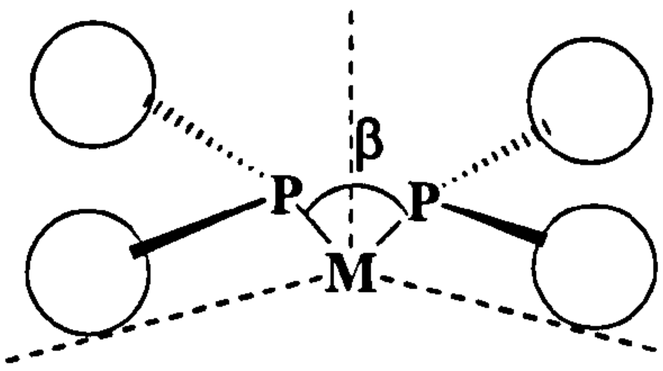

Figure 1.5

Computer modelled geometries can be used to estimate natural ligand bite angles. The metal centre is a dummy atom, the M-P distance is fixed at 2.315 Å for Rh, and the force constant for the P-M-P bond angle is set to 0 kcal mol^{-1} deg^{-1} to eliminate any contribution of the metal. The flexibility range is defined as the accessible range of bite angles within 3 kcal mol^{-1} of the minimum energy. For some ligands it is of crucial importance to perform a systematic conformer search to make sure the lowest energy conformation is used for the bite angle calculation.[15] Steric interactions between the ligand and the substrate depend also on the bite angle and thus can play a pivotal role.

1.4 Bulky phosphine ligands

Since 1980, research in bulky phosphines has grown greatly in the areas of coordination chemistry and catalysis.

1.4.1 Coordination properties of bulky phosphines

A series of generalisations were made by Shaw,[16] which described the effects of sterically demanding tertiary phosphine ligands. These are summarised below with updated examples. A new section on agostic C-H interactions has also been added.

1.4.1.1 Very bulky tertiary phosphines such as those of type PBu^t_2R (R = alkyl or aryl) will not coordinate in mutually cis-positions.

Tertiary phosphines such as PMe_3, PEt_3, PPh_3 *etc.* will generally coordinate in either mutually *cis*- or *trans*-positions, but ligands such as PBu^t_3 or $PRBu^t_2$ will almost always co-ordinate in mutually *trans*-positions.[17]

For example, the presence of bulky phosphine ligands in $[OsH(OH)(CO)(PBu^t_2Me)_2]$ makes its crystal structure atypical.[18] The reason for this is the intermolecular interactions between hydroxyl groups of centrosymmetrically related neighbouring molecules. This interaction is a consequence of the square-pyramidal geometry (Figure 1.6) with nearly linear *trans*-phosphines (∠P-Os-P = 175.3°).

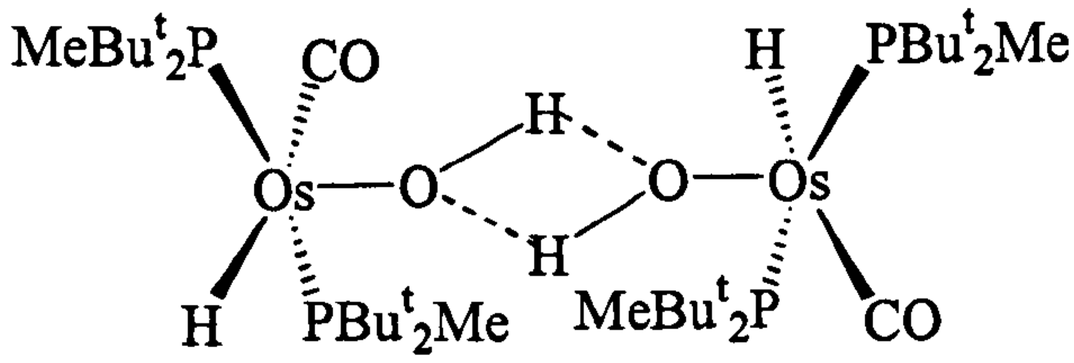

Figure 1.6

1.4.1.2 There are strong non-bonding interactions between a bulky tertiary phosphine and other ligands e.g. Cl, Br, CO, alkyl etc. on the metal.

The best evidence for this comes from variable temperature ^{31}P NMR spectroscopy.[16] Three rotamers are observed for $[RhCl(CO)(PBu^t_2Et)_2]$ when its solution is cooled to –60 °C (Figure 1.7).

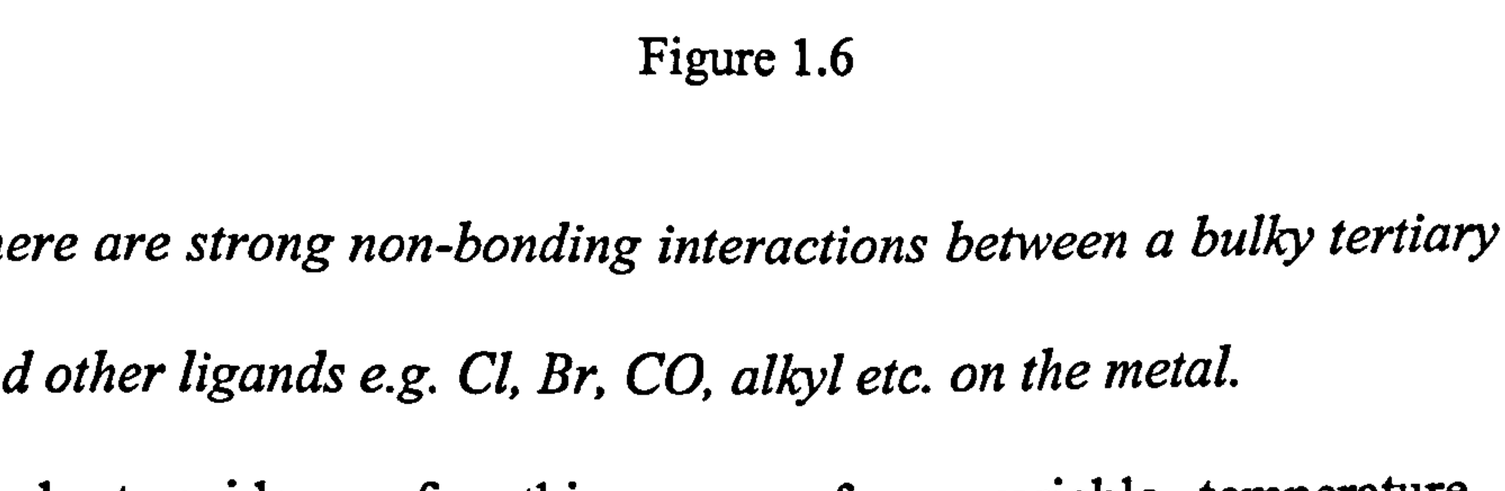

Figure 1.7

1.4.1.3 In order to reduce steric strain coordinatively unsaturated complexes are often formed.

A good example of this is the reaction between $[FeCl_2(CO)_4]$ and (i) PPr^i_3 or (ii) PBu^t_2Me. A dicarbonyl (18*e*) complex is formed when L = PPr^i_3, but with L = PBu^t_2Me the unsaturated (14*e*) species is favoured (Equation 1.3).[19]

$$[FeCl_2(CO)_2L_2] \underset{}{\overset{-2CO}{\rightleftharpoons}} [FeCl_2L_2]$$

$L = PPr^i_3$ $\qquad\qquad$ $L = PBu^t_2Me$

Equation 1.3

Bulky phosphine ligands can be used to make very reactive unsaturated ruthenium complexes. Caulton and co-workers have studied the π–stabilization degree of unsaturation in $[RuH(X)CO(PBu^t_2Me)_2]$, where X = I, Cl, OPh, OH, OCH_2CF_3, $OSiPh_3$, $OSiMe_2Ph$, $OSiMe_3$.[20] They reasoned that when the X groups are good π-donors they stabilise to the 16*e* complexes by the synergic effect of the M-X σ-bond and X→ M π-bond *via* lone pairs on X.

The synthesis of $[RuCl_2(CO)_2(d^tbpe)]$, (d^tbpe = $Bu^t_2PCH_2CH_2PBu^t_2$) an 18*e* complex, has also been reported. The $[RuCl_2(CO)_2(d^tbpe)]$ complex can be reduced to $[RuH_2(CO)_2(d^tbpe)]$ (**1.3**) containing *cis*-hydrides. The dihydrido complex will react with CO at 25 °C to form $[Ru(CO)_3(d^tbpe)]$.[21]

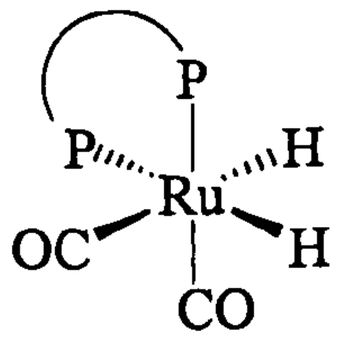

1.3

The reaction of $[Cp^*Ru(OMe)]_2$ with PCy_3 produces the very reactive alkoxo derivative $[Cp^*Ru(OMe)(PCy_3)]$ (**1.4**), which was reacted with H_2 to form (**1.5**). In addition, protonation of (**1.4**) with HBF_4 led to methanol elimination and dehydrogenation of the phosphine ligand to produce (**1.6**).[22]

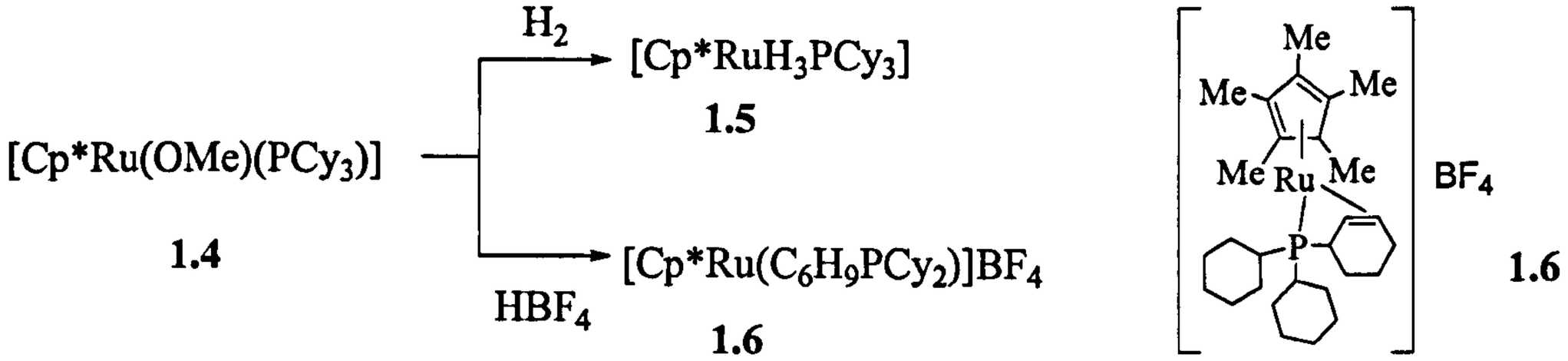

Equation 1.4

The interest in unsaturated ruthenium complexes with bulky phosphines ligands has grown over the last 10 years, due to their performance as catalysts in ring-opening metathesis.[23] A very reactive 14-electron ruthenium hydride complex $[RuHCl(PPr^i_3)]$ (**1.7**) has been isolated and fully characterized.[24,25] Complex (**1.7**) is a crucial intermediate in the preparation of the Grubbs ruthenium catalyst (**1.8**) (see Section 1.4.2.4).

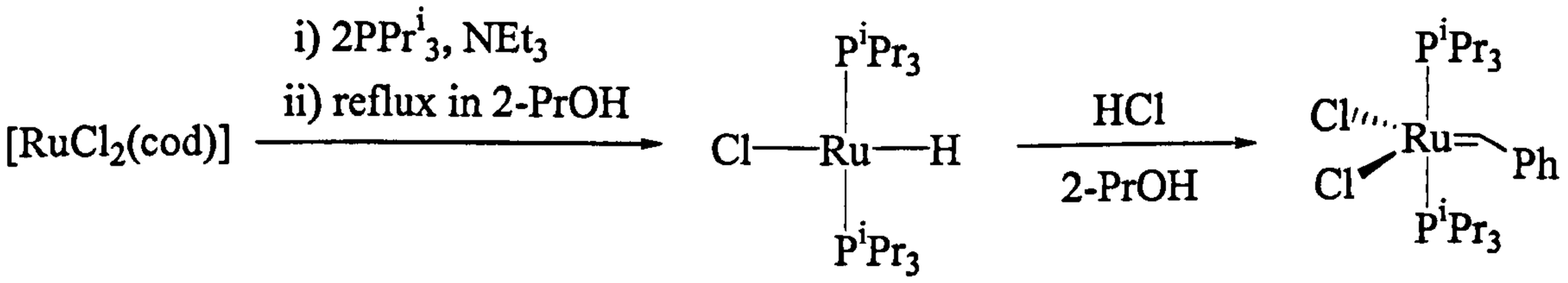

1.4.1.4 The other associated ligands are preferably small

Because bulky phosphines are very sterically demanding, having the other coordinating ligands relatively small (e.g. H), can reduce the steric strain; compounds (**1.9**), (**1.10**), (**1.11**) and (**1.12**) are good examples.[16]

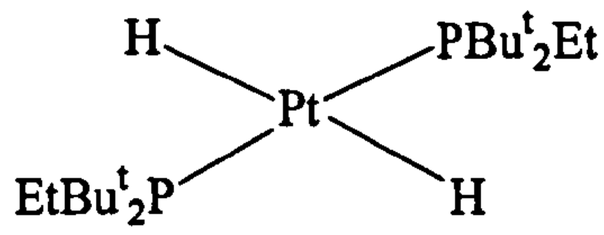

1.9

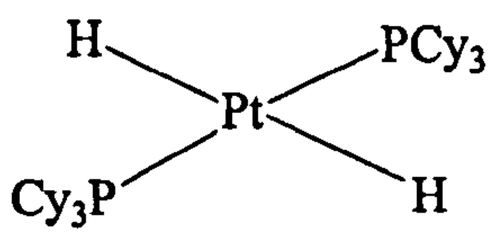

1.10

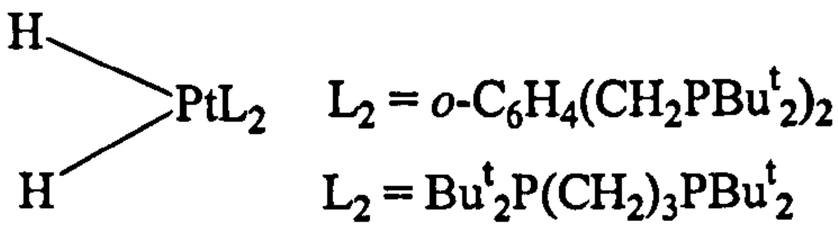

1.11-1.12

1.4.1.5 Bulky phosphines may assist in the kinetic stabilisation of complexes

An unusual cationic ruthenium complex (**1.13**) with bulky phosphine ligands has been reported which has a bidentate coordinated dichloromethane molecule.[26] The salt (**1.13**) results from the metathesis of $[RuH(OTf)(CO)L_2]$ with 1 equiv. of $NaBAr_4$.

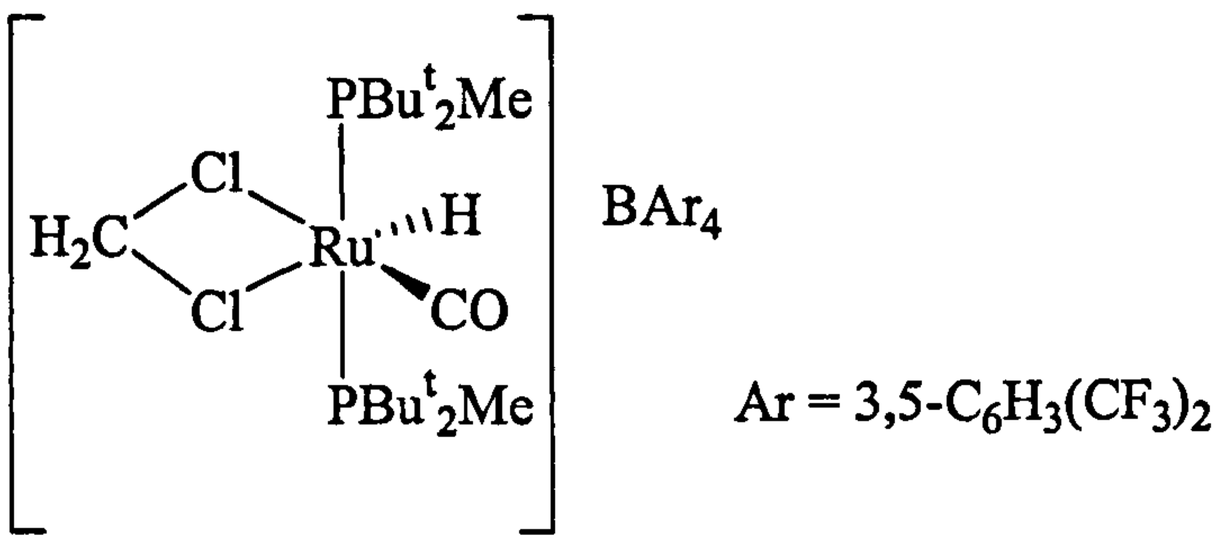

1.13

Bulky phosphine groups have been used to stabilize the Ni(II) phosphine-imine catalyst in the polymerisation of ethene.[27] The phosphine-imine complexes (**1.14**) are stable after 7 h at 70° in the polymerisation of ethene, whereas the Ni(II)-α-bis-imine phosphines (**1.15**) decompose within 30 min of the reaction.[27]

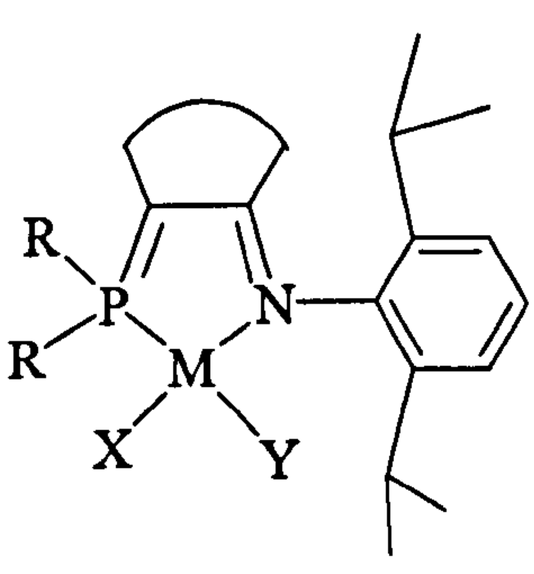

M = Pd, X = Cl
M = Ni, X = Br

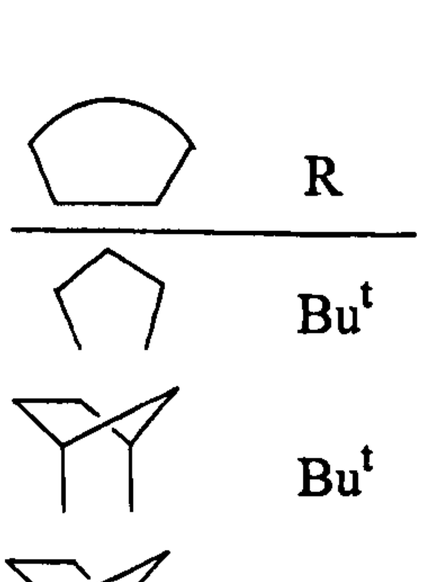

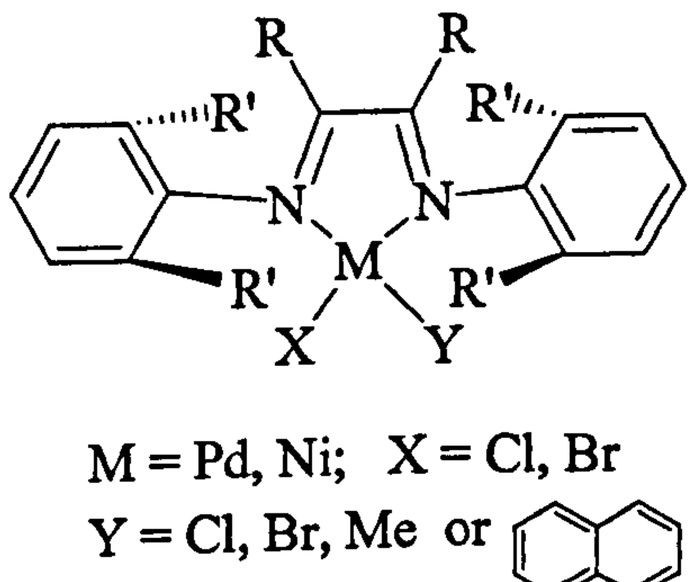

M = Pd, Ni; X = Cl, Br
Y = Cl, Br, Me or

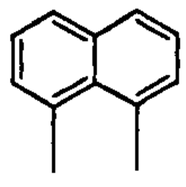

R = H, Me
R' = Me, Et' P^{ri}

1.14 **1.15**

A series of platinum complexes of the general formula $[Pt(Me_2NCS_2)(PR_3)(alkyl)]$ have been synthesised by Reger *et al.*[28] The complexes undergo alkyl isomerization as shown in Equation 1.5.[28] The equilibrium position from the linear to branched product can be changed from 9:1 (**1.16**) to 25:1 (**1.19**) by replacement of the methyl group for cyclohexyl in the phosphine ligand.

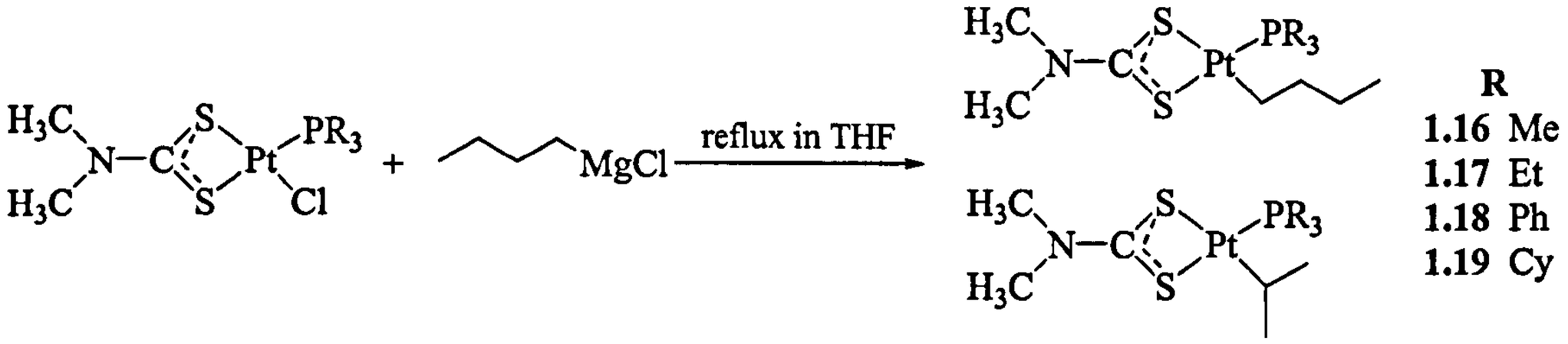

Equation 1.5

1.4.1.6 The decarbonylation of alcohols is a common reaction with metal complexes containing bulky tertiary phosphine ligands.

A good example of this generalization is given by complexes of type $[RhHCl_2(PBu^t_2R)_2]$ which react in seconds with methoxide ions in methanol at 20 °C to give *trans*-$[RhCl(CO)(PBu^t_2R)_2]$.[16]

Recently the decarbonylation of aldehydes, formates and formamides by the $[RuHCl(PPr^i_3)_2]_2$ complex has been reported. The reactions are shown in Scheme 1.1, Equation 1.6 and Equation 1.7.[29] The decarbonylation of aldehydes and formates is complete and quantitative within 30 min at room temperature.

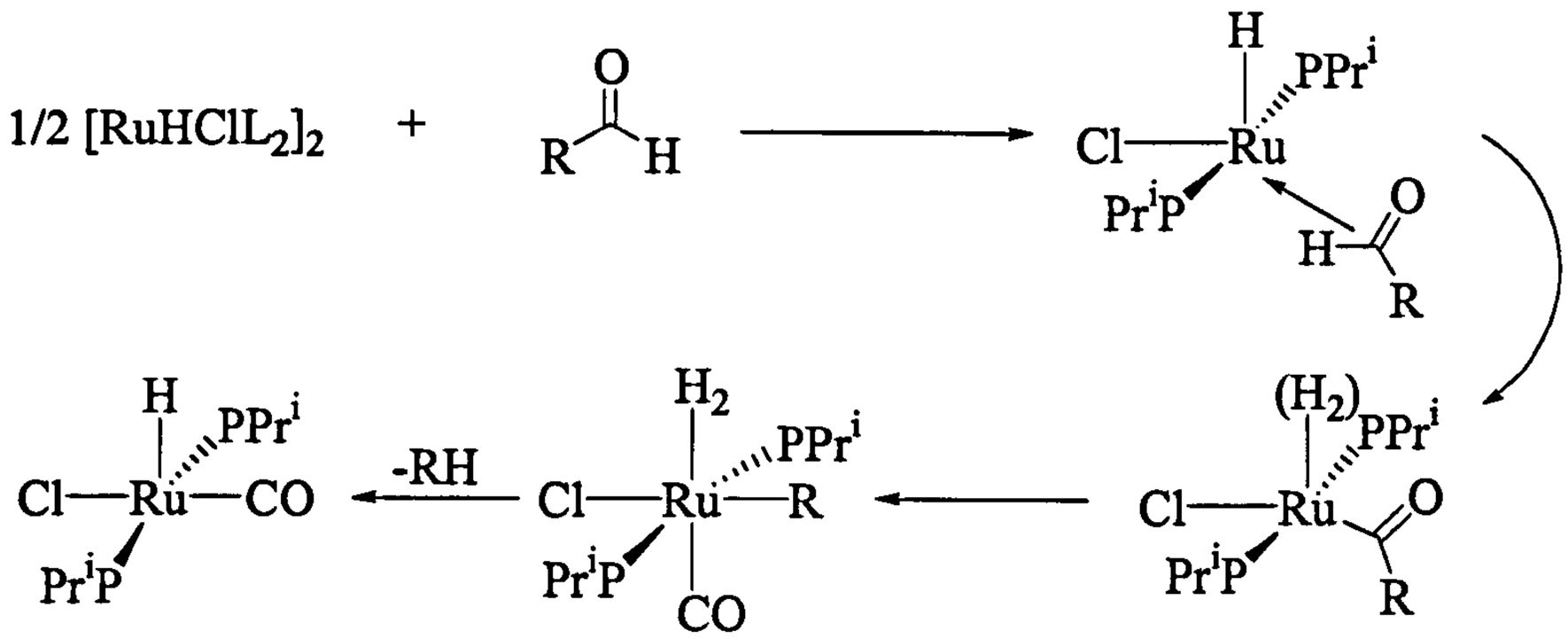

Scheme 1.1

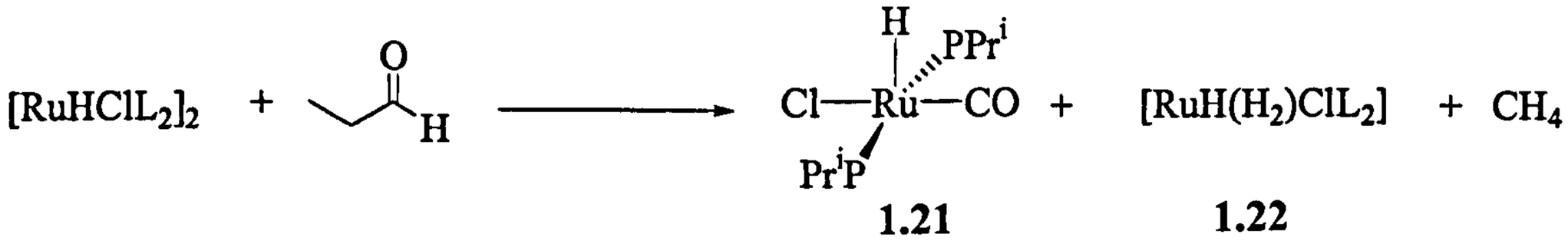

Equation 1.6

The decarbonylation of formamides with complexes containing bulky phosphine ligands is complete at room temperature after 2 days, but at 80 °C can be complete in 3 h (Equation 1.7).[29]

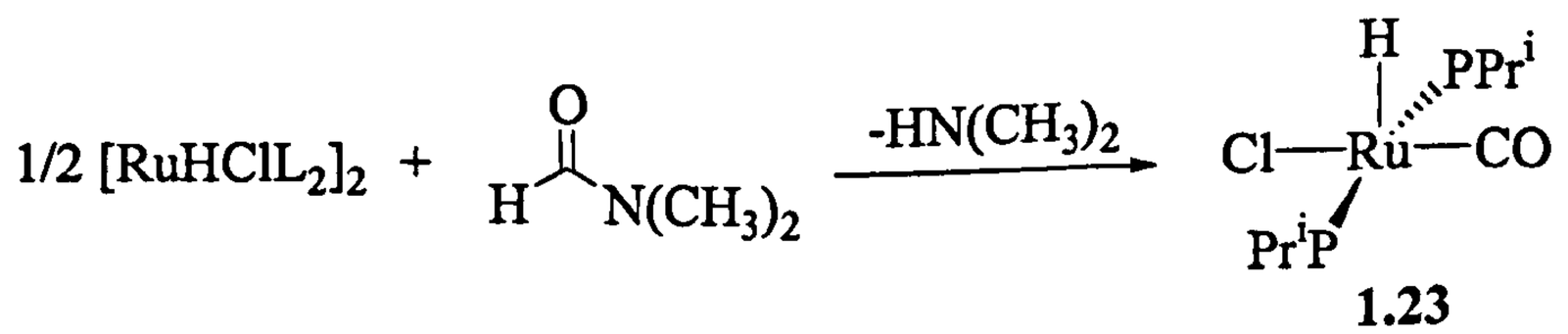

Equation 1.7

1.4.1.7 Metal-metal bond formation is favoured by very bulky phosphine ligands

An example of this effect was observed by Shaw in 1973.[30] An alcoholic ruthenium(III) chloride solution was first carbonylated and to the resulting complex was

added the very bulky ligands PBu^t_2Ph, $PBu^t_2(CH_2Bu^t)$ or PBu^t_3 (Equation 1.8). Only one tertiary phosphine complexed to each ruthenium and a binuclear ruthenium(I) complex **(1.24)** was formed, reducing the steric strain due to the bulky phosphines.[16]

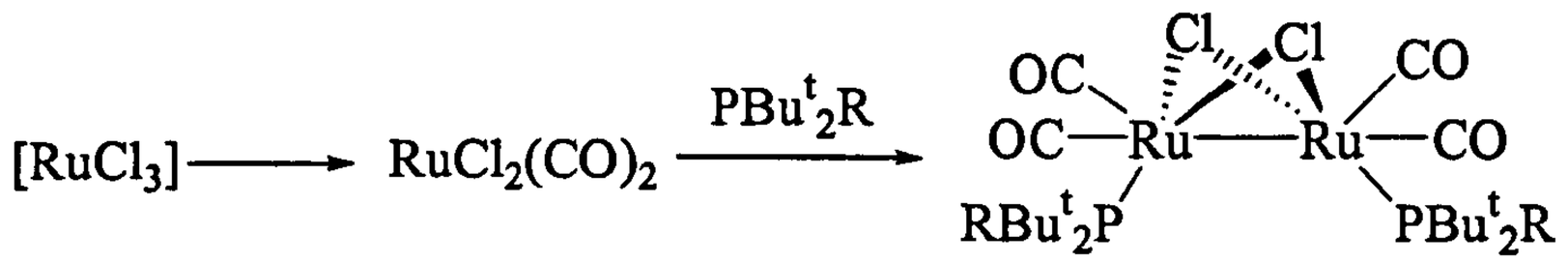

1.24

Equation 1.8

1.4.1.8 Very bulky phosphines assist in cyclometallation

This generalization came from observations on the influence the size of R_1 and R_2 (Equation 1.9) have on the cyclometallation process. With phenyl substituents it would not always occur but if R_1 and R_2 are bulky substituents the reaction often occurs readily. It was found that cyclometallation increases in the order (R_1 or R_2) Me < Ph < Bu^t and clearly steric effects are dominant over electronic effects.[16]

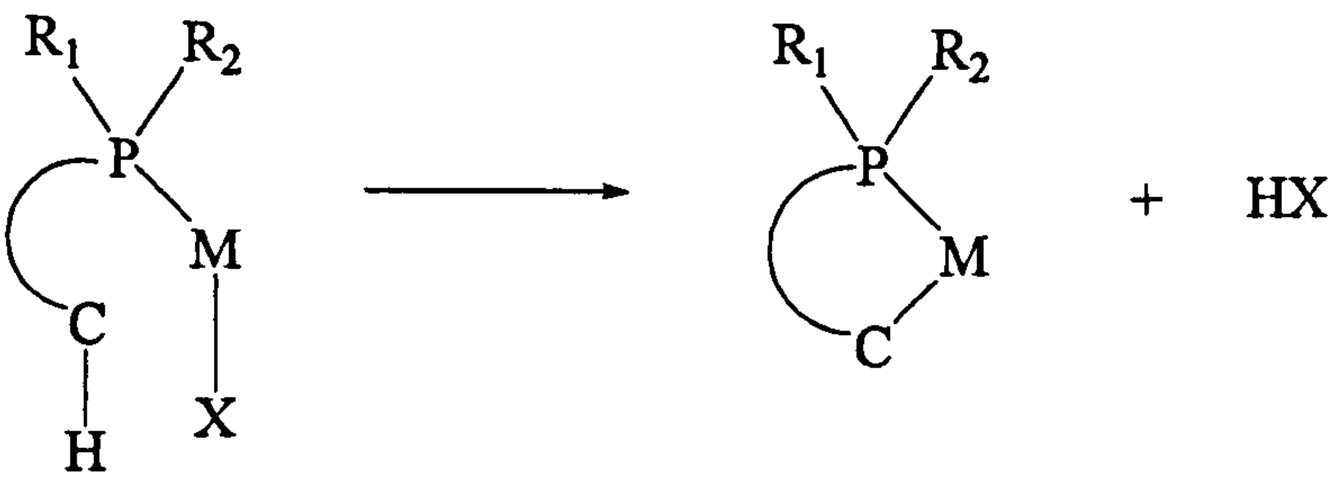

Equation 1.9

An example of this reaction is shown in Equation 1.10 where the bulky phosphine substituents in PBu^t_2 promote C-H activation of the pro-chiral ferrocenylmethylphosphine to form the cyclopalladated complex **(1.25)**.[31] The product was obtained in 70% yield as a racemic mixture (due to the planar chirality).

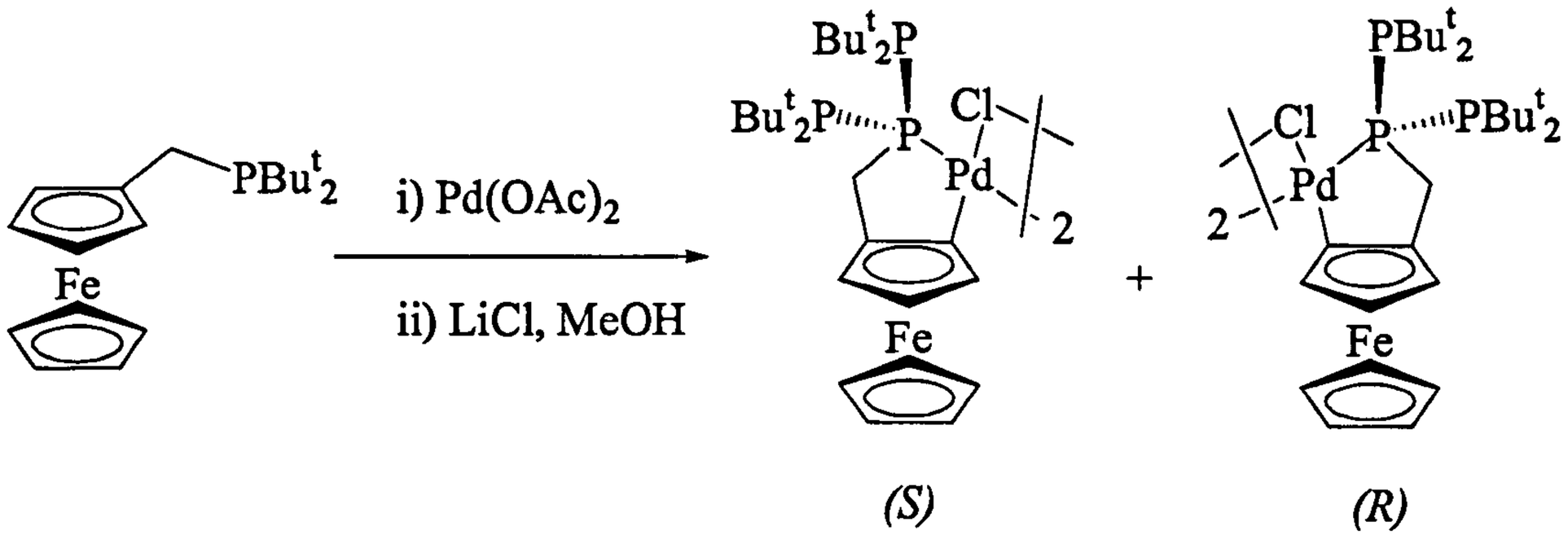

1.25 (S) **1.25** (R)

Equation 1.10

Cyclometallated phosphine-based pincer complexes such as (**1.26**) have recently been reviewed.[32] They have been used in applications such as the Heck reaction[33,34] and in the activation of C-C[35] and C-O bonds (see Section 1.4.2.2).[32,36]

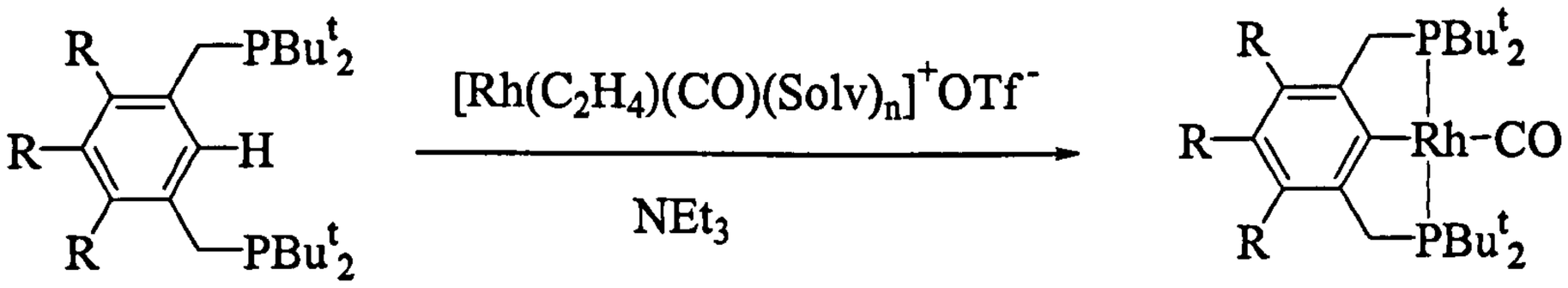

R = H, OMe

1.26

1.4.1.9 Large ring formation is promoted by very bulky phosphine ligands

Until the early 1980's large chelate rings (> 8-membered) were thought to be unstable when compared to open-chain (polymeric) structures. However, it has been shown that a variety of long chain diphosphines with sterically demanding substituents on the donor atoms will form large ring chelates (12- to 72-membered). For example $Bu^t_2P(CH_2)_4C{\equiv}C(CH_2)_4PBu^t_2$ and $Bu^t_2PC{\equiv}C(CH_2)_nC{\equiv}PBu^t_2$ (n = 4 or 5) formed large chelate rings whereas $Me_2P(CH_2)_{12}PMe_2$ and $Ph_2P(CH_2)_{10}PPh_2$ gave intractable polymeric materials.[16]

1.4.1.10 β-agostic Interactions

Complexes where the metal atom forms a M····H—C, two electron and three-centre (agostic) interaction, are important in hydrogenation,[37] hydroformylation and alkene oligomerization.[9]

Spencer *et al.*[38] reported the synthesis of a series of cationic platinum complexes $[Pt(norbonyl)L_2)]^+$ (L_2 = bulky diphosphine) (Scheme 1.2) in which the norbornyl ligand binds to the platinum *via* σ-alkyl and β-C-H agostic interactions, forming a 14*e* complex.

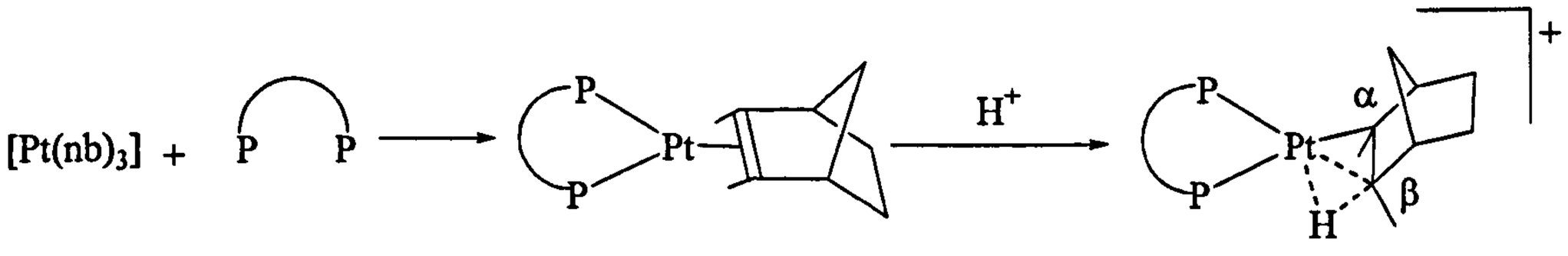

1.27 $Cy_2P(CH_2)_2PCy_2$,
1.28 $Bu^t_2P(CH_2)_2PBu^t_2$,
1.29 $Cy_2P(CH_2)_3PCy_2$,
1.30 $Bu^t_2P(CH_2)_3PBu^t_2$,
1.31 *o*-$(Bu^t_2PCH_2)_2C_6H_4$

Scheme 1.2

Further investigation of these complexes showed a connection between the strength of the agostic interaction and size of the diphosphine ligand. Increasing the bulkiness of the groups at the phosphorus promotes kinetic stabilisation of the agostic interaction.[39]

Spencer has shown in several studies[40-43] that bulky phosphines stabilise β-agostic complexes. Brookhart *et al.*[44] has also shown that electronic effects are sometimes also important in the stabilization of β-agostic interactions.

1.4.2 Bulky phosphines in catalysis

Bulky phosphine ligands are very important in catalysis, e.g. carbonylation, olefin metathesis reactions, Heck reactions and cross-coupling reactions. In this section we will describe recent reports of bulky phosphine ligands in these reactions which are most pertinent to the research described in Chapter 2 and Chapter 4.

1.4.2.1 Carbonylation

Some large scale chemical processes are based on synthesis gas which is derived from methane[45] (Equation 1.11).

$$CH_4 + H_2O \longrightarrow CO + 3\,H_2$$

Equation 1.11

The alkoxycarbonylation of olefins is of industrial importance since a wide range of products can be obtained such as high molecular weight polyketones, which are useful due to their engineering thermoplastic properties, and methyl propanoate (when n = 1 in Equation 1.12) which is an intermediate in the production of acrylic polymers.[46]

$$CH_3OH + CO + H_2C{=}CH_2 \xrightarrow{[Cat]} H\text{-}(CH_2\text{-}CH_2C(=O))\text{-}_nOCH_3$$

Equation 1.12

The catalysts used in the reaction in Equation 1.12 are usually of type $[L_nPdX_2]$, where L is a phosphine ligand and X is the anion of an acid HX. The complex is generated as in Equation 1.13.

$$[Pd(OAc)_2] + n\,L + HX\,(excess) \longrightarrow [L_nPdX_2] + 2HOAc$$

Equation 1.13

In the alkoxycarbonylation of alkenes, the palladium catalyst shows a pronounced selectivity dependence on the nature of the phosphine ligand. In the CO/ethene reaction, monodentate phosphines generally give methyl propanoate, whilst bidentate phosphines generally produce high molecular weight co-polymers.[47] The reasons for this are complex and require a detailed examination of the proposed mechanism.[47]

The catalysts (**1.27-1.29**) have been shown to have exceptional activity,[48] selectivity and stability in the formation of methyl propanoate.

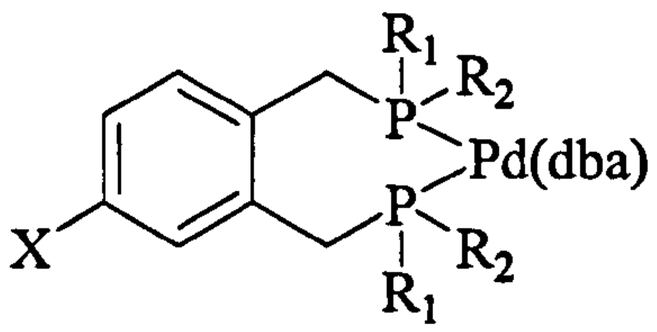

1.27 $R_1 = R_2 = Bu^t$, $X = H$

1.28 $R_1 = R_2 = Bu^t$, $X = NO_2$

1.29 $R_1 = R_2 = Bu^t$, $X = OMe$

Complexes (**1.27-1.29**) were formed by the addition of the diphosphine to $[Pd_2(dba)_3]$ (dba = *trans,trans*-$(PhCH{=}CH)_2CO$). These catalysts were shown to convert ethene, CO and methanol to methylpropanoate at a rate of 50 000 mol/mol cat/h with a selectivity of 99.98%. It was reported that the activity was reduced by a factor of 60 when the t-butyl substituents on the phosphine were replaced by i-propyl groups.[48]

A later report of the catalytic system[49] with d^tbpx showed that the formation of methyl propanoate occurs *via* a hydride (cycle A) (Scheme 1.3) rather than a methoxycarbonyl cycle (cycle B). All the intermediates in this cycle have been identified by multinuclear NMR spectroscopy and ^{13}C-labelling.

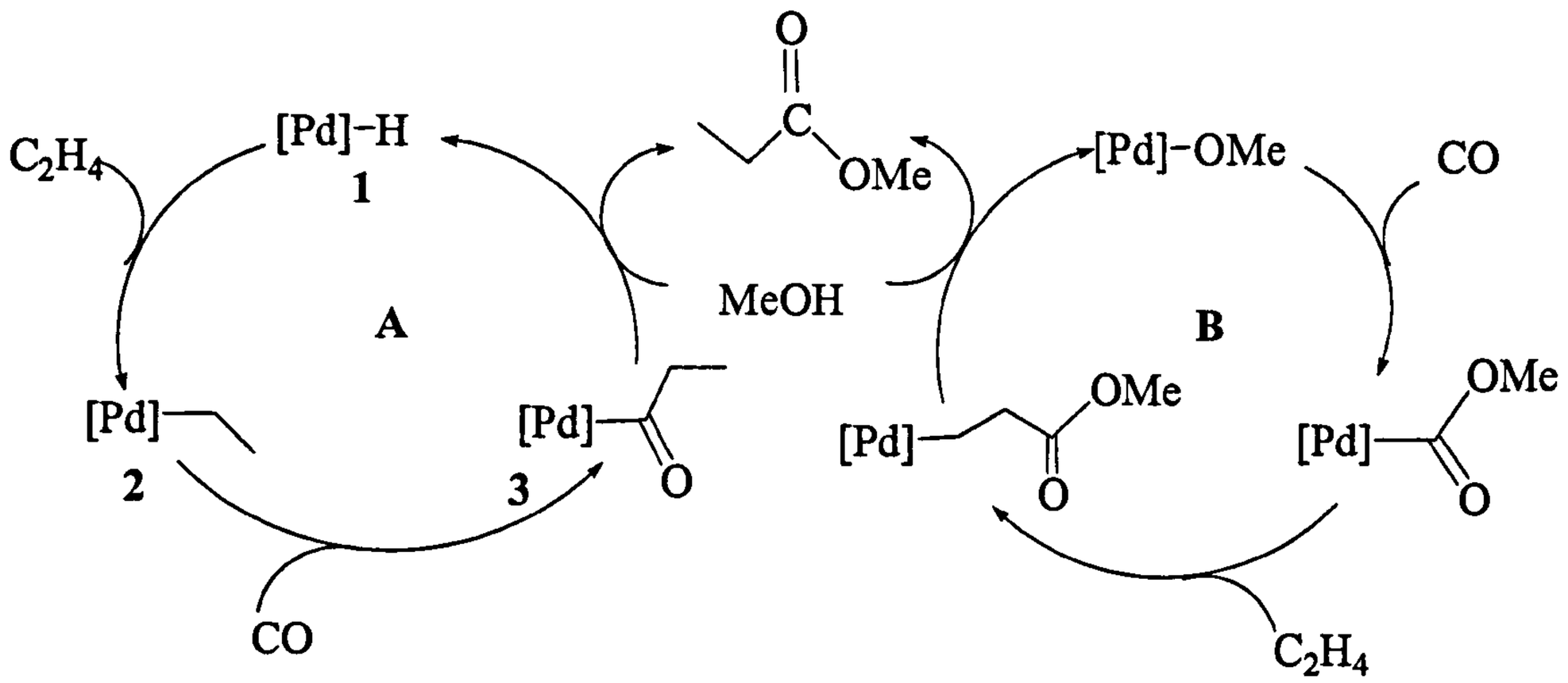

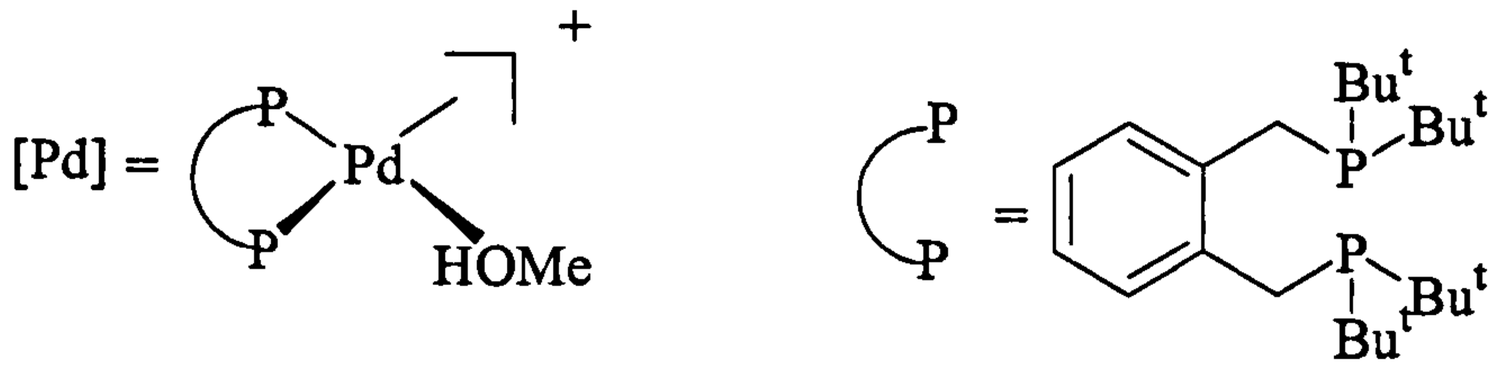

Scheme 1.3

A more detailed spectroscopic study[50] showed that the reaction of [PdH(L-L)(MeOH)]$^+$ with ethene produced a β-C-H interaction as shown below (Figure 1.8).

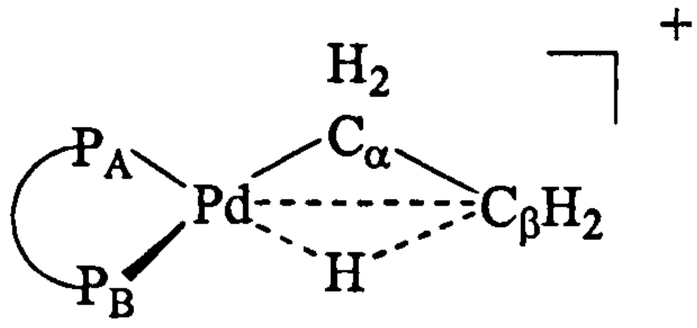

Figure 1.8

The agostic interaction was confirmed in different solvents such as Pr^{n}OH, THF and EtCN. This species (Figure 1.8) had been reported before by Spencer *et al.*, synthesised by the protonation of [Pd(L-L)(C_2H_4)], but no NMR data was reported.[51]

Recently highly active palladium(II) catalysts with bis(phospha-adamantyl)-diphosphine ligands e.g. **(1.30)** have been reported for the selective methoxycarbonylation of 1-tetradecene and internal isomers giving the linear ester with good selectivity (80%).[52] When the catalyst, made by the complexation of [Pd(OAc)$_2$] and **(1.30)**, was used in the methoxycarbonylation of ethene, methyl propanoate was

produced with very high selectivity (>99%). This result may be connected with the unusual properties of *meso/rac*-**(1.30)**. Ligand *meso/rac*-**(1.30)** possesses a significantly larger cone angle ($\theta = 173^{o}$)[53] than the xylenylphosphine (d^{t}bpp) ($\theta = 155^{o}$), which has been reported as an excellent ligand for the formation of methyl propanoate (see above).[54]

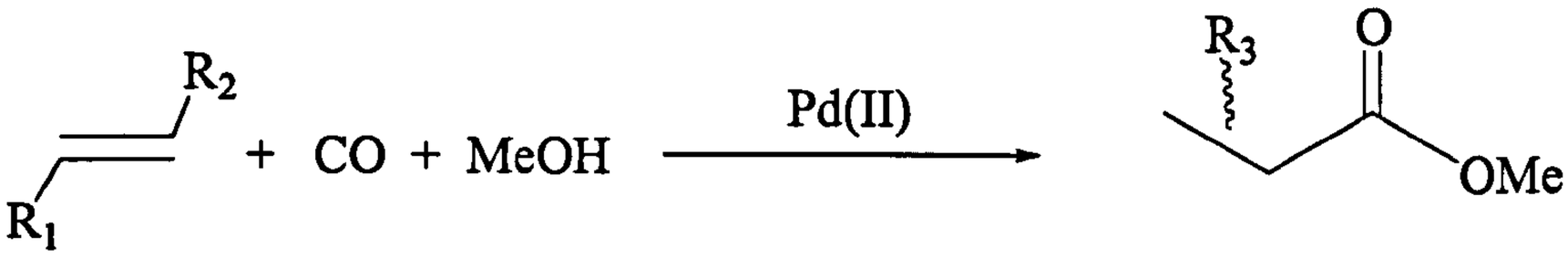

Equation 1.14

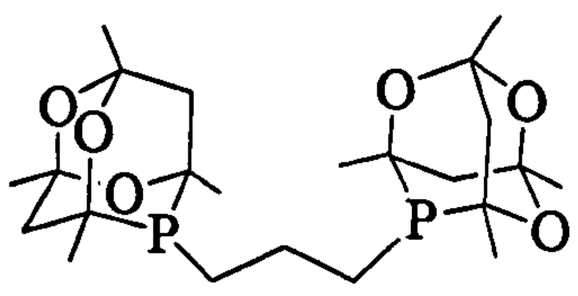

rac-**1.30**

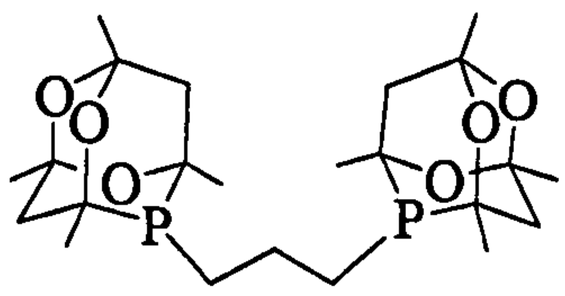

meso-**1.30**

The catalysis was markedly affected by the length of the ligand backbone. When **(1.31)** was used in the methoxycarbonylation of ethene under the same conditions as **(1.30)**, a polyketone with low molecular weight was obtained.[52]

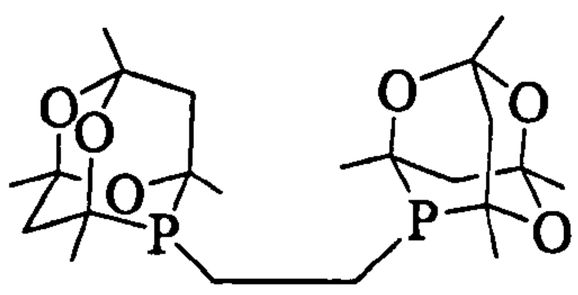

rac-**1.31**

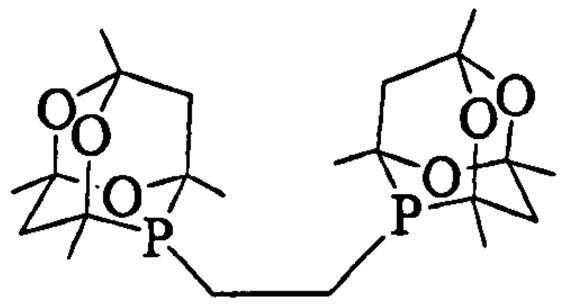

meso-**1.31**

Interesting results were found when the ligands **(1.32-1.35)** were tested in the same palladium-catalyzed methoxycarbonylation of ethene in methanol.[55]

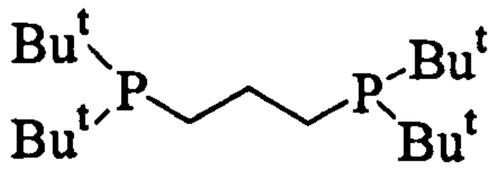

(d^{t}bpp) **1.32**

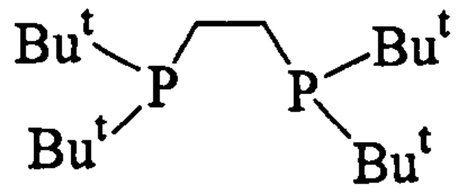

(d^{t}pe) **1.33**

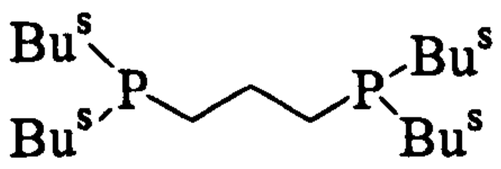

(d^{s}bpp) **1.34**

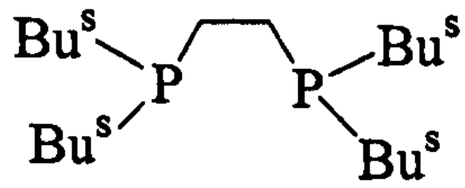

(d^{s}bpe) **1.35**

When (d^{t}bpp) was used under high temperature conditions (120 °C), the formation of methyl propanoate was 25 000 mol/mol cat/h. but when the less sterically demanding ligand (d^{s}bpp) was used, diethyl ketone was formed in 75% yield.[55] The most impressive result was observed with ligand (d^{t}bpe) which, under the same conditions, increased the diethyl ketone selectivity to 98% and with an activity of 90 000 mol/mol cat/h. However, in this reaction 20 bar of H_2 was used to inject the methanolic catalyst solution into the autoclave at the reaction temperature instead of using 10 bar of CO as in the previous reactions.

An explanation of this effect has been proposed in terms of a different catalytic cycle.[55] It was proposed that the effect of hydrogen was to speed up the rate of the reaction by direct hydrogenolysis of the oxo-chelate (**A**) shown in Scheme 1.4. However, no detailed mechanistic study has been carried out to prove that H_2-assisted regeneration of the Pd-hydride (**B**) from the Pd-methoxide (**C**) occurs rather than rapid methanol protonolysis *via* the enolate (**D**).

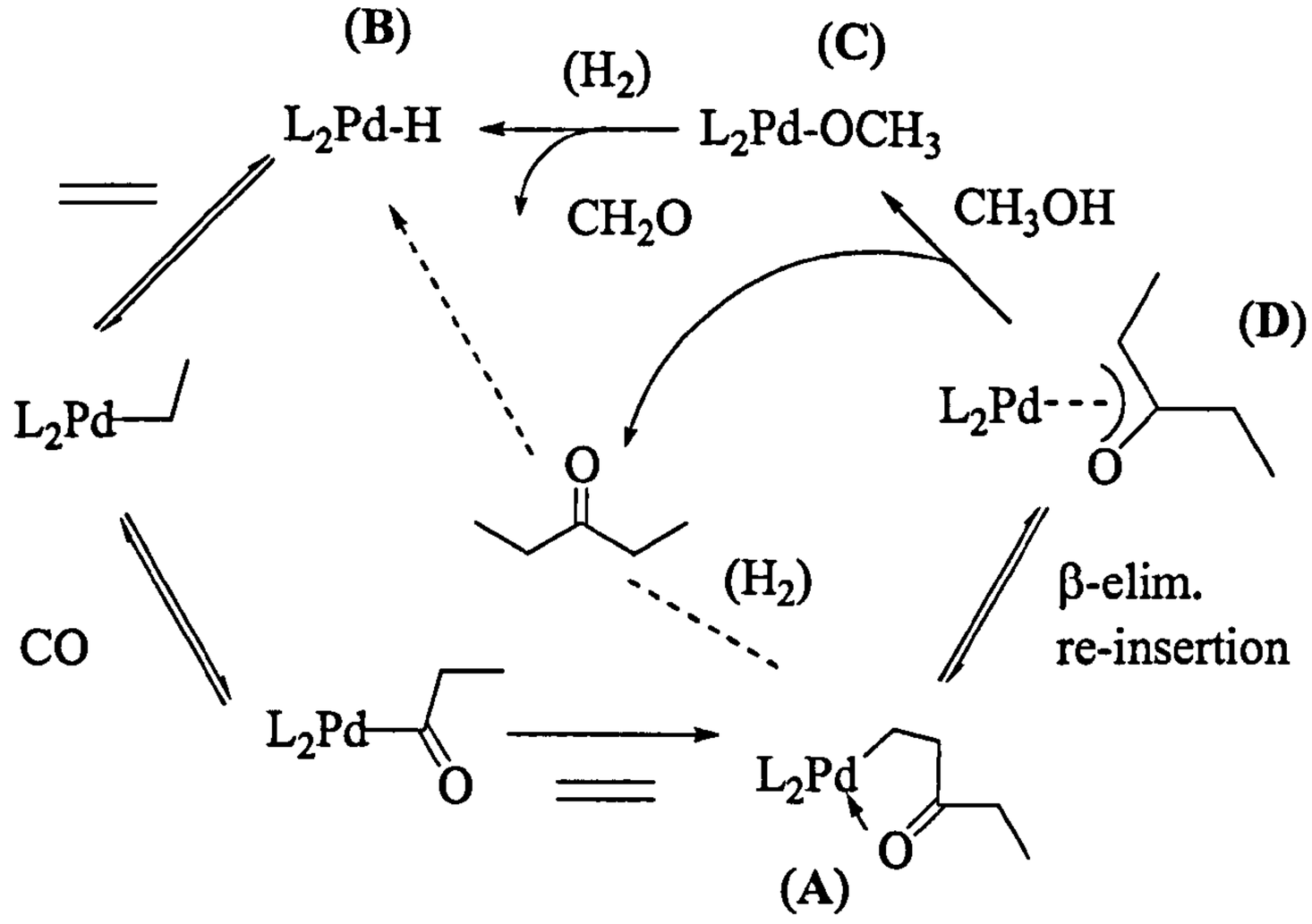

Scheme 1.4

1.4.2.2 Heck catalysis with bulky pincer P-C-P palladium complexes

Cyclometallated pincer complexes are of interest due to their ability to balance stability and reactivity. The stability of the tridentate systems P-C-P is extraordinary, they are thermally stable, and no decomposition is observed at temperatures up to 180 °C and they are also not sensitive to oxygen or moisture.[56]

Reactivity can be controlled by systematic ligand modifications, including altering the backbone (alkyl, aryl) **(1.36, 1.37)**, changing the nature of the metal centre, and utilizing a wide range of substituents on the phosphorus atoms.

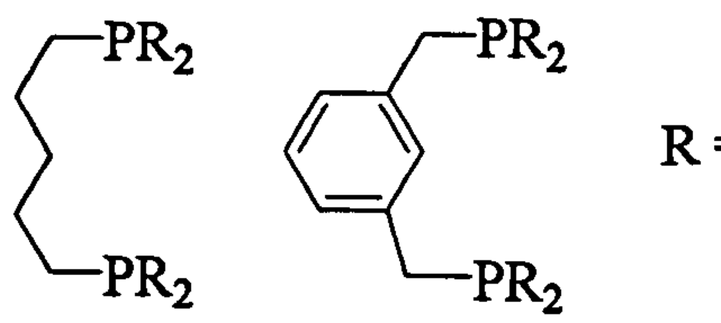

1.36 **1.37**

An extensive review of cyclometallated phosphine-based pincer complexes has been recently published.[56] Palladium pincer complexes **(1.38 - 1.43)**, and many other metal complexes using ligands **(1.36, 1.37)** have been shown to be excellent catalysts

for the dehydrogenation of alkenes,[57] ketone reduction by hydrogen transfer,[58] Suzuki biaryl coupling,[59] and Heck olefin arylation.[60,61]

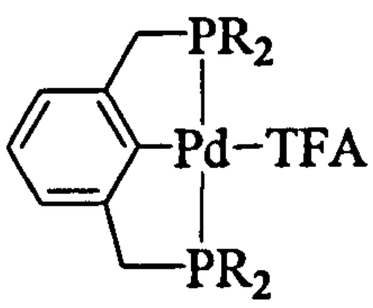

1.38 R = Pr^i

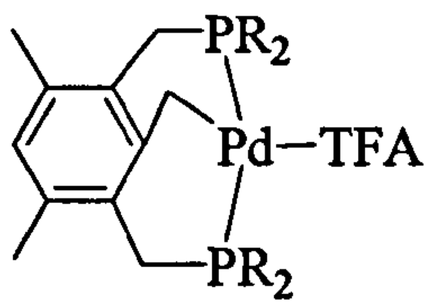

1.39 R = Pr^i
1.40 R = Bu^t

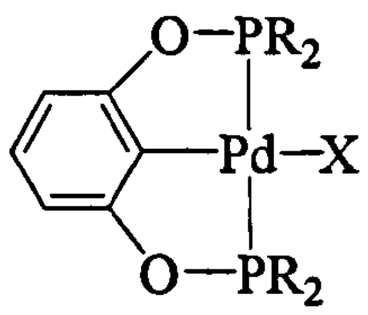

1.41 R =4-$MeOC_6H_4O$, X = I
1.42 R =Pr^i, X = Cl

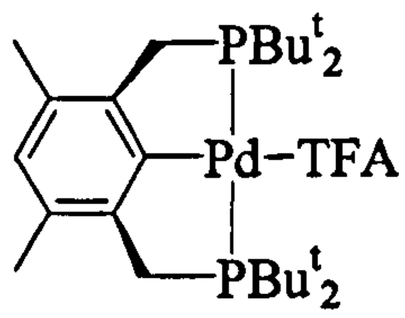

1.43

Milstein's pincer complexes (**1.38 - 1.40**) were the first to be used in the Heck reaction (Equation 1.15), with turnover numbers (TONs) > 100 000, very high yields and no observable catalyst degradation.[60] Another good example of the excellent performance of pincer complexes as catalysts is (**1.41**), which has shown TONs of c*a.* 10^8 when used in the intramolecular Heck reaction to afford carboxylic ring systems (Equation 1.16).

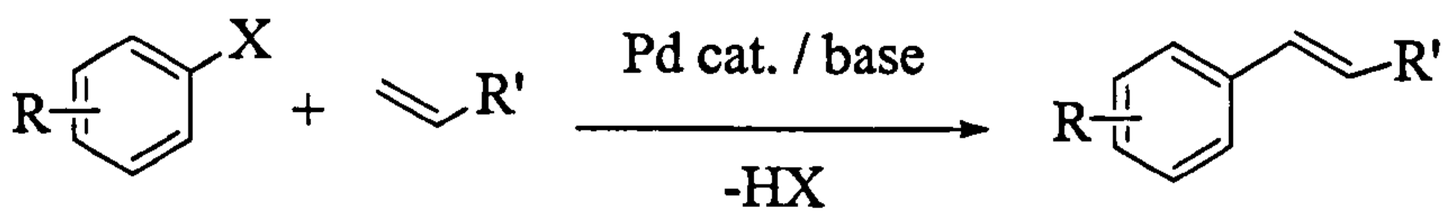

Equation 1.15

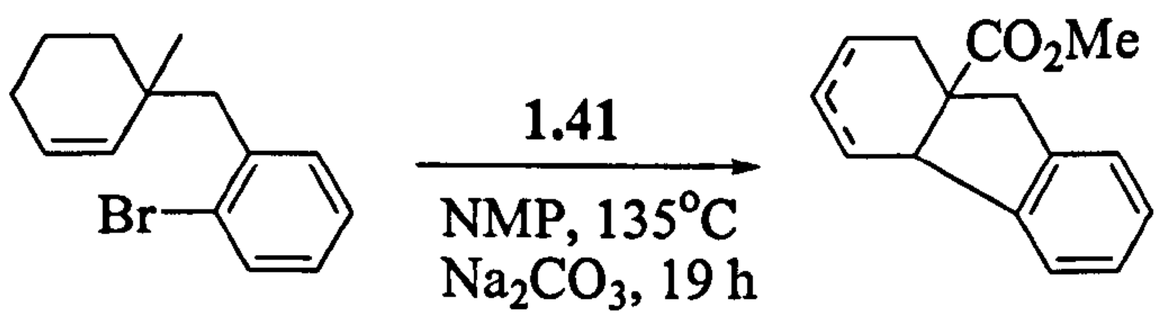

Equation 1.16

Nanosize multimetallic pincer compounds e.g. (**1.44**), are a new development introduced by van Koten *et al*[62] as Lewis-acid catalysts in the double Michael reaction between methyl vinyl ketone and ethyl α-cyanoacetate (Equation 1.17).

Cat =

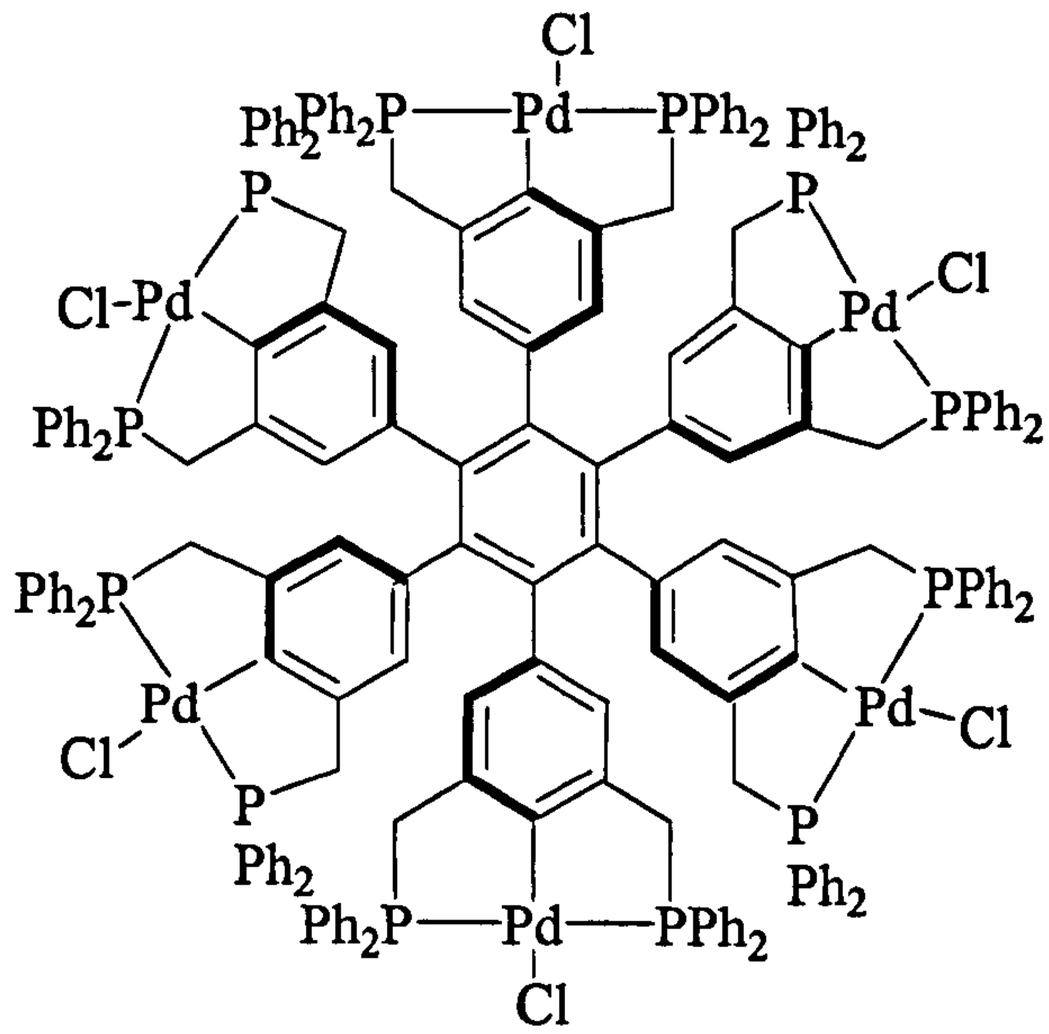

1.44

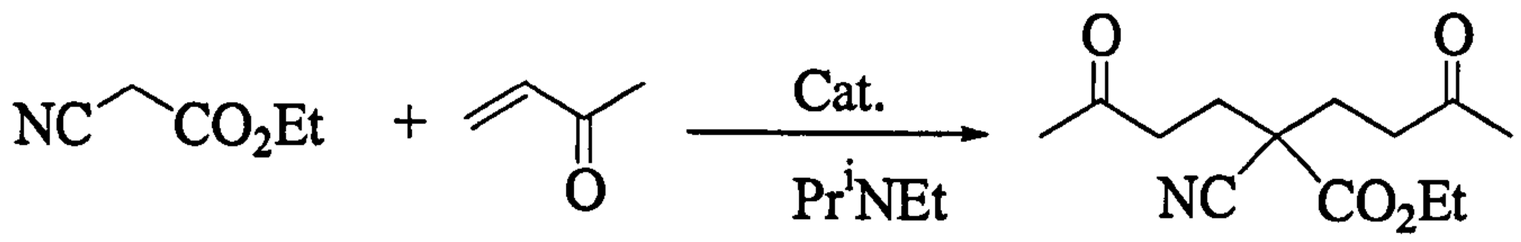

Equation 1.17

1.4.2.3 Bulky phosphines for palladium-catalyzed arylations

Electron-rich bulky alkylphosphine and N-heterocyclic carbene ligands have made palladium catalyzed α-arylation of ketones a useful process for a broad range of enolates, including those derived from amides, esters, aldehydes, nitriles, malonates, cyanoesters, nitroalkanes, sulfones, and lactones.[63,64] The bulky phosphine d^{t}bpf **(1.45)** (Equation 1.18) has proven to be a very fast catalyst with high TONs in just a few hours at 70°C, and many arylations have been performed at room temperature.[65]

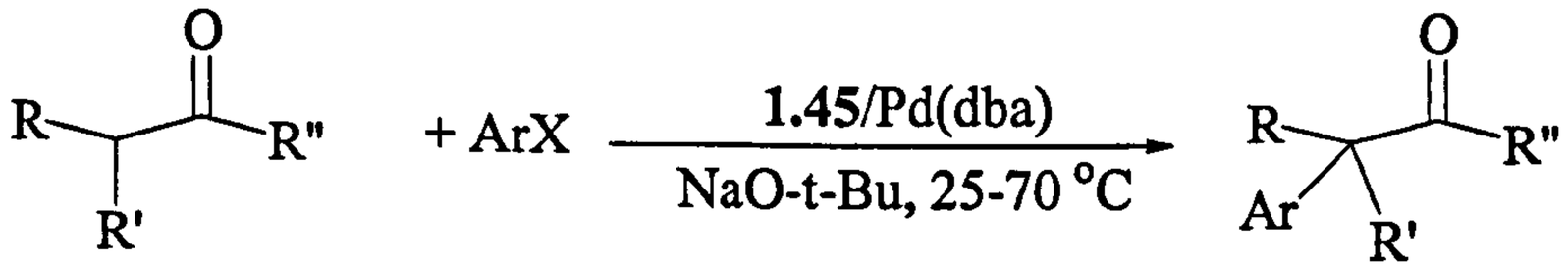

Equation 1.18

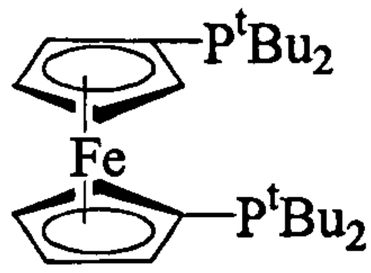

d^{t}bpf 1.45

Tri-t-butyl-phosphine has been used as a ligand in the arylation of esters at room temperature (Equation 1.19).[65]

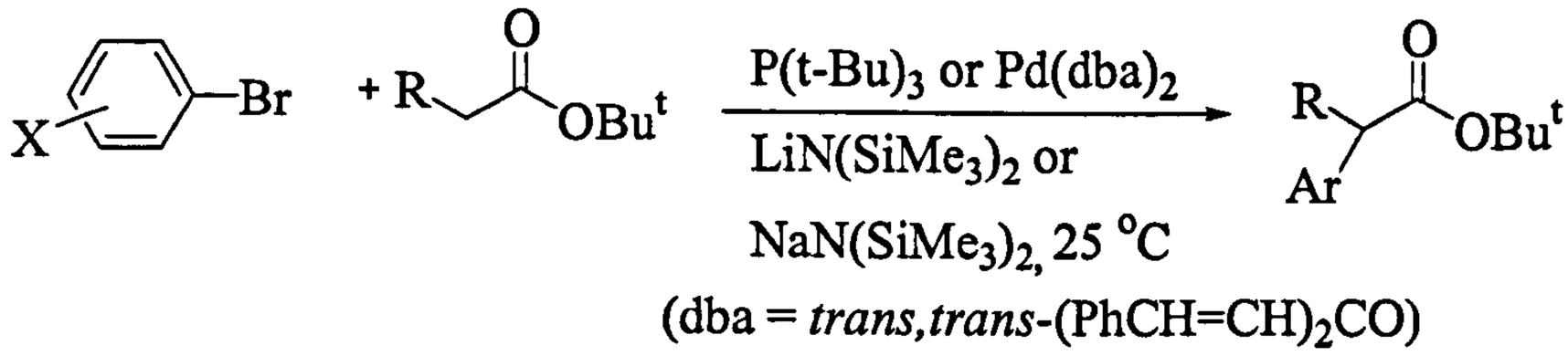

Equation 1.19

Buchwald *et al.*[66] have shown that the bulky phosphine ligand (**1.46**) promotes C-H functionalization in the palladium-catalyzed synthesis of oxindole ring systems under mild conditions (Equation 1.20). The oxindole ring system is an important structural unit in numerous natural products and pharmaceutically active compounds.

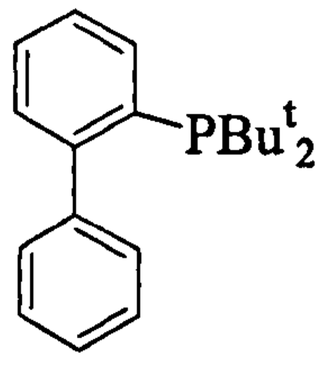

1.46

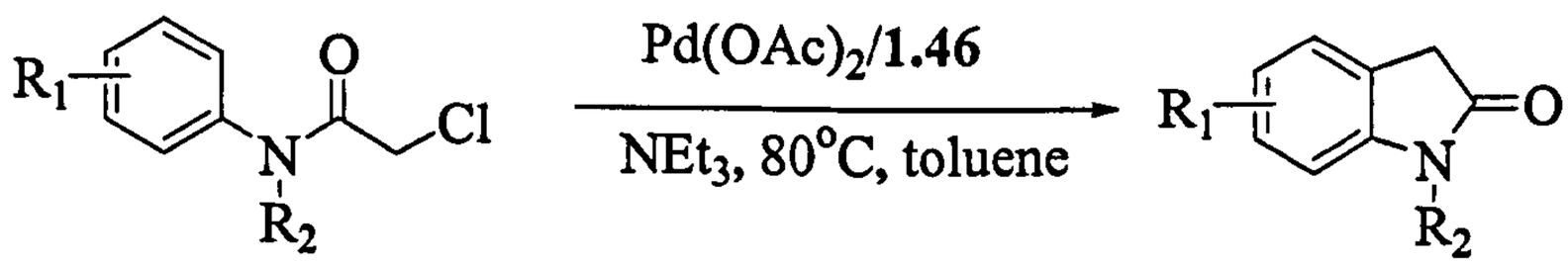

Equation 1.20

Recently ligand **1.47** has been shown to be very active in the palladium-catalyzed Suzuki-Miyaura coupling reaction of unactivated aryl tosylates (Equation

1.21).[67] This catalytic system can be used for a wide range of substrates under mild conditions.

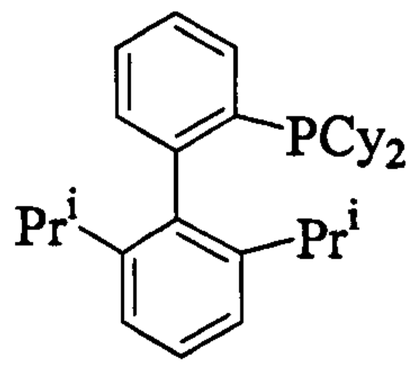

1.47

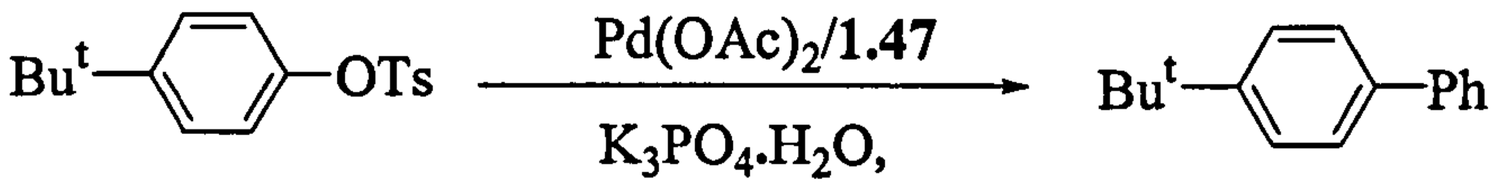

Equation 1.21

1.4.2.4 Grubbs metathesis catalysts

Olefin metathesis is a catalyticreaction in which alkenes are converted into new products via the rupture and reformation of carbon-carbon double bonds.[68] There are a variety of olefin metathesis reactions (Figure 1.9), including ring-opening metathesis polymerisation (ROMP), ring-closing metathesis (RCM), acyclic diene metathesis polymerization (ADMET), ring-opening metathesis (ROM), and cross-metathesis (CM or XMET) reactions.

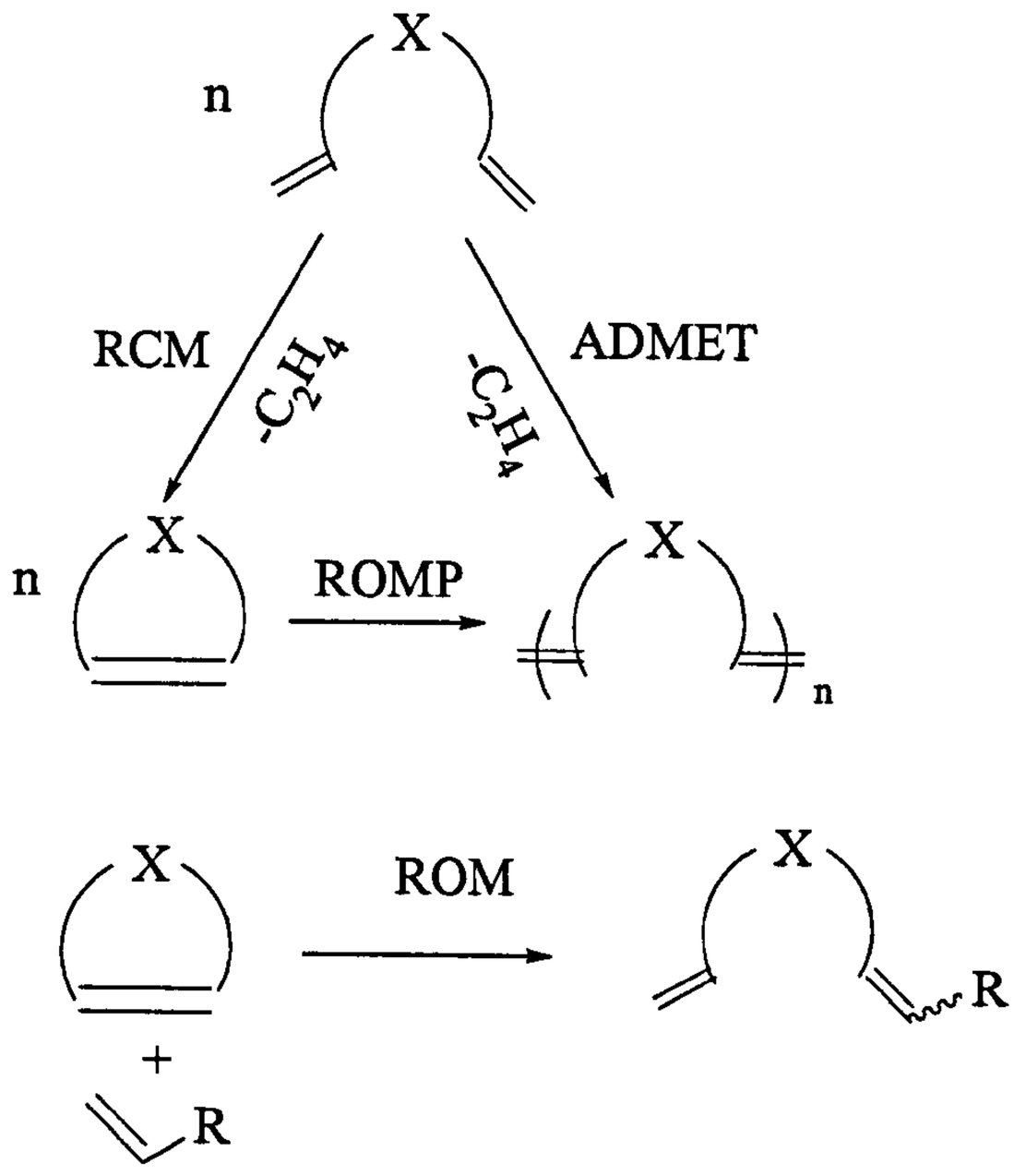

Figure 1.9

Grubbs carbene complexes (**1.49, 1.50**), first and second generation respectively, have demonstrated remarkable efficiency in the metathesis of olefins. In addition, a growing number of newly discovered processes mediated by these complexes have been recently reviewed.[69]

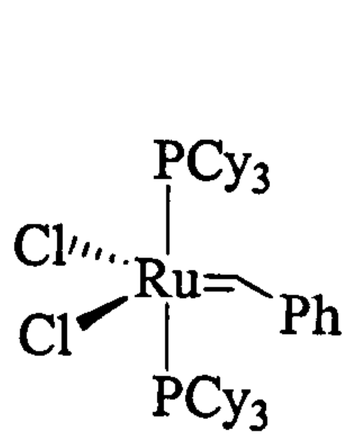

1.49

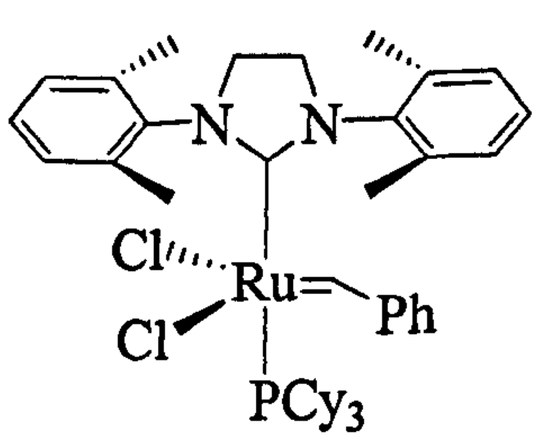

1.50

For example, the Grubbs catalyst (**1.50**) showed good activity and stability for the RCM reaction (Equation 1.22) and CM reaction (Equation 1.23).[70] The product of

Equation 1.23 is a medicinal natural product possessing antioxidant and anti-inflammatory properties.

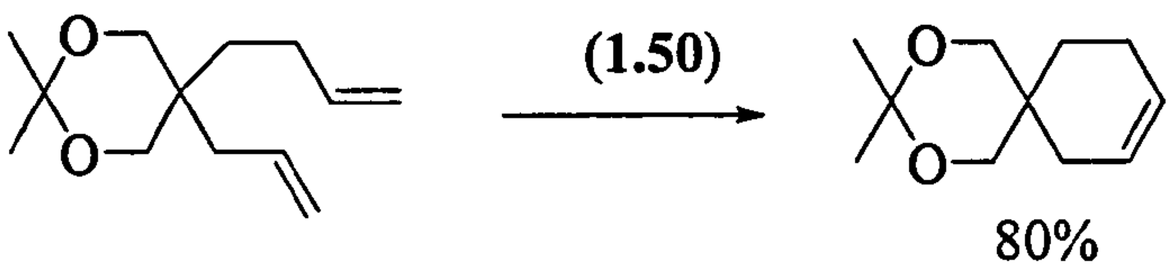

Equation 1.22

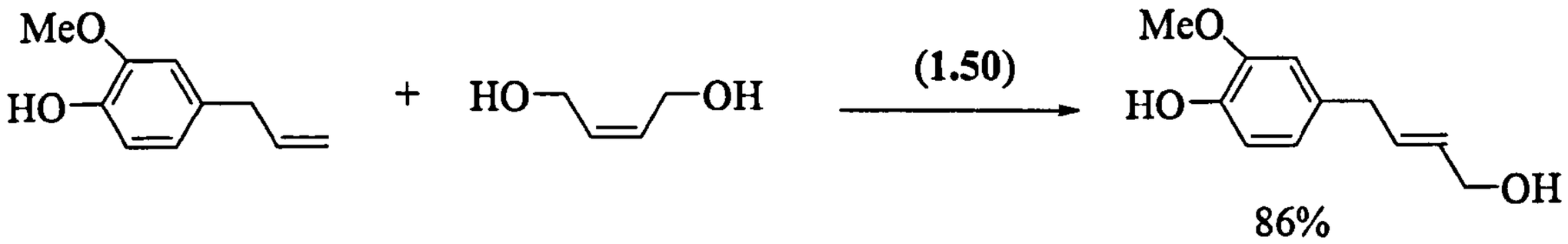

Equation 1.23

1.5 Aims

The aims of this project were to prepare new bulky cage-phosphine and cage-diphosphine ligands by hydrophosphination and to investigate their coordination chemistry and catalytic activity in hydroformylation. The objectives for the ligands were:

i) To separate the *meso/rac*-diastereoisomers by recrystallization or selective complexation.

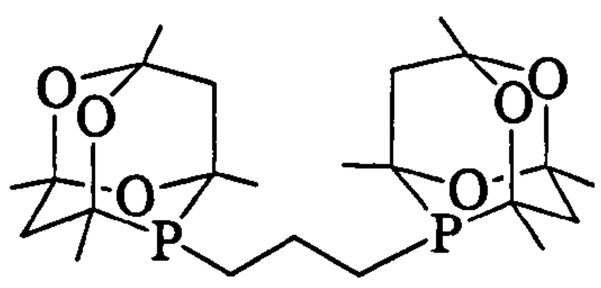

meso-

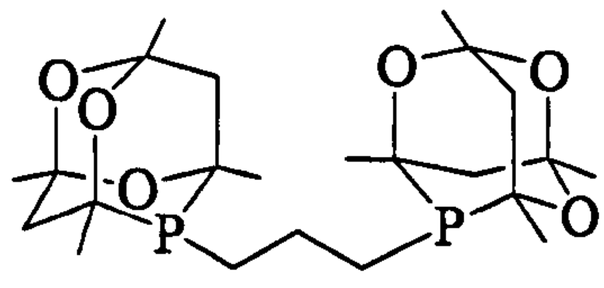

rac-

ii) The synthesis of the new bidentate tetramethyl-trioxa-phospha-adamantanes

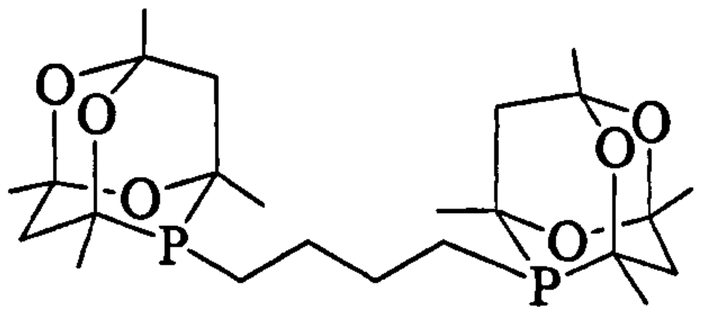

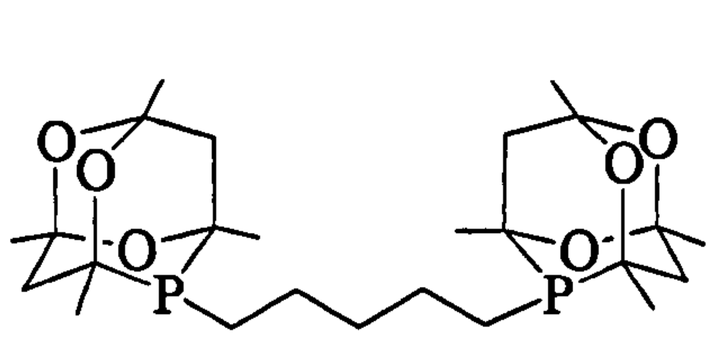

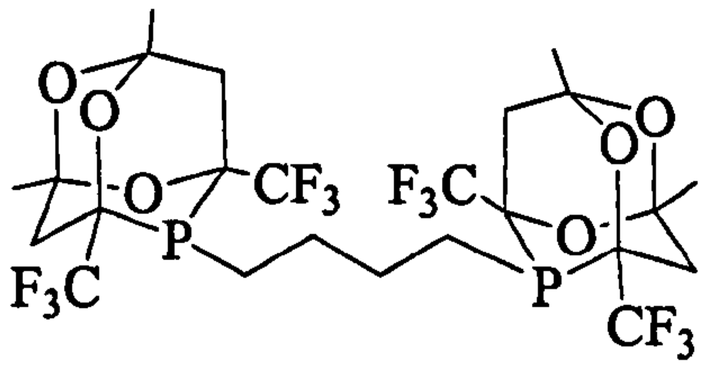

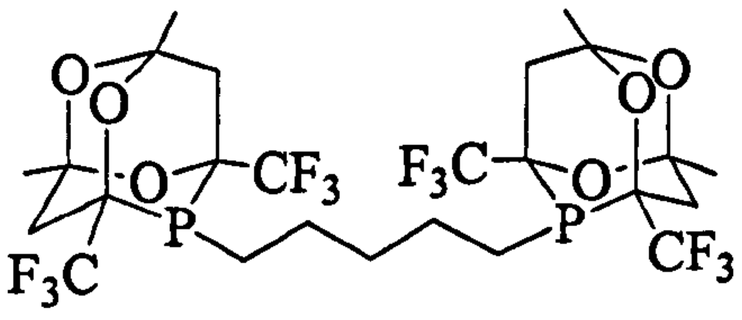

iii) The synthesis of the new bidentate tetraethyl-trioxa-phospha-adamantanes

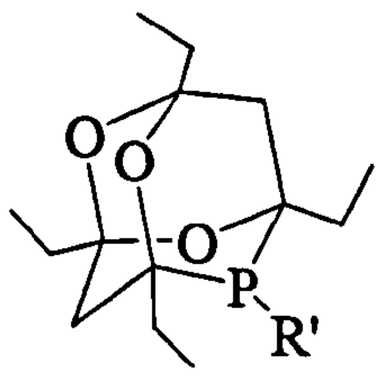

R' = H, Ph

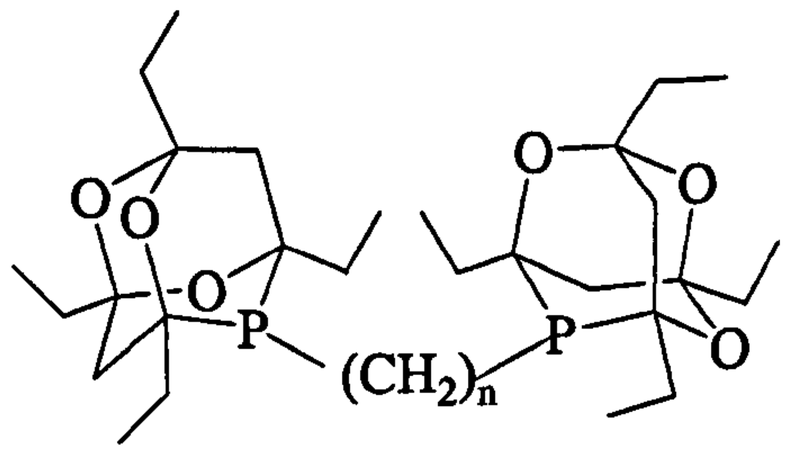

n = 3, 4, 5

Chapter 2

Bidentate tetramethyl-trioxa-phospha-adamantanes and their coordination chemistry

2.1 Introduction

The main features of bulky phosphines, their coordination chemistry and use in catalysis have been described in Chapter 1. In this chapter the chemistry of bulky phosphines based on tetramethyl-trioxa-phospha-adamantane cages is discussed.

In 1961, Epstein and Buckler[71] reported the first example of a 1,3,5,7-tetramethyl-4,6,8-trioxa-2-phospha-adamantane. They found that solutions of 2,4-pentanedione in aqueous hydrochloric acid readily absorbed PH_3 and a white crystalline solid was precipitated in 49% yield. This was characterized as the cage secondary phosphine *adamphos* **(2.1)** (Equation 2.1) on the basis of chemical and spectroscopic evidence.

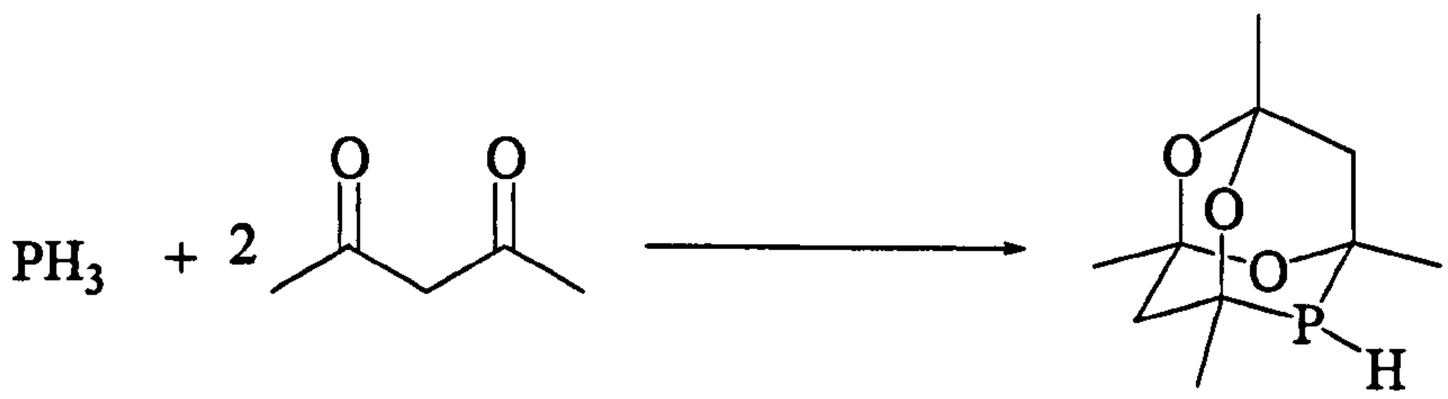

2.1

Equation 2.1

Using similar conditions to those in Equation 2.1 and using primary phosphines they synthesised compounds **(2.2)**, **(2.3)** and **(2.4)**.

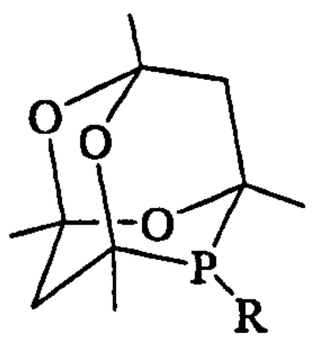

2.2 R = *n*-C_8H_{17}
2.3 R = *i*-C_4H_9
2.4 R = C_6H_5

In 1962, the use of **(2.2)**, **(2.3)** and **(2.4)** as gasoline additives was patented. In the same year the synthesis of **(2.5)** and **(2.6)** was reported.[72]

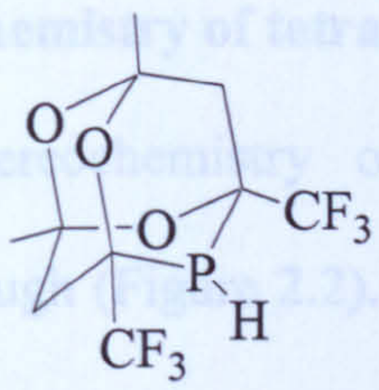

2.5

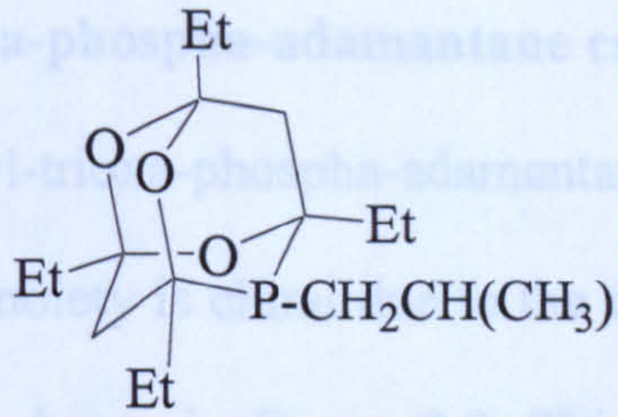

2.6

Compound (**2.1**) is atypical of a secondary phosphine in that it is air-stable. An explanation of this stability can be offered from an examination of the crystal structure.[73]

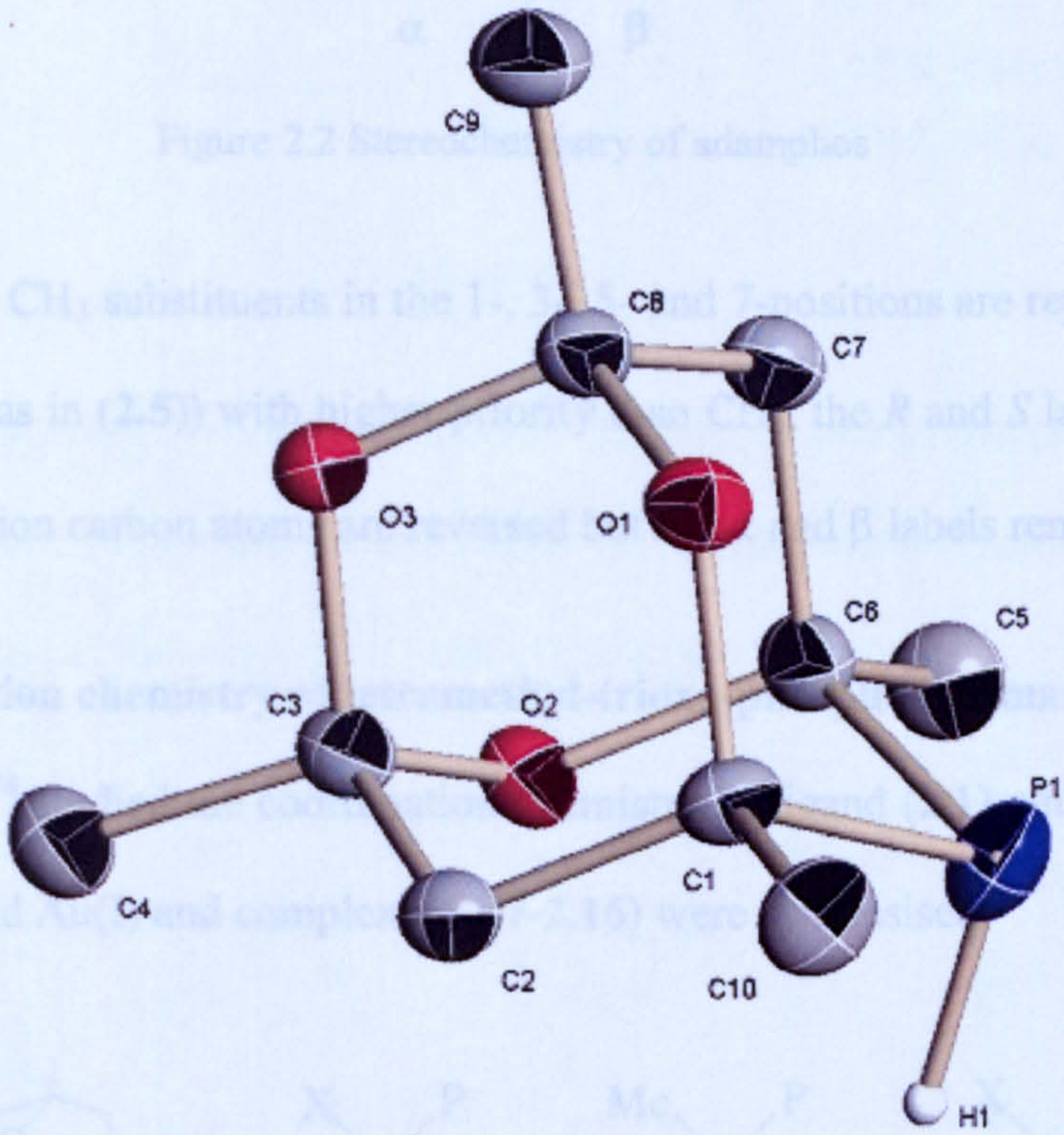

Figure 2.1 Molecular structure of **2.1**

Pugh[73] reported the crystal structure of (**2.1**). It can be observed in Figure 2.1 that the P-H bond is positioned pseudo-axially, which means the pseudo-equatorial lone pair on the phosphorus is sterically protected by the methyl groups (C_5 and C_{10}).

2.2 Stereochemistry of tetramethyl-trioxa-phospha-adamantane cages

The stereochemistry of tetramethyl-trioxa-phospha-adamantane cages was described by Pugh (Figure 2.2).[73] The cage moiety is chiral due to the four stereogenic centres at the 1-, 3-, 5- and 7- positions as shown in Figure 2.2. This results in two enantiomers for all phospha-adamantane cages. The enantiomers are labelled α and β.

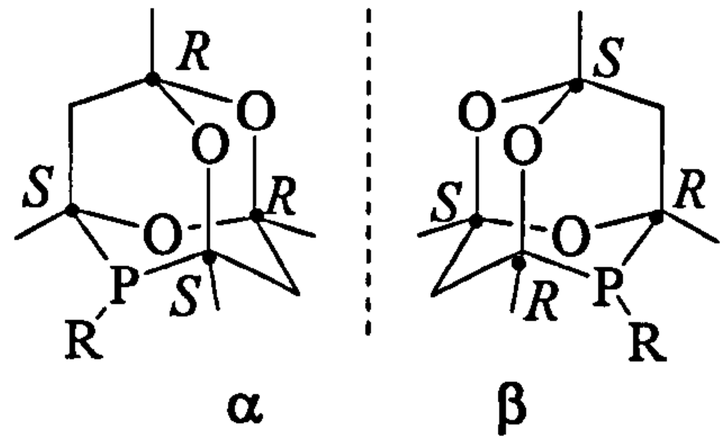

Figure 2.2 Stereochemistry of adamphos

When the CH_3 substituents in the 1-, 3-, 5- and 7-positions are replaced by other groups (e.g. CF_3 as in (**2.5**)) with higher priority than CH_3, the *R* and *S* labels for the 1-, 3-, 5- and 7-position carbon atoms are reversed but the α and β labels remain.

2.3 Coordination chemistry of tetramethyl-trioxa-phospha-adamantanes

Downing[74] studied the coordination chemistry of ligand (**2.1**) with Pt(II), Pd(II), Rh(I) and Ir(I) and complexes (**2.7-2.16**) were synthesised.

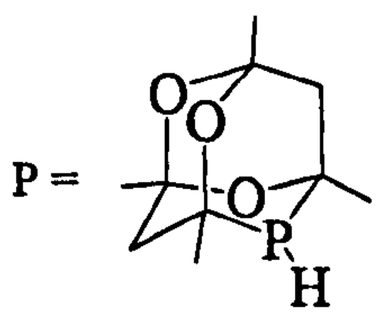

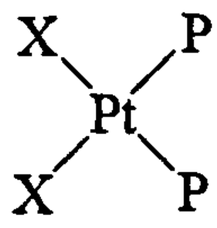

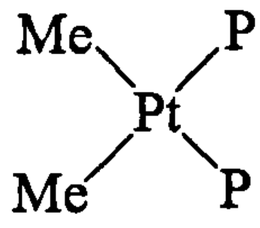

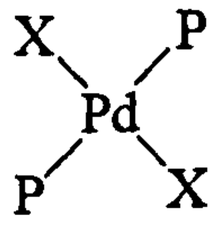

2.7 X = Cl
2.8 X = Br
2.9 X = I

2.10

2.11 X = Cl
2.12 X = Br
2.13 X = I

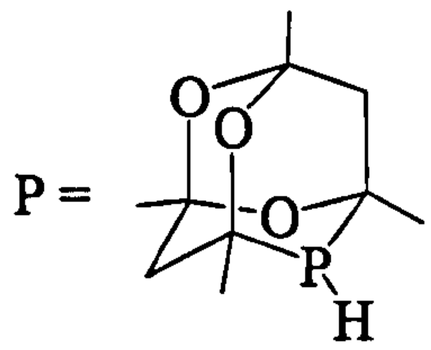

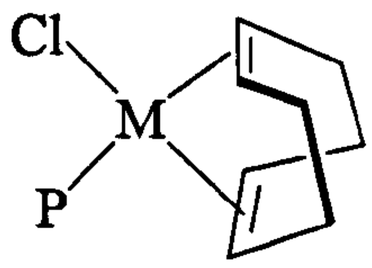

2.14 M = Rh
2.15 M = Ir

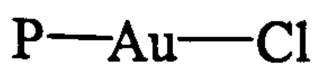

2.16

Pugh[73] has also reported the synthesis of monodentate cage ligands (Equation 2.2) (**2.17-2.19**).[73]

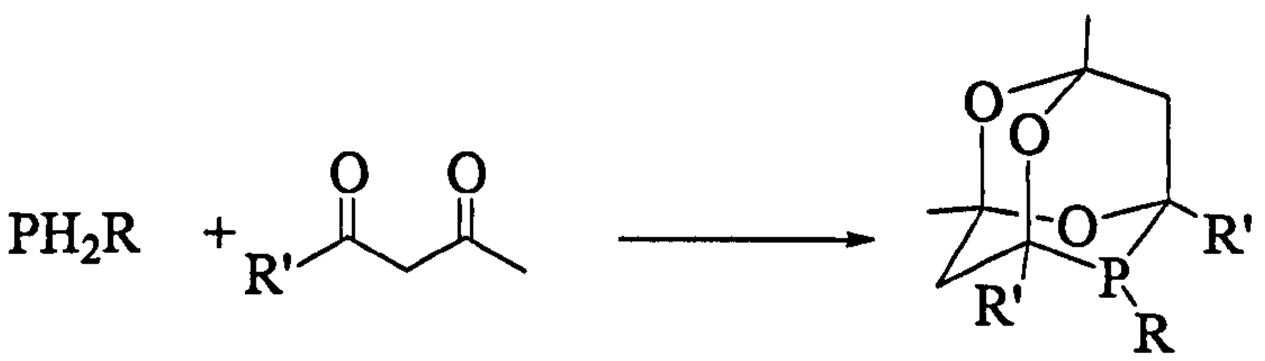

2.17 R = Ph R' = CF_3
2.18 R = *i*-propyl R' = CH_3
2.19 R = Cy, R' = CH_3

Equation 2.2

The coordination chemistry of ligands (**2.17-2.19**) was investigated with Pt(II), Pd(II), and Rh(I) complexes and the complexes (**2.20-2.26**) showed *trans*-configuration, as expected because of the large steric bulk of the cage moiety.

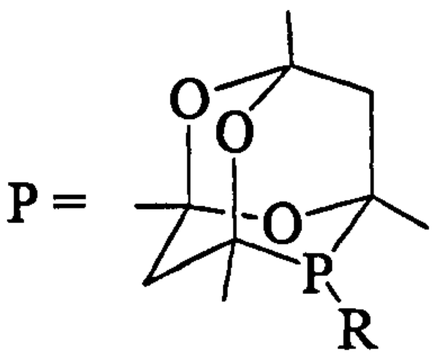

2.17-2.19

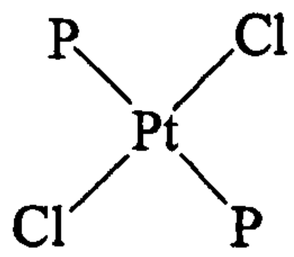

2.20 R = *i*-propyl
2.21 R = Cy

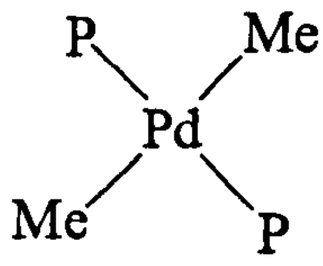

2.22 R = Ph
2.23 R = *i*-propyl
2.24 R = Cy

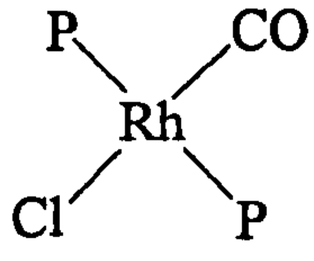

2.25 R = Ph
2.26 R = *i*-propyl

Gee[75] reported the first bidentate tetramethyl-trioxa-phospha-adamantanes (**2.27-2.30**) in 1997. The reaction of the diprimary phosphines $H_2P(CH_2)_nPH_2$ (n = 2 or 3) in aqueous HCl gave the diastereomeric mixtures *meso/rac*-(**2.27-2.30**) in *ca.* 60% yield.

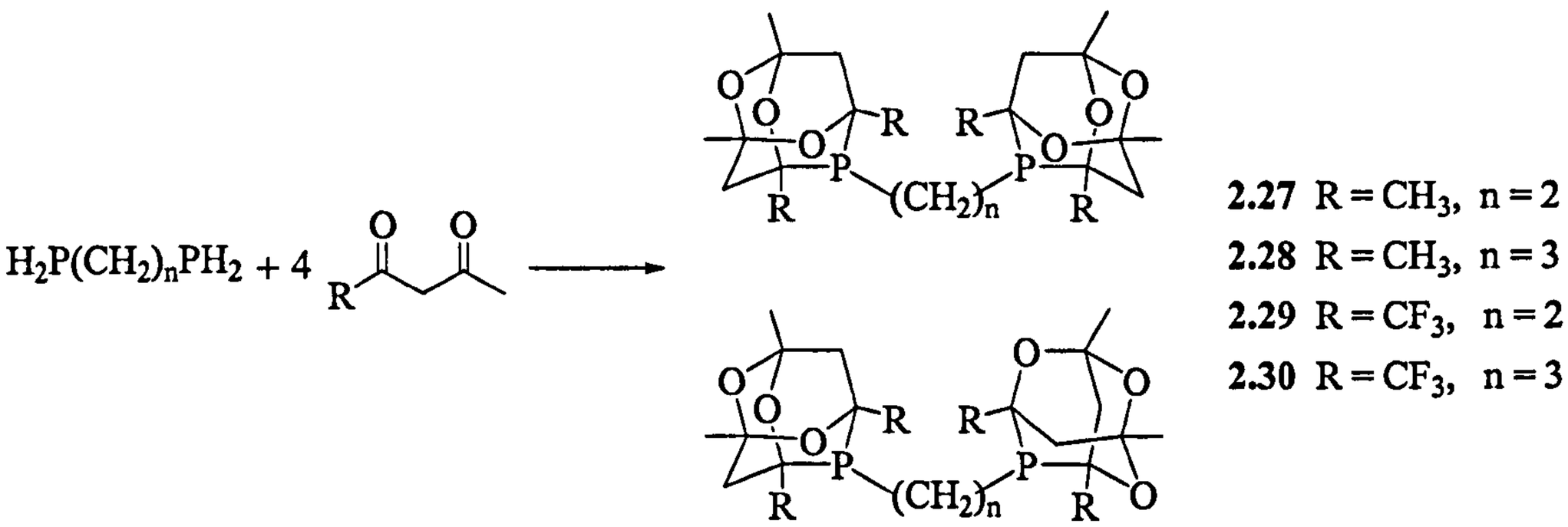

2.27 R = CH_3, n = 2
2.28 R = CH_3, n = 3
2.29 R = CF_3, n = 2
2.30 R = CF_3, n = 3

Equation 2.3

The coordination chemistry of these ligands with Pd(II), Pt(II) and Rh(I) has also been reported,[53] and the chelates (**2.31-2.45**) have been fully characterised.

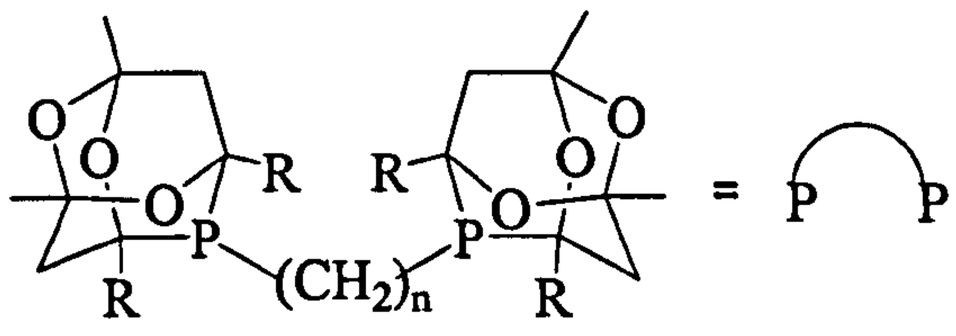

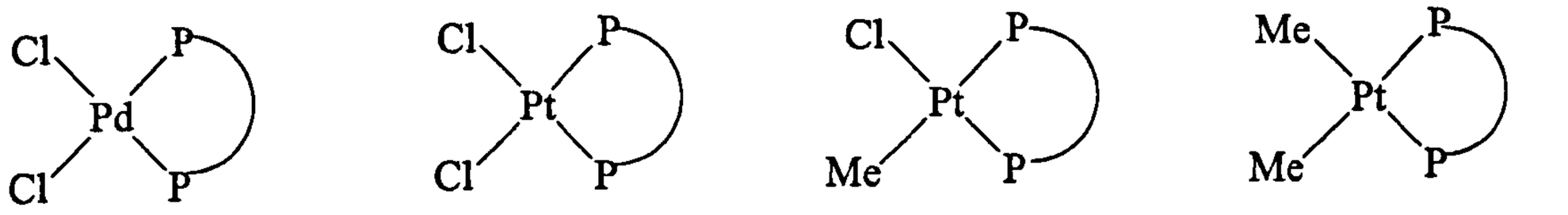

2.31 R = CH_3, n = 2
2.32 R = CH_3, n = 3
2.33 R = CF_3, n = 3

2.34 R = CH_3, n = 2
2.35 R = CH_3, n = 3

2.36 R = CH_3, n = 3

2.37 R = CH_3, n = 2
2.38 R = CH_3, n = 3

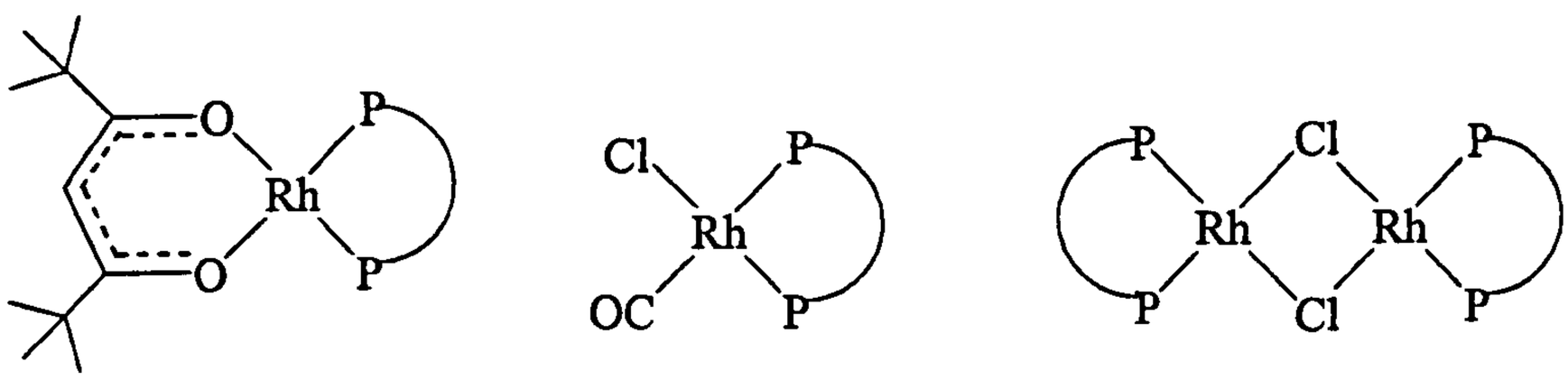

2.39 R = CH_3, n = 2
2.40 R = CH_3, n = 3
2.41 R = CF_3, n = 2

2.42 R = CH_3, n = 2
2.43 R = CF_3, n = 2
2.44 R = CF_3, n = 3

2.45 R = CH_3, n = 2

The diphosphine (**2.28**) affords highly active palladium catalysts for the methoxycarbonylation of ethene to form methyl propanoate, which has been described in Section 1.4.2.1.[76,77]

Ligands (**2.46**) and (**2.47**) were synthesised by Pugh.[73]

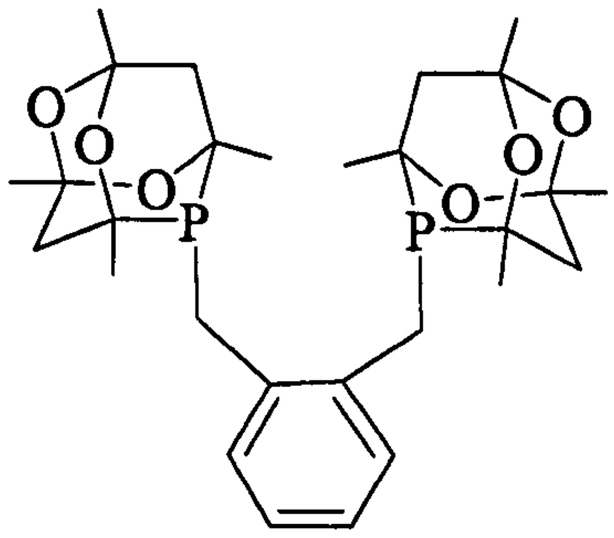

2.46

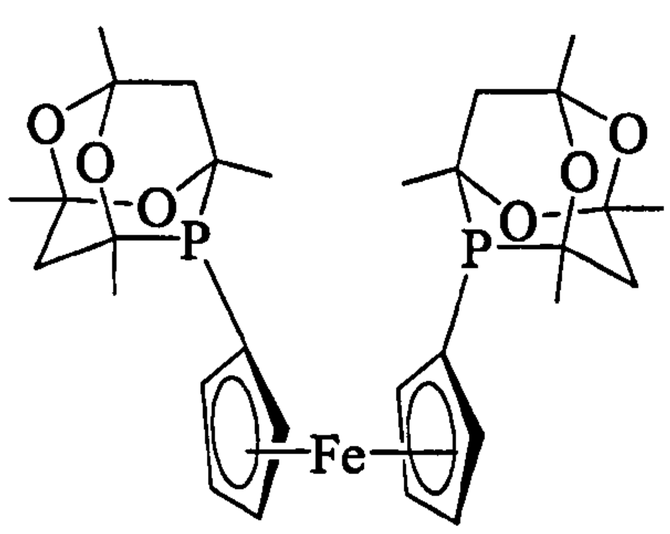

2.47

Platinum(II) and palladium(II), chelates are formed with the bidentate ligand (**2.46**) and (**2.47**) as shown below (**2.48, 2.49** and **2.50**). Oligomeric species were also observed in by $^{31}P\{^{1}H\}$ NMR spectroscopy with (**2.50**).[73]

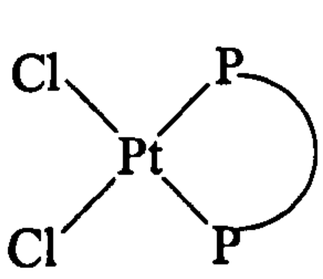

2.48 = **2.46**

2.49 = **2.47**

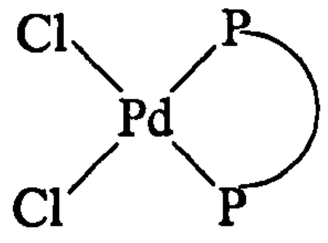

2.50 = **2.46**

Recently the catalytic activity of palladium complexes of ligands (**2.51-2.53**) in the Suzuki cross-coupling reactions (Equation 2.4) of aryl halides has been reported.[78] Palladium complexes derived from ligands (**2.51-2.53**) were shown to be very active catalysts for the Suzuki reaction in comparison to other phosphines used in this process. PBu^{t}_{3}, one of the best ligands for the catalysis in terms of its activity in the Suzuki reaction requires special conditions to avoid oxidation. In comparison, the cage ligands (**2.51-2.53**) are crystalline, air-stable and easier to handle.

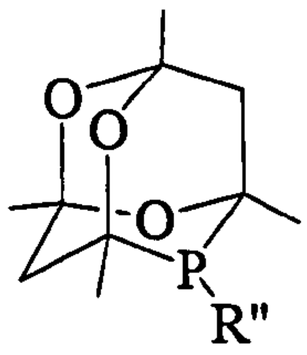

2.51 R" = Ph
2.52 R" = 2-tolyl
2.53 R" = $C_{14}H_{29}$

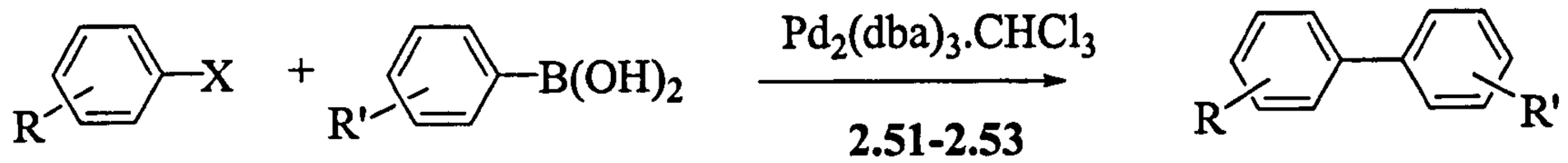

Equation 2.4

2.4 Separation of the diastereoisomers *meso*- and *rac*-1,3-bis(^{Me}adamphosphino)-propane

2.4.1 Recrystallization of *meso/rac*-(2.54)

Pugh[73] reported that when the 1:1 mixture of *meso*- and *rac*-(**2.54**) (Figure 2.3) was repeatedly recrystallized from CH_2Cl_2/methanol, a solid of 97% pure *rac*-isomer was obtained in low yield. We wished to improve the separation of the *rac*-isomer in order to attempt a resolution into optical isomers. The *meso*-isomer was also required in high purity for catalysis studies.

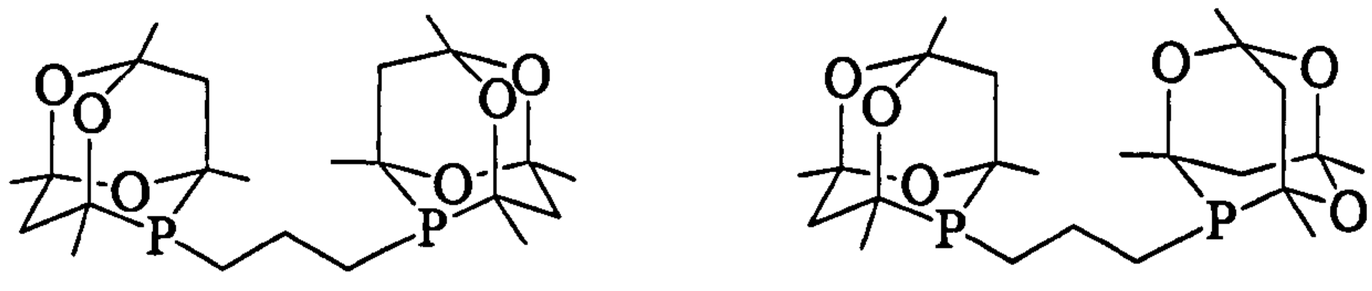

meso-**2.54** *rac*-**2.54**

Figure 2.3 *meso*- and *rac*-1,3-bis(^{Me}adamphosphino)propane diastereoisomers

2.4.1.1 Recrystallization from a mixture of CH_2Cl_2 and methanol

Repeating Pugh's procedure,[73] the recrystallization of 1:1 *meso/rac*-(**2.54**) from CH_2Cl_2/methanol (1:5), gave a good separation of the diastereoisomers, where the *rac*-(**2.54**) crystallised and the *meso*-isomer remained in the mother liquor. The $^{31}P\{^1H\}$ NMR spectrum after two recrystallizations showed *meso/rac*-(**2.54**) in a ratio of ca. 5:95.

Due to the low overall recovery of this method we aspired to improve it and attempted recrystallisation from other solvents.

Attempts to recrystallize from acetonitrile, THF and diethyl ether were unsuccessful due to low solubility but ethanol and methanol were found to be effective as described below.

2.4.1.2 Recrystallization from ethanol

The recrystallization of *meso/rac*-**(2.54)** from ethanol gave a moderate separation of the diastereoisomers. After one recrystallization of the crude solid, the $^{31}P\{^{1}H\}$ NMR spectrum showed *meso/rac*-**(2.54)** in a ratio of *ca.* 10:90.

2.4.1.3 Recrystallization from methanol

The recrystallization of 1:1 *meso/rac*-**(2.54)** from methanol gave a good separation of the diastereoisomers. After one recrystallization of the crude solid, the $^{31}P\{^{1}H\}$ NMR spectrum showed *meso/rac*-**(2.54)** in a ratio of *ca.* 6:94 and with 80% recovery. Thus this was the method of choice for the separation.

2.4.2 Selective complexation of *meso/rac*-(2.54)

The selective complexation of *meso*- and *rac*-**(2.54)** from a 1:1 diastereomeric mixture was first observed by Gee.[75] In her work, 2.0 equivalents of 1:1 *meso/rac*-**(2.54)** were added to 1.0 equivalent of [Pt(norbornene)$_3$]. The *meso*-diastereoisomer preferentially complexed to Pt(0) over the *rac*-diastereoisomer in a ratio of 12:1 (Figure 2.4). Gee[75] explained, if one considers that for *rac*-**(2.54)** each cage has the same absolute configuration for the two cages (labelled α and β as described above), the molecule has C_1 symmetry and therefore the phosphorus atoms are non-equivalent **(2.55)** resulting in an AB pattern in the $^{31}P\{^{1}H\}$ NMR spectrum (Figure 2.4). The two singlets were assigned to the two complexes **(2.56)** and **(2.57)**. These arise because *meso*-**(2.54)** gives two C_s-symmetric diastereoisomers as a result of each cage having the opposite absolute configuration (α and β). This reaction therefore offers a possible opportunity to separate the diastereoisomers, but it is very expensive. We decided to explore further the selective complexation of the *meso*- and *rac*-diastereoisomers **(2.54)**.

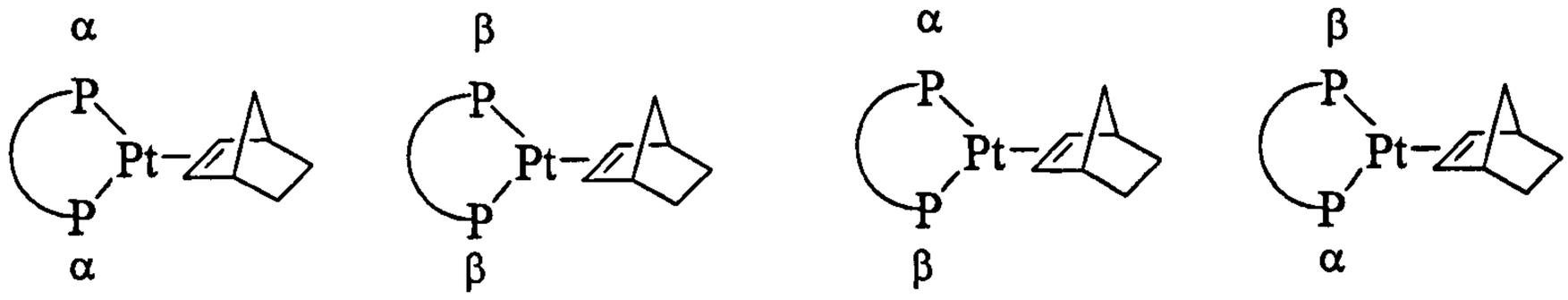
α
β
P
Pt
P
α
β
α
β
α
β
2.55
2.56
2.57

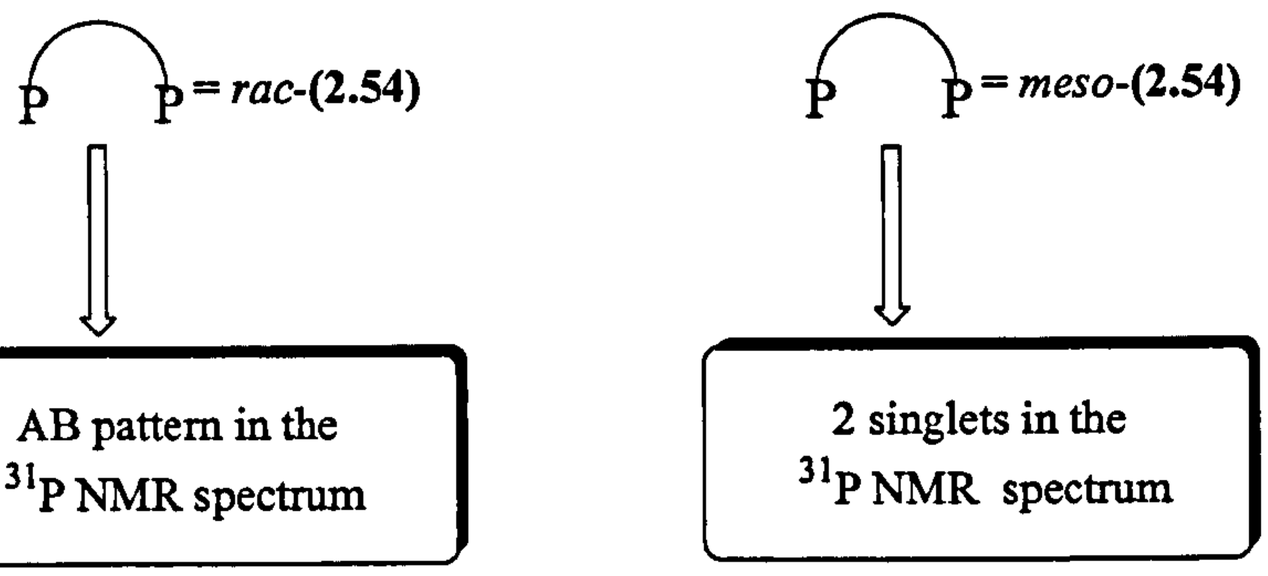
P P = *rac*-(2.54)
AB pattern in the ^{31}P NMR spectrum
P P = *meso*-(2.54)
2 singlets in the ^{31}P NMR spectrum

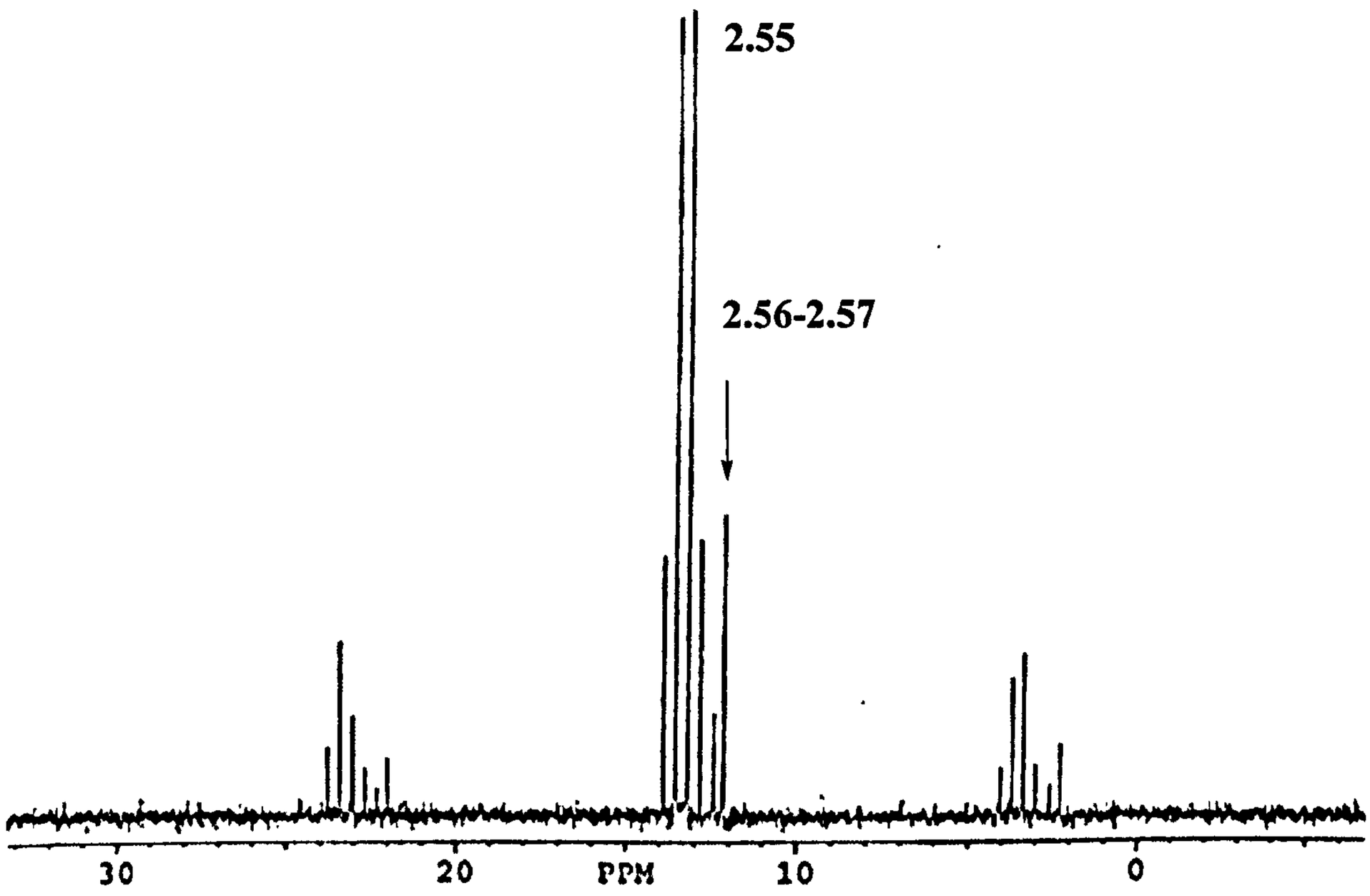
2.55
2.56-2.57
30
20
PPM
10
0

Figure 2.4

2.4.2.1 Complexation with nickel(II)

The reaction of 2.0 equivalents of *meso/rac*-(**2.54**) with 1.0 equivalent of $NiCl_2.6H_2O$ in ethanol gave a purple precipitate. The solid was isolated and then treated with aqueous KCN and diethyl ether for decomplexation of the ligand. The $^{31}P\{^1H\}$ NMR spectrum of the ethereal layer showed that both *meso*- and *rac*-diastereoisomers are complexed by the nickel centre in a proportion of *ca.* 1:1 and so no selective complexation was observed.

Single crystals of the purple complex (**2.58**) were grown from acetone, the crystal structure determination (Figure 2.5) was carried out by Dr. Katie Heslop. The crystal structure was of the *meso*-isomer and was solved in the orthorhombic space group Cmc2(1) with four formula units per unit cell. The method of data collection, structure solution and refinement are summarised in the Appendix. Selected bond lengths and angles for the nickel(II) complex (**2.58**) are shown in (Table 2.1). The complex has tetrahedral geometry at the metal centre that can be rationalised by the large steric bulk of (**2.54**).

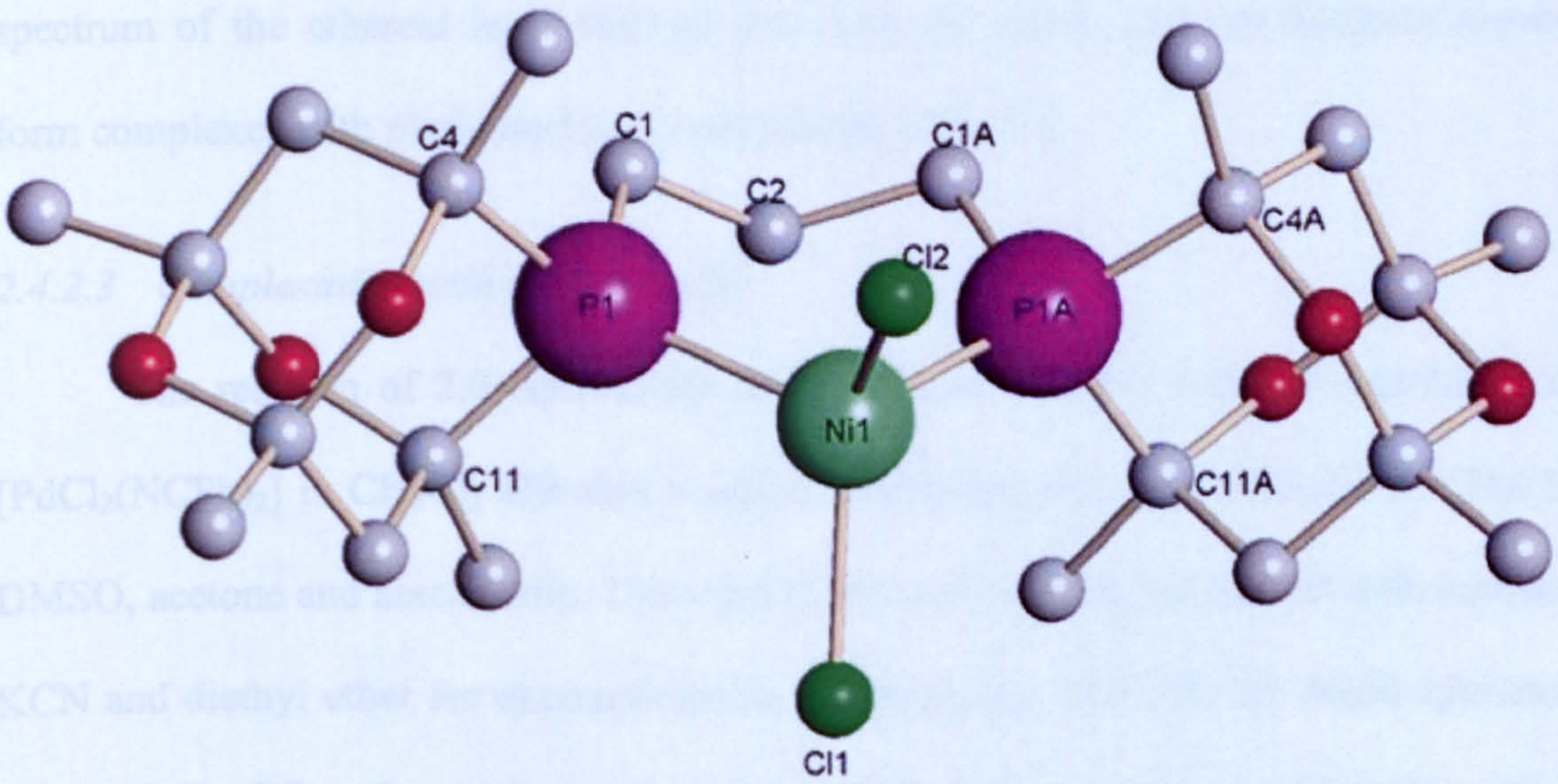

Figure 2.5 Molecular structure of the nickel(II) complex(**2.58**). Selected atoms are labelled

Table 2.1 Selected bond lengths and angles for the nickel(II) complex **(2.58)**

Bond	Lengths [Å]	Bond	Angles [°]
Ni(1)-Cl(2)	2.187(3)	Cl(2)-Ni(1)-Cl(1)	122.48(9)
Ni(1)-Cl(1)	2.232(3)	Cl(2)-Ni(1)-P(1)	108.26(7)
Ni(1)-P(1)	2.3260(18)	Cl(1)-Ni(1)-P(1)	107.80(7)
Ni(1)-P(1A)	2.3260(18)	C(1)-P(1)-Ni(1)	114.52(18)
P(1)-C(1)	1.818(5)	C(11)- P(1)-Ni(1)	116.64(19)
P(1)-C(4)	1.876(5)	P(1)-Ni(1)-P(1A)	99.91(9)
C(1)-C(2)	1.543(7)	C(1)-P(1)-C(4)	106.2(2)
C(2)-C(1A)	1.543(7)	C(4)-P(1)-C(11)	94.3[(2)]

2.4.2.2 Complexation with platinum(II)

The reaction of 2.0 equivalents of *meso/rac*-(**2.54**) with 1.0 equivalent of $[PtCl_2(cod)]$ in CH_2Cl_2 afforded a pale yellow precipitate that was insoluble in CH_2Cl_2, DMSO, acetone and acetonitrile. The solid (**2.59**) was isolated and then treated with aqueous KCN and diethyl ether for decomplexation of the ligand. The $^{31}P\{^1H\}$ NMR spectrum of the ethereal layer showed that both the *meso*- and *rac*-diastereoisomers form complexes with platinum(II) in a proportion of *ca.* 3:1.

2.4.2.3 Complexation with palladium(II)

The reaction of 2.0 equivalents of 1:1 *meso/rac*-(**2.54**) with 1.0 equivalent of $[PdCl_2(NCPh)_2]$ in CH_2Cl_2 afforded a yellow precipitate that was insoluble in CH_2Cl_2, DMSO, acetone and acetonitrile. The solid (**2.60**) was isolated and treated with aqueous KCN and diethyl ether for decomplexation of the ligand. The $^{31}P\{^1H\}$ NMR spectrum (Figure 2.6) of the ethereal layer showed that both the *meso*- and *rac*-diastereoisomers form complexes with palladium(II) in a proportion of *ca.* 5:1. Therefore this was the

most successful of the selective complexations attempted but still inferior to the original Pt(0) method.[75]

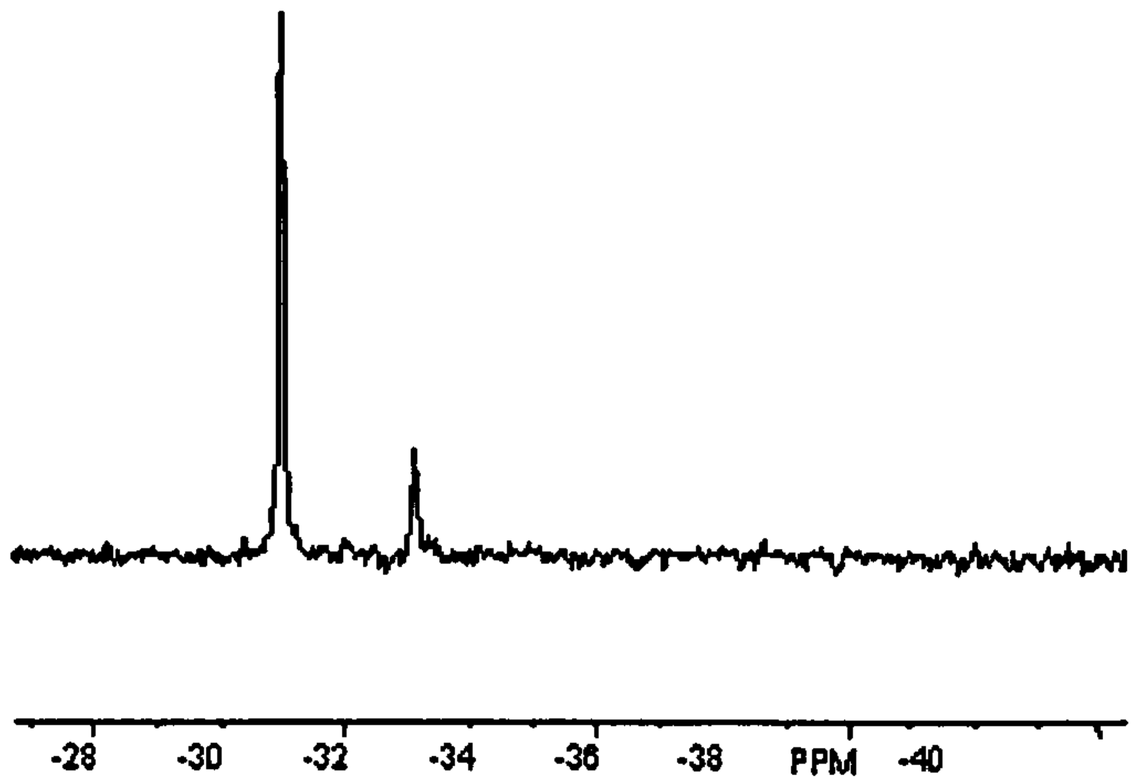

Figure 2.6 $^{31}P\{^{1}H\}$ NMR spectrum after the decomplexation of the palladium complex (**2.60**)

2.4.3 Attempted resolution of *rac*-1,3-bis(^Meadamphosphino)-propane (2.54)

Wild[79-81] has investigated a series of homochiral forms of chloro-bridged palladium(II) complexes containing cyclometallated *N,N*-dimethyl(α-methylbenzyl)amines and related naphthylamines for the resolution of chiral bidentate trivalent phosphines, an example of which is shown in Scheme 2.1.

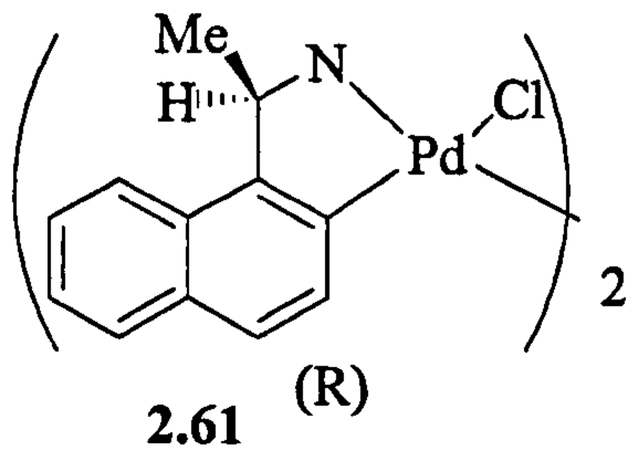

2.61 (R)

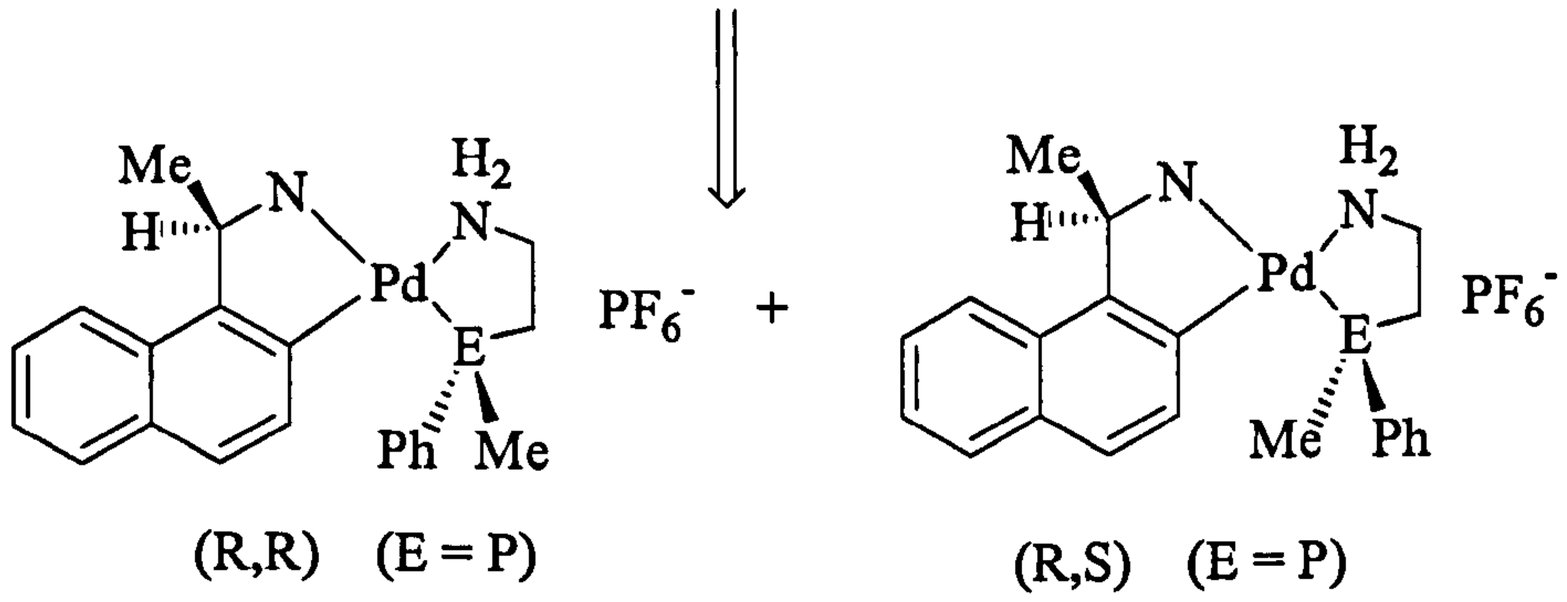

(R,R) (E = P) (R,S) (E = P)

Scheme 2.1

Repeated attempts to separate the *rac*-enantiomers (**2.54**) with (**2.61**), following the literature procedure[81] were unsuccessful. Addition of 2.0 equivalents of *rac*-(**2.54**) to 1.0 equivalent of binuclear (**2.61**) in methanol gave a solution which was then treated with NH_4PF_6 to form the salt. The $^{31}P\{^1H\}$ NMR spectrum of the resultant solution showed many peaks and no solid crystallised so the separation had not been unsuccessful.

2.4.4 Conclusion

The *rac*-(**2.54**) can be separated from *meso*-(**2.54**) by recrystallization, with the best result (94:6 and 80% recovery) when methanol is used.

The selective complexation of *meso*-(**2.54**) with Pd(II) (5:1), Pt(II) (3:1) and Ni(II) (1:1) gave modest results compared with the ratio found by Gee[75] in the complexation with Pt(0) (12:1) which is the best result obtained to date.

2.5 Synthesis and coordination chemistry of bidentate tetramethyl-trioxa-phospha-adamantanes

2.5.1 Synthesis of *meso/rac*-1,4-bis(^{Me}adamphosphino)butane (2.64)

The preparation of 1:1 *meso/rac*-1,4-bis(^{Me}adamphosphino)butane is a multi-step process. The first step is the reaction of dibromobutane and triethylphosphite[82] to produce the phosphonate (**2.62**) *via* a Michaelis–Arbuzov reaction. The second step is the reduction of the phosphonate (**2.62**) to afford the diprimary phosphine[83] (**2.63**) (Scheme 2.2).

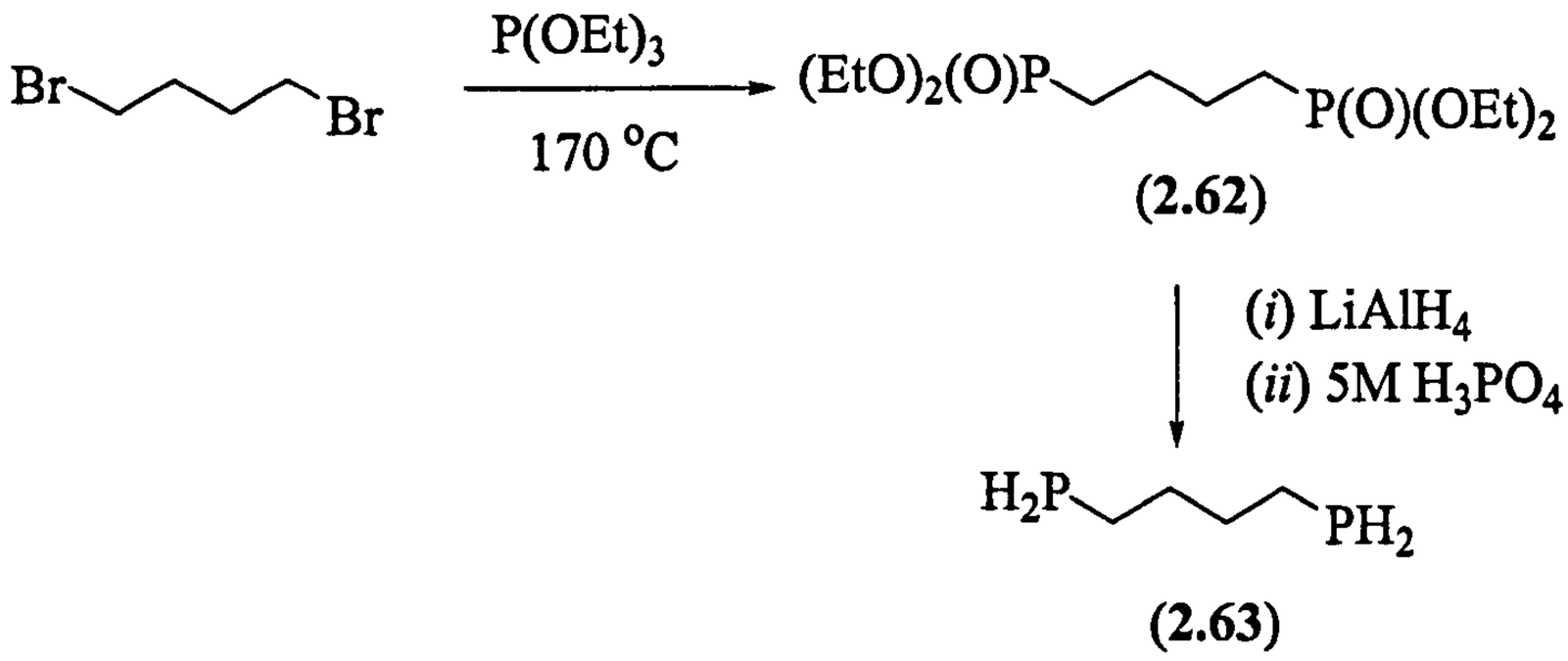

Scheme 2.2 Preparation of the diprimary phosphine

The reaction between **(2.63)** and 2,4-pentanedione in 5M HCl afforded 1:1 *meso/rac*-1,4-bis(^{Me}adamphosphino)butane **(2.64)** in 60% yield as a white solid (Scheme 2.3). The $^{31}P\{^{1}H\}$ NMR spectrum of **(2.64)** showed two singlets at –28.5 and –29.6 ppm in a ratio *ca.* 1:1 corresponding to the *meso*- and *rac*-diastereoisomers. The white solid product was further characterized by $^{31}P\{^{1}H\}$ NMR, $^{13}C\{^{1}H\}$ NMR and ^{1}H NMR spectroscopy, mass spectrometry and elemental analysis (see Experimental). The product is air-stable and soluble in CH_2Cl_2, methanol, ethanol and diethyl ether.

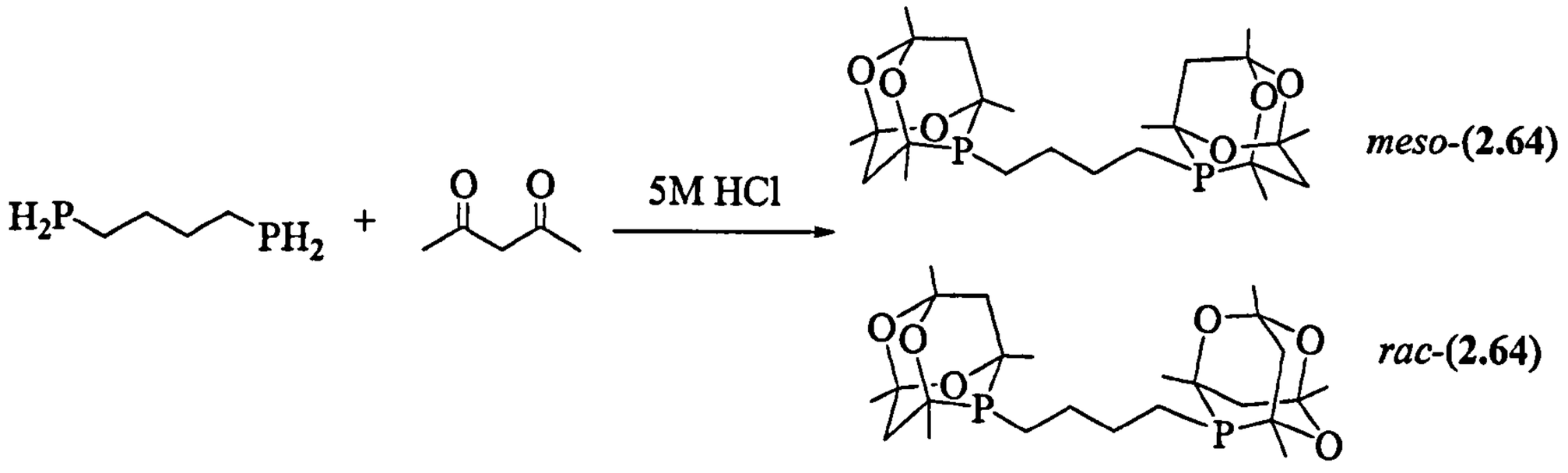

Scheme 2.3 Preparation of **(2.64)**

The preparation of *meso/rac*-**(2.64)** by the hydrophosphination of acetylacetone has the disadvantage of using a diprimary phosphine which is pyrophoric, air-sensitive, has an unpleasant odour and requires a lengthy synthesis. In view of this, the next

section describes an alternative synthesis of **(2.64)** that avoids using a diprimary phosphine.

2.5.2 Synthesis of (2.64) from the adamphosphine-borane adduct

The addition of n-butyllithium to the adamphos-borane adduct **(2.65)**[73] in THF followed by addition of dibromopropane afforded the *meso/rac*-1,4-bis(^Me^adamphosphino)butane borane adduct **(2.66)** (Scheme 2.4).

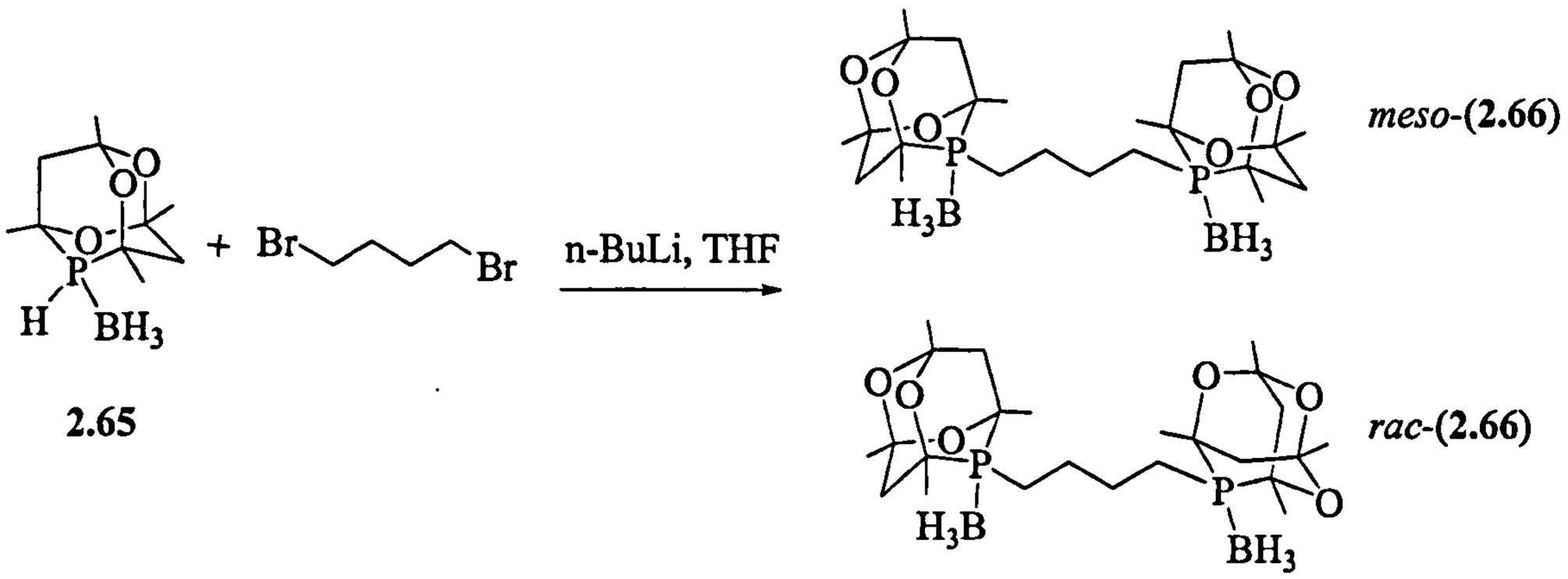

2.65

meso-**(2.66)**

rac-**(2.66)**

Scheme 2.4 Preparation of the borane adduct of **(2.66)**

Treatment of **(2.66)** with silica gave **(2.64)** in 50% yield as a white solid (Scheme 2.5).

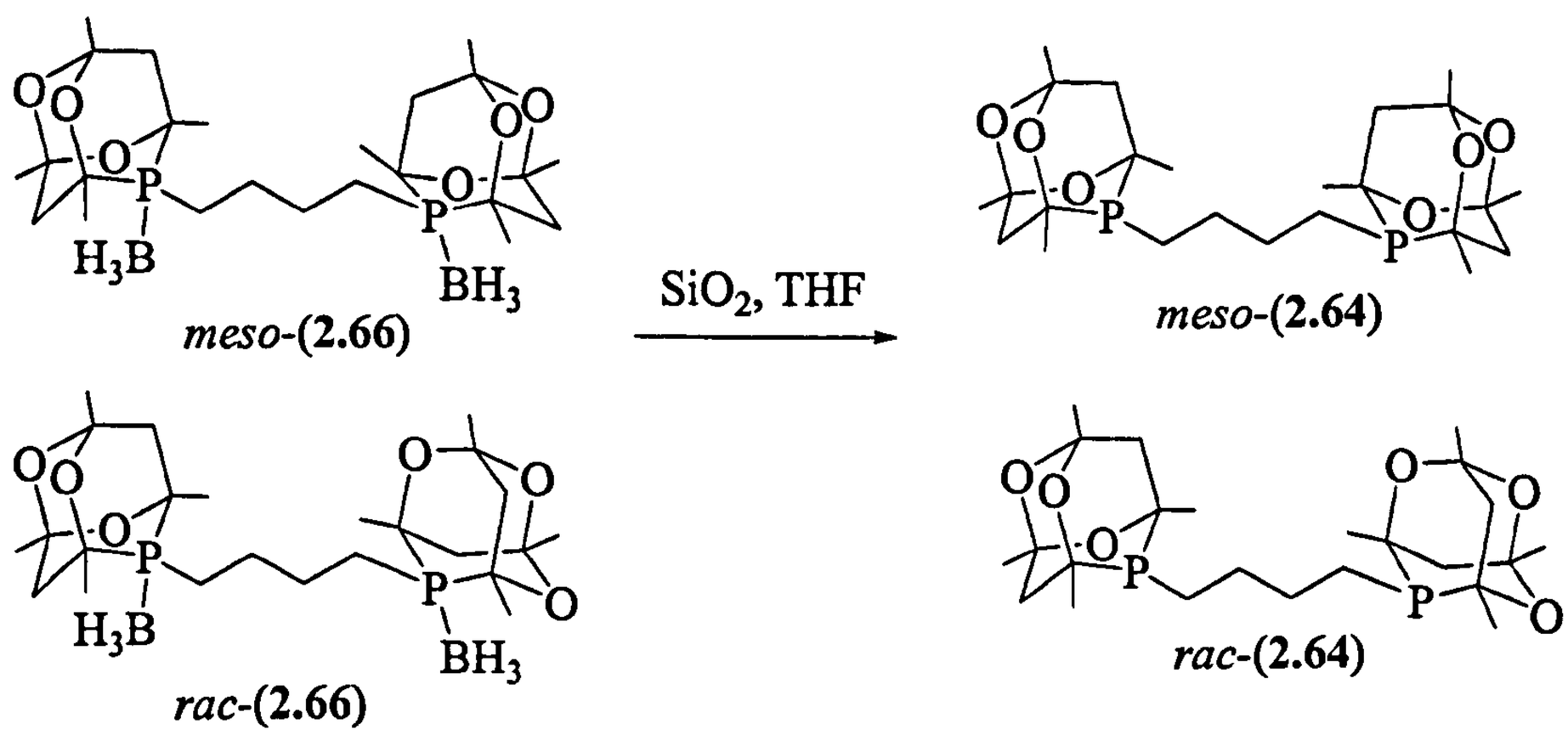

meso-**(2.66)**

meso-**(2.64)**

rac-**(2.66)**

rac-**(2.64)**

Scheme 2.5 Deprotection of the borane adduct **(2.66)**

The crude *meso/rac*-(**2.64**) was recrystallized from methanol and the $^{31}P\{^{1}H\}$ NMR spectrum showed two singlets at –28.5 and –29.6 ppm in a ratio of 2:1 corresponding to the two diastereoisomers in 62% recovery. The white product was fully characterized by $^{31}P\{^{1}H\}$, $^{13}C\{^{1}H\}$ and ^{1}H NMR spectroscopy, mass spectrometry and elemental analysis (see Experimental).

2.5.3 Dichloroplatinum(II) complex of (2.64)

The reaction of 1.0 equivalent of *meso/rac*-(**2.64**) with 1.0 equivalent of $[PtCl_2(cod)]$ in CH_2Cl_2 gave a pale yellow solution. The solvent was evaporated and a pale yellow solid was recovered in 97% yield. The solid was fully characterized as *meso/rac*-(**2.67**) by $^{31}P\{^{1}H\}$ NMR, mass spectroscopy, elemental analysis and X-ray crystallography (Figure 2.7).

The $^{31}P\{^{1}H\}$ NMR spectrum showed a singlet at δ –4.9 ppm with platinum satellites (^{1}J(PtP) 3513 Hz). The presence of two diastereoisomers was confirmed by $^{13}C\{^{1}H\}$ NMR from the observation of two doublets for P-CH_2 in the P-CH_2-CH_2-CH_2-CH_2-P backbone. The presence of only one signal in the $^{31}P\{^{1}H\}$ NMR spectrum can be explained as an overlapping of the two diastereoisomers signals.

A crystal structure of *meso*-(**2.67**) was obtained confirming that a seven-membered chelate ring is present. The structure shows that one of the carbon atoms in the backbone is in the same plane as the $PtCl_2P_2$ plane, whereas the other three carbons in the backbone are perpendicular to them and forming an arch.

The crystal structure was of the *meso*-isomer and was solved in the monoclinic space group $P2_1/c$ with four formula units per unit cell. The method of data collection, structure solution and refinement are summarised in the Appendix. Selected bond lengths and angles for the platinum(II) complex (**2.67**) are shown in Table 2.2.

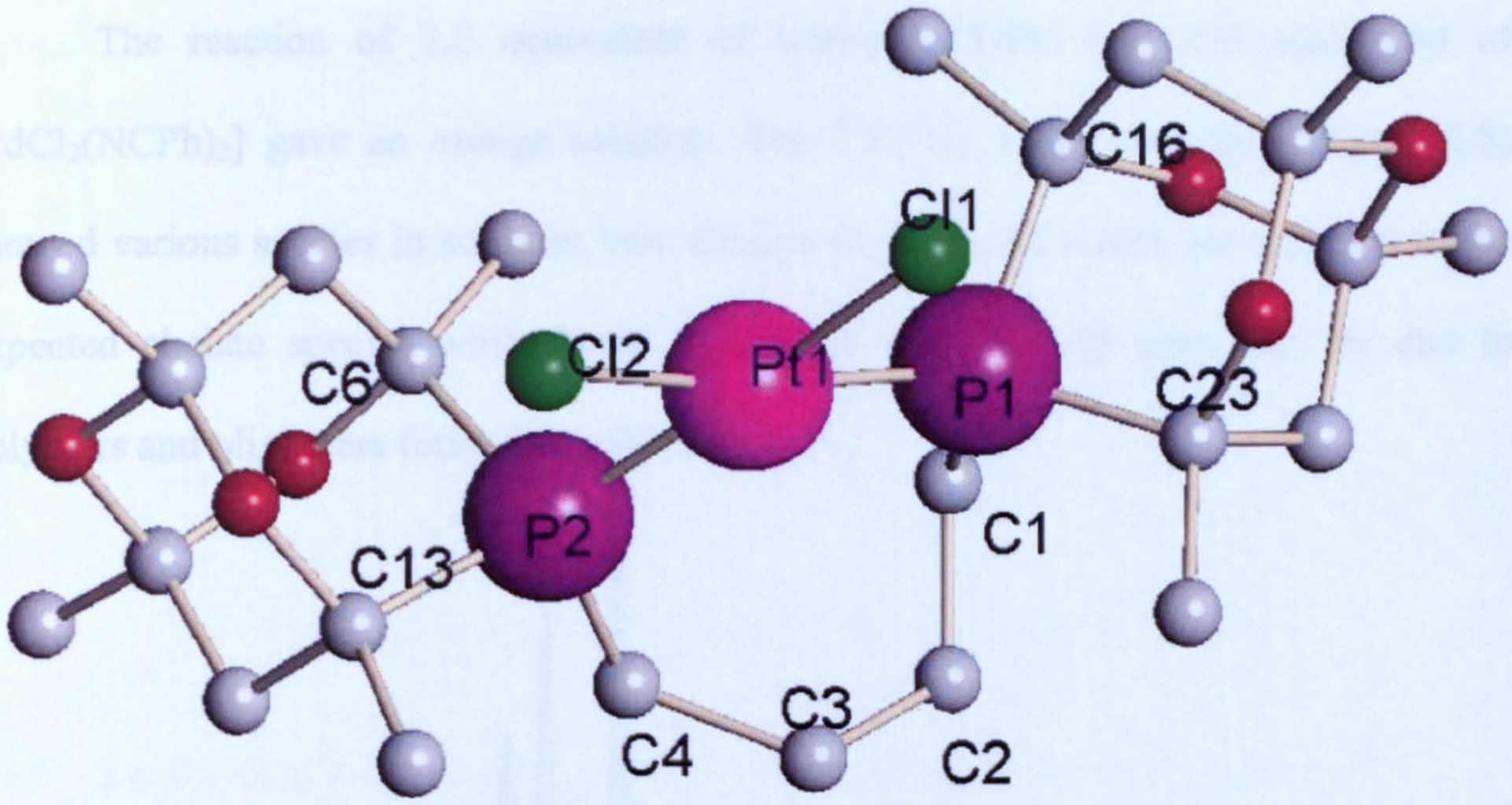

Figure 2.7 Molecular structure of *meso*-[$PtCl_2$(**2.64**)] (**2.67**); selected atoms are labelled

Table 2.2 Selected bond lengths and angles for [$PtCl_2$(**2.64**)] (**2.67**)

Bond	Lengths [Å]	Bond	Angles [°]
Pt(1)-P(1)	2.273(4)	P(1)-Pt(1)-P(2)	99.38(14)
Pt(1)-P(2)	2.282(4)	P(1)-Pt(1)-Cl(1)	87.04(13)
Pt(1)-Cl(1)	2.335(4)	P(1)-Pt(1)-Cl(2)	169.64(14)
Pt(1)-Cl(2)	2.339(4)	P(2)-Pt(1)-Cl(1)	173.56(14)
P(1)-C(1)	1.825(14)	P(2)-Pt(1)-Cl(2)	90.85(14)
P(1)-C(16)	1.866(14)	C(13)-P(2)-C(6)	92.9(6)
P(1)-C(23)	1.870(13)	P(2)-Pt(1)-Cl(2)	90.85(14)
P(2)-C(4)	1.824(14)	C(16)-P(1)-C(23)	93.7(6)
P(2)-C(13)	1.887(16)	C(4)-P(2)-Pt(1)	117.3(5)
P(2)-C(6)	1.888(14)	C(6)-P(2)-Pt(1)	114.2(4)
C(1)-C(2)	1.53(2)	C(1)-P(1)-Pt(1)	116.1(5)
C(2)-C(3)	1.49(2)	C(23)-P(1)-Pt(1)	117.3(4)

2.5.4 Dichloropalladium(II) complex of (2.64)]

The reaction of 1.0 equivalent of *meso/rac*-(**2.64**) with 1.0 equivalent of $[PdCl_2(NCPh)_2]$ gave an orange solution. The $^{31}P\{^1H\}$ NMR spectrum (Figure 2.8) showed various species in solution, two singlets at *ca*. 4 and 5 ppm are assigned to the expected chelate species while broad multiplets from 7 - 12 ppm may be due to polymers and oligomers formed in solution.

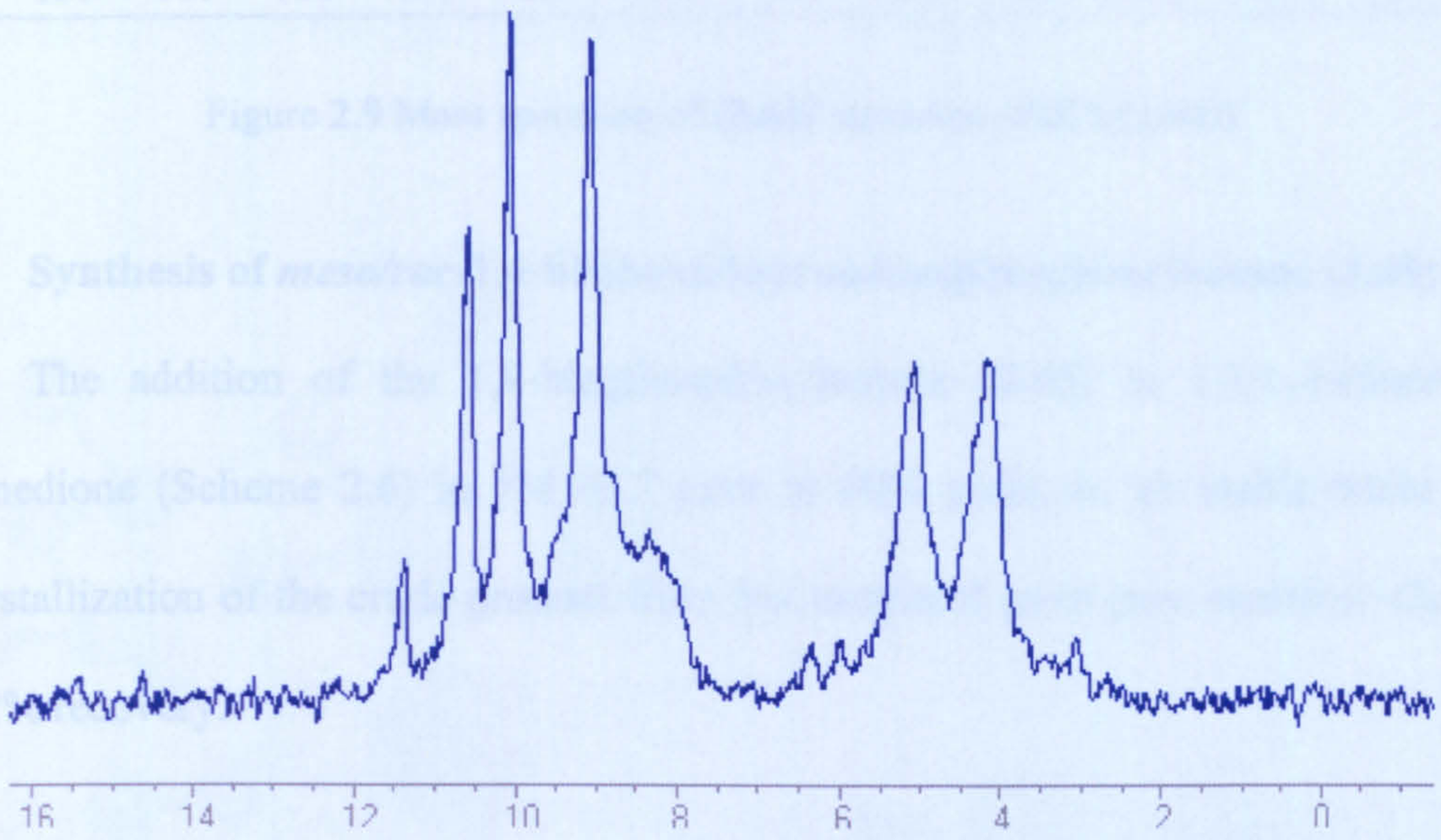

Figure 2.8 $^{31}P\{^1H\}$ NMR of the orange solution obtained from the reaction of *meso/rac*-(**2.64**) with $[PdCl_2(NCPh)_2]$

The formation of polymers and oligomers is likely to be consequence of the length of the backbone in the ligand making it difficult for the chelate to form and therefore competitive oligomerization takes place. The mass spectrum shows the molecular ion of the chelate species (627 M^+-Cl) with an intensity of 40% (Figure 2.9).

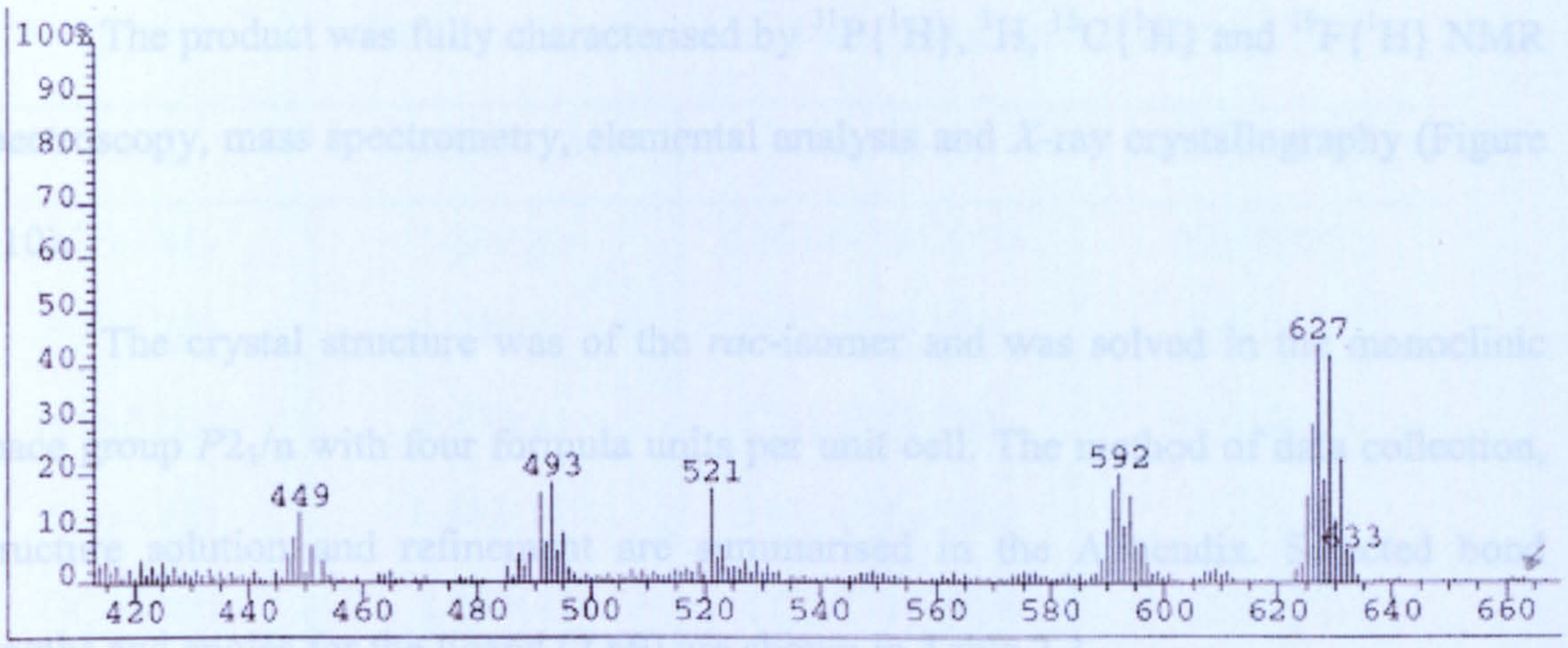

Figure 2.9 Mass spectrum of (**2.68**) *meso/rac*-[$PdCl_2$(**2.64**)]

2.5.5 Synthesis of *meso/rac*-1,4-bis(hexafluoroadamphosphino)butane (2.69)

The addition of the 1,4-bis(phosphino)butane (**2.63**) to 1,1,1,-trifluoro-2,4-pentanedione (Scheme 2.6) in 5M HCl gave in 60% yield, an air stable white solid. Recrystallization of the crude product from hot methanol gave pure *meso/rac*-(**2.69**) in *ca.* 62% recovery.

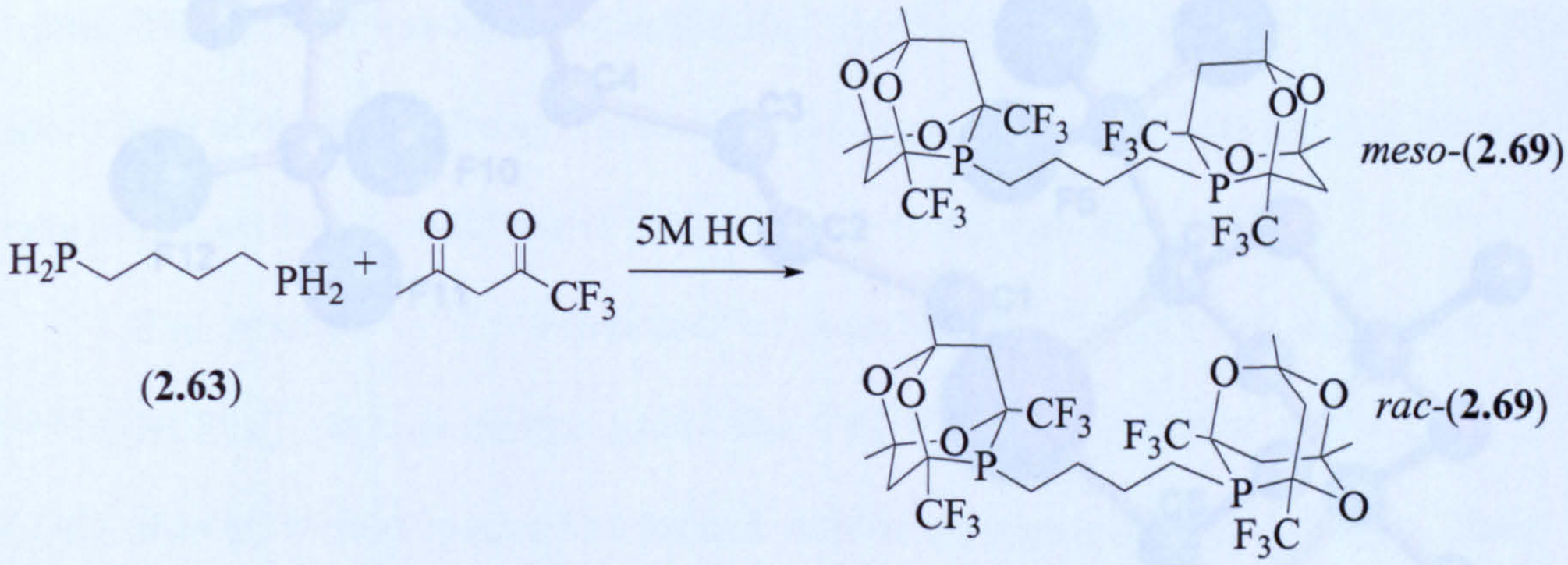

Scheme 2.6 Synthesis of *meso/rac*-1,4-bis(hexafluoroadamphosphino)butane (**2.69**)

The $^{31}P\{^{1}H\}$ NMR spectrum of the white solid showed two septets overlapping at –34.0 ppm, corresponding to the diastereoisomers *meso/rac*-1,4-bis(hexafluoro-adamphosphino)butane (**2.69**). Both signals are septets as a result of coupling between the phosphorus and 6 fluorine atoms.

The product was fully characterised by $^{31}P\{^{1}H\}$, ^{1}H, $^{13}C\{^{1}H\}$ and $^{19}F\{^{1}H\}$ NMR spectroscopy, mass spectrometry, elemental analysis and *X*-ray crystallography (Figure 2.10).

The crystal structure was of the *rac*-isomer and was solved in the monoclinic space group $P2_1/n$ with four formula units per unit cell. The method of data collection, structure solution and refinement are summarised in the Appendix. Selected bond lengths and angles for the ligand (**2.69**) are shown in Table 2.3.

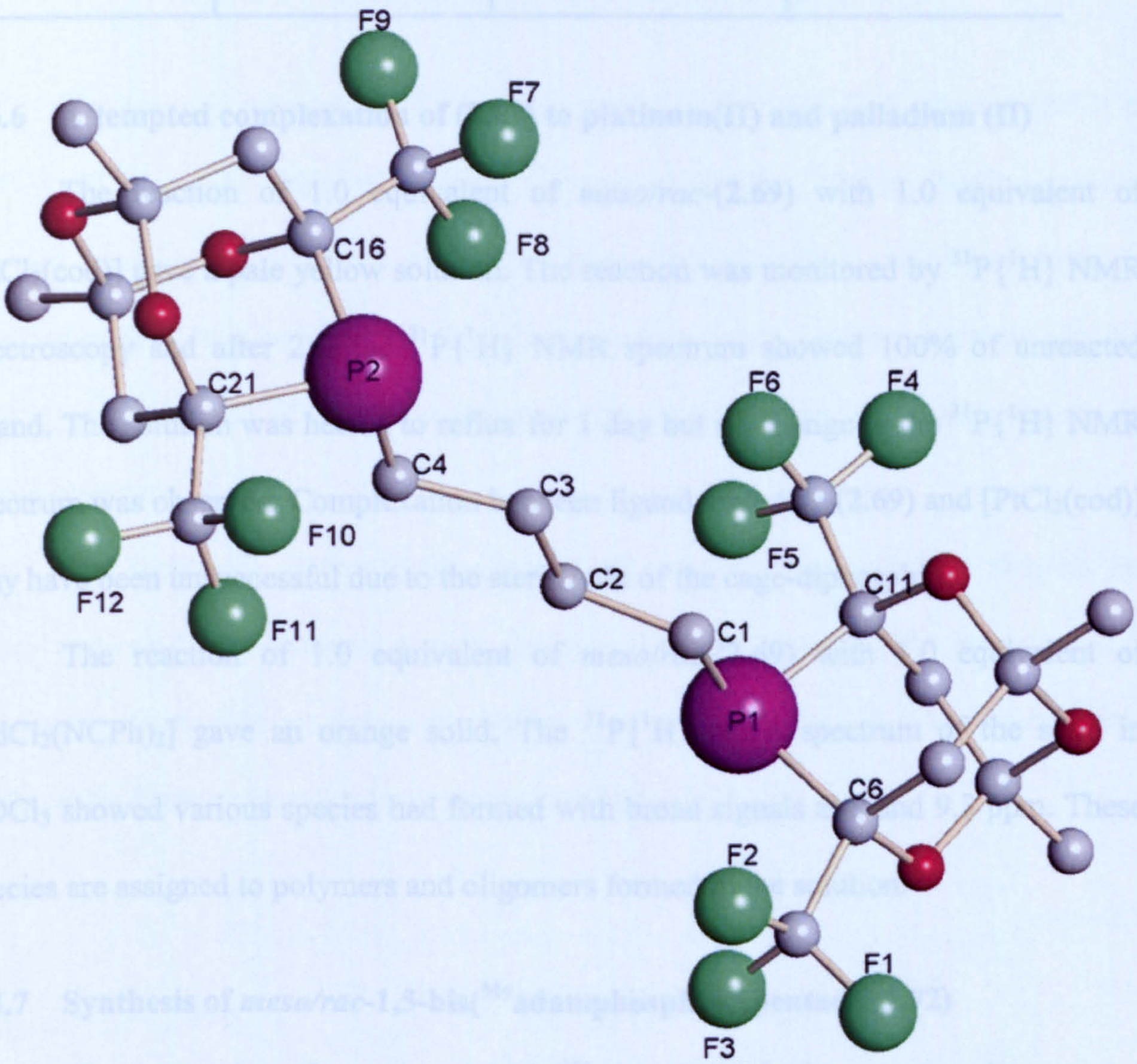

Figure 2.10 Molecular structure of *rac*-(**2.69**) selected atoms are labelled

Table 2.3 Selected bond lengths and angles for **(2.69)**

Bond	Lengths [Å]	Bond	Angles [°]
P(1)-C(1)	1.842(4)	C(6)-P(1)-C(11)	89.14(18)
P(1)-C(6)	1.888(4)	F(3)-C(5)-F(2)	108.0(4)
P(1)-C(11)	1.892(4)	C(1)-P(1)-C(6)	103.04(18)
F(1)-C(5)	1.343(14)	F(2)-C(5)-C(6)	110.6(3)
O(2)-C(6)	1.439(4)	C(2)-C(1)-P(1)	111.9(3)
C(5)-C(6)	1.531(6)	O(4)-C(11)-C(17)	103.4(5)
C(2)-C(3)	1.524(5)	O(4)-C(11)-P(1)	107.1(3)

2.5.6 Attempted complexation of (2.69) to platinum(II) and palladium (II)

The reaction of 1.0 equivalent of *meso/rac*-**(2.69)** with 1.0 equivalent of $[PtCl_2(cod)]$ gave a pale yellow solution. The reaction was monitored by $^{31}P\{^1H\}$ NMR spectroscopy and after 2 h the $^{31}P\{^1H\}$ NMR spectrum showed 100% of unreacted ligand. The solution was heated to reflux for 1 day but no change in the $^{31}P\{^1H\}$ NMR spectrum was observed. Complexation between ligand *meso/rac*-**(2.69)** and $[PtCl_2(cod)]$ may have been unsuccessful due to the steric bulk of the cage-diphosphine.

The reaction of 1.0 equivalent of *meso/rac*-**(2.69)** with 1.0 equivalent of $[PdCl_2(NCPh)_2]$ gave an orange solid. The $^{31}P\{^1H\}$ NMR spectrum of the solid in $CDCl_3$ showed various species had formed with broad signals at 8 and 9.3 ppm. These species are assigned to polymers and oligomers formed in the solution.

2.5.7 Synthesis of *meso/rac*-1,5-bis(^{Me}adamphosphino)pentane (2.72)

The preparation of *meso/rac*-1,5-bis(^{Me}adamphosphino)pentane involves several steps. The first step is the reaction of dibromopentane and triethylphosphite[82] to produce the phosphonate **(2.70)** *via* a Michaelis–Arbuzov reaction. The second step is the

reduction of the phosphonate (**2.70**) to afford the diprimary phosphine[83] (**2.71**) (Scheme 2.7).

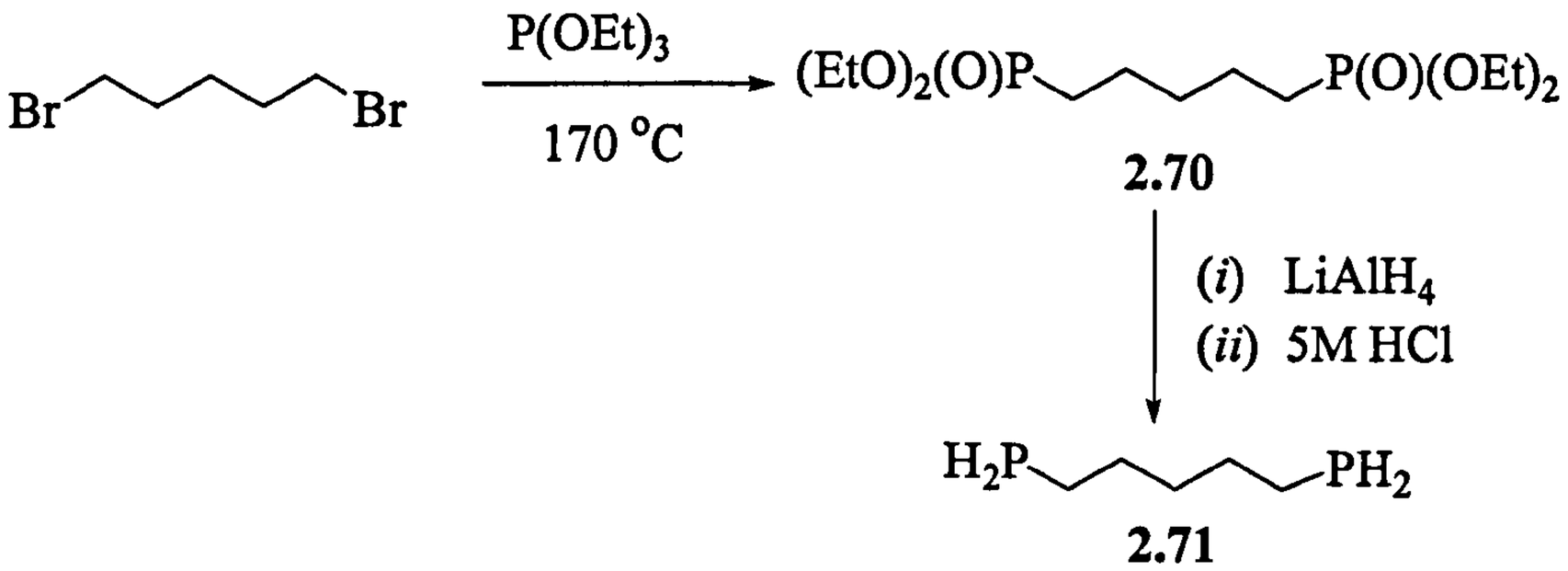

Scheme 2.7 Preparation of the 1,5-diprimary phosphine (**2.71**)

The reaction between (**2.71**) and 2,4-pentanedione in 5M HCl afforded (**2.72**) in 70% yield as an air-stable white solid (Scheme 2.8). The $^{31}P\{^{1}H\}$ NMR spectrum showed a broad singlet at -28.3 ppm corresponding to *meso/rac*-1,5-bis(^{Me}adamphosphino)pentane (**2.72**). The product was further characterized by $^{31}P\{^{1}H\}$, $^{13}C\{^{1}H\}$ and ^{1}H NMR spectroscopy, mass spectrometry and elemental analysis (see Experimental).

The broadness of the NMR signals is due to overlapping of the singlets for *meso-* and *rac*-(**2.72**) diastereoisomers, because the more separated the cages are (*i.e.* the longer the backbone) the more similar their environment and thus the chemical shifts of the diastereoisomers occur closer together.

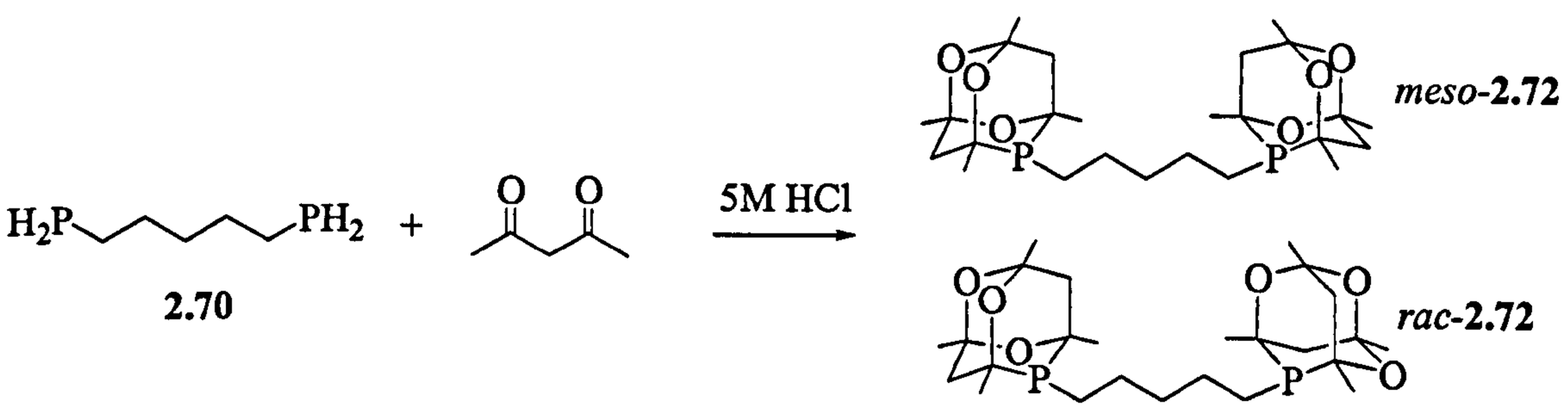

Scheme 2.8 Preparation of (**2.72**)

2.5.8 Dichloroplatinum(II) complex of (2.72)

The reaction of 1.0 equivalent of *meso/rac*-(**2.72**) with 1.0 equivalent of $[PtCl_2(cod)]$ gave a mixture of products. Two groups of broad signals (marked * and **X** in Figure 2.11) were observed in the ^{31}P NMR spectrum from 0.5 - 2.0 ppm with broad platinum satellites (^1J(PtP) 2683 Hz) (^1J(PtP) 2595 Hz) indicating the presence of several species in which (from the magnitude of ^1J(PtP)) the phosphines are *trans*. The experiment was repeated in 10 times dilution in an attempt to promote the formation of the chelate, but no difference in the spectrum was observed. The broadness of the signals (Figure 2.11) indicates that the product is a mixture of oligomers. The 5-carbon backbone militates against the formation of a chelate, as noted in Section 2.5.4 for the 4-carbon backbone diphosphine ligand.

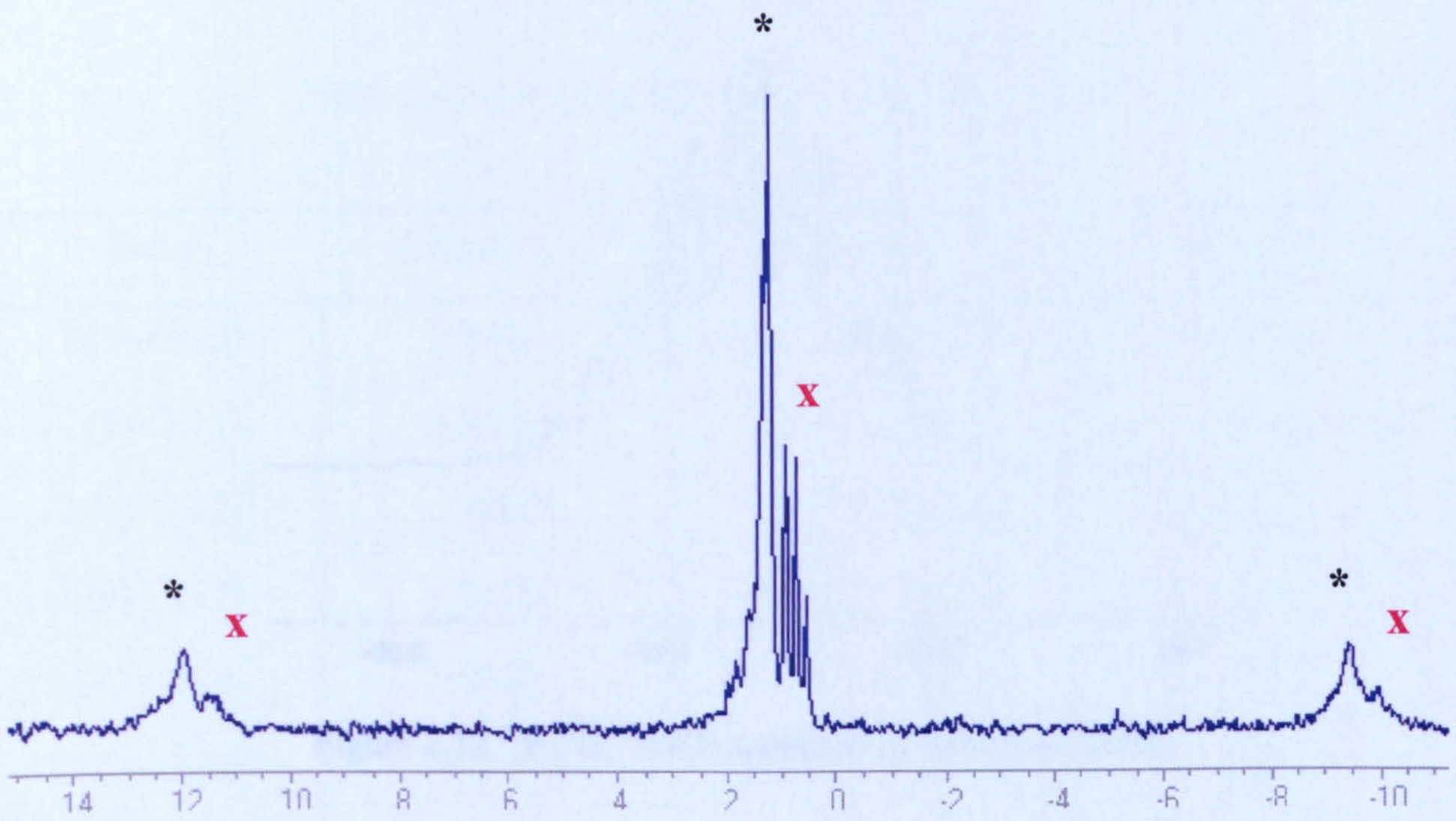

Figure 2.11 $^{31}P\{^1H\}$ NMR spectrum obtained from the reaction of *meso/rac*-(**2.72**) with $[PtCl_2(cod)]$

2.5.9 Synthesis of *meso/rac*-1,5-bis(hexafluoroadamphosphino)pentane (2.73)

The addition of 1,5-bis(phosphino)pentane (**2.70**) to 1,1,1,-trifluoro-2,4-pentanedione in 5M HCl yielded a white solid (**2.73**) (Scheme 2.9).

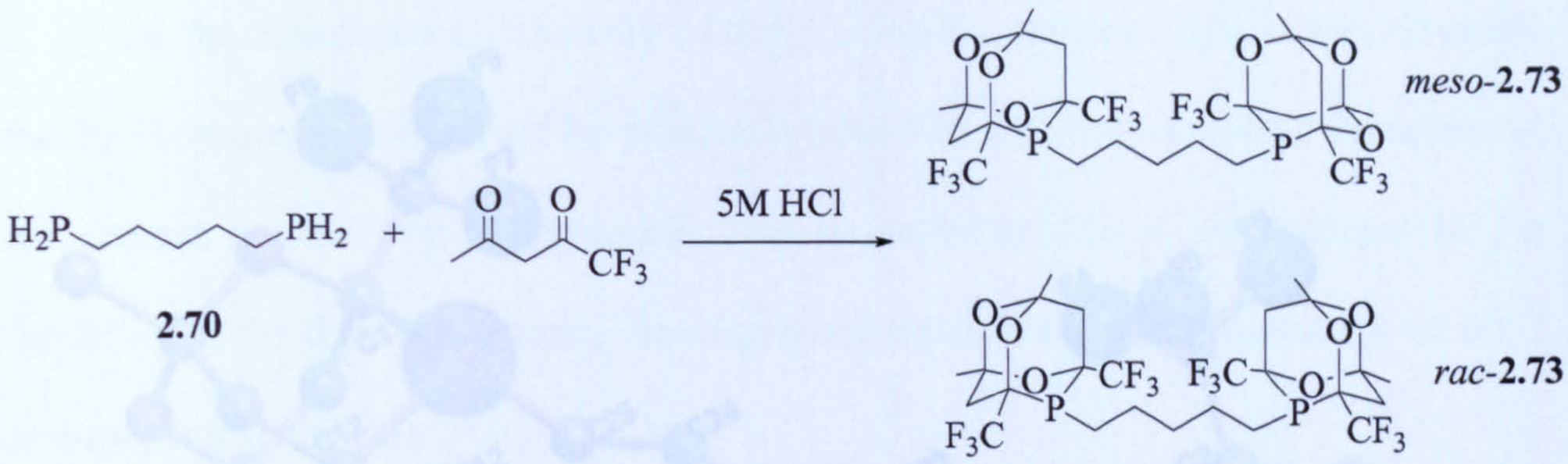

2.70

Scheme 2.9 Preparation of (**2.73**)

The $^{31}P\{^{1}H\}$ NMR spectrum showed two overlapping signals centre at –33.4 ppm corresponding to the diastereoisomers *meso/rac*-1,5-bis(hexafluoroadamphos-phino)-pentane (**2.73**). Coupling between the phosphorus and six fluorine atoms leads to two overlapping septets in the $^{31}P\{^{1}H\}$ NMR spectrum (Figure 2.12).

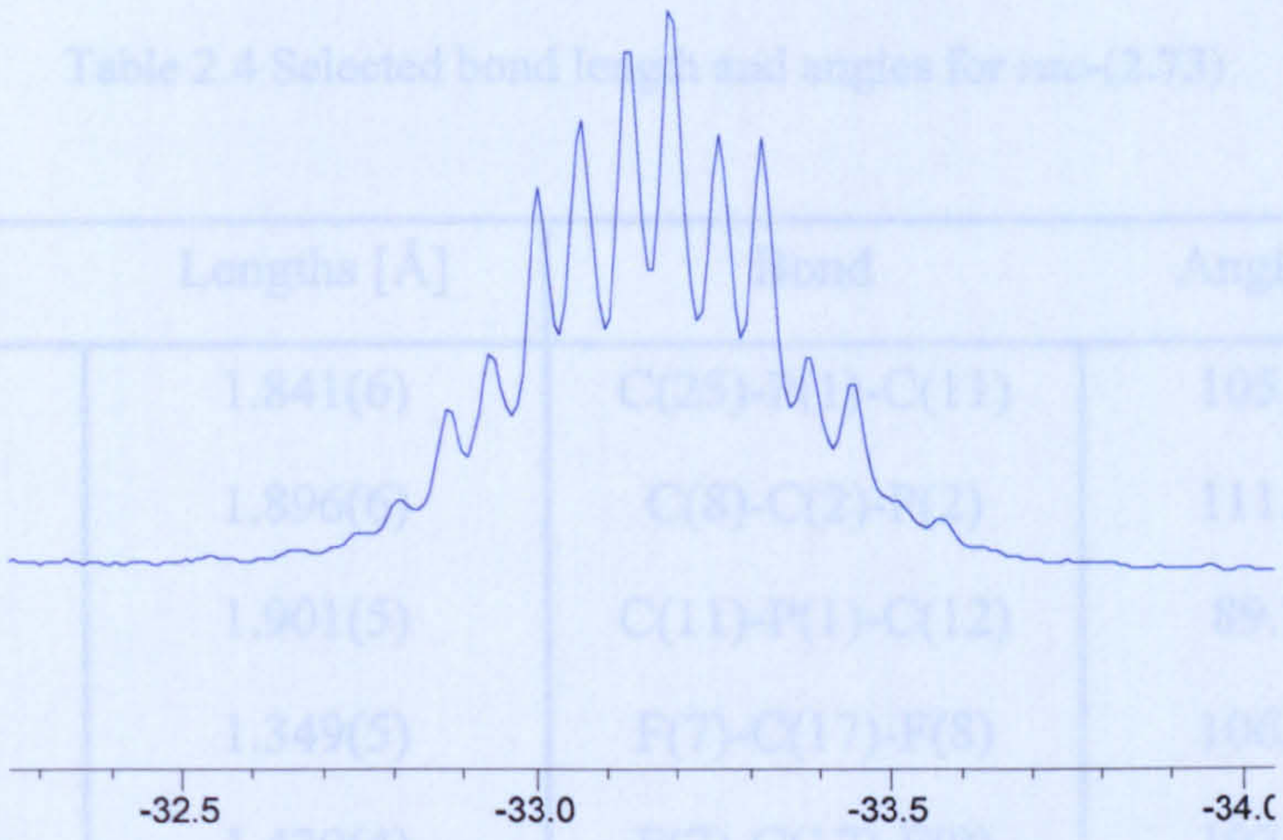

Figure 2.12 $^{31}P\{^{1}H\}$ NMR spectrum of *meso/rac*-(**2.73**)

The product was fully characterised by $^{31}P\{^{1}H\}$, ^{1}H and $^{13}C\{^{1}H\}$ spectroscopy, mass spectrometry, elemental analysis and *X*-ray crystallography (Figure 2.13).

The crystal structure was of the *rac*-isomer and was solved in the monoclinic space group $P2_1/c$ with four formula units per unit cell. The method of data collection, structure solution and refinement are summarised in the Appendix. Selected bond lengths and angles for the ligand (**2.73**) are shown in Table 2.4.

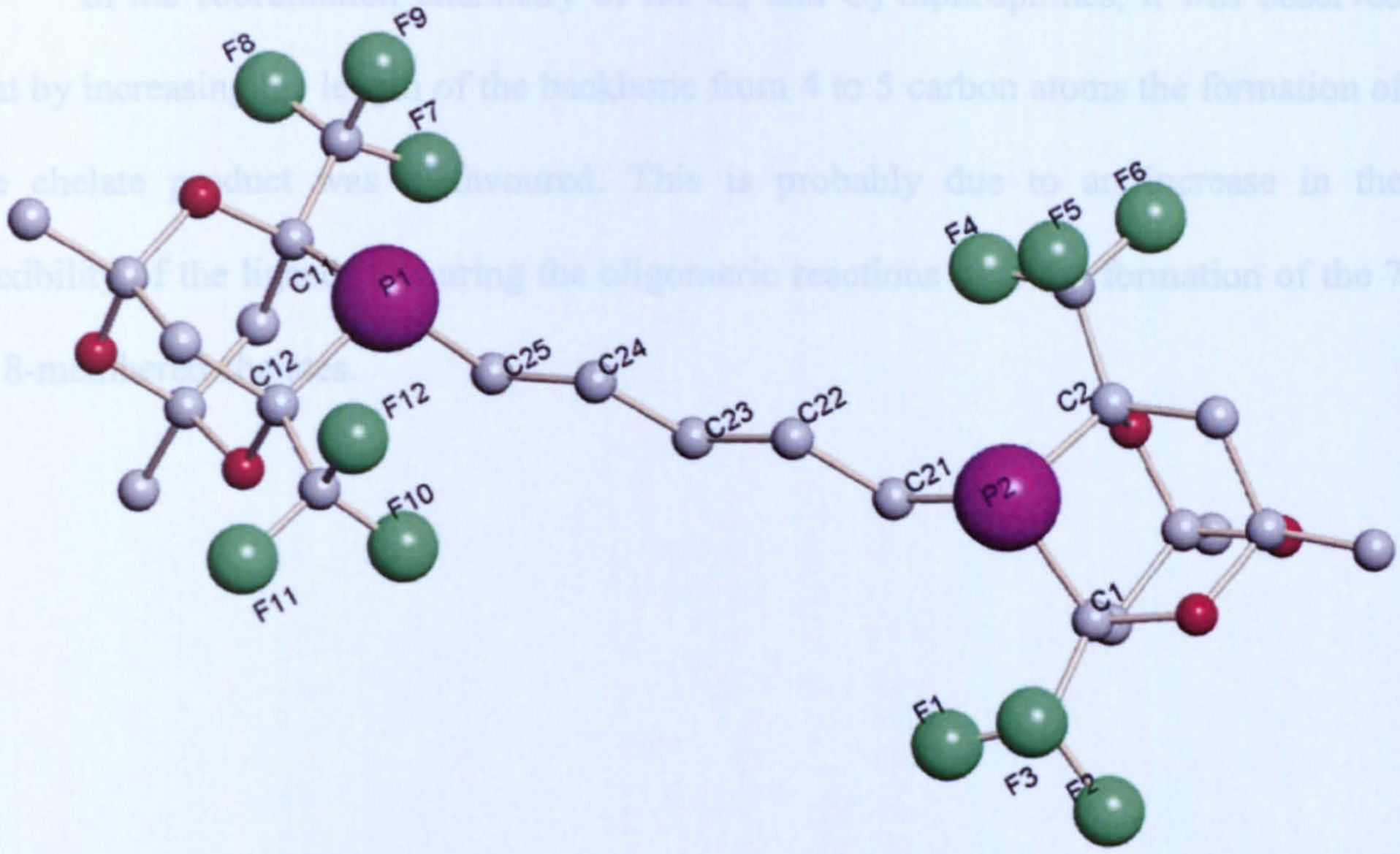

Figure 2.13 Molecular structure of *rac*-(**2.73**) selected atoms are labelled

Table 2.4 Selected bond length and angles for *rac*-(**2.73**)

Bond	Lengths [Å]	Bond	Angles [°]
P(1)-C(25)	1.841(6)	C(25)-P(1)-C(11)	105.5(2)
P(1)-C(11)	1.896(6)	C(8)-C(2)-P(2)	111.1(4)
P(1)-C(12)	1.901(5)	C(11)-P(1)-C(12)	89.7(2)
F(9)-C(17)	1.349(5)	F(7)-C(17)-F(8)	106.9(4)
O(2)-C(6)	1.439(4)	F(7)-C(17)-F(9)	107.0(4)
C(21)-C(22)	1.527(8)	O(1)-C(11)-C12	109.2(3)
C(17)-C(11)	1.524(8)	F(4)-C(10)-C(11)	113.1(4)

2.6 Conclusion

The new bidentate phospha-adamantane cages with C_4 and C_5 backbones were synthesised in good yields.

In the coordination chemistry of the C_4 and C_5 diphosphines, it was observed that by increasing the length of the backbone from 4 to 5 carbon atoms the formation of the chelate product was disfavoured. This is probably due to an increase in the flexibility of the ligand, favouring the oligomeric reactions over the formation of the 7 or 8-membered chelates.

Chapter 3

Monodentate and bidentate tetraethyl-trioxa-phospha-adamantanes and their coordination chemistry

3.1 Introduction

In Chapter 2 the synthesis of new bidentate tetramethyl-trioxa-phospha-adamantanes with variation in the backbone and some variation of the 6,8-substituents (methyl to trifluoromethyl) were described. In this Chapter the synthesis of tetraethyl-trioxa-phospha-adamantanes (shown below) is presented.

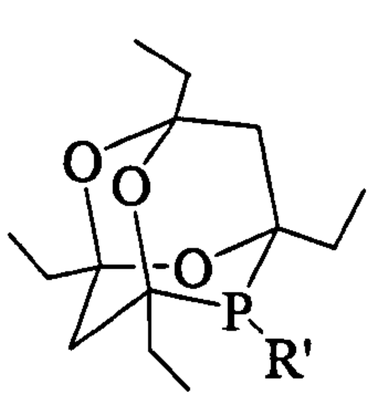

R' = H, Ph

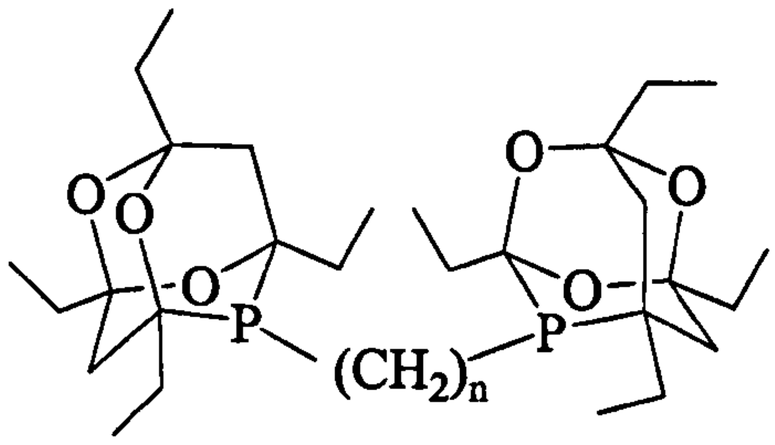

n = 3, 4, 5

The aim was to increase further the bulkiness of the ligand by increasing the size of the substituents on the cage, and to investigate their performance as ligands for Rh-catalyzed hydroformylation.

3.2 Chemistry of monodentate 1,3,5,7-tetraethyl-2,4,8-trioxa-6-phospha-adamantanes

3.2.1 Synthesis of 1,3,5,7-tetraethyl-2,4,8-trioxa-6-phospha-adamantane (^{Et}CgPH)

The compound ^{Et}CgPPh (**3.1**) was prepared by passing phosphine gas through a deoxygenated solution of 3,5-heptanedione in aqueous 5M HCl at –12 °C for 16 h (Equation 3.1). After this time the solution was neutralized with deoxygenated 5M NaOH; the product was extracted into $CHCl_3$, passed through a silica column and then isolated as a pale yellow oil in up to 15% yield. The $^{31}P\{^1H\}$ NMR spectrum of **(3.1)** showed a singlet at –57.9 ppm.

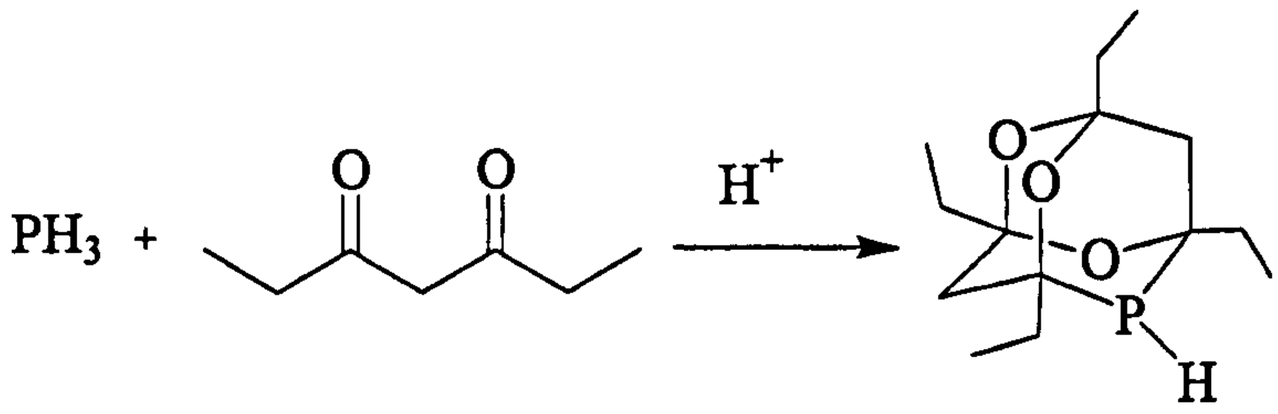

3.1

Equation 3.1

The temperature of the reaction (-12 °C) was chosen on the basis of related optimisation by Pugh[73] for the synthesis of ^{Me}CgPH.

In the first attempt of the synthesis of (**3.1**), low solubility of the hydrophobic heptanedione in the aqueous medium was observed, and therefore in subsequent attempts ethanol was added to the reaction mixture to increase the solubility of the 3,5-heptanedione. Unfortunately after passage of PH_3 for 8 h, the $^{31}P\{^1H\}$ NMR spectrum showed two unidentified peaks at 52.1 and 52.6 ppm, and the desired product ^{Et}CgPH (**3.1**) was not present.

The concentration of the acid catalyst was increased, which accelerated the reaction and also improved the solubility of the heptanedione. Thus by passing phosphine gas through a solution of 3,5-heptanedione in 8M aqueous HCl at –12 °C, the reaction time was reduced from 16 h to 6 h and the yield of (**3.1**) was increased to 75%. The $^{31}P\{^1H\}$ NMR spectrum showed a singlet at –57.9 ppm and the identity of (**3.1**) was confirmed by mass spectrometry and elemental analysis (see Experimental).

A mechanism was proposed by Gee[75] for the acid-catalysed addition of a PH_2 group to two equivalents of $RC(O)CH_2C(O)R$ (R = Me, CF_3) (Scheme 3.1). In steps (i) and (ii) "normal" carbonyl additions take place, followed in steps (iii) and (iv) by intramolecular nucleophilic attack to form two cyclic hemiketals. Finally cage formation occurs by an intramolecular condensation. The overall reaction is therefore a hydrophosphination/dehydration reaction.

In the mechanism (Scheme 3.1) the reaction is acid-catalysed and thus increasing the concentration of the acid increased the rate of the reaction. In the synthesis of the ^{Me}CgPH,[73,74] the concentration of the acid was 5M and after 1 day this gave a 50% yield. In the synthesis of ^{Et}CgPH (**3.1**) the concentration of the acid was 8M and gave 75% yield after 6 h. In the formation of the ^{Et}CgPH (**3.1**) the more bulky 1,3-diketone, restricts the attack of the PH_2 group (step (ii)). Increasing the concentration of the acid from 5M (^{Me}CgPH) to 8M (^{Et}CgPH) gave a large increase in the reaction rate to counteract this effect.

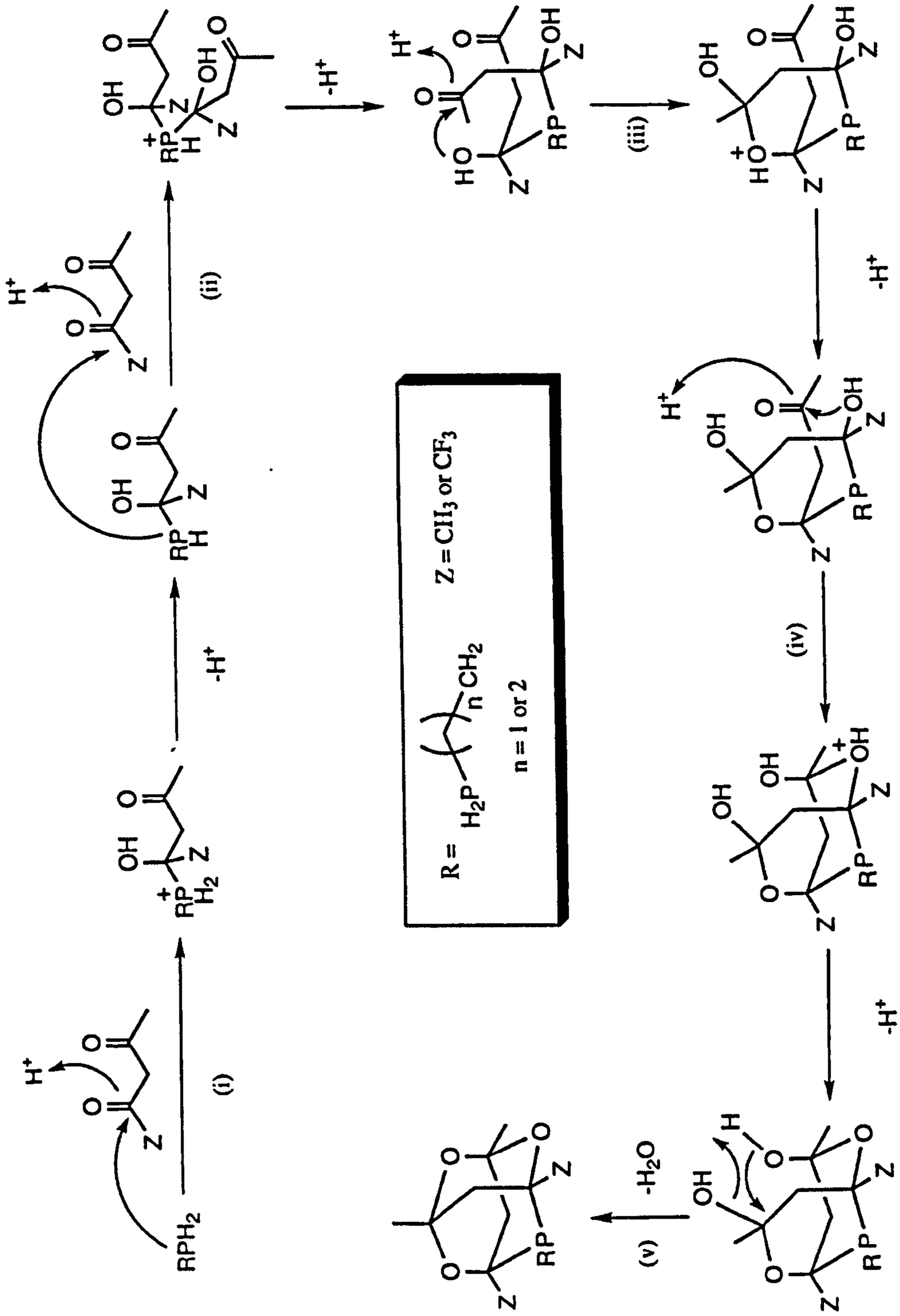

Scheme 3.1 Mechanism of the cage formation via hydrophosphination[75]

3.2.2 Dichloroplatinum(II) complex of (3.1)

The reaction of ^{Et}CgPH (**3.1**) with [$PtCl_2$(cod)] in CH_2Cl_2 gave a pale yellow solution. The solvent was evaporated and a pale yellow solid was recovered in 98% yield. The solid was further characterized as a mixture of *meso*- and *rac*-[$PtCl_2$(^{Et}CgPH)$_2$] (**3.2**) (Equation 3.2) by $^{31}P\{^1H\}$ NMR spectroscopy, mass spectrometry, elemental analysis.

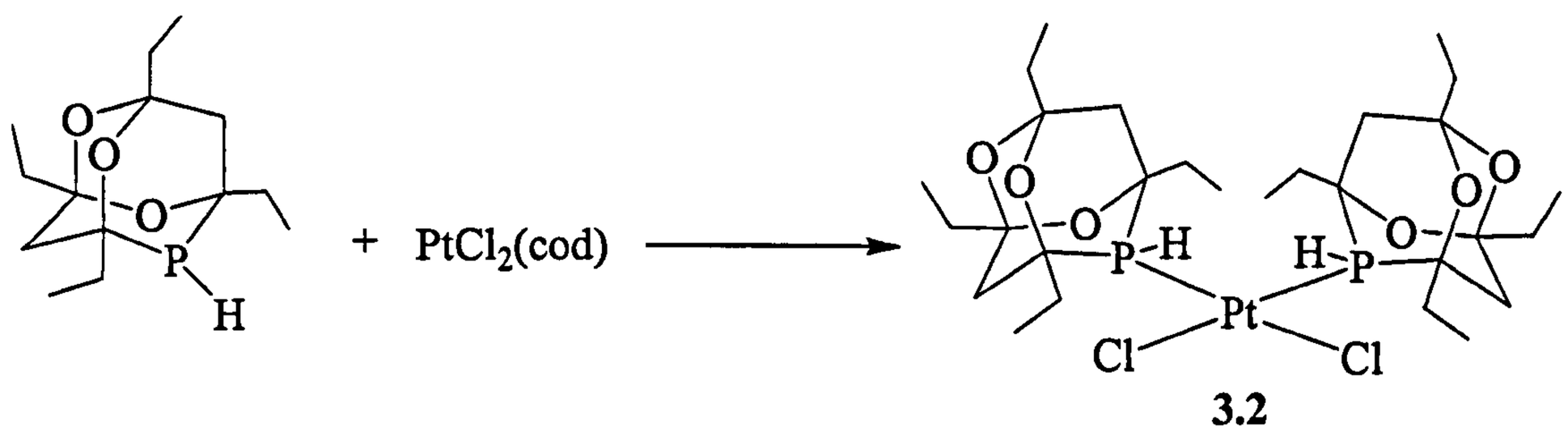

3.2

Equation 3.2

The ^{Et}CgPH (**3.1**) is chiral and as a consequence *meso*- and *rac*-diastereoisomers of (**3.2**) are observed. The $^{31}P\{^1H\}$ NMR spectrum showed that the main products are two singlets at 1.4 and 1.7 ppm with platinum satellites (^1J(PPt) 3308 Hz) that correspond to *meso*/*rac*-(**3.2**).

A preliminary investigation of the solid state structure of compound (**3.1**) has been carried out by K. Heslop (see Figure 3.1). The compound appears to crystallise in space group P2(1)/c with two molecules in the asymmetric unit. The crystal used was of very poor quality and it has only been possible to establish the gross molecular geometry of the complex. It has not been possible to differentiate between the oxygen and carbon atoms in the cage groups and the positions of the oxygen atoms shown in Figure 3.1 are arbitrarily assigned. Bond length data are not reliable and have not been included in this thesis.

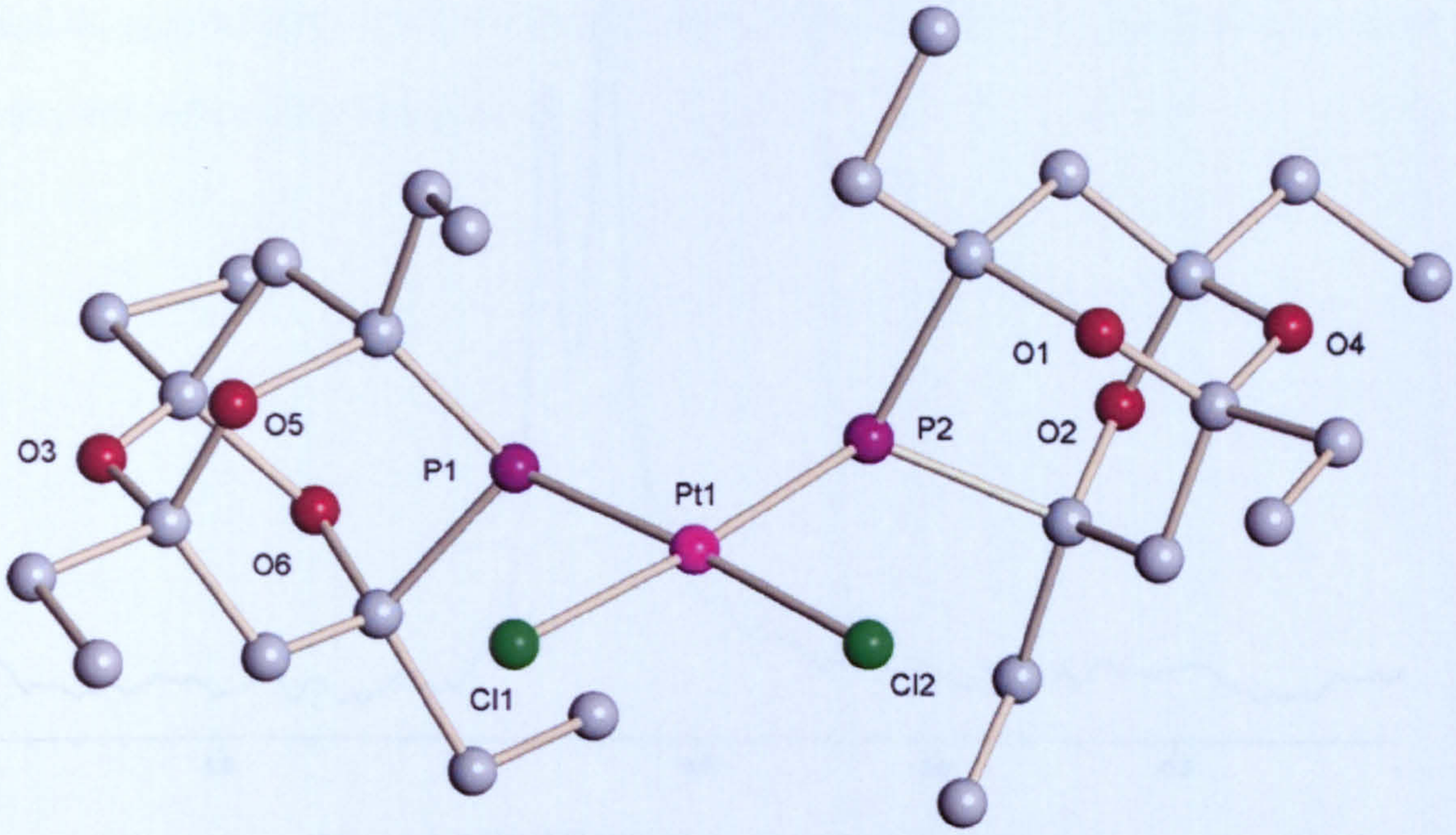

Figure 3.1 Molecular structure of the *cis*-$[PtCl_2(^{Et}CgPH)_2]$ (**3.2**). Selected atoms are labelled

3.2.3 Synthesis of the dichloropalladium(II) complex (3.3)

The reaction of $^{Et}CgPH$ (**3.1**) with $[PdCl_2(NCPh)_2]$ in CH_2Cl_2 gave a yellow solution. The solvent was evaporated and a pale yellow solid was recovered in 97% yield. The solid was further characterized as a mixture of *meso*- and *rac*-$[PdCl_2(^{Et}CgPH)_2]$ (**3.3**) by $^{31}P\{^1H\}$ NMR spectroscopy, mass spectrometry and elemental analysis. The $^{31}P\{^1H\}$ NMR spectrum (Figure 3.2) showed two singlets corresponding to the *meso*/*rac*-(**3.3**).

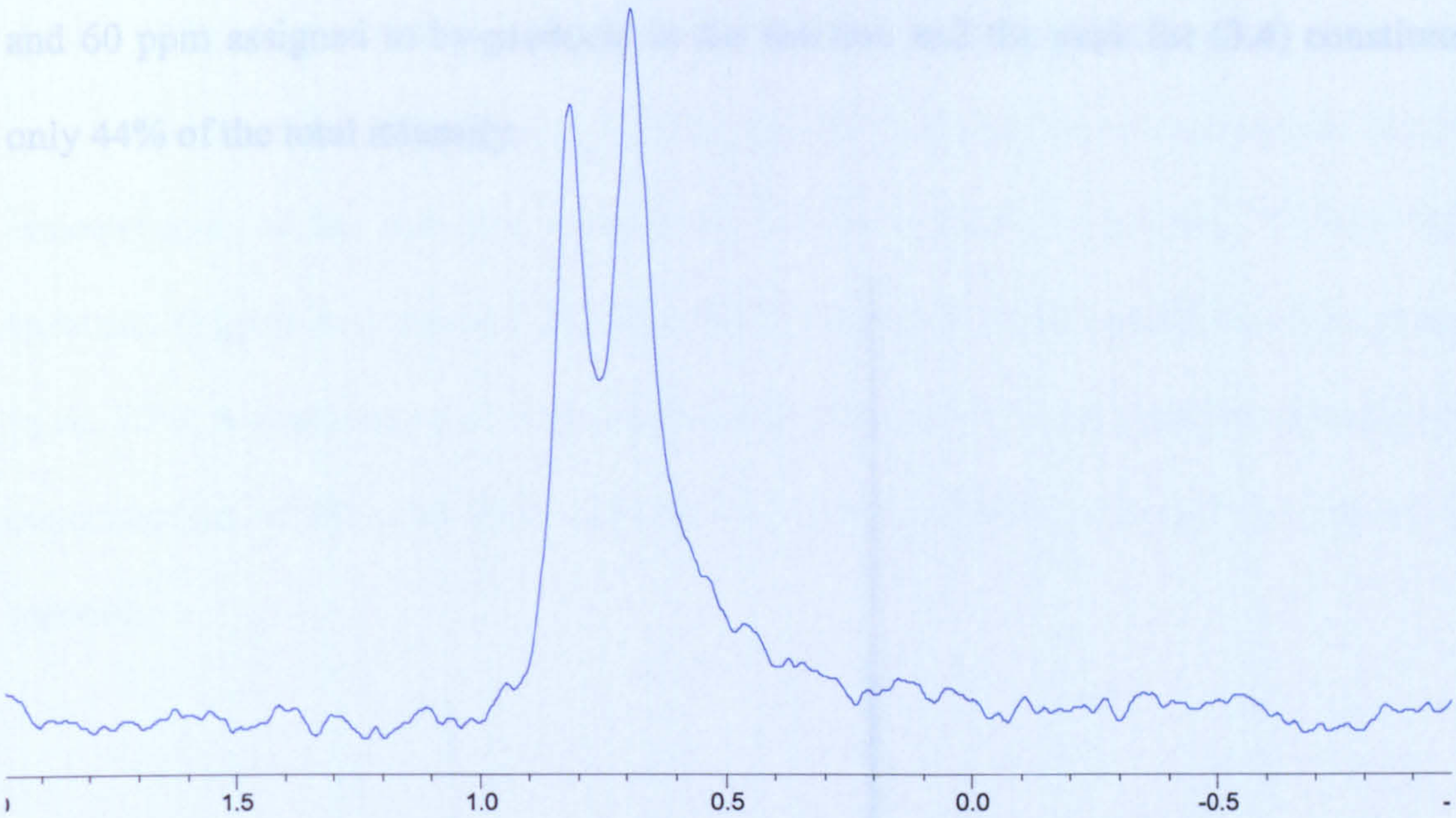

Figure 3.2 $^{31}P\{^{1}H\}$ NMR spectrum of *meso/rac*-(**3.3**)

3.2.4 Synthesis of 1,3,5,7-tetraethyl-6-phenyl-2,4,8-trioxa-6-phospha-adamantane ^{Et}CgPPh (3.4)

In collaboration with Mr. Andrew Ward, the synthesis of the ^{Et}CgPPh (**3.4**) was attempted following the method described by Marr[84] for the synthesis of ^{Me}CgPPh. Phenyl phosphine was added to a deoxygenated solution of 2.0 equivalents of 3,5-heptanedione in 12M HCl (Equation 3.3).

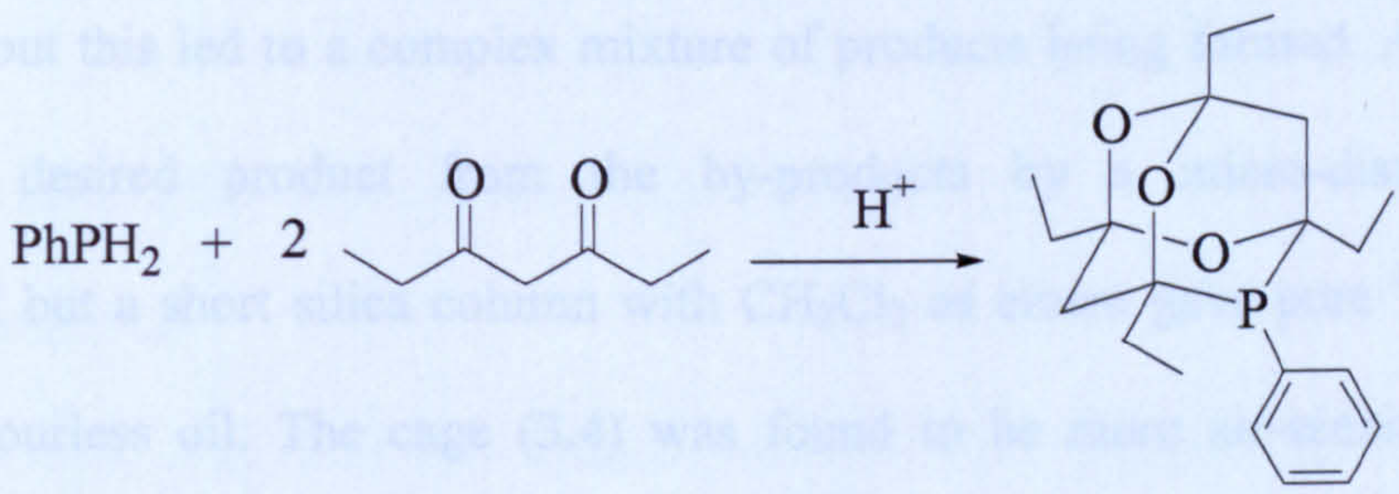

3.4

Equation 3.3

The reaction was monitored by $^{31}P\{^{1}H\}$ NMR spectroscopy over 3 days, after which time the spectrum (Figure 3.3) showed that the desired product had formed (δ = –30.6 ppm). However it can be seen (Figure 3.3) that there are several peaks between 30

and 60 ppm assigned to by-products in the reaction and the peak for (**3.4**) constituted only 44% of the total intensity.

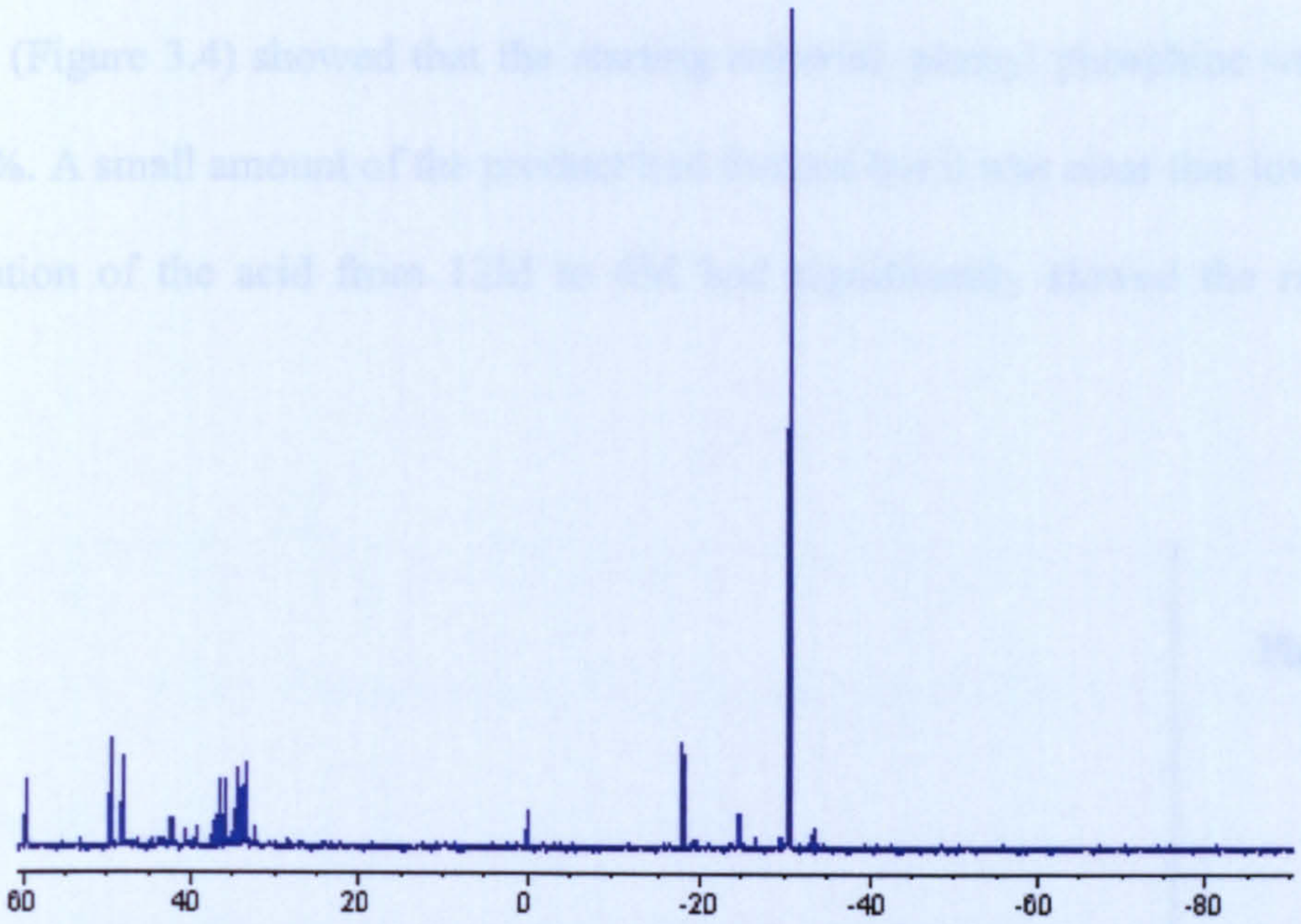

Figure 3.3 $^{31}P\{^{1}H\}$ NMR spectrum of ^{Et}CgPPh (**3.4**) reaction using 12M HCl after 3 days

The reaction was allowed to proceed for a further 23 days but little increase in the amount of (**3.4**) was observed, and in addition, no change was observed in the peak profile of the by-products. A sample of the reaction mixture was then heated to reflux for 3 hours but this led to a complex mixture of products being formed. An attempt to isolate the desired product from the by-products by a micro-distillation was unsuccessful but a short silica column with CH_2Cl_2 as eluent gave pure ^{Et}CgPPh as a viscous, colourless oil. The cage (**3.4**) was found to be more air-sensitive than the ^{Me}CgPPh and had to be stored under N_2.

The formation of the (**3.4**) is significantly slower than the ^{Me}CgPPh under similar conditions and the yield of the product was low; this prompted us to investigate the effect of the acid on the reaction as described below.

*3.2.4.1 The effect of the acid concentration in the synthesis of (**3.4**)*

The reaction (Equation 3.3) was repeated under similar conditions but the concentration of the acid was reduced to 6M HCl. After 3 days the $^{31}P\{^{1}H\}$ NMR spectrum (Figure 3.4) showed that the starting material, phenyl phosphine was present in *ca*. 80%. A small amount of the product had formed but it was clear that lowering the concentration of the acid from 12M to 6M had significantly slowed the rate of the reaction.

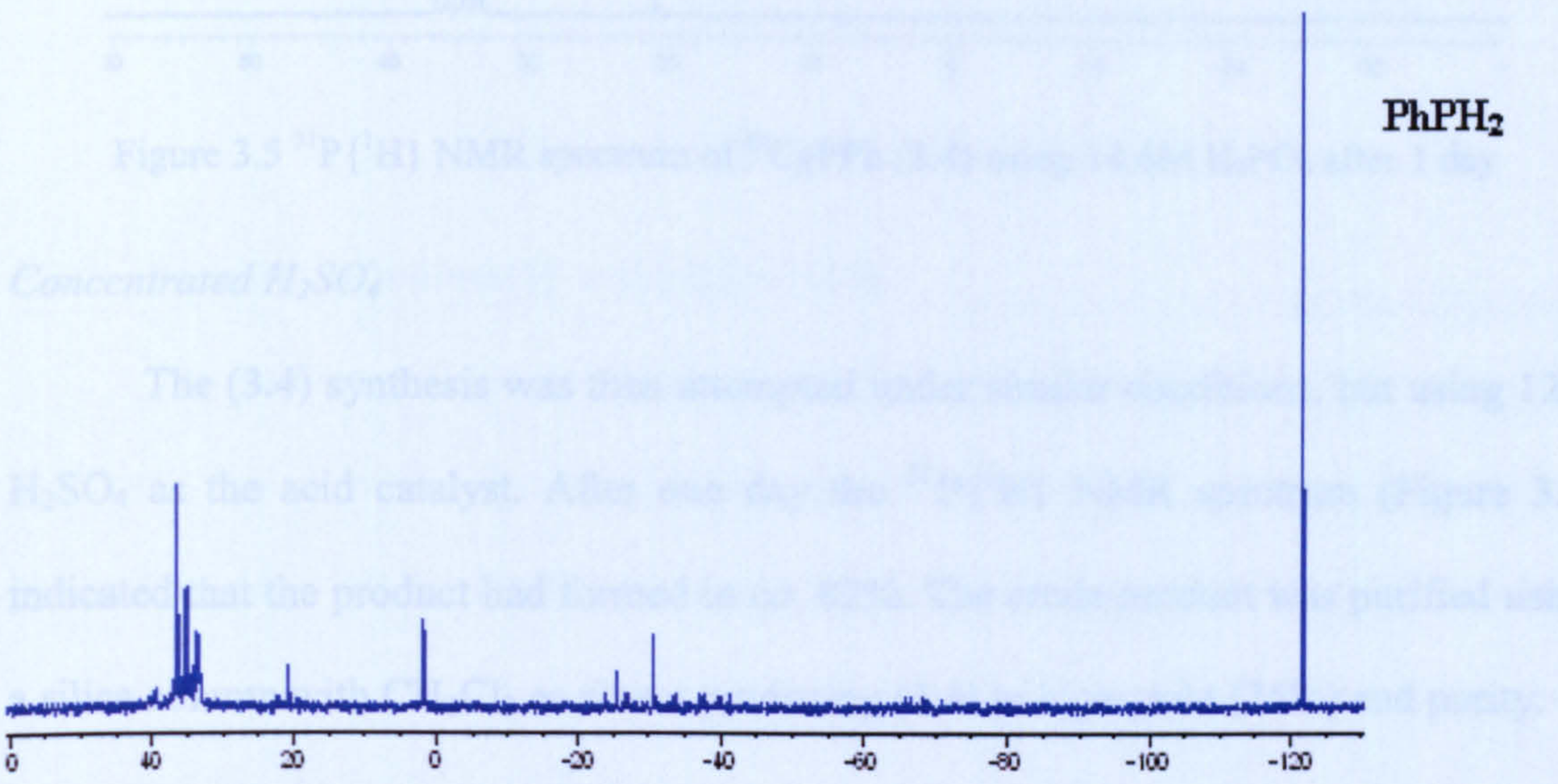

Figure 3.4 $^{31}P\{^{1}H\}$ NMR spectrum of ^{Et}CgPPh (**3.4**) using 6M HCl after 3 days

*3.2.4.2 Variation of the acid in the synthesis of (**3.4**)*

Concentrated H_3PO_4

The synthesis of (**3.4**) was repeated under similar conditions to those described in Section 3.2.4 but using concentrated H_3PO_4 (14.6M) instead of 12M HCl. The reaction was monitored by $^{31}P\{^{1}H\}$ NMR spectroscopy and after 1 day the spectrum (Figure 3.5) showed the desired product in *ca*. 62%. The reaction was repeated using 8M H_3PO_4, but little difference was observed in the $^{31}P\{^{1}H\}$ NMR spectrum. Pure (**3.4**) was obtained in high yield (56%) by column chromatography using CH_2Cl_2 as eluent.

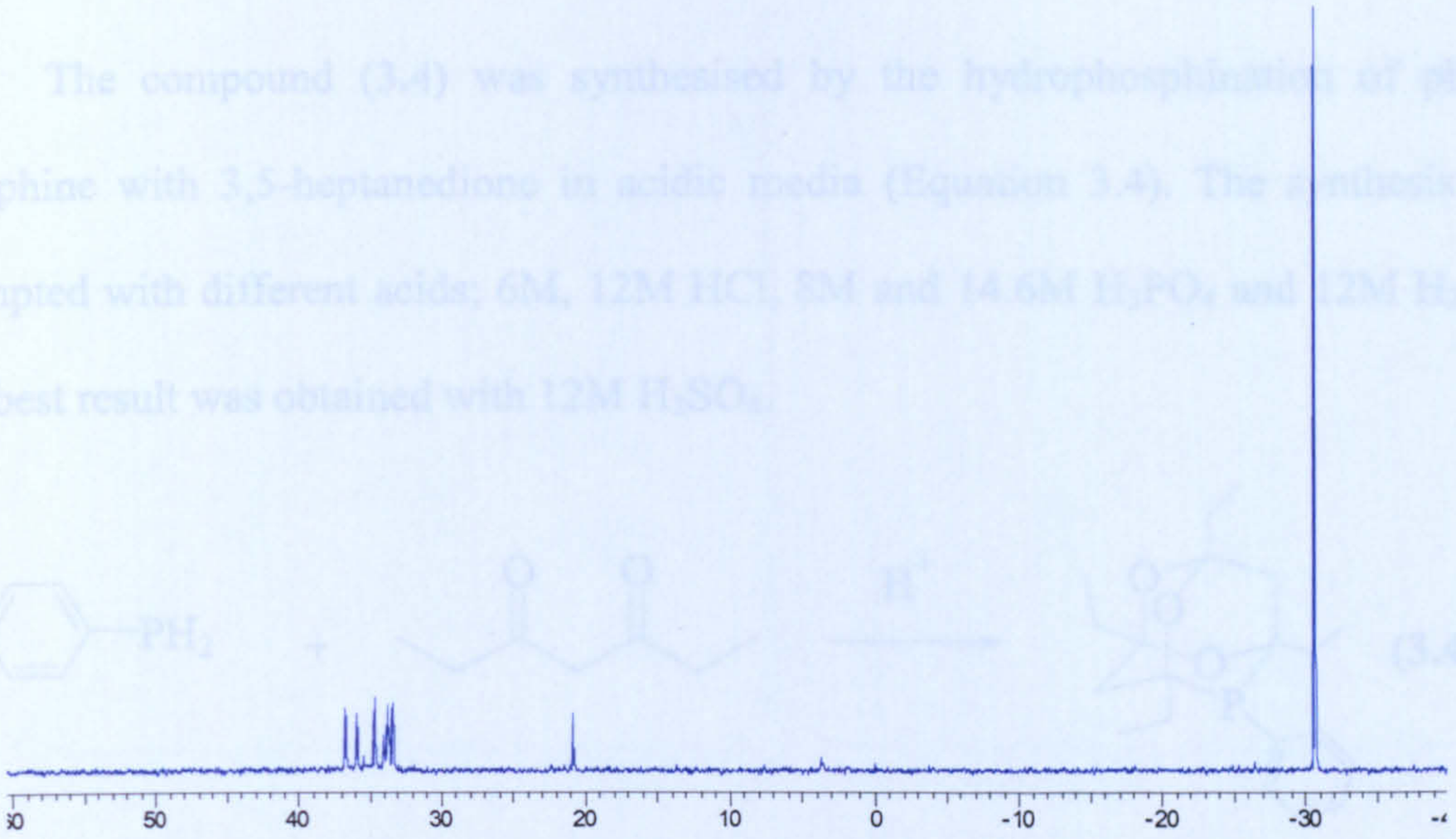

Figure 3.5 $^{31}P\{^{1}H\}$ NMR spectrum of ^{Et}CgPPh (**3.4**) using 14.6M H_3PO_4 after 1 day

Concentrated H_2SO_4

The (**3.4**) synthesis was then attempted under similar conditions, but using 12M H_2SO_4 as the acid catalyst. After one day the $^{31}P\{^{1}H\}$ NMR spectrum (Figure 3.6) indicated that the product had formed in *ca*. 82%. The crude product was purified using a silica column with CH_2Cl_2 as eluent producing (**3.4**) in high yield (75%) and purity.

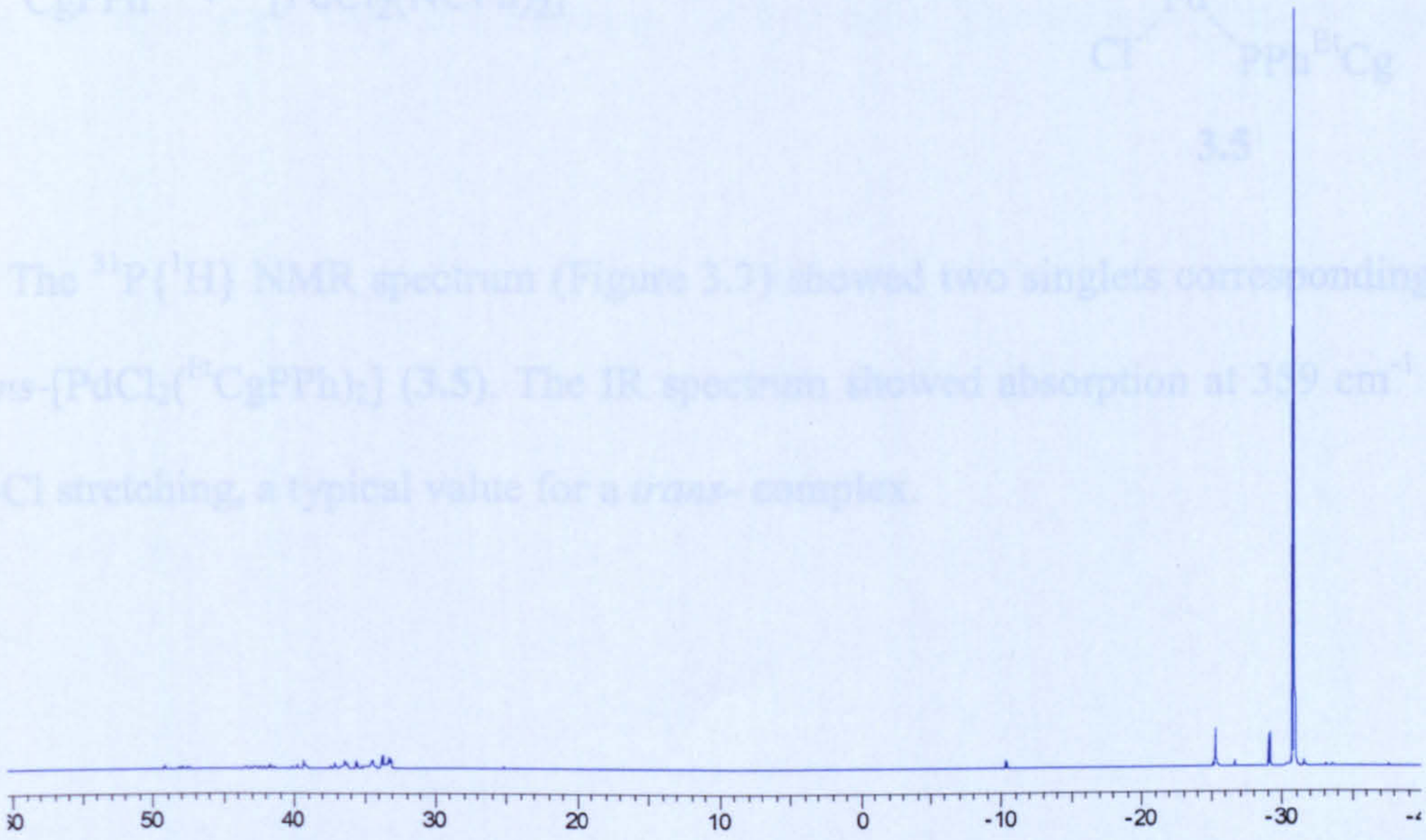

Figure 3.6 $^{31}P\{^{1}H\}$ NMR spectrum of ^{Et}CgPPh (**3.4**) using 12M H_2SO_4 after 1 day

3.2.4.3 Conclusion

The compound **(3.4)** was synthesised by the hydrophosphination of phenyl phosphine with 3,5-heptanedione in acidic media (Equation 3.4). The synthesis was attempted with different acids; 6M, 12M HCl, 8M and 14.6M H_3PO_4 and 12M H_2SO_4. The best result was obtained with 12M H_2SO_4.

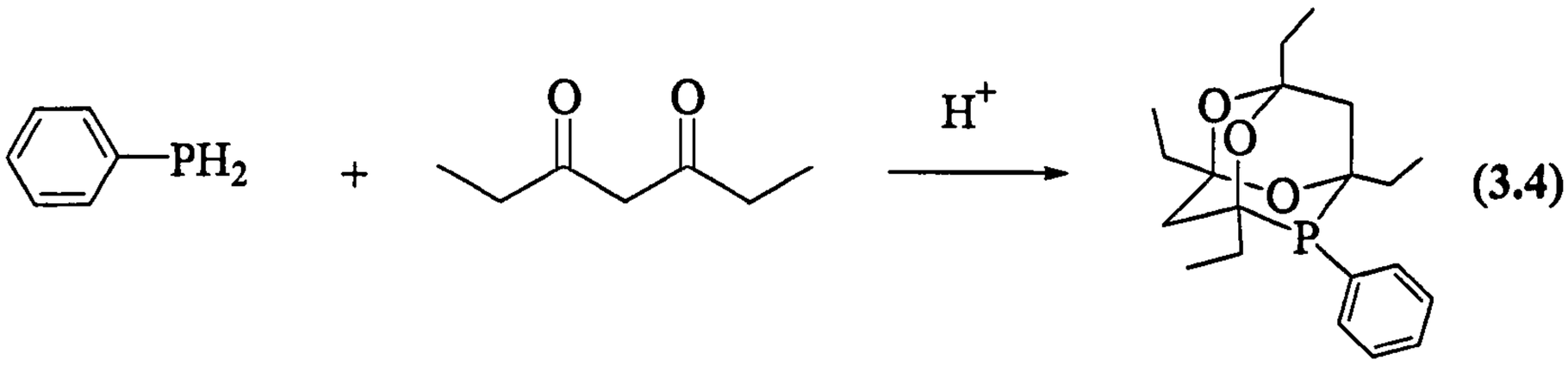

(3.4)

Equation 3.4

3.2.5 Dichloropalladium(II) complex of (3.4)

The reaction of 2.0 equiv. of **(3.4)** with $[PdCl_2(NCPh)_2]$ in CH_2Cl_2 gave a yellow solution. The solvent was evaporated and the solid was isolated and further characterized by $^{31}P\{^1H\}$ NMR, elemental analysis, and X-ray crystallography.

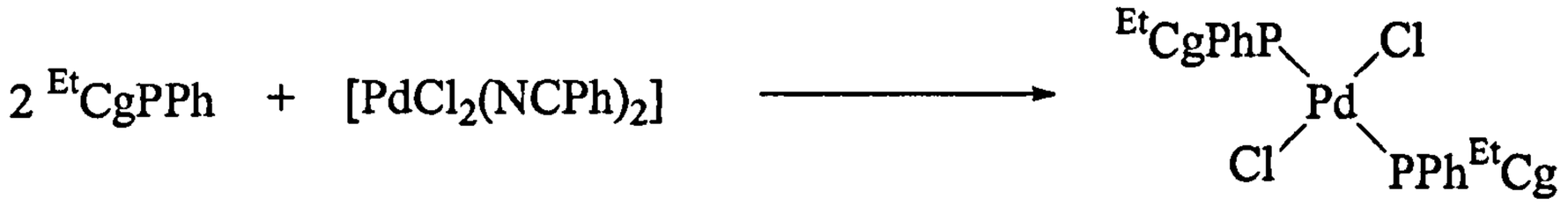

3.5

The $^{31}P\{^1H\}$ NMR spectrum (Figure 3.7) showed two singlets corresponding to the *trans*-$[PdCl_2(^{Et}CgPPh)_2]$ **(3.5)**. The IR spectrum showed absorption at 359 cm^{-1} for the Pd-Cl stretching, a typical value for a *trans*- complex.

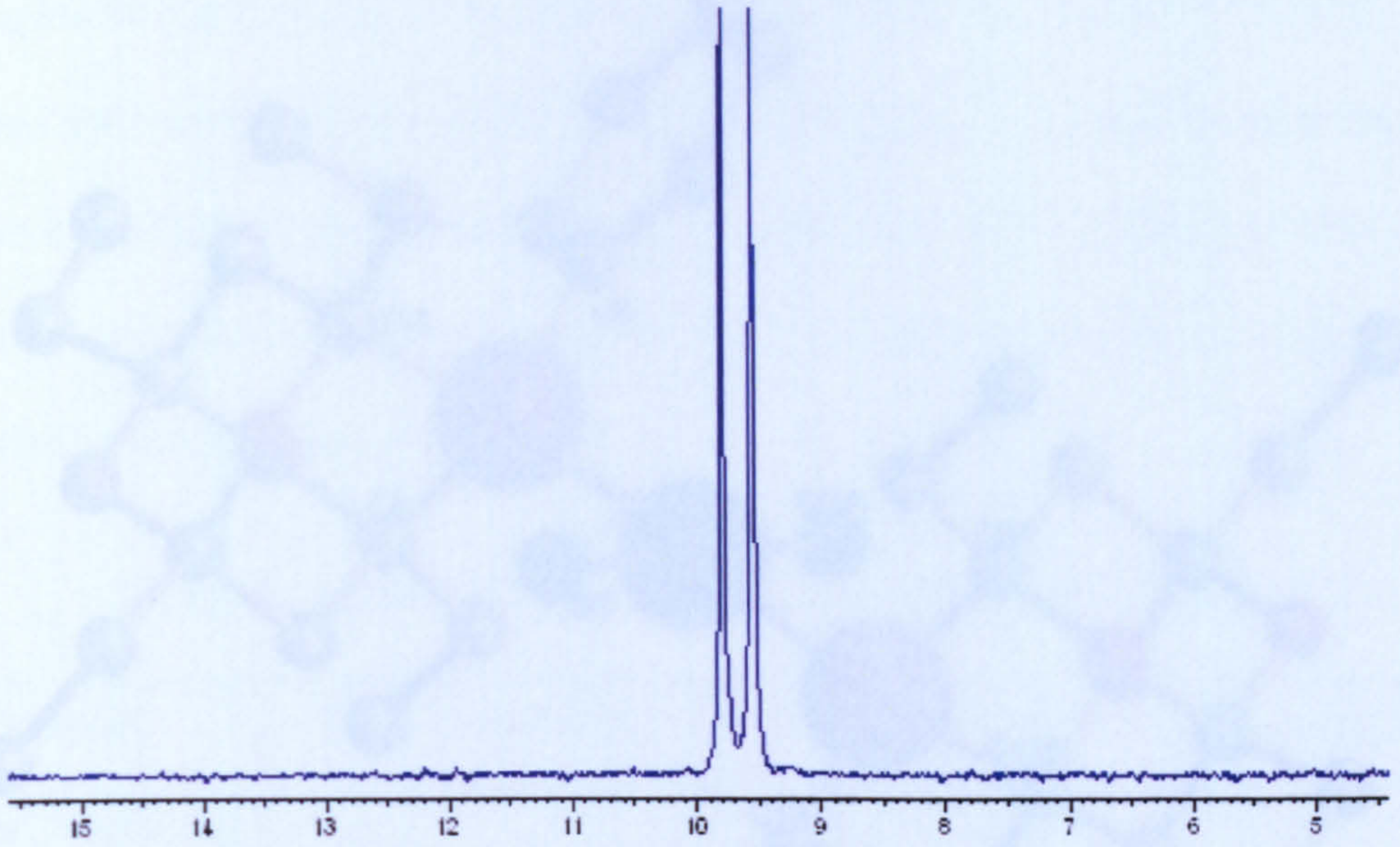

Figure 3.7 $^{31}P\{^{1}H\}$ NMR spectrum of (**3.5**)

Crystals of *trans*-$[PdCl_2(^{Et}CgPPh)_2]$ (**3.5**) were grown by the diffusion of hexane into CH_2Cl_2 solution and the structure determination was carried out by Miss A. Baber of this department, confirming the *trans*- orientation of the ligands. The structure was solved in the monoclinic space group $P2_1/c$ with four formula units per unit cell. The molecular structure is shown in Figure 3.8. The method of data collection, structure solution and refinement are summarised in the Appendix. The cone angle of the ligand (**3.5**) is 157°.

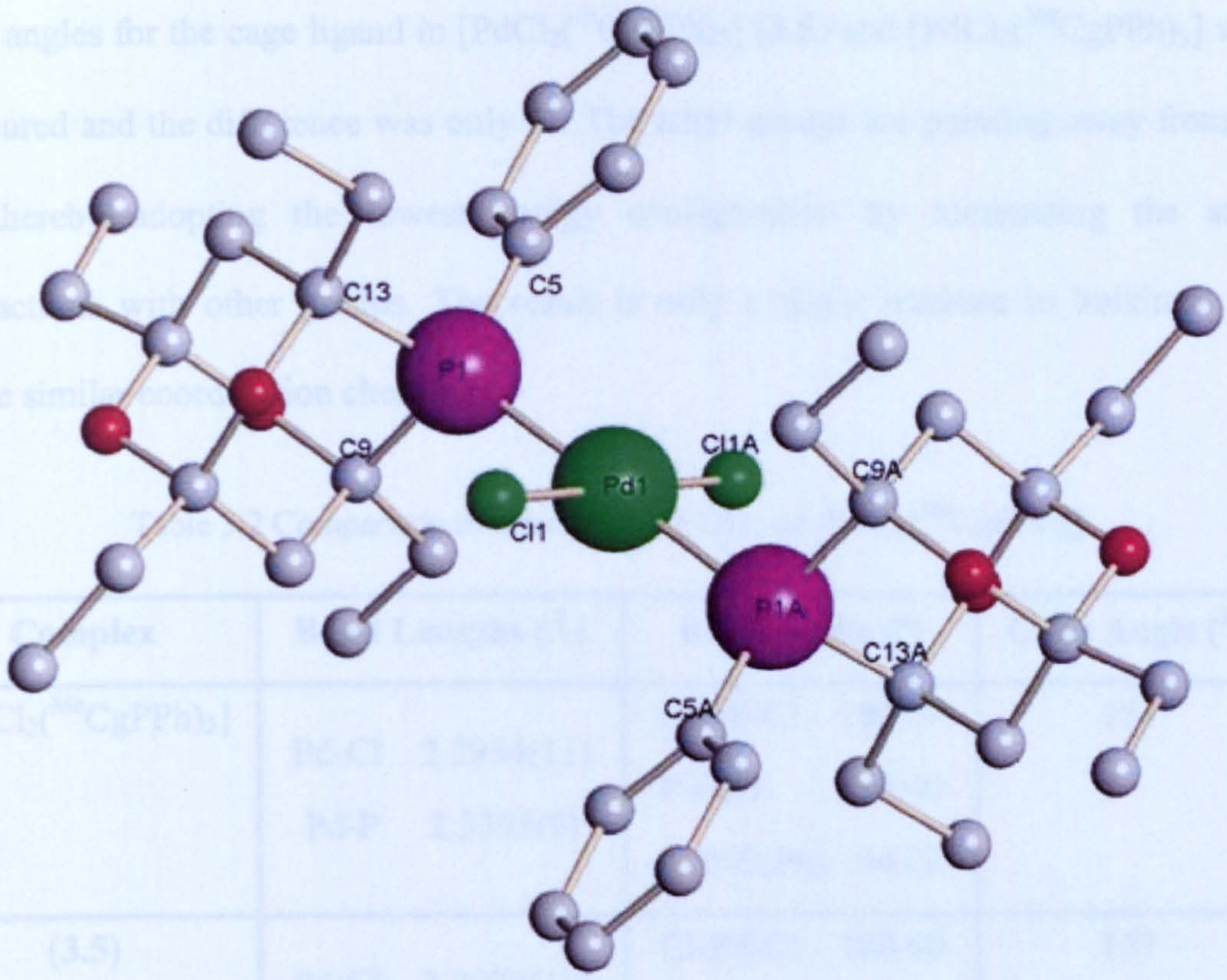

Figure 3.8 Molecular structure of the *trans-meso*-$[PdCl_2(^{Et}CgPPh)_2]$ (**3.5**). Selected atoms are labelled.

Table 3.1 Selected bond lengths and angles for the palladium(II) complex (**3.5**)

Bond	Lengths [Å]	Bond	Angles [°]
Pd(1)-Cl(1)	2.2978(10)	Cl(2)-Pd(1)-Cl(1A)	180.00(5)
Pd(1)-P(1A)	2.3383(9)	Cl(1)-Pd(1)-P(1A)	85.60(3)
P(1)-C(5)	1.816(4)	Cl(1A)-Pd(1)-P(1A)	94.40(3)
P(1)-C(9)	1.863(4)	P(1A)-Pd(1)-P(1)	180.00(4)
C(4)-C(5)	1.393(5)	C(5)-P(1)-C(9)	111.55(17)
O(1)-C(9)	1.445(5)	C(5)-P(1)-C(13)	103.98(16)
C(5)-C(6)	1.394(5)	C(9)-P(1)-C(13)	94.78(16)

The complex has a square planar geometry. A comparison with the $^{Me}CgPPh$ analogue[85] (Table 3.1) shows that both complexes, *trans*-$[PdCl_2(^{Me}CgPPh)_2]$ and *trans*-$[PdCl_2(^{Et}CgPPh)_2]$ (**3.5**), have similar bond lengths between the Pd, P and Cl atoms. The

cone angles for the cage ligand in $[PdCl_2(^{Et}CgPPh)_2]$ (**3.5**) and $[PdCl_2(^{Me}CgPPh)_2]$ were measured and the difference was only 3°. The ethyl groups are pointing away from the Pd thereby adopting the lowest energy configuration by minimising the steric interactions with other groups. The result is only a slight increase in bulkiness and hence similar coordination chemistry.

Table 3.2 Comparison of the complex (**3.5**) and $[PdCl_2(^{Me}CgPPh)_2]$

Complex	Bond Lengths (Å)	Bond Angle (°)	Cone Angle (°)
$[PdCl_2(^{Me}CgPPh)_2]$	Pd-Cl 2.2934(11) Pd-P 2.3395(9)	Cl-Pd-Cl 180.00 P-Pd-P 180.00 C-P-C(Ph) 94.02	154
(**3.5**)	Pd-Cl 2.2978(10) Pd-P 2.3383(9)	Cl-Pd-Cl 180.00 P-Pd-P 180.00 C-P-C(Ph) 94.78	157

3.2.6 Preliminary studies of the dichloroplatinum(II) complex of (3.4)

The reaction of 2.0 equivalents of $^{Et}CgPPh$ (**3.4**) with of $[PtCl_2(cod)]$ in CH_2Cl_2 gave a pale yellow solution. The reaction was monitored by $^{31}P\{^1H\}$ NMR spectroscopy and the spectrum of the solution showed that starting material and two Pt species were present (Equation 3.5).

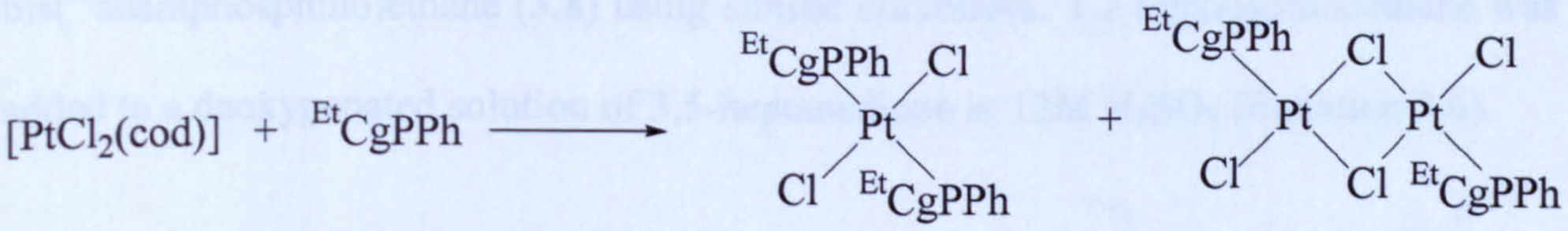

3.6 **3.7**

Equation 3.5

The $^{31}P\{^1H\}$ NMR spectrum (Figure 3.9) revealed two pairs of singlets, due to *meso/rac*-diastereoisomers; one at *ca.* 4.2 ppm (P^3), which is assigned to the monomer

meso/rac-(**3.6**), and one at *ca.* 15.3 ppm (P^4) assigned to the dimer *meso/rac*-(**3.7**); each with Pt satellites (J_{Pt-P} 2682 Hz and 4570 Hz respectively). Further investigation of this reaction should be carried out.

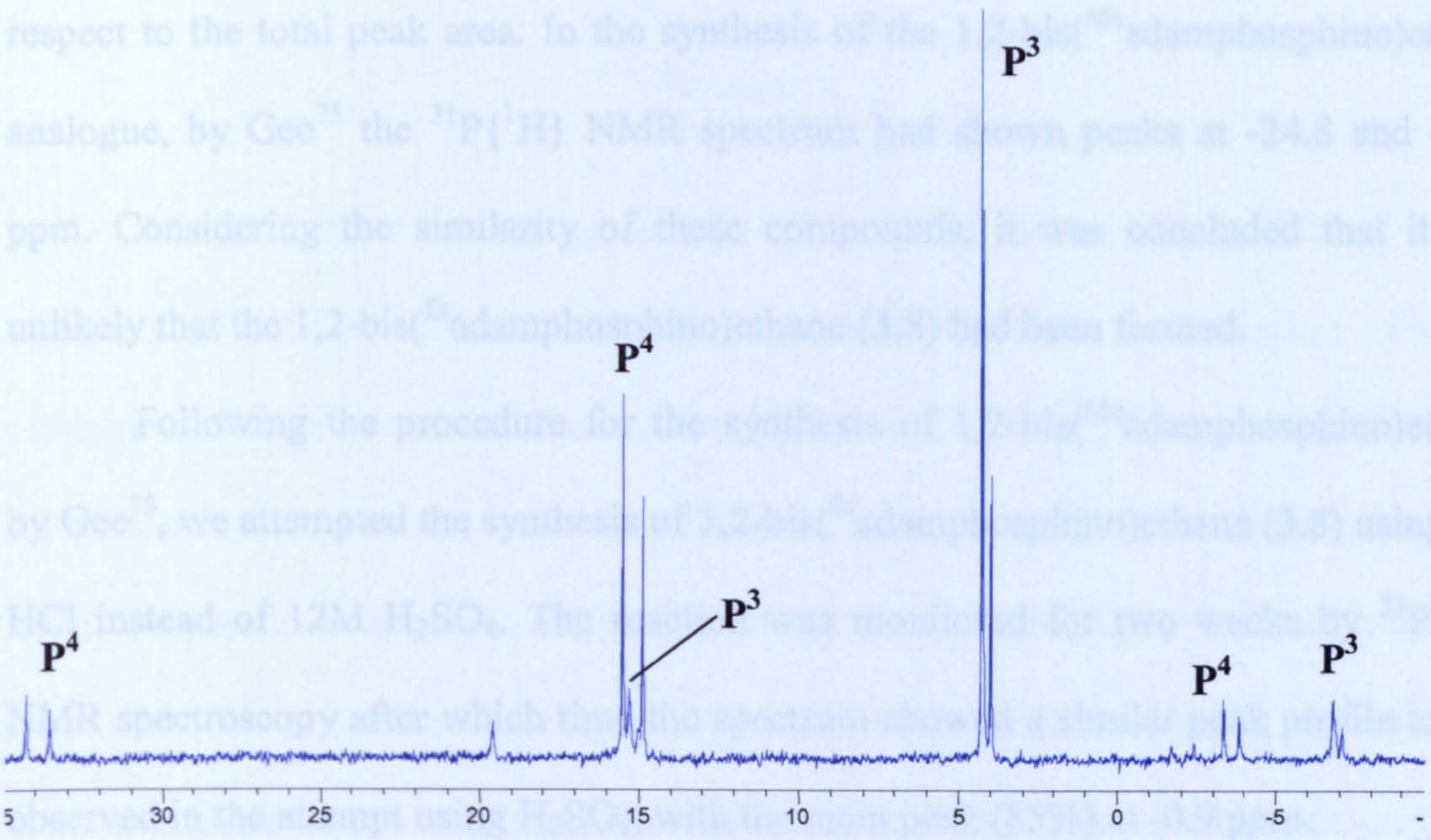

Figure 3.9 $^{31}P\{^1H\}$ NMR spectrum of ^{Et}CgPPh (**3.4**)and $[PtCl_2(cod)]$

3.3 Chemistry of bidentate tetraethyl-trioxa-phospha-adamantanes

3.3.1 Attempted synthesis of 1,2-bis(^{Et}adamphosphino)ethane

The positive results obtained in the synthesis of the monodentate ^{Et}CgPPh (**3.4**) (Section 3.2.4.1) prompted us to attempt the synthesis of the bidentate ligand 1,2-bis(^{Et}adamphosphino)ethane (**3.8**) using similar conditions. 1,2-Diphosphinoethane was added to a deoxygenated solution of 3,5-heptanedione in 12M H_2SO_4 (Equation 3.6).

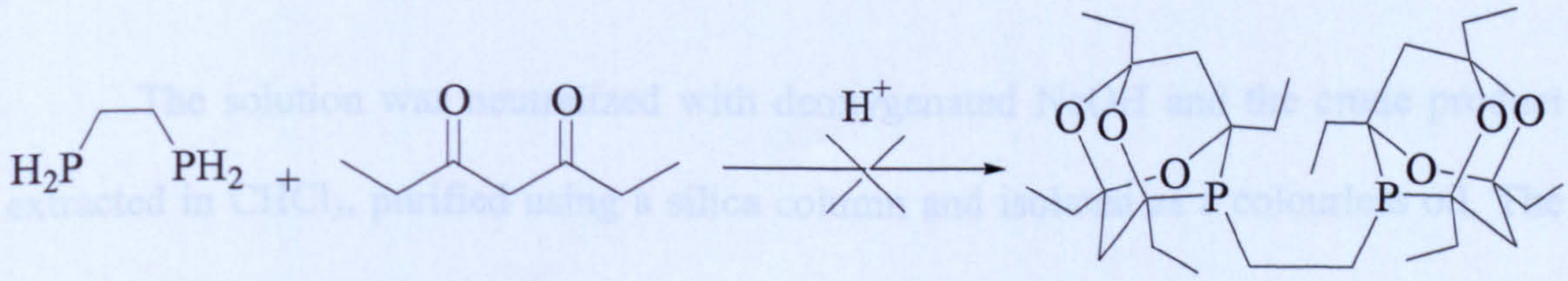

(3.8)

Equation 3.6

The reaction was monitored by $^{31}P\{^{1}H\}$ NMR spectroscopy over one week until the starting material had been completely consumed. The spectrum showed that several peaks had formed and the major product was a singlet at –1.2 ppm in 65% yield with respect to the total peak area. In the synthesis of the 1,2-bis(^{Me}adamphosphino)ethane analogue, by Gee[75] the $^{31}P\{^{1}H\}$ NMR spectrum had shown peaks at -24.8 and -24.9 ppm. Considering the similarity of these compounds, it was concluded that it was unlikely that the 1,2-bis(^{Et}adamphosphino)ethane (**3.8**) had been formed.

Following the procedure for the synthesis of 1,2-bis(^{Me}adamphosphino)ethane by Gee[75], we attempted the synthesis of 1,2-bis(^{Et}adamphosphino)ethane (**3.8**) using 5M HCl instead of 12M H_2SO_4. The reaction was monitored for two weeks by $^{31}P\{^{1}H\}$ NMR spectroscopy after which time the spectrum showed a similar peak profile to that observed in the attempt using H_2SO_4, with the main peak (85%) at -0.9 ppm.

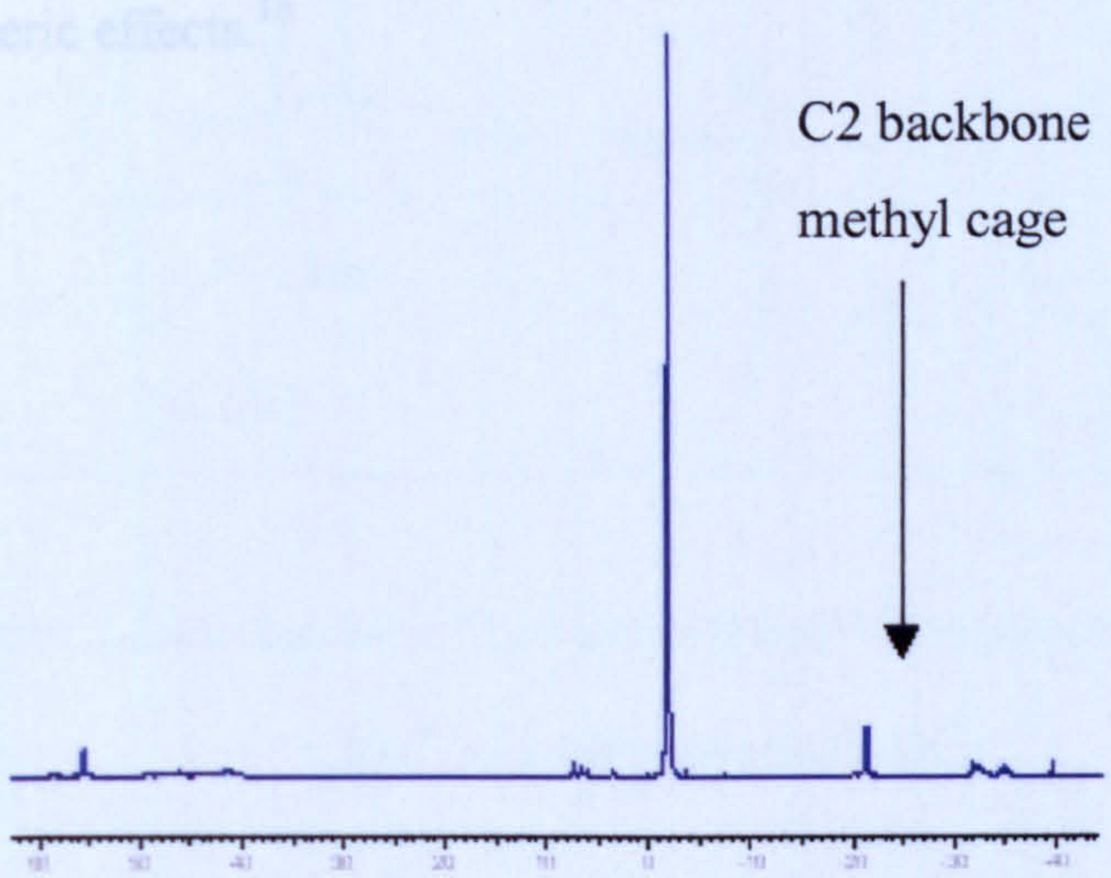

Figure 3.10 $^{31}P\{^{1}H\}$ NMR spectrum of attempted synthesis of 1,2-bis(^{Et}adamphosphino)ethane

The solution was neutralized with deoxygenated NaOH and the crude product extracted in $CHCl_3$, purified using a silica column and isolated as a colourless oil. The product was characterized by elemental analysis and mass spectrometry and the results indicated that instead of the desired bidentate ligand, the product of the reaction was (**3.9**) (shown in Equation 3.7).

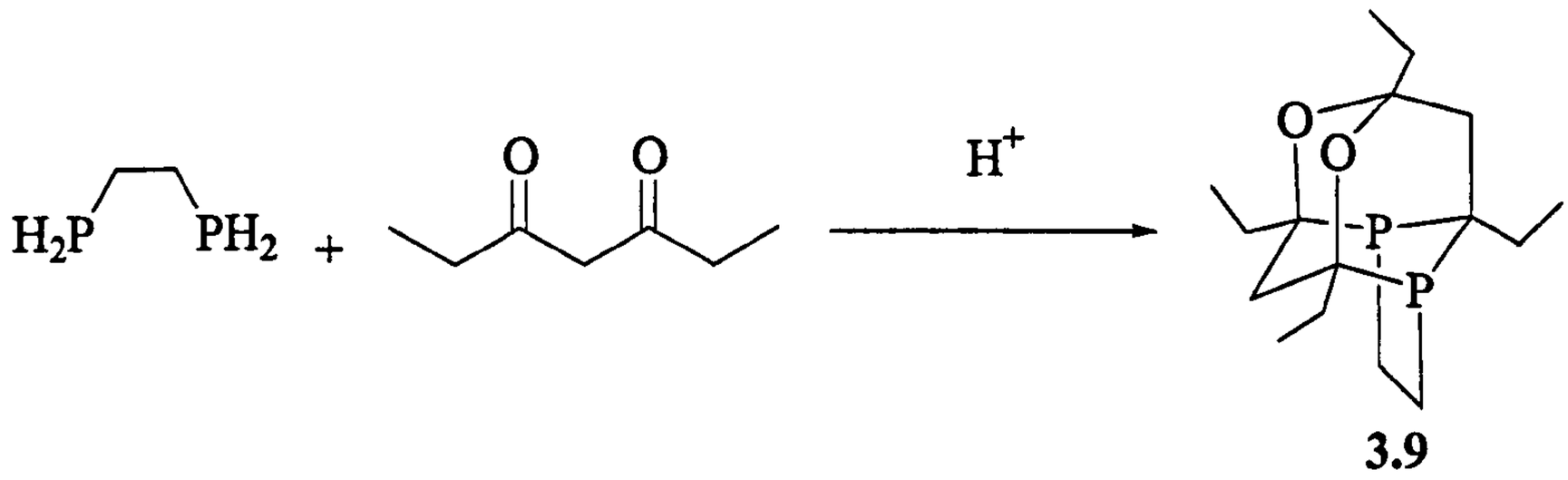

3.9

Equation 3.7

A similar product was present in the reaction carried out by Gee,[75] in the synthesis of 1,2-bis(^{Me}adamphosphino)ethane, but in a very low amount (5%). A mechanism was proposed by Gee[75] for the formation of this by-product, Scheme 3.2. This mechanism shows the formation of a 5-membered ring after the hydrophosphination step (i). The increase in the yield of this by-product shows that the ethyl group in the ketone has a significant influence on the course of the reaction. This is an example of the Thorpe-Ingold or the *gem*- dialkyl effect, in which cyclisation is promoted by steric effects.[16]

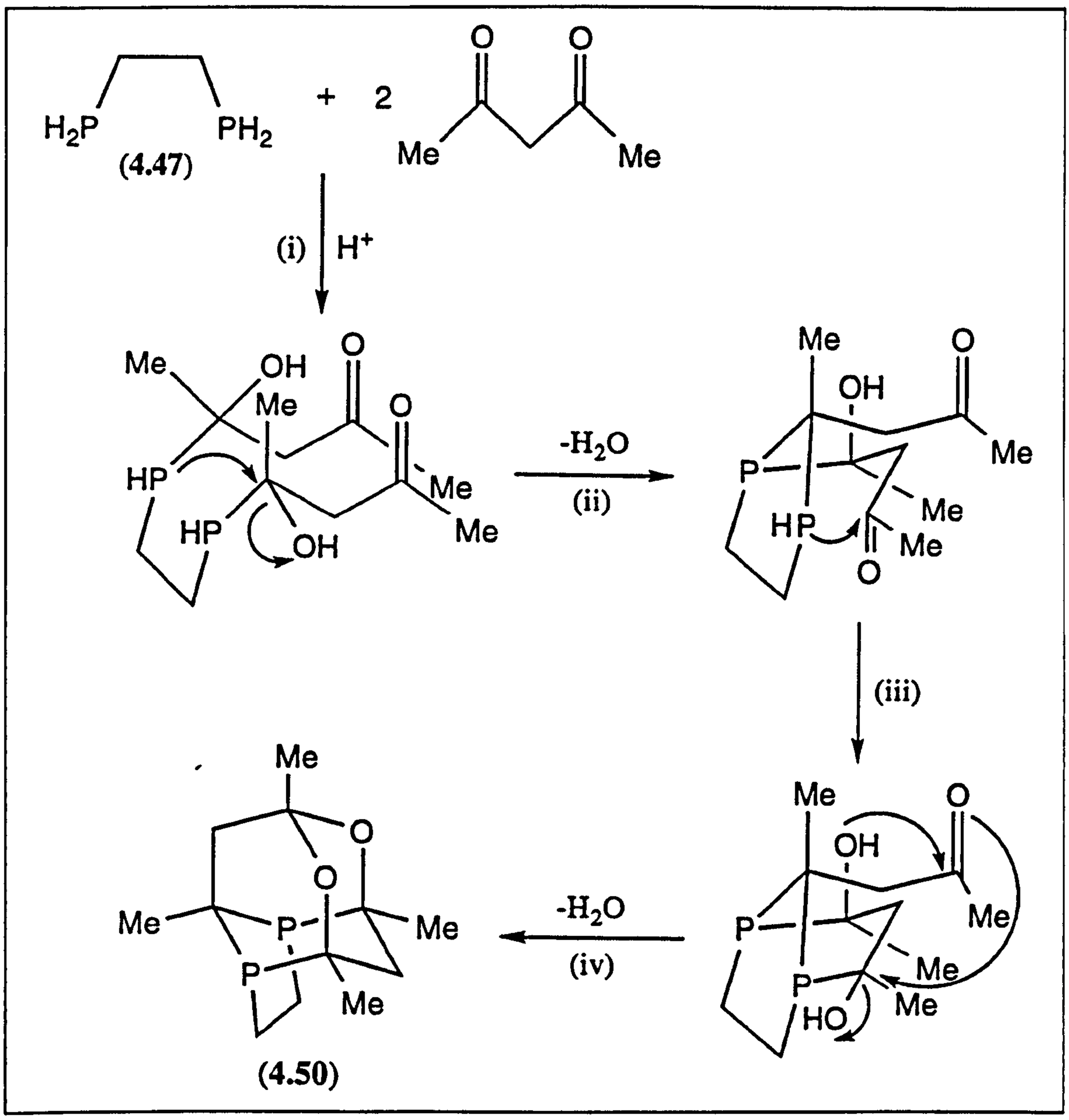

Scheme 3.2 Mechanism of by-product formation in the synthesis of 1,2-bis(^{Me}adamphosphino)ethane[75]

3.3.2 Synthesis of *meso/rac*-1,3-bis(^{Et}adamphosphino)propane (3.10)

The synthesis of the 1,3-bis(^{Et}adamphosphino)propane **(3.10)** (Equation 3.8) was attempted by the addition of the 1,3-diphosphinopropane to a deoxygenated solution of 3,5-heptanedione in 6M HCl. The reaction was monitored by $^{31}P\{^{1}H\}$ NMR and the spectrum showed, after one month, the desired product in 47% yield. In a second attempt, the acid concentration was increased from 6M to 10M but no significant

change was observed in the $^{31}P\{^{1}H\}$ NMR spectrum nor in the reaction time. In view of the results discussed above in Section 3.2.4.2 where changing the acid increased the rate and yield of the hydrophosphination reaction, the effect of changing acid to H_2SO_4 and H_3PO_4 on Equation 3.8 reaction was studied.

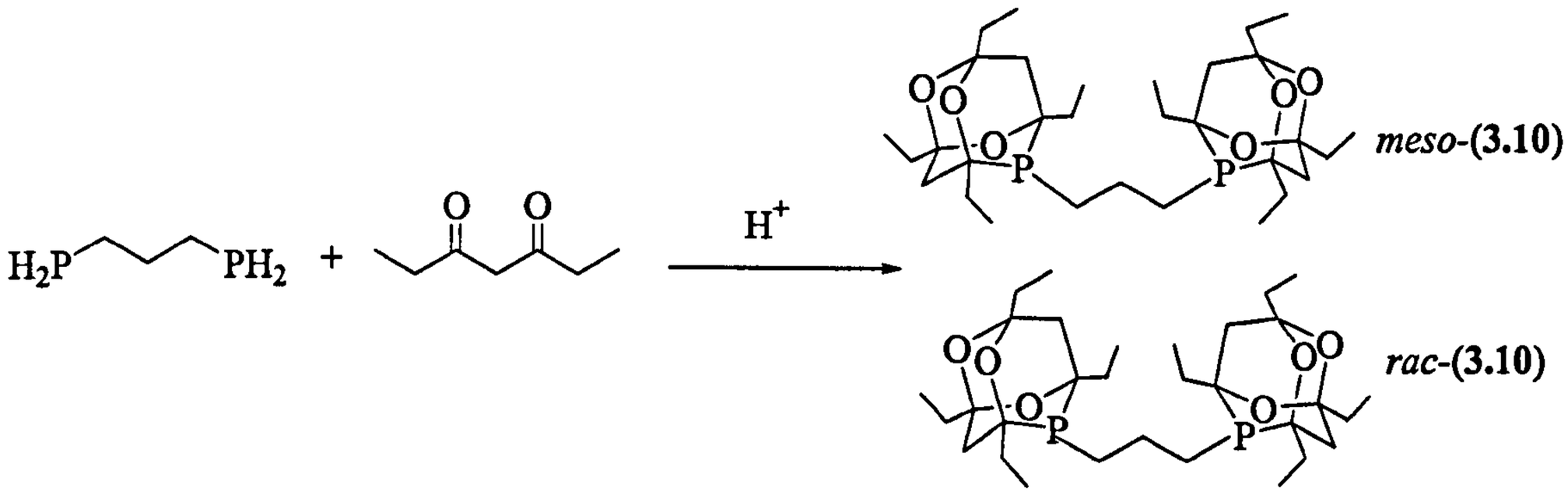

Equation 3.8

3.3.2.1 Variation of the acid type on the synthesis of 1,3-bis(^{Et}adamphosphino) propane

Concentrated H_3PO_4

The synthesis of 1,3-bis(^{Et}adamphosphino)propane **(3.10)** (Equation 3.8) was attempted with 8M H_3PO_4. The $^{31}P\{^{1}H\}$ NMR spectrum of the reaction mixture showed after 2 weeks the desired product had formed in only 2.5%, with an unidentified major product at 26.6 ppm (51%).

Concentrated H_2SO_4

The synthesis of 1,3-bis(^{Et}adamphosphino)propane **(3.10)** was attempted, (Equation 3.8) with 12M H_2SO_4. The $^{31}P\{^{1}H\}$ NMR spectrum of the reaction mixture showed that after 36 h, the desired product had formed in *ca.* 85% yield. The crude product was neutralized with 5M NaOH, extracted with $CHCl_3$ and purified with a silica column using $Et_2O/CHCl_3$ 80:20 as eluent. The product was isolated as a pale yellow oil in high yield (80%) and high purity.

The $^{31}P\{^{1}H\}$ NMR spectrum showed two singlets at –37.9 and –38.2 ppm in a ratio of *ca* 1:1 corresponding to the *meso*- and *rac*-**(3.10)** diastereoisomers. The product was further characterized by ^{1}H and $^{13}C\{^{1}H\}$ NMR spectroscopy, mass spectrometry and elemental analysis.

3.3.3 Dichloroplatinum(II) complex (3.11)

The reaction of *meso/rac*-**(3.10)** with 1.0 equiv. of $[PtCl_2(cod)]$ in CH_2Cl_2 gave a pale yellow solution. The solvent was removed in *vacuo* and a pale yellow solid was recovered and characterized as *meso/rac*-**(3.11)** by $^{31}P\{^{1}H\}$ NMR, mass spectrometry and elemental analysis.

The $^{31}P\{^{1}H\}$ NMR spectrum (Figure 3.11) showed two signals at –15.7 and –19.4 ppm with platinum satellites (^{1}J(PtP) 3388 Hz and ^{1}J(PtP) 3386 Hz). The presence of two peaks in the $^{31}P\{^{1}H\}$ NMR spectrum is due to the existence of the *meso*- and *rac*-diastereoisomers in a ratio of 1.2:1. In the $^{31}P\{^{1}H\}$ NMR spectrum, there is a separation of almost 4 ppm between the two signals for the diastereoisomers. This may imply that the environment of the phosphorus atoms in the two structures are quite different and it would be of interest to investigate any differences in catalytic activities between the diastereoisomers. Pugh[73] found that catalytic activity of the *meso*-1,3-bis(^{Me}adamphosphino)propane was 3.6 times faster than the *rac*-isomer in the hydrocarbonylation of propene.

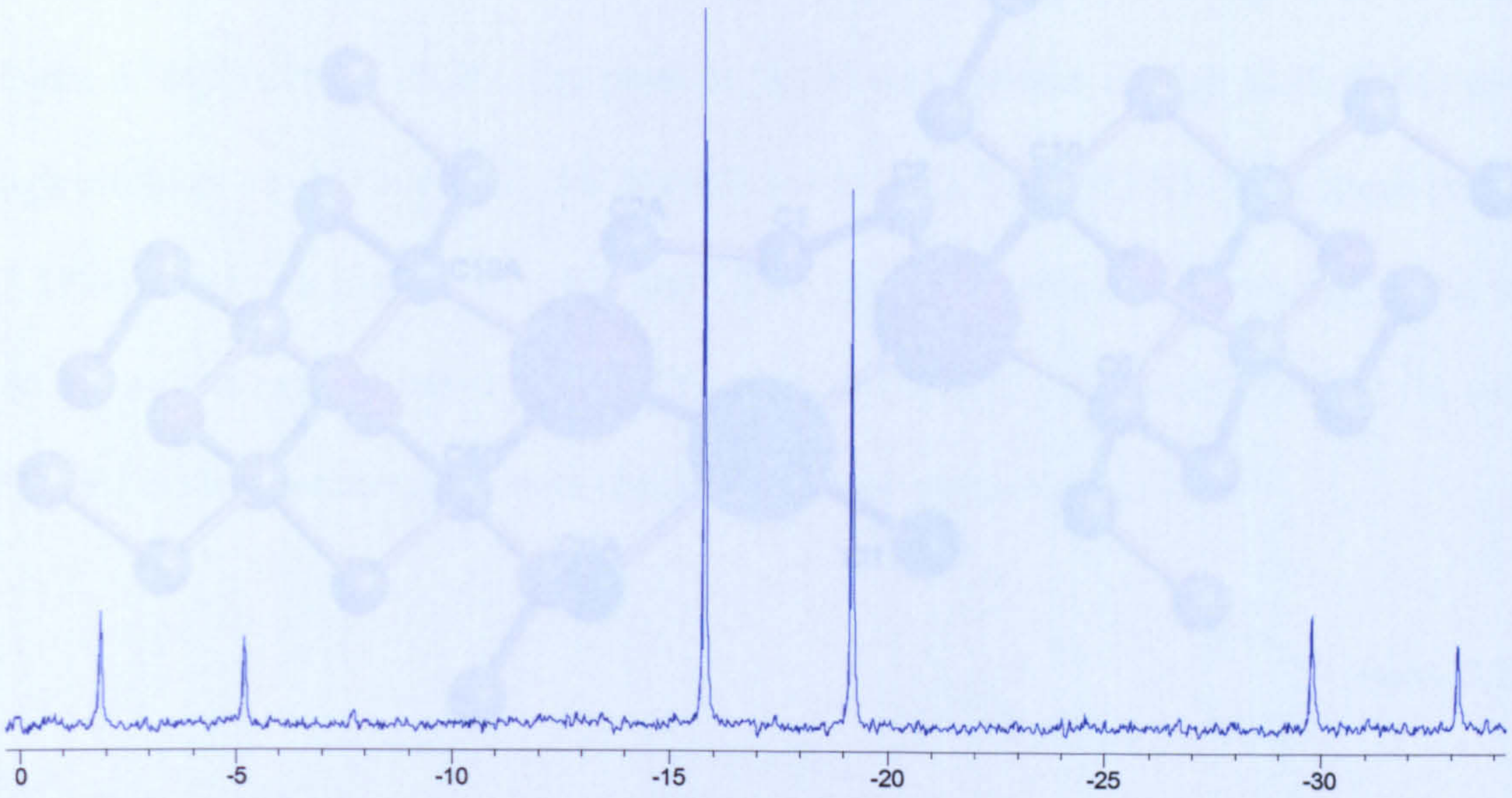

Figure 3.11 $^{31}P\{^{1}H\}$ NMR spectrum of *meso/rac*-[$PtCl_2$(**3.11**)]

3.3.4 Dichloropalladium(II) complex of (3.10)

The reaction of *meso/rac*-(**3.10**) with 1.0 equiv. of [$PdCl_2(NCPh)_2$] in CH_2Cl_2 gave a yellow solution. The $^{31}P\{^{1}H\}$ NMR spectrum showed that several products had formed, but two predominant singlets (89%) at 0.4 and 2.7 ppm were assigned to the chelate products (**3.12**). Others peaks from 8.7 to 10.1 ppm may be binuclear species. Single crystals were grown by slow evaporation of the solvent. The structure determination was carried out by Miss A. Baber of this department, confirming the *cis*-orientation of the ligands around the palladium(II) metal. The structure was solved in the monoclinic space group P2(1)/m with four formula units per unit cell, and the crystal was shown to be exclusively the *meso*-diastereoisomer. The method of data collection, structure solution and refinement are summarised in the Appendix. The molecular structure is shown in Figure 3.12.

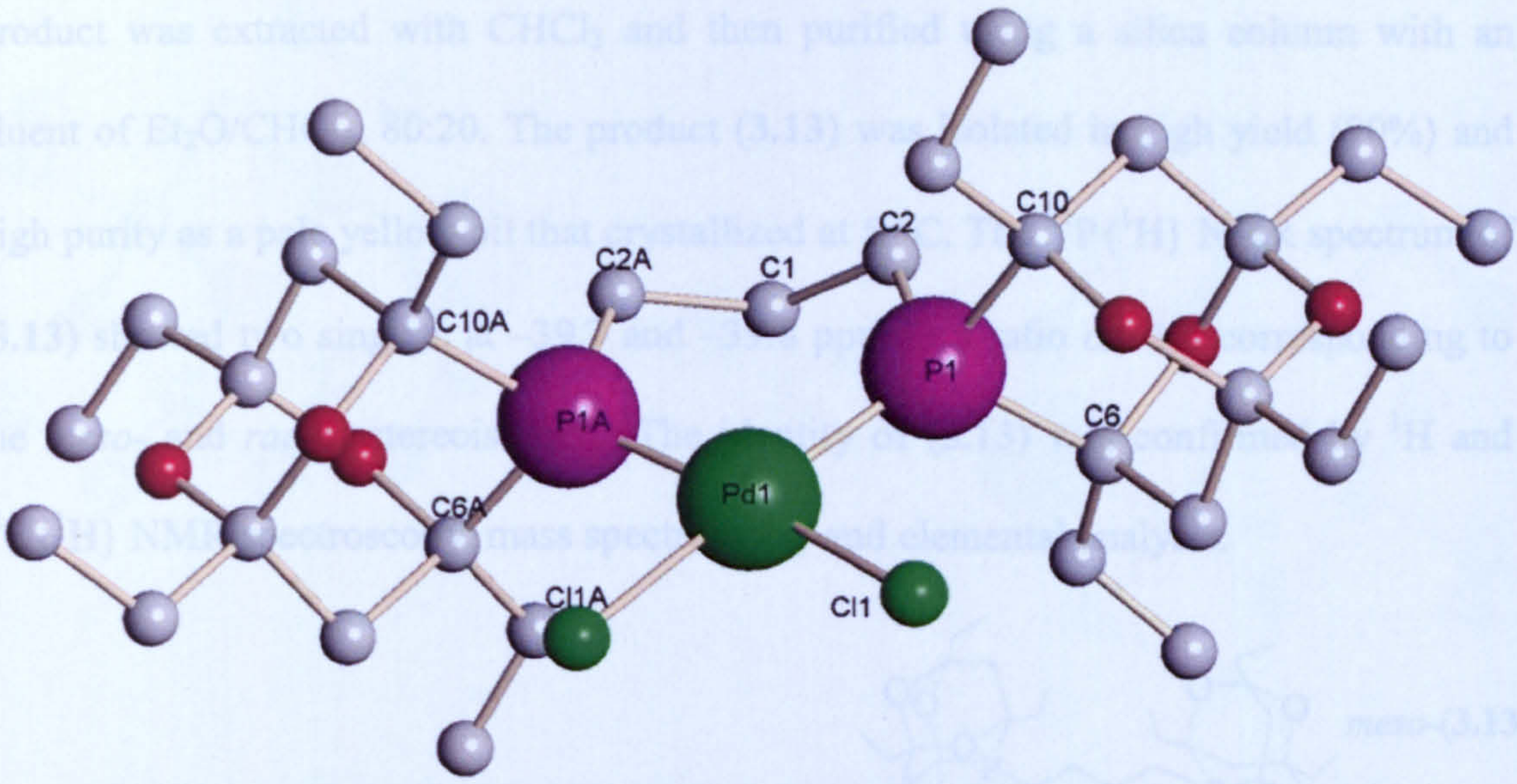

Figure 3.12 Molecular structure of the ligand (**3.12**). Selected atoms are labelled

Table 3.3 Selected bond lengths and angles for the palladium(II) complex (**3.12**)

Bond	Lengths [Å]	Bond	Angles [°]
Pd(1)-Cl(1A)	2.351(8)	Cl(1A)-Pd(1)-Cl(1)	83.9(4)
Pd(1)-P(1A)	2.283(8)	P(1)-Pd(1)-Cl(1)	173.4(3)
P(1)-C(2)	1.76(3)	P(1)-Pd(1)-P(1A)	96.40(4)
P(1)-C(6)	1.89(3)	C(2)-P(1)-Cl(6)	98.9(13)
C(1)-C(2)	1.58(3)	C(2)-P(1)-C(10)	104.1(14)
O(1)-C(6)	1.42(3)	C(6)-P(1)-C(10)	94.3(13)
C(5)-C(6)	1.394(5)	C(10)-P(1)-Pd(1)	115.3(9)

3.3.5 Synthesis of *meso/rac*-1,4-bis(^{Et}adamphosphino) butane (3.13)

The synthesis of 1,4-bis(^{Et}adamphosphino)butane (**3.13**) was carried out by the addition of 1,4-diphosphinobutane to a deoxygenated solution of 3,5-heptanedione in a aqueous solution of 12M H_2SO_4 (Equation 3.9). The reaction was monitored by $^{31}P\{^1H\}$ NMR spectroscopy for 2 days, after which time the reaction had gone to completion and a yellow oil had appeared. The mixture was neutralized with 5M NaOH, the crude

product was extracted with $CHCl_3$ and then purified using a silica column with an eluent of $Et_2O/CHCl_3$, 80:20. The product **(3.13)** was isolated in high yield (90%) and high purity as a pale yellow oil that crystallized at 5 °C. The $^{31}P\{^1H\}$ NMR spectrum of **(3.13)** showed two singlets at –39.7 and –39.8 ppm in a ratio *ca.* 1:1 corresponding to the *meso*- and *rac*-diastereoisomers. The identity of **(3.13)** was confirmed by ^1H and $^{13}C\{^1H\}$ NMR spectroscopy, mass spectrometry and elemental analysis.

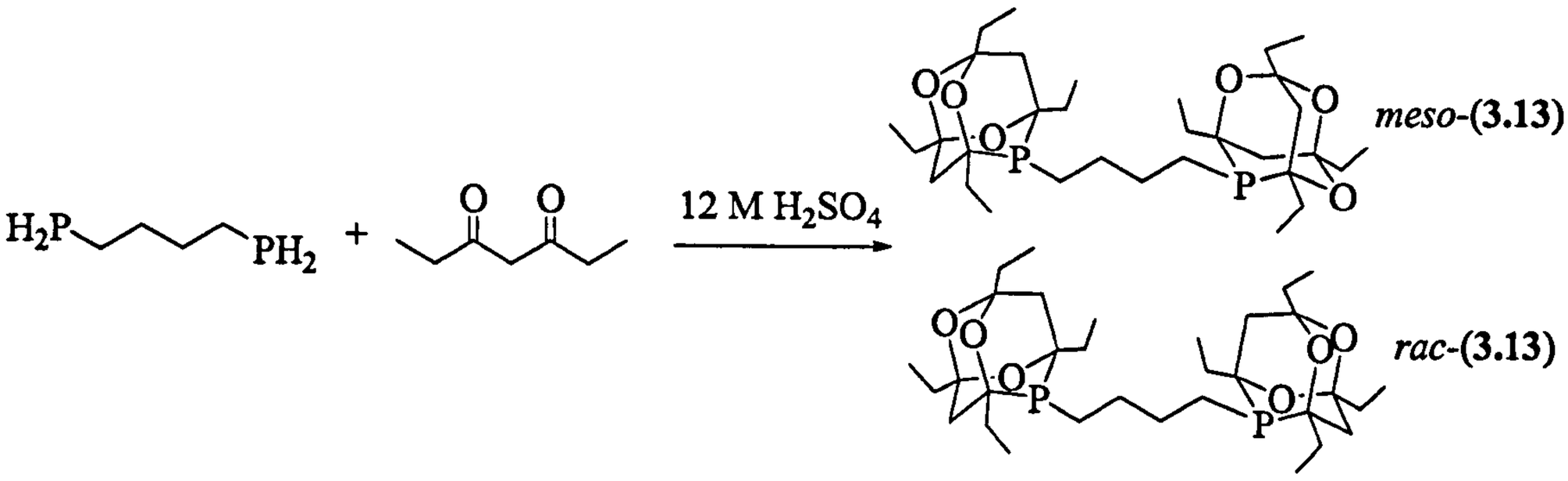

Equation 3.9

Single crystals of the *meso* form cage-diphosphine **(3.13)** suitable for *X*-ray diffraction were grown by the slow evaporation of solvent from a dichloromethane solution. The structure determination was carried out by Miss A. Baber of this department, confirming the molecular structure of the ligand. The structure was solved in the triclinic space group P-1 with one molecule per unit cell. The molecular structure is shown in Figure 3.13. The method of data collection, structure solution and refinement are summarised in the Appendix.

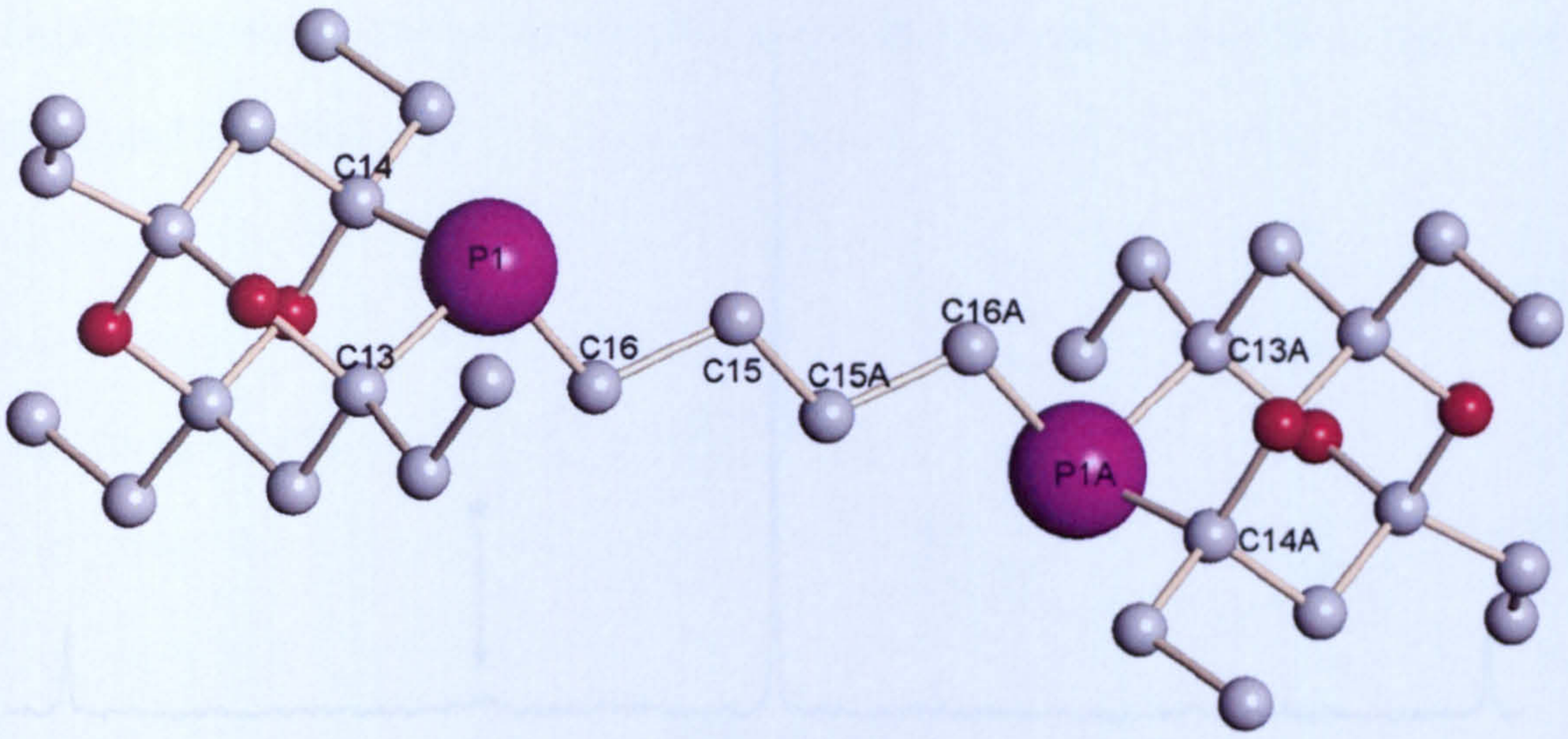

Figure 3.13 Molecular structure of the ligand (**3.13**). Selected atoms are labelled

Table 3.4 Selected bond lengths and angles for ligand (**3.13**)

Bond	Lengths [Å]	Bond	Angles [°]
P(1)-C(16)	1.850(5)	C(16)-P(1)-C(14)	102.7(3)
P(1)-C(14)	1.870(6)	C(16)-P(1)-C(13)	102.8(3)
P(1)-C(13)	1.894(6)	C(14)-P(1)-C(13)	92.4(3)
O(2)-C(13)	1.452(7)	C(12)-O(2)-C(13)	113.9(5)
C(16)-C(15)	1.527(7)	C(11)-O(1)-C(14)	115.1(5)

3.3.6 Dichloroplatinum(II) complex of (3.13)

The reaction of *meso/rac*-(**3.13**) with 1.0 equiv. of $[PtCl_2(cod)]$ in CH_2Cl_2 gave a pale yellow solution. The solvent was removed in *vacuo* and a pale yellow solid was recovered. The solid was characterized as *meso/rac*-(**3.14**) by $^{31}P\{^1H\}$ NMR (Figure 3.14), mass spectrometry and elemental analysis.

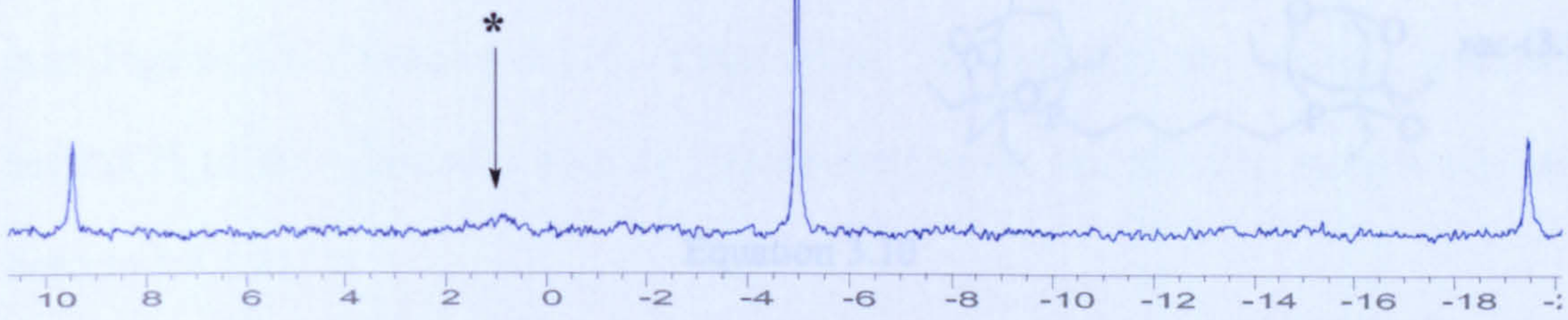

Figure 3.14 $^{31}P\{^{1}H\}$ NMR spectrum of the dichloroplatinum(II) complex (**3.14**)

The $^{31}P\{^{1}H\}$ NMR spectrum of (**3.14**) showed one signal at –5 ppm with platinum satellites (^{1}J(PtP) 3512 Hz). The presence of two peaks in the $^{31}P\{^{1}H\}$ NMR spectrum is expected due to the existence of the *meso*- and *rac*-diastereoisomers. The observed single in the $^{31}P\{^{1}H\}$ NMR spectrum is presumably due to coincidental equivalence. The broad signal at *ca.* 1 ppm (marked * in Figure 3.14) is possibly due to the presence of oligomeric complexes (see Section 3.3.7 for further discussion).

3.3.7 Synthesis and characterisation of *meso/rac*-1,5-bis(^{Et}adamphosphino)-pentane (3.15)

The synthesis of the *meso/rac*-1,5-bis(^{Et}adamphosphino)pentane (**3.15**) was carried out by the addition of 1,5-diphosphinopentane to a deoxygenated solution of 3,5-heptanedione in an aqueous solution of 12M H_2SO_4 (Equation 3.10). The reaction was monitored by $^{31}P\{^{1}H\}$ NMR spectroscopy over 2 days, after which time the reaction had gone to completion and a yellow oil had formed in the reaction mixture. The mixture was neutralized with a deoxygenated solution of 5M NaOH, the crude product was extracted with $CHCl_3$ and then purified using a silica column with an eluent of

$Et_2O/CHCl_3$, 80:20. The product (**3.15**) was isolated as a pale yellow oil in high yield (90%) and high purity.

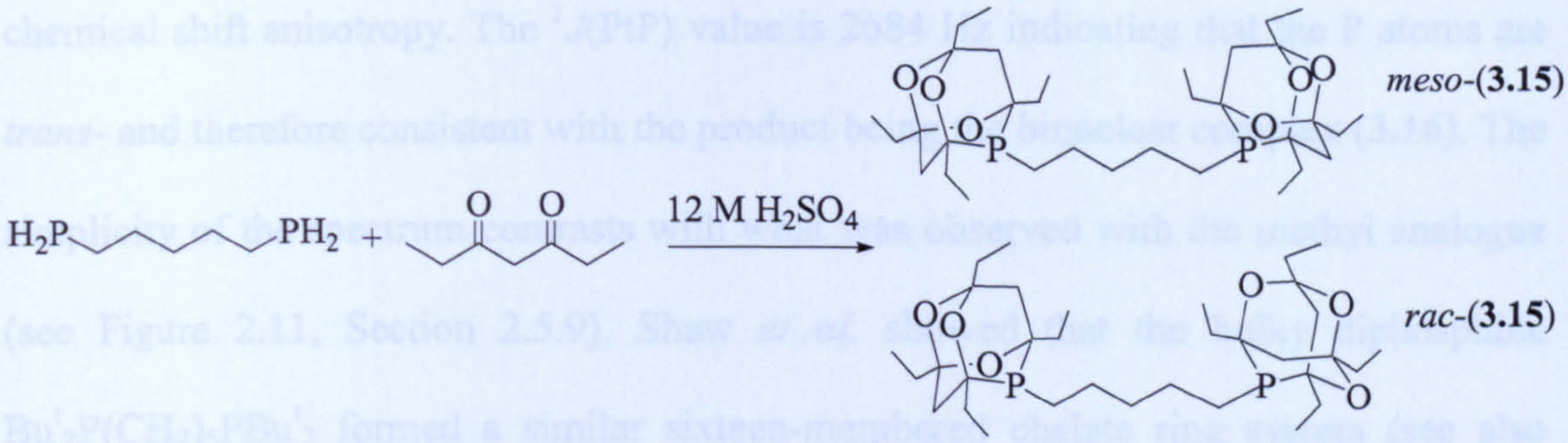

Equation 3.10

The $^{31}P\{^1H\}$ NMR spectrum of (**3.15**) showed two singlets at -36.4 and -36.5 ppm in a ratio *ca.* 1:1 corresponding to the *meso*- and *rac*-diastereoisomers (Figure 3.15). The isomers were characterized by ^1H and $^{13}C\{^1H\}$ NMR spectroscopy, mass spectrometry and elemental analysis.

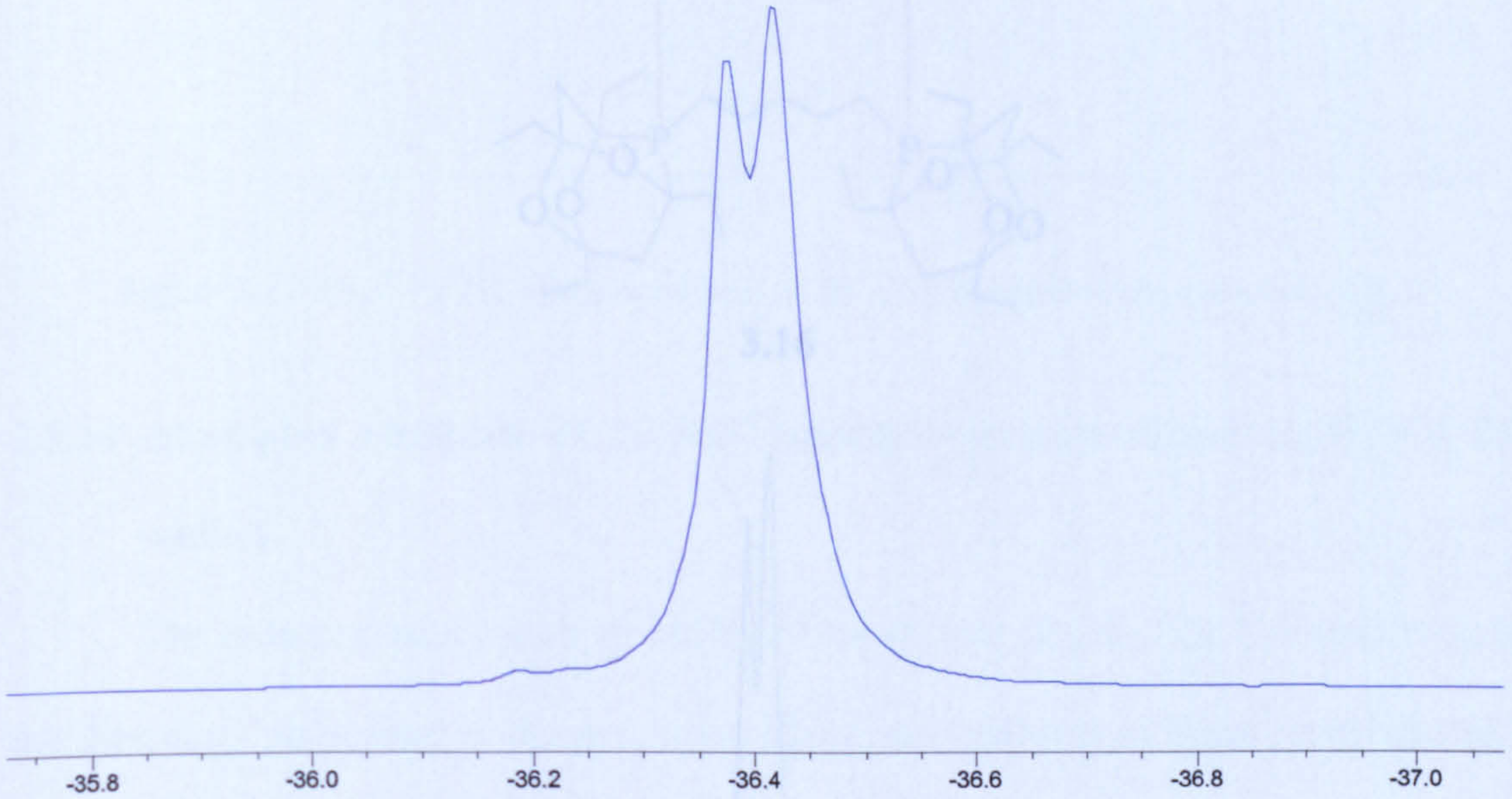

Figure 3.15 $^{31}P\{^1H\}$NMR spectrum of 1,5-bis(^{Et}adamphosphino)pentane (**3.15**)

3.3.8 Dichloroplatinum(II) complex of (3.15)

The reaction of *meso/rac*-(**3.15**) with 1.0 equiv. of $[PtCl_2(cod)]$ in CH_2Cl_2 gave a pale yellow solution. The solvent was removed in *vacuo* and a pale yellow solid was isolated.

The $^{31}P\{^{1}H\}$ NMR spectrum (Figure 3.16) of the product showed two singlets at 1.5 ppm with broad platinum satellites. The platinum satellites are broad due to chemical shift anisotropy. The ^{1}J(PtP) value is 2684 Hz indicating that the P atoms are *trans*- and therefore consistent with the product being the binuclear complex (**3.16**). The simplicity of the spectrum contrasts with what was observed with the methyl analogue (see Figure 2.11, Section 2.5.9). Shaw *et al.* showed that the bulky diphosphine $Bu^{t}_{2}P(CH_2)_5PBu^{t}_{2}$ formed a similar sixteen-membered chelate ring system (see also Section 1.4.1.9).[16]

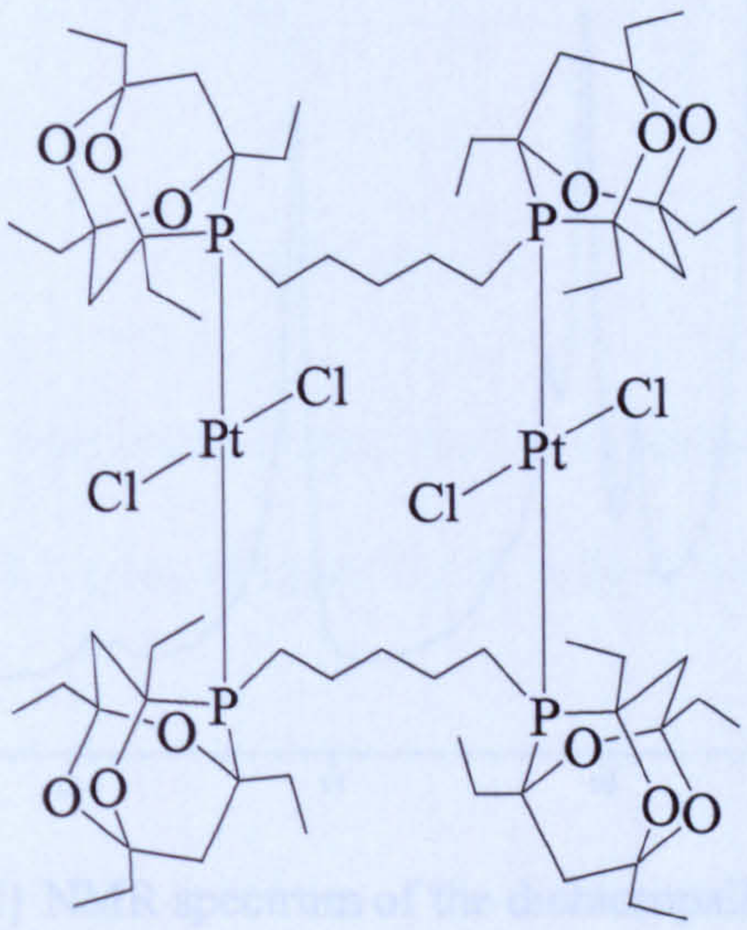

3.16

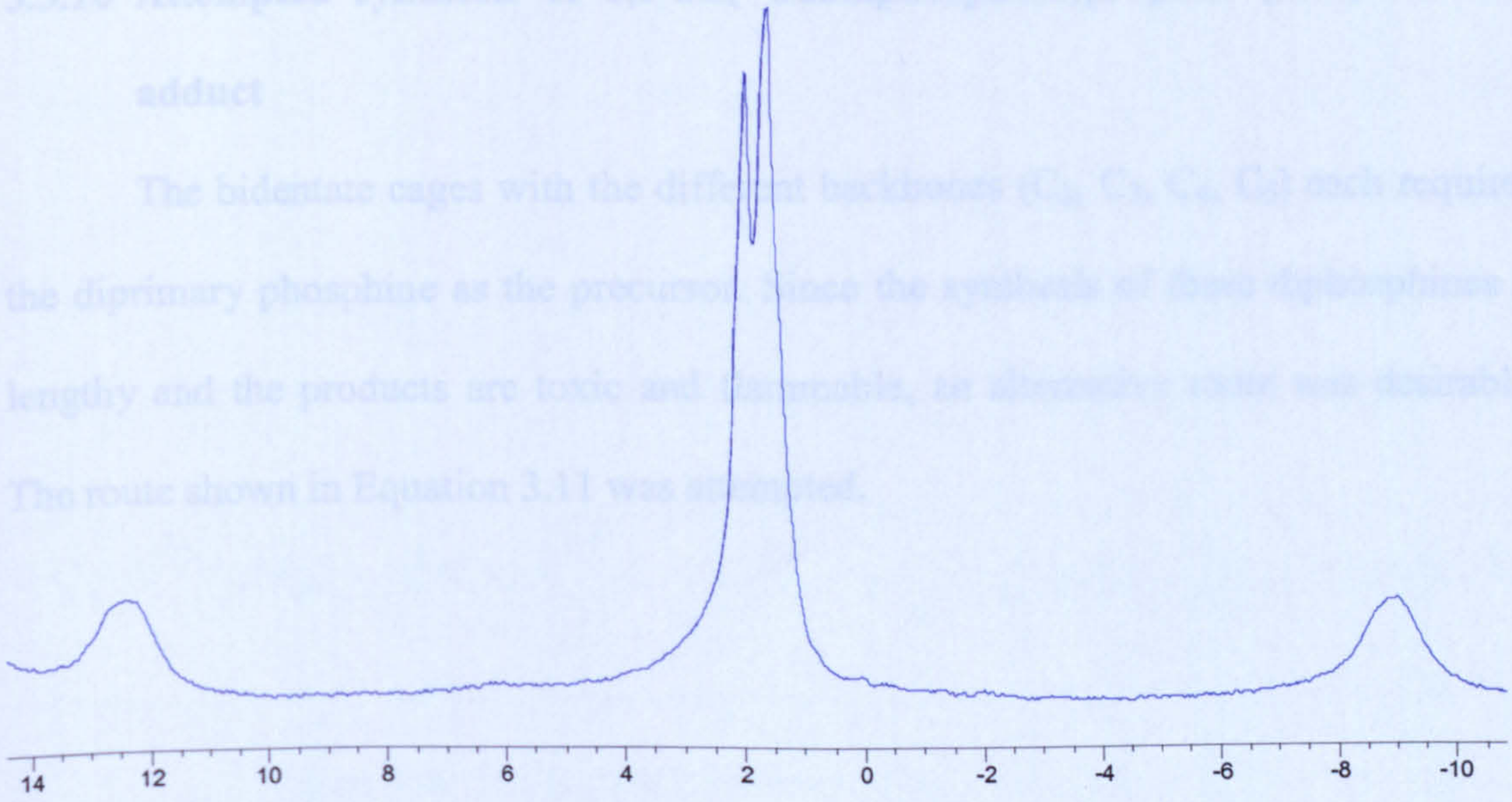

Figure 3.16 The $^{31}P\{^{1}H\}$ NMR spectrum of the dichloroplatinum(II) complex of 1,5-bis(^{Et}adam-phosphino)pentane (**3.16**)

3.3.9 Dichloropalladium(II) complex of (3.15)

The reaction of *meso/rac*-(**3.15**) with 1.0 equiv. of $[PdCl_2(NCPh)_2]$ in CH_2Cl_2 gave a yellow solution. The $^{31}P\{^1H\}$ NMR spectrum (Figure 3.17) of the solution showed that various products had formed; signals from 9 ppm to 11.5 ppm were observedand were assigned to mononuclear, binuclear and oligonuclear products. The flexibility of the C_5 backbone makes chelation more difficult and hence multinuclear complexes were expected to form.

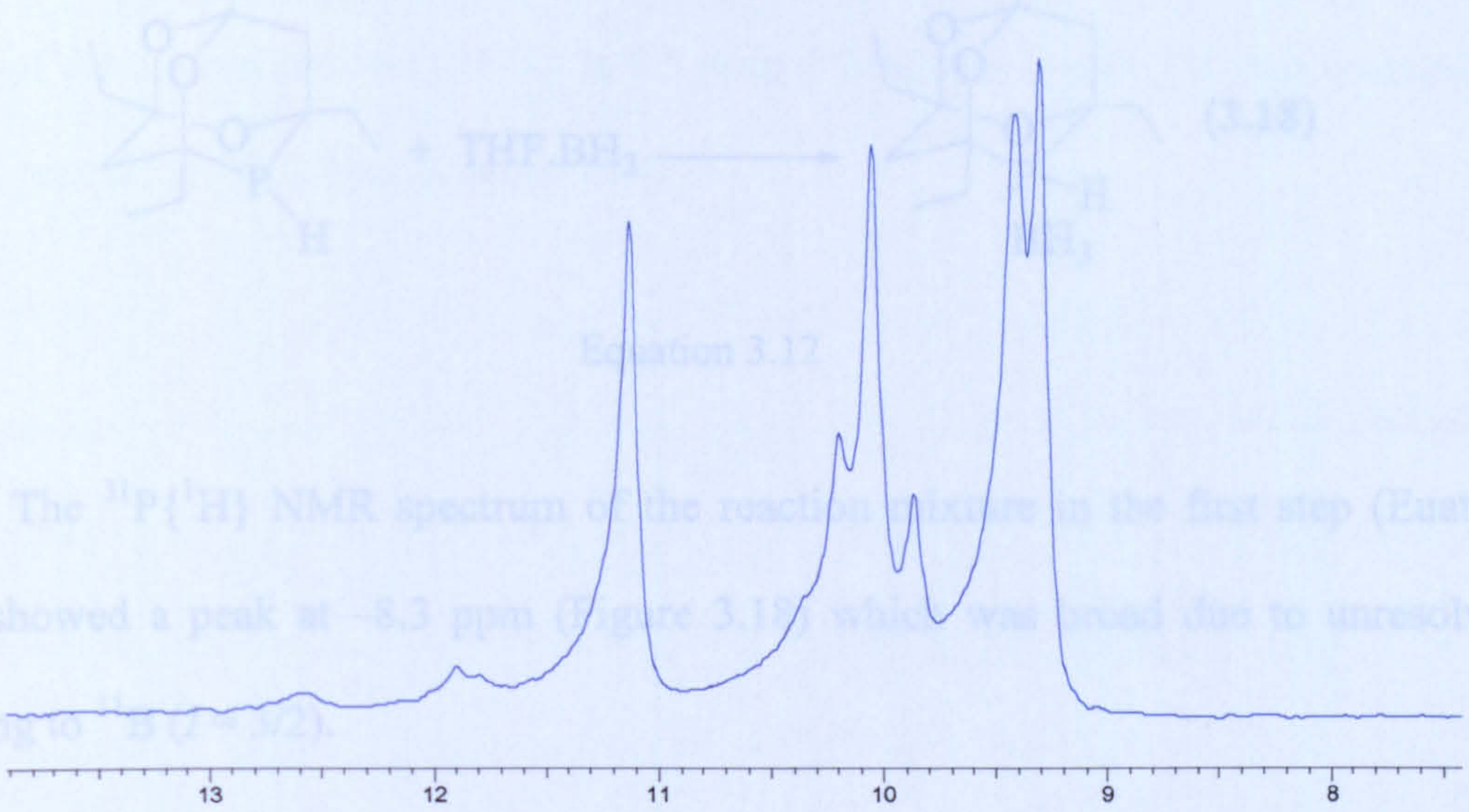

Figure 3.17 The $^{31}P\{^1H\}$ NMR spectrum of the dichloropalladium complex of **3.15**

3.3.10 Attempted synthesis of 1,3-bis(^{Et}adamphosphino)propane (3.10) via BH_3 adduct

The bidentate cages with the different backbones (C_2, C_3, C_4, C_5) each required the diprimary phosphine as the precursor. Since the synthesis of these diphosphines is lengthy and the products are toxic and flammable, an alternative route was desirable. The route shown in Equation 3.11 was attempted.

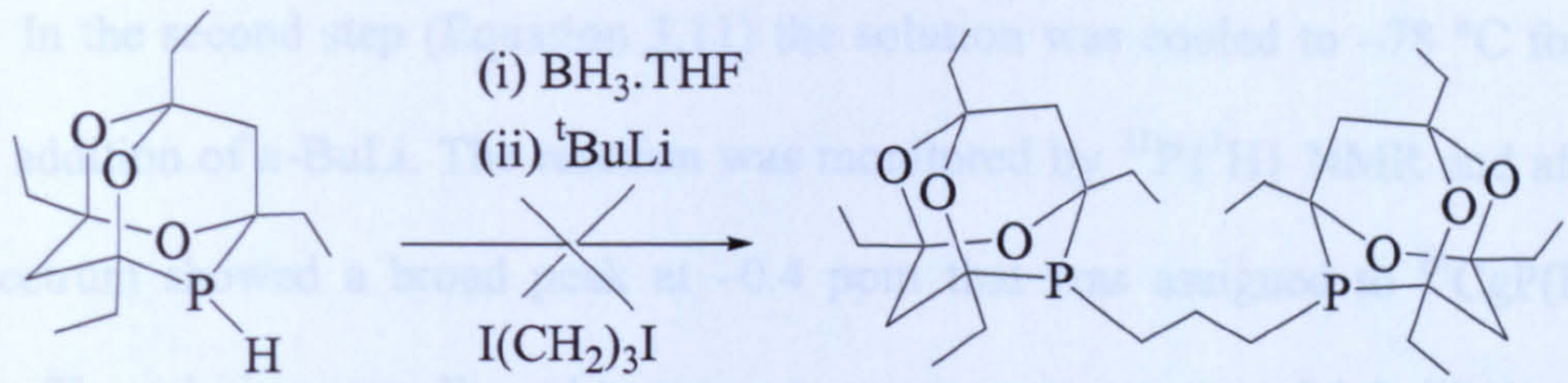

Equation 3.11

The borane adduct below (**3.18**) was first made according to Equation 3.12.

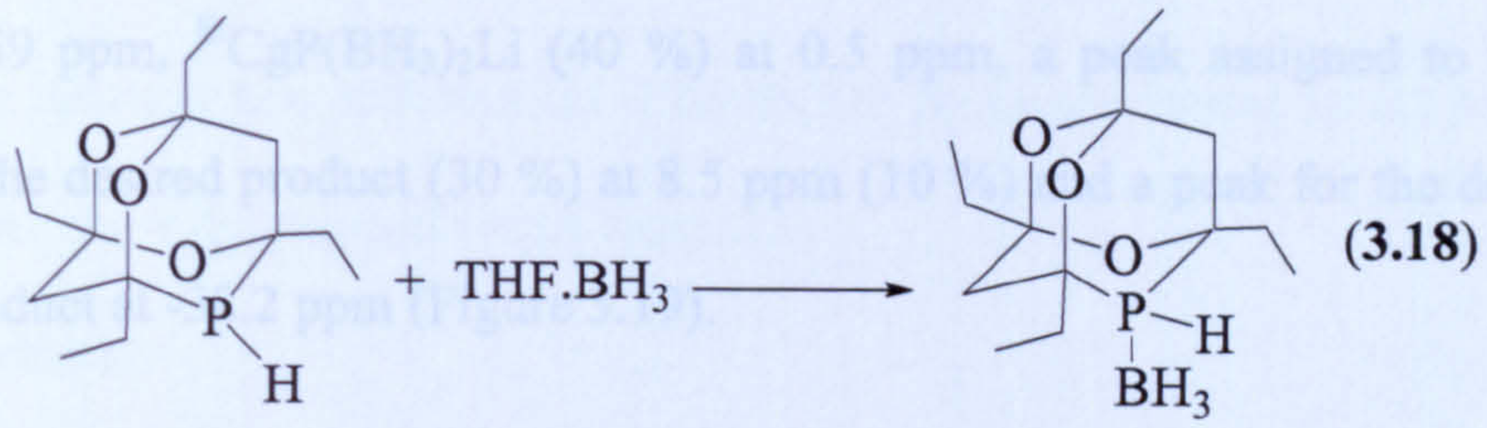

Equation 3.12

The $^{31}P\{^{1}H\}$ NMR spectrum of the reaction mixture in the first step (Euation 3.12) showed a peak at –8.3 ppm (Figure 3.18) which was broad due to unresolved coupling to ^{11}B ($I = 3/2$).

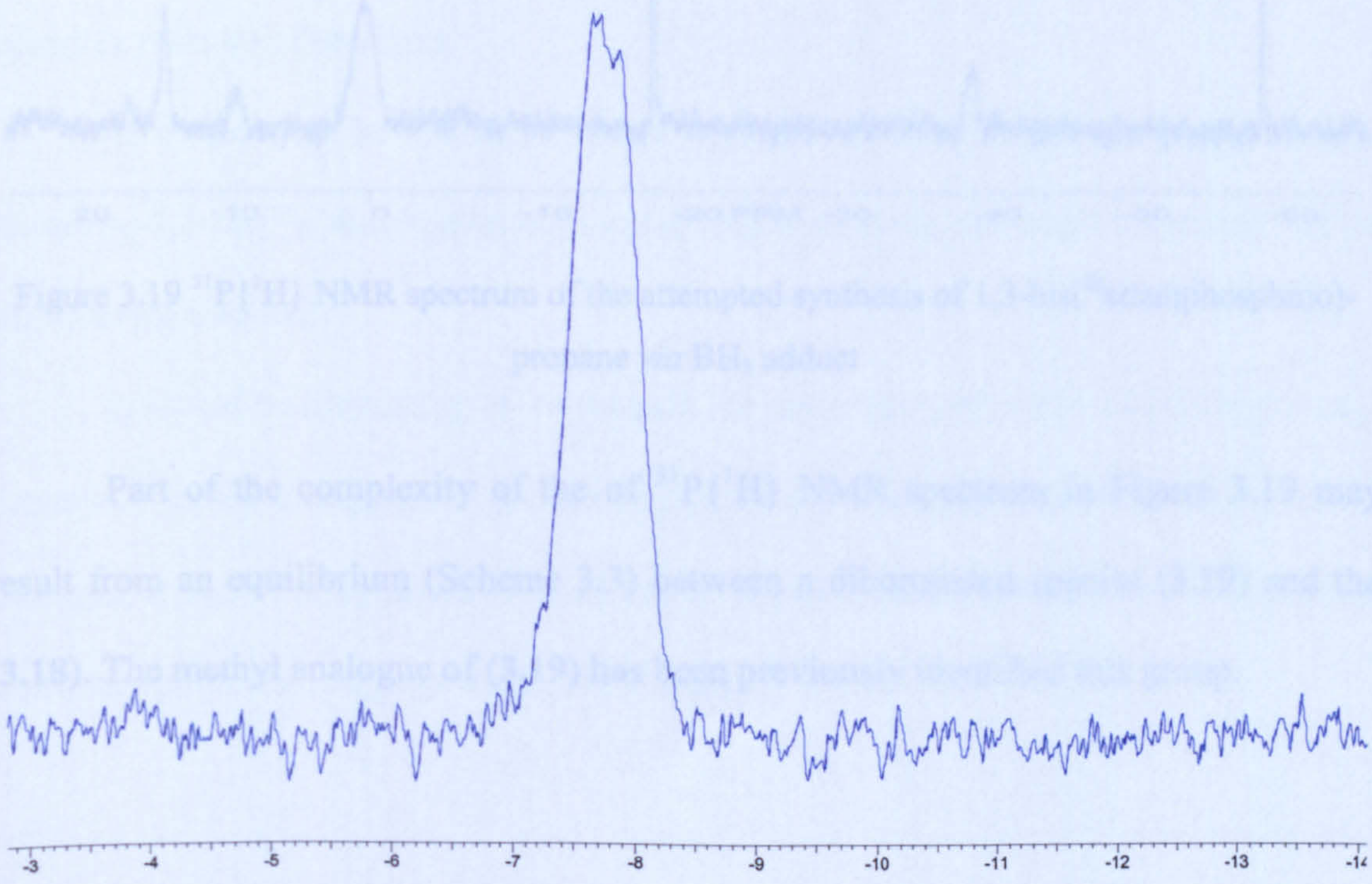

Figure 3.18 $^{31}P\{^{1}H\}$ NMR spectrum of the borane adduct (**3.18**)

In the second step (Equation 3.11) the solution was cooled to –78 °C followed by the addition of *n*-BuLi. The reaction was monitored by $^{31}P\{^{1}H\}$ NMR and after 2 h the spectrum showed a broad peak at –0.4 ppm that was assigned to $^{Et}CgP(BH_3)Li$ species. The solution was allowed to warm to room temperature and 1,3-diiodopropane was added to the solution. The $^{31}P\{^{1}H\}$ NMR spectrum of the reaction mixture (Figure 3.19) showed several peaks, corresponding to; $^{Et}CgP(BH_3)Li$ (11%) at 14 ppm, $^{Et}CgPH$ (6%) at –59 ppm, $^{Et}CgP(BH_3)_2Li$ (40 %) at 0.5 ppm, a peak assigned to the borane adduct of the desired product (30 %) at 8.5 ppm (10 %) and a peak for the deboronated desired product at -38.2 ppm (Figure 3.19).

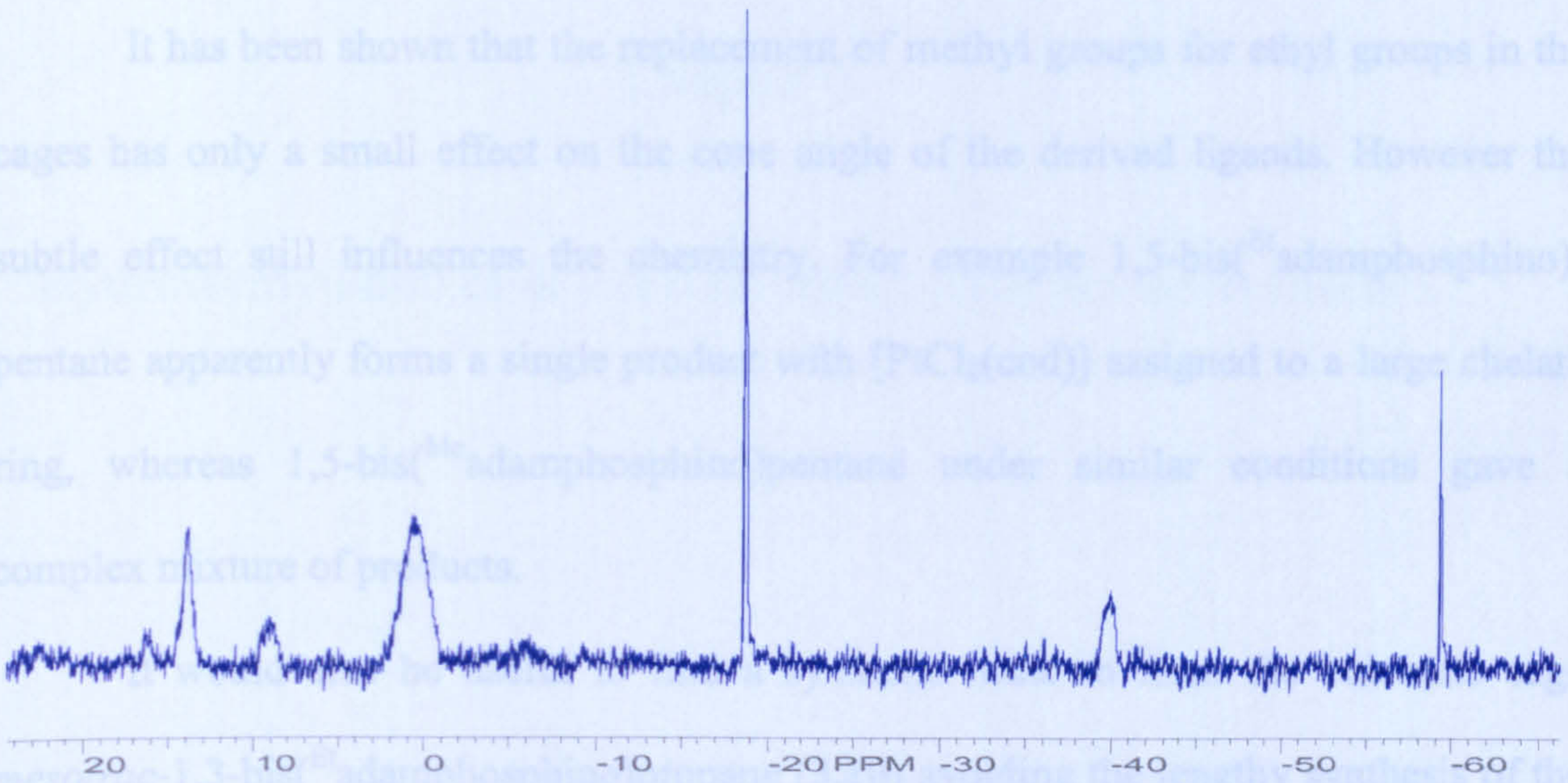

Figure 3.19 $^{31}P\{^{1}H\}$ NMR spectrum of the attempted synthesis of 1,3-bis(^{Et}adamphosphino)-propane *via* BH_3 adduct

Part of the complexity of the of $^{31}P\{^{1}H\}$ NMR spectrum in Figure 3.19 may result from an equilibrium (Scheme 3.3) between a diboronated species (**3.19**) and the (**3.18**). The methyl analogue of (**3.19**) has been previously identified this group.

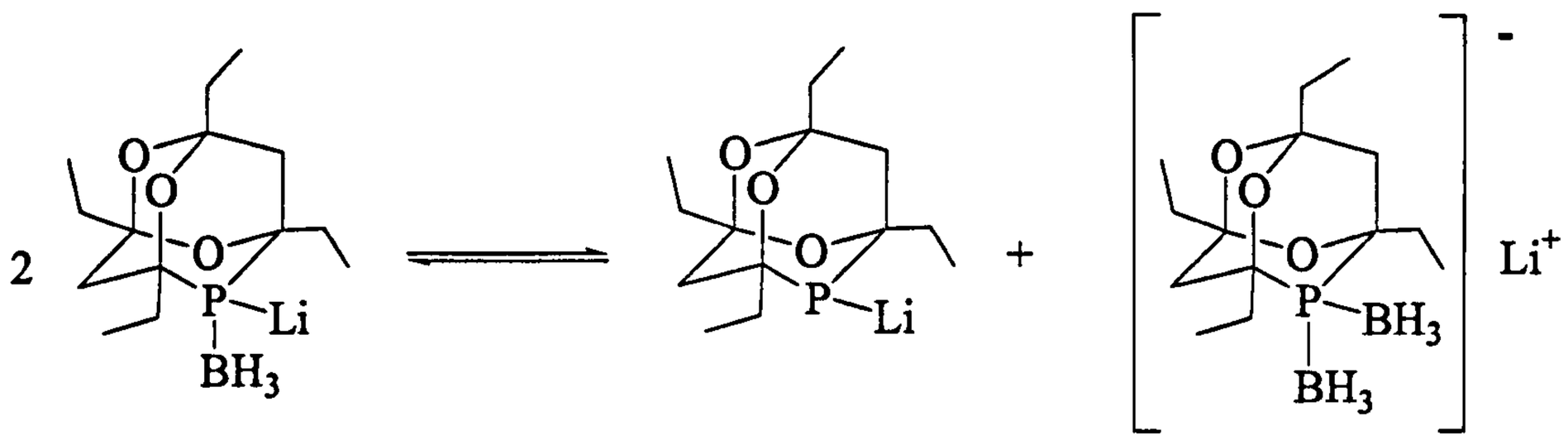

3.19

Scheme 3.3 Possible equilibrium for borane/lithium adduct

The reaction was refluxed for 4 hours but no improvement in the reaction was observed and more by-products were formed.

3.4 Conclusion

It has been shown that the replacement of methyl groups for ethyl groups in the cages has only a small effect on the cone angle of the derived ligands. However the subtle effect still influences the chemistry. For example 1,5-bis(^{Et}adamphosphino)-pentane apparently forms a single product with $[PtCl_2(cod)]$ assigned to a large chelate ring, whereas 1,5-bis(^{Me}adamphosphino)pentane under similar conditions gave a complex mixture of products.

It would also be useful to find a synthetic route to form the bidentate cage *meso/rac*-1,3-bis(^{Et}adamphosphino)propane (**3.10**) avoiding the lengthy synthesis of the diprimary phosphine.

It would be interesting to investigate the electronic and steric effects in the cage moiety by further changing the substituents in the α-carbon position of the diketone. For example, a phenyl or cyclohexyl group could be incorporated into the diketone, and the diprimary phosphine cage synthetic route could be used.

Chapter 4

Hydroformylation catalysis with trioxa-phospha-adamantanes

4.1 Introduction

In this chapter we will review large scale hydroformylation processes, approaches to some current challenges such as catalyst separation, hydroformylation of internal olefins and the hydroformylation of epoxides. This will put into context the hydroformylation results to be presented for our ligands, for which synthesis was described in previous chapters.

4.2 Hydroformylation

Ever since the discovery of cobalt-catalyzed hydroformylation by Otto Roelen[86] in 1938, the industrial importance of this reaction has been recognized[87-89] and it is now one of the world's most important homogeneously catalyzed reactions. In the course of this reaction a new carbon-carbon bond is formed and, simultaneously, the synthetically valuable aldehyde function is introduced (Equation 4.1).

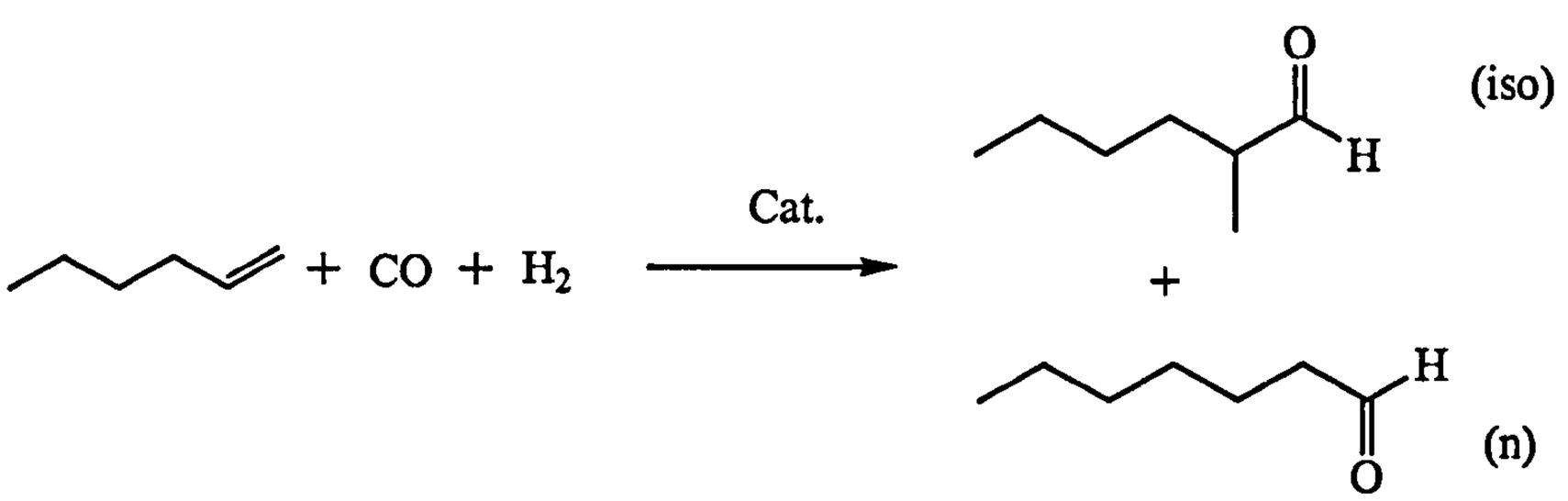

Equation 4.1

The aldehydes are then often reduced by hydrogenation to alcohol, which are used as raw materials in the synthesis of plasticizers, soaps and detergents. Aldehydes are raw materials for other very useful chemicals as shown in Figure 4.1.[2]

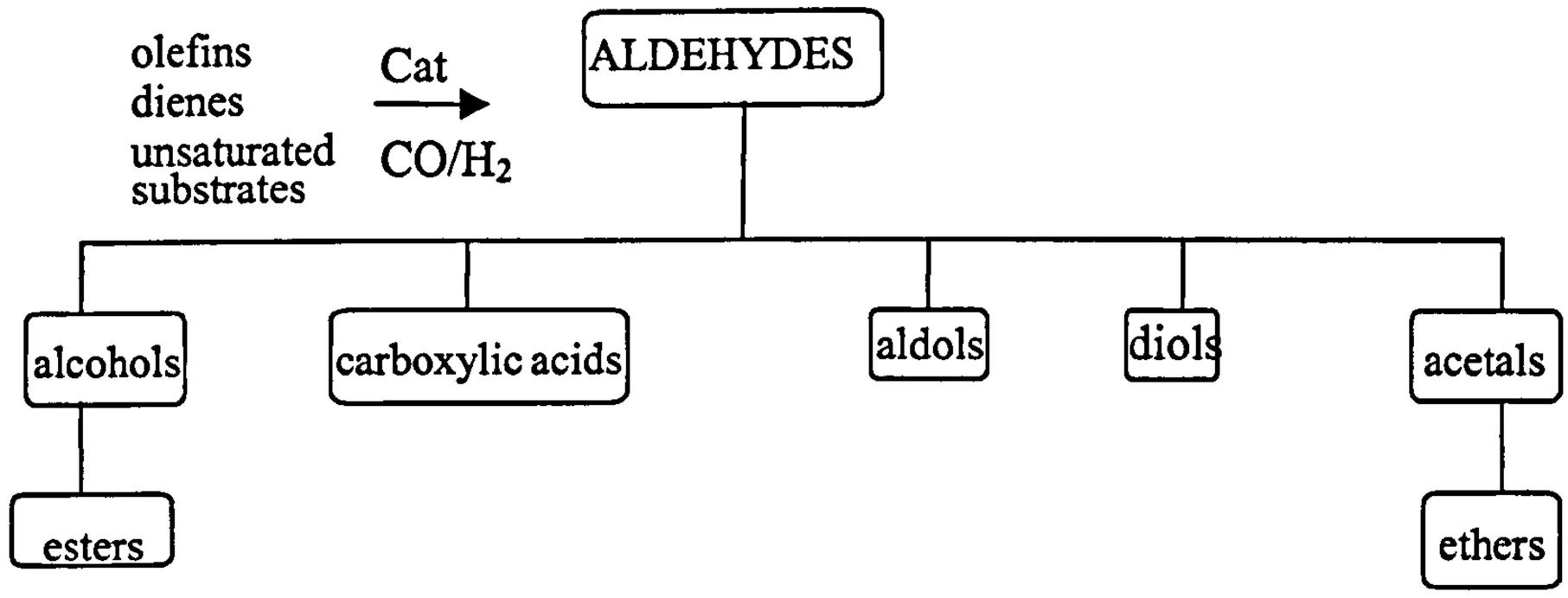

Figure 4.1

In the first two decades after the discovery of hydroformylation, the catalytic system was based on [$HCo(CO)_4$], but high temperatures and pressures were required to ensure the catalyst stability.[90] In 1968, it was reported[91] that the addition of a tertiary phosphine could stabilise the catalyst to such an extent that reaction pressures below 100 atm were feasible. Although the phosphine modified Co catalytic system is less reactive than the unmodified catalyst, the increased electron density on the metal centre affords a better hydrogenation catalyst which results in the formation of alcohols rather than aldehydes as the primary products.[90] Thus, where alcohols are required as the end product, the extra hydrogenation step is obviated. Unfortunately, this improved hydrogenation capability also resulted in substantial amounts of the olefin feedstock being lost *via* the competing hydrogenation of the alkenes to alkanes.[90]

The replacement of [$HCo(CO)_4$] by [$RhH(CO)(PPh_3)$] was a great development as the process can operate under much milder conditions, below 100 °C and at only a few atmospheres). The Rh system produces aldehydes with no loss of alkene by hydrogenation.[92] The first industrial application of the rhodium catalysis was in the hydroformylation of propene by the Union Carbide Corporation (UCC). The LPO process (low pressure oxo),[93] was designed to trap the catalyst in the reactor system and to separate the catalyst and aldehydes by distillation under reaction conditions. This

process involved a high-boiling solvent for the catalyst, an excess of PPh_3 ligand, and gas injection through the reactor to remove the butanals formed. The original UCC process has been refined, with what has been called the "gas recycle process": The products are removed from the catalyst by passing a large amount of gas through the reaction (which is recycled) to evaporate the aldehydes.

The PPh_3-rhodium catalyst for the UCC process has since been replaced by the diphosphite **(4.1)**-rhodium catalyst. The new catalyst is more active and more selective.[87]

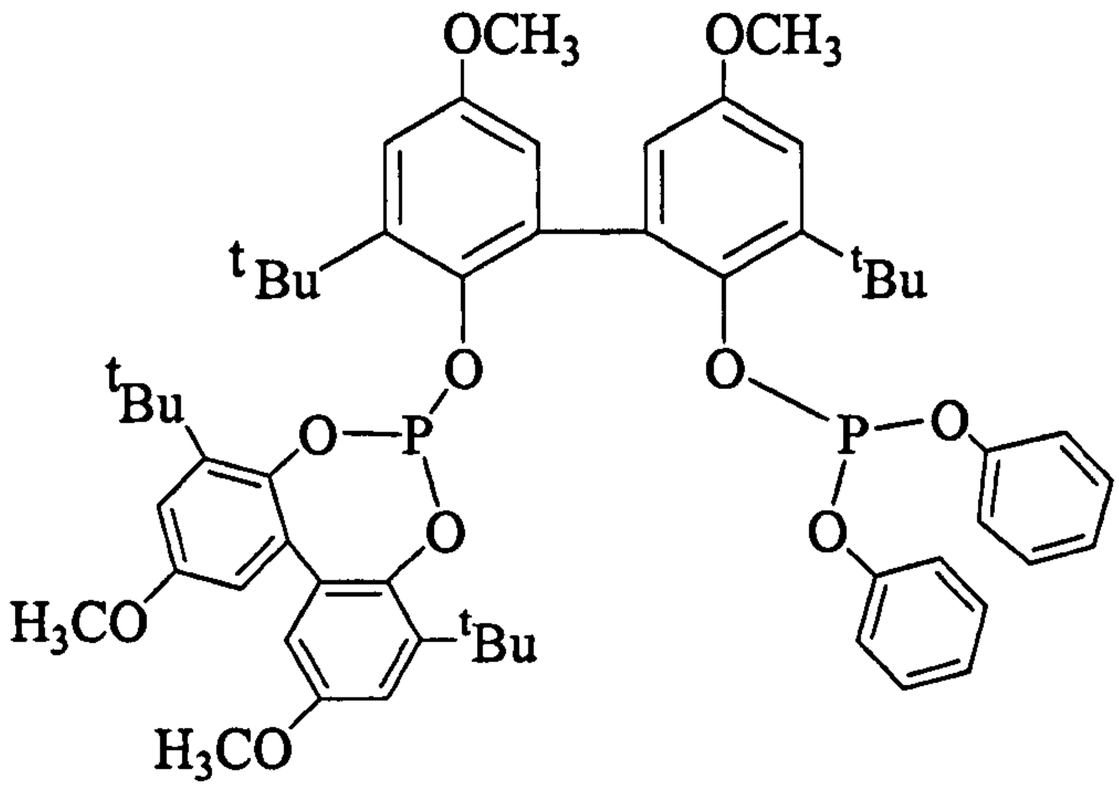

4.1

In the Ruhrchemie/Rhône-Poulenc (RCH/RP) process, propene or butene and a H_2/CO mixture are fed into the reactor which contains an aqueous solution with a water soluble catalyst [(*meta*-sulfonated triphenylphosphine, as sodium salt **(4.1)** (TPPTS)] (Figure 4.2). The effluent from the reactor is passed through a phase separator. The aqueous solution is recycled back to the reactor and the crude aldehydes are sent to a distillation column. The process is used for the production of C_4 and C_5 aldehydes. The aqueous biphasic catalyst has two main advantages; long lifetime of the rhodium catalyst used and an overall more economical process.

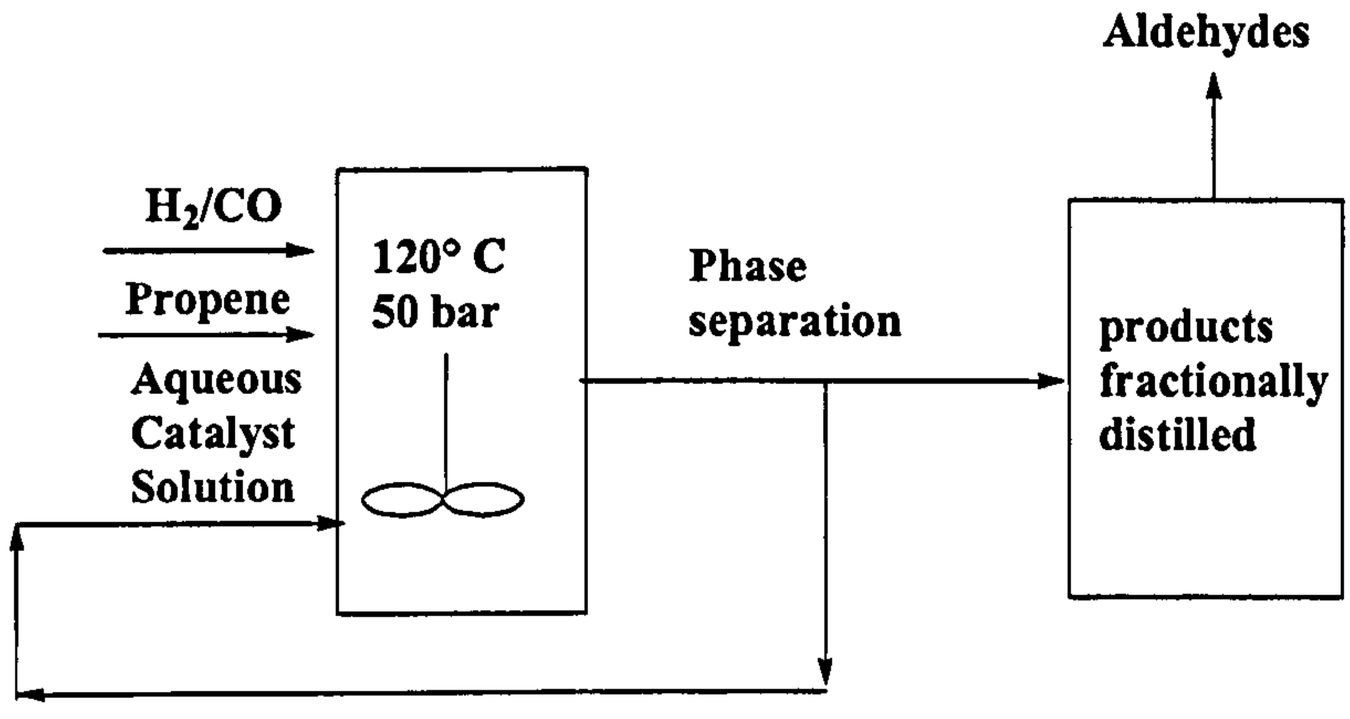

Figure 4.2 RCH/RP Process

Since the discovery of rhodium(I)-phosphine complexes as chemoselective hydroformylation catalysts, further development of new catalytic systems have been aimed at controlling the chemo-, regio-, and stereoselectivity. Major advances have been made towards this goal during the last decades.[94]

The generally accepted, dissociative mechanism for $[RhH(CO)(PPh_3)_3]$ catalyzed hydroformylation, as proposed by Wilkinson,[95] is shown in Scheme 4.1.

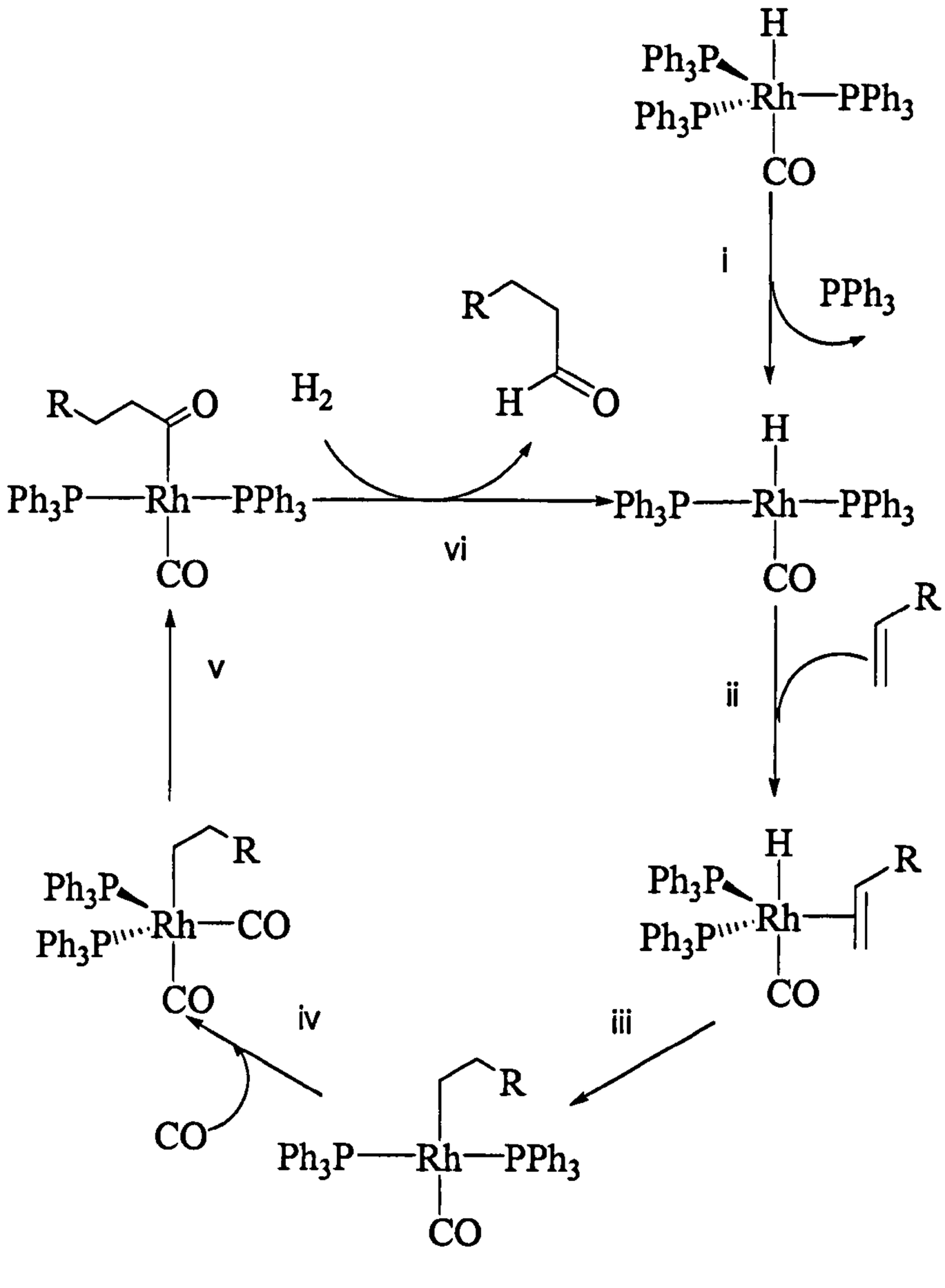

Scheme 4.1

The mechanism begins with the dissociation of a molecule of PPh_3 (step i) from $[HRh(CO)(PPh_3)_3]$, followed by coordination of the alkene (step ii). The hydride migration (step iii) is the source of the very high selectivity for the linear product. Step vi involves the rate-limiting oxidative addition of hydrogen followed by reductive elimination of the product aldehyde.[9]

4.3 Current challenges in hydroformylation

Since the discovery of the hydroformylation process, many improvements to the catalyst's activity and selectivity have been made.[2,90,96] Also, due to the cost of the metal complex catalyst, its recovery has been a central issue for a long time. One of the

long-standing problems of hydroformylation chemistry, the low pressure hydroformylation of internal and more highly substituted olefins, still awaits a practical solution.[97] It is known that the reactivity of hydroformylation catalysts decreases exponentially with the degree of olefin substitution.[98] This section describes some current approaches and some other challenges in hydroformylation catalysis.

4.3.1 Separation of long chain aldehydes from the catalyst in hydroformylation

One of the limitations of using rhodium catalysts is that only low boiling products can be easily separated from the catalyst solution by distillation.[87] When less volatile compounds are involved, such recovery of the catalyst is not feasible because the thermally sensitive rhodium complexes decompose below the boiling point of the product. For the longer chain products, which are important in detergent manufacture, cobalt catalysts are still used despite their lower activity and selectivity.[99]

Many approaches to the separation and/or catalyst reuse problem are being investigated.[2,90,94,100] To overcome the separation problems, several approaches have been investigated as described below.

Fluorous biphasic systems

A catalyst is rendered soluble in fluorocarbons usually by adding fluorous tails to known catalysts. The substrate and products are dissolved in the inmiscible organic phase.[101-106] The great advantage of this type of system over the aqueous biphasic approach is that by careful choice of the fluorous and organic solvents, [97, 107, 108] a single phase is formed at the operating temperature, but phase separation occurs on cooling. In the past few years the fluorous phosphorus ligands, $P[OCH_2CH_2(CF_2)_7CF_3]_3$ and $P[CH_2CH_2(CF_2)_5CF_3]_3$, have been used in hydroformylation reactions as modifying ligands in fluorous multiphase systems and have demonstrated not only high stability but also shown a great advantage in the separation of high molecular weight aldehydes

from the catalysts.[2,109,110] It has been shown that, by operating in the absence of organic solvents and using triarylphosphines with "fluorous ponytails", it is possible to obtain high linear selectivities at low catalyst loading in hydroformylation reactions with >99.5% retention of rhodium in the fluorous phase.[105,111]

A recent example of a fluorobiphasic ligand (**4.2**) (poly[fluoroacrylate-*co*-4-(phenylphosphino)styrene]) is shown in Equation 4.2. This ligand has been used in the hydroformylation of styrene, acrylates and 1-hexene, with $[Rh(acac)(CO)_2]$. In the hydroformylation of 1-hexene 99% selectivity was reported.[106]

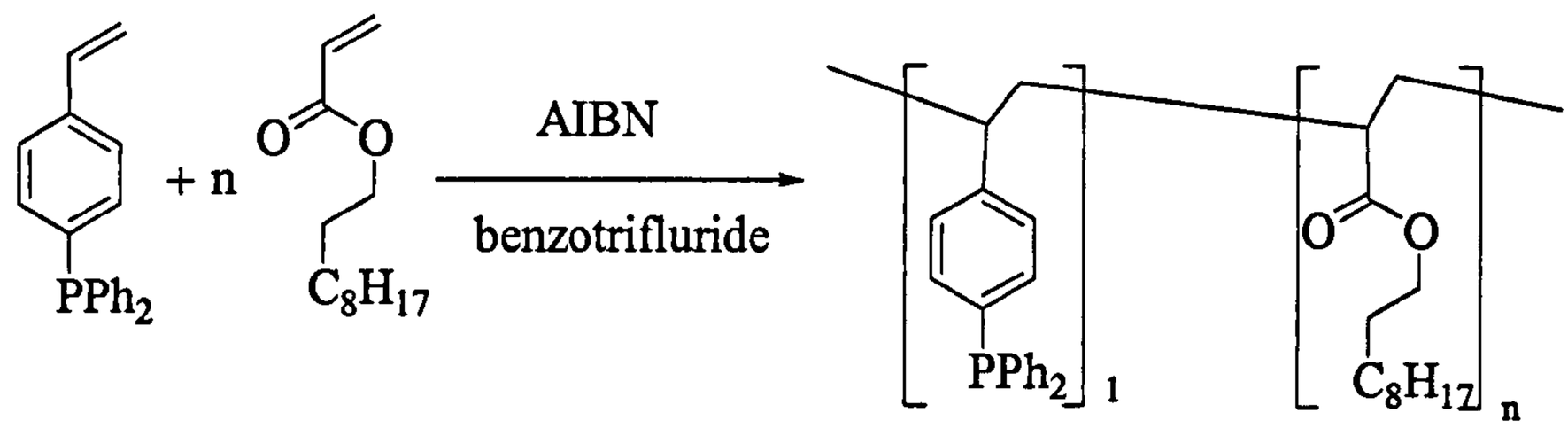

n = 5, n = 9

4.2

Equation 4.2

Aqueous biphasic systems

These use the same principles as those involved in the Rhone-Poulenc/Ruhr Chemie process,[99] where a water-soluble catalyst $[HRh(CO)(TPPTS)_3]$ (TPPTS = **4.3**), remains in the water at all times and the product aldehydes are separated by decantation.

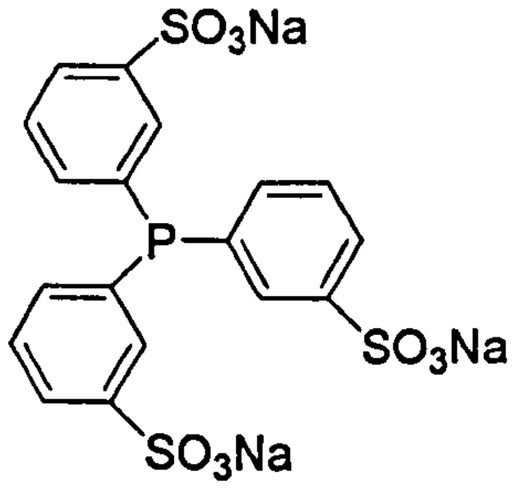

4.3

The catalysis takes place in the aqueous phase and the system works well for alkenes up to octene, but higher olefins suffer from the disadvantage of lower rates limited by the solubility of the olefins in water.[112,113]

The hydroformylation of propene has been performed using the water-soluble catalyst Rh/BINAS-Na (**4.4**) (99:1 *n:i* ratio).[114]

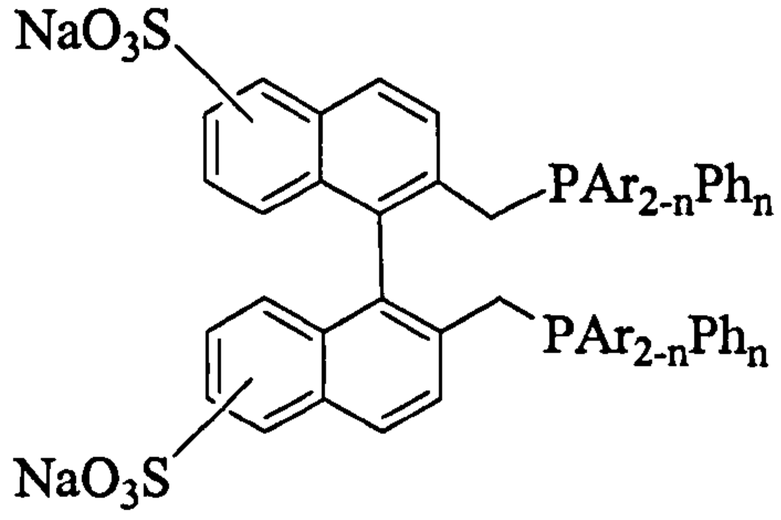

BINAS-Na

$Ar = m\text{-}C_6H_4\text{-}SO_3Na^+$

4.4

Some recently reported water soluble phosphines include $Ph_2PCH_2CH_2C(O)NHC(CH_3)_2CH_2SO_3Li$, $Ph_2PCH_2CH(COOLi)(CH_2COOLi)$, $Ph_2PCH_2CH(CH_3)(COOH)$ and $Ph_2PCH_2CH(CH_3)(COONa)$ which have been successfully applied to the rhodium-catalyzed hydroformylation of methyl acrylate,[115] 1-hexene[116] and C_4 unsaturated alcohols.[117]

In the latest research in biphasic hydroformylation a new system called "thermo-regulated phase transfer catalysis" (TRPTC) also known as a "smart" system, has been described.[120] This involves the use of non-ionic water-soluble phosphine ligands bearing polyoxyethylene moieties. These undergo changes in their hydrogen bonding patterns with temperature,[100,118,119] and the catalyst is separated and recycled.[121] The polyoxyethylene chains are hydrophilic groups, which demonstrate temperature-dependent solubility. As a result, their metal complexes are soluble in the aqueous phase

at lower temperatures, and are soluble in the organic phase on heating above the cloud point (Figure 4.3).[122] The cloud point is defined as the temperature at which the polyoxyethylene moiety loses its solubility through disruption of the hydrogen bonds to water molecules, and precipitates from the aqueous phase.

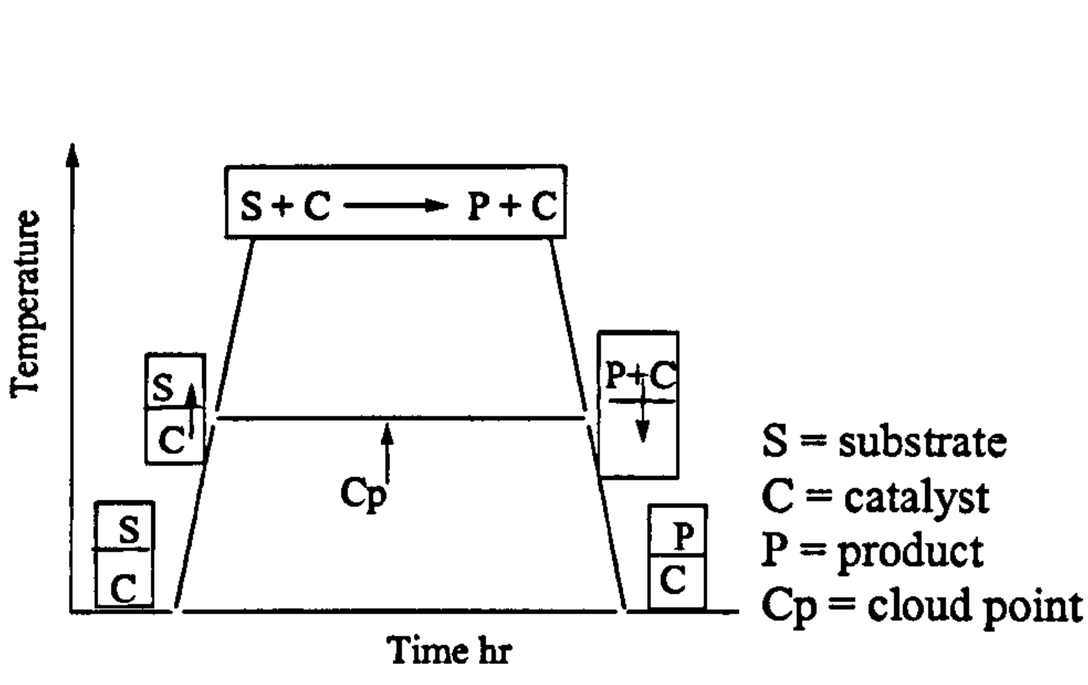

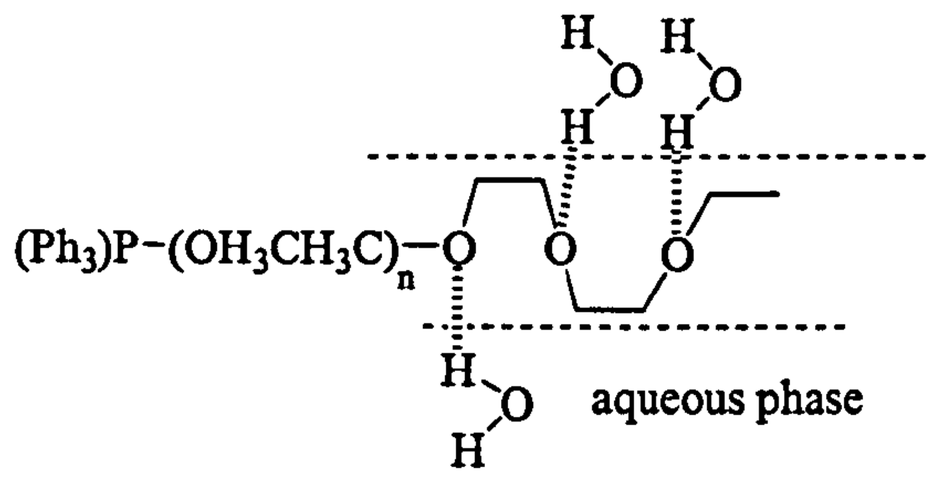

Figure 4.3

Supercritical fluids

One other method reported to solve the problem of separating rhodium-based catalysts from long-chain aldehydes involves the use of supercritical fluids such as $scCO_2$.[123-129] These fluids are gases heated above their critical temperature (T_c) and pressurized above their critical pressure (P_c). $scCO_2$ offers several advantages over conventional organic solvents, which make it very attractive as a solution to the separation problem.[96, 123, 130] These advantages include; (i) $scCO_2$ density is comparable to that of organic liquids, and will solubilise a wide range of organic substrates; (ii) the design, scale-up and operation of reactors operating in one phase are much simpler than multiphase reactors; (iii) $scCO_2$ is non-flammable, non-toxic, environmentally acceptable, readily available in large quantities and has a low critical temperature and a moderate critical pressure; (iv) scCO has no gas-liquid phase boundary; and (v) scCO facilitates easy product and catalyst separation.

Research in this area has mainly focussed on the use of analogues of rhodium/triphenylphosphine complexes, since the parent complex shows rather low

solubility and activity.[131] Better solubility has been achieved by using fluoroalkyl- or fluoroalkoxy- substituted arylphosphines **(4.5-4.10).**[101,123,125,128,130,132,133] These ligands are analogous to those used to enhance the solubility of similar catalysts in fluorous biphasic systems.[101,102,127]

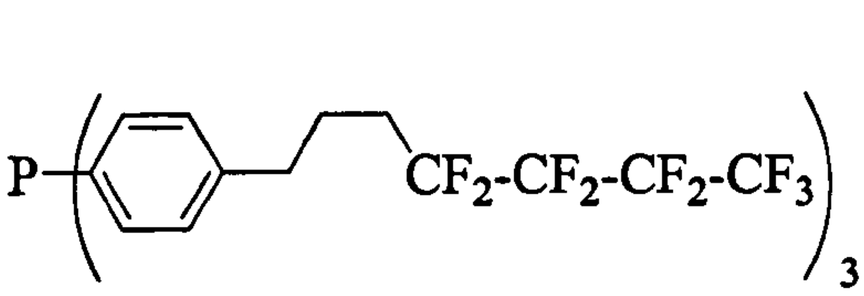

4.5

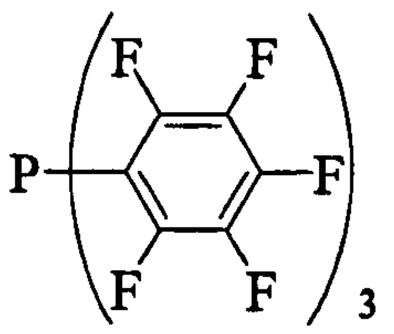

4.6

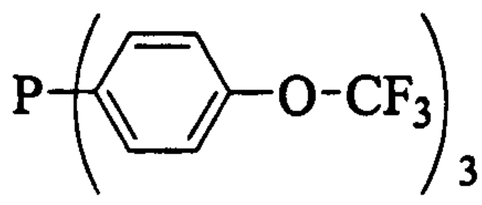

4.7

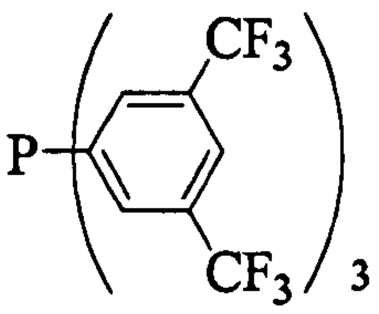

4.8

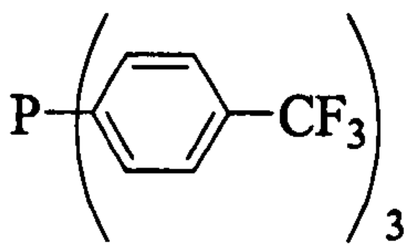

4.9

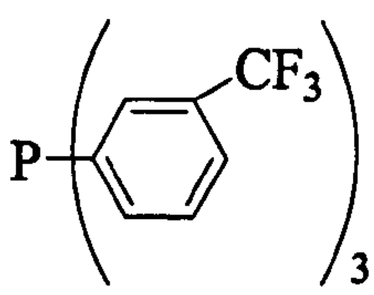

4.10

Using catalysts that are insoluble in $scCO_2$ has great advantages in terms of separation.[124] Ligands **(4.11)** and **(4.12)** have afforded insoluble metal complexes that have been used in the hydroformylation reaction of hex-1-ene in $scCO_2$, and showed high activity and selectivity. The products were removed from the reaction by flushing them into a second autoclave and decompressing them to give the aldehyde product, containing no detectable amounts of rhodium; the catalyst could be reused several times.[124]

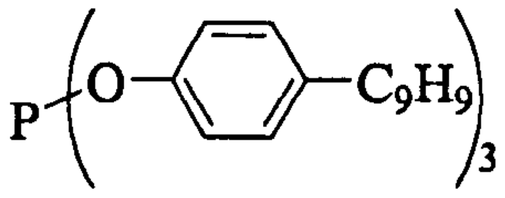

4.11

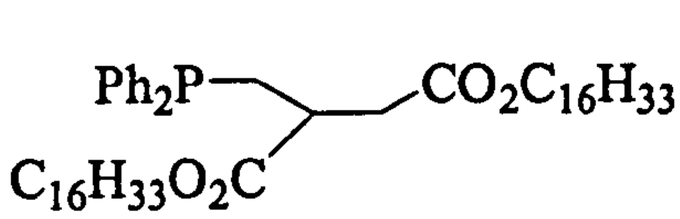

4.12

Other methods for immobilizing the catalyst, which are not going to be discussed further here include anchoring of ionic catalysts to insoluble supports,[134,135]

anchoring of insoluble catalysts to insoluble supports[136] and anchoring homogeneous catalysts to dendrimer supports.[137-139]

4.3.2 Hydroformylation of internal olefins

4.3.2.1 Phosphabenzene

Rhodium-phosphine catalysts are significantly more active than cobalt-phosphine systems for the hydroformylation of terminal olefins. However, their activity for the hydroformylation of internal and higher olefins is still rather low.[98]

Strong π-acceptor ligands, such as phosphites, have been observed to give more active hydroformylation catalysts for both the hydroformylation of internal and terminal olefins.[140] Unfortunately, technical application of phosphites has been hampered by their inherent lability to hydrolysis.[2,141] Hence, the development of new classes of π-acceptor ligands remains an important task. In 1996, phosphabenzenes were shown to be good ligands for the hydroformylation of terminal and internal olefins.[142]

Märkl made the first preparation of these compounds in 1966.[143,144] The interest in phosphabenzene derivatives as potential ligand candidates for transition metal catalysed reactions is due to several reasons, including the novelty of such applications, the ease of preparation, their stability, and the unique electronic properties of these systems.[145]

Many complexes of phosphabenzenes are known,[146] and some examples are **(4.13-4.16)**. Phosphabenzenes may vary their coordination mode according to the metal to which they are bound.

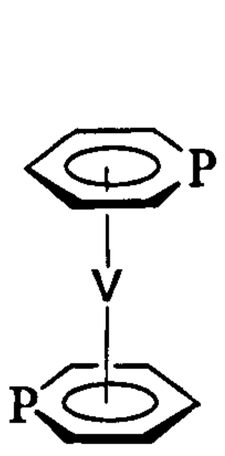

4.13

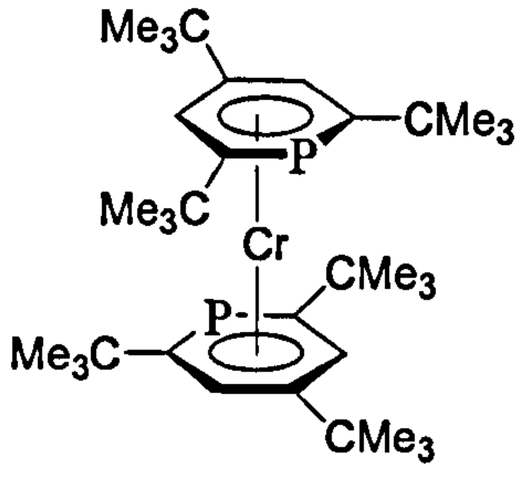

4.14

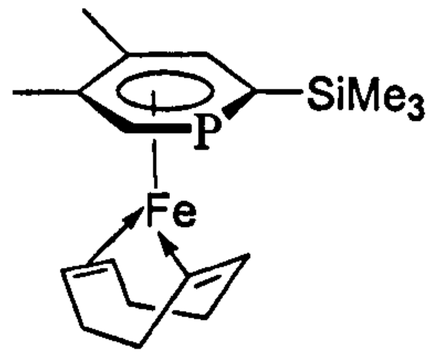

4.15

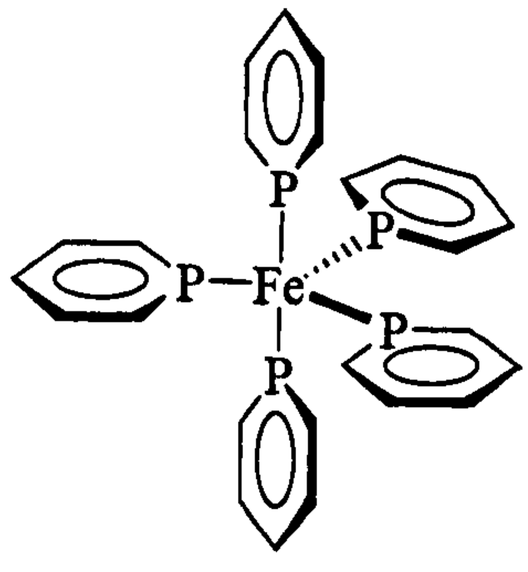

4.16

In general there are three conventional binding modes: η^1, η^6, and mixed (Figure 4.4). The η^1-binding mode is typically observed with late transition metals in low oxidations states.[147] The η^6 is favoured by early transition metals in low oxidation states.[148] Metals in the centre of the transition series tend to exhibit mixed binding.[145]

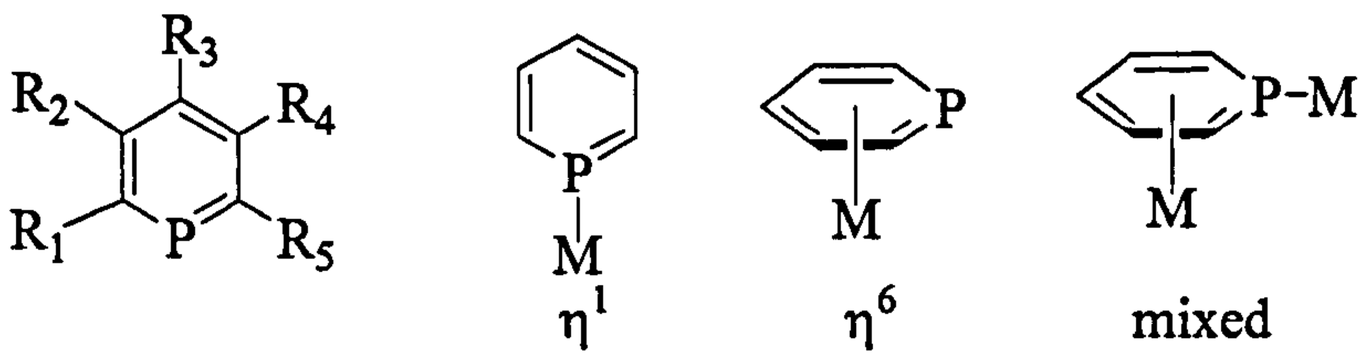

η^1 η^6 mixed

Figure 4.4

Rhodium-catalysts modified with bulky monophosphabenzenes, phosphines and phosphonites have been compared in the hydroformylation of styrene (Equation 4.3).[97] The phosphabenzene catalyst showed the highest activity and excellent regioselectivity to form the branched aldehyde product.

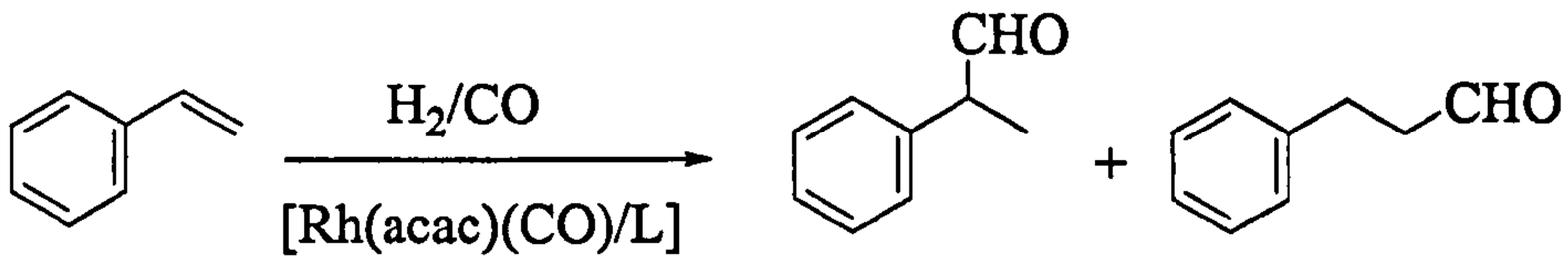

L = 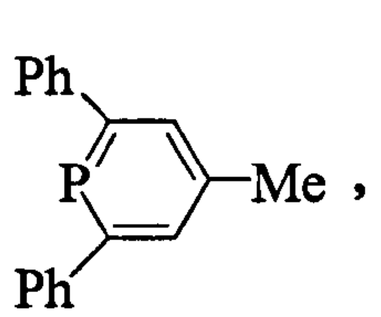 , 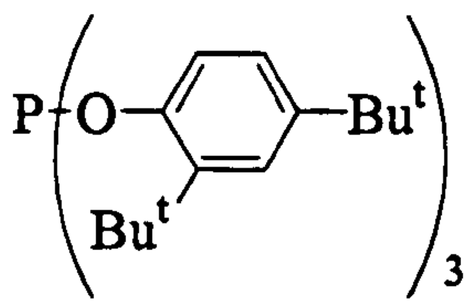 , PPh_3

4.17 **4.18** **4.19**

Equation 4.3

A series of phosphabenzenes (**4.20-4.26**), and their catalytic activity in the hydroformylation of terminal and internal olefins has also been reported.[97]

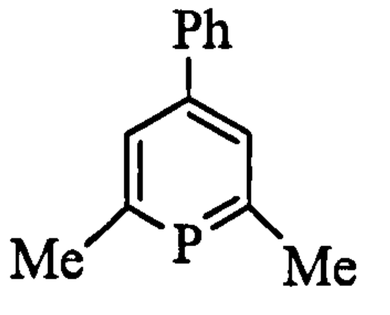

4.20

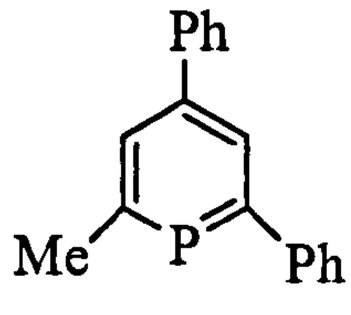

4.21

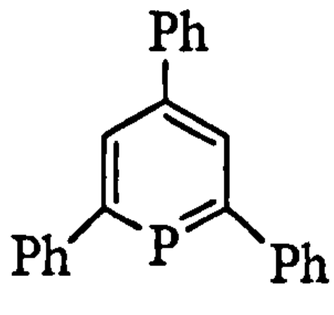

4.22

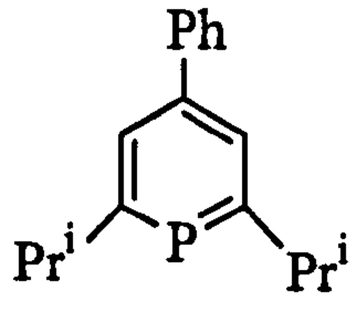

4.23

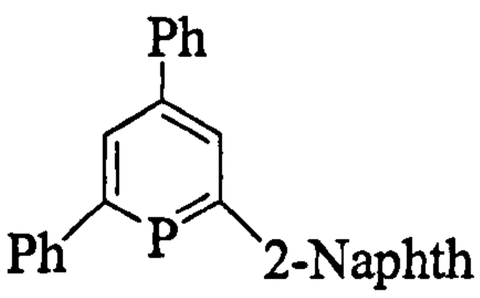

4.24

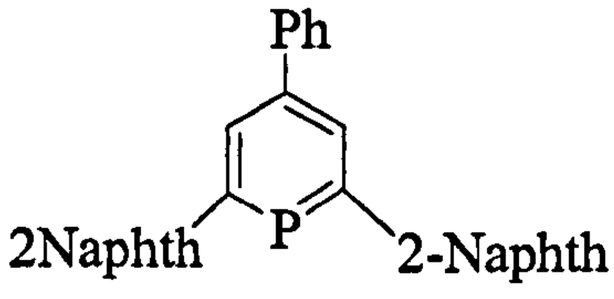

4.25

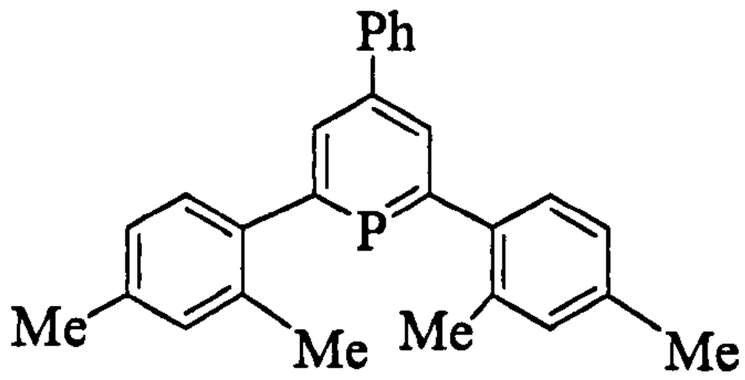

4.26

The study showed that phosphabenzene **4.26** provided the most active rhodium catalyst for the hydroformylation of 1-octene. Even more impressive results were obtained in the hydroformylation of internal olefins including 1,1-disubstituted (Equation 4.4), trisubstituted (Equation 4.5) and tetrasubstituted alkenes (Equation 4.6).

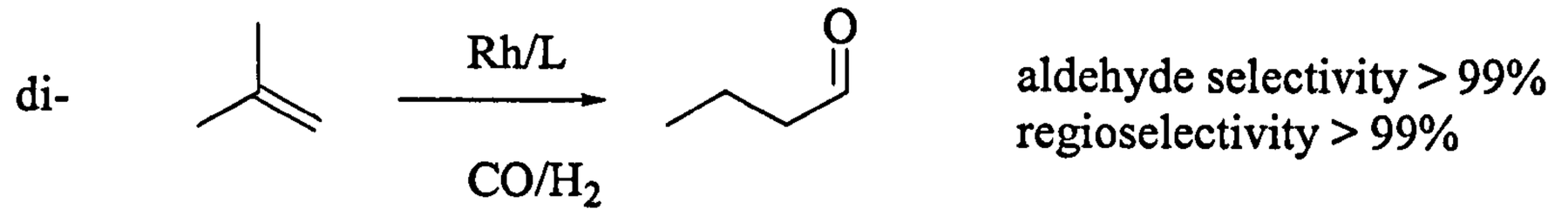

Equation 4.4

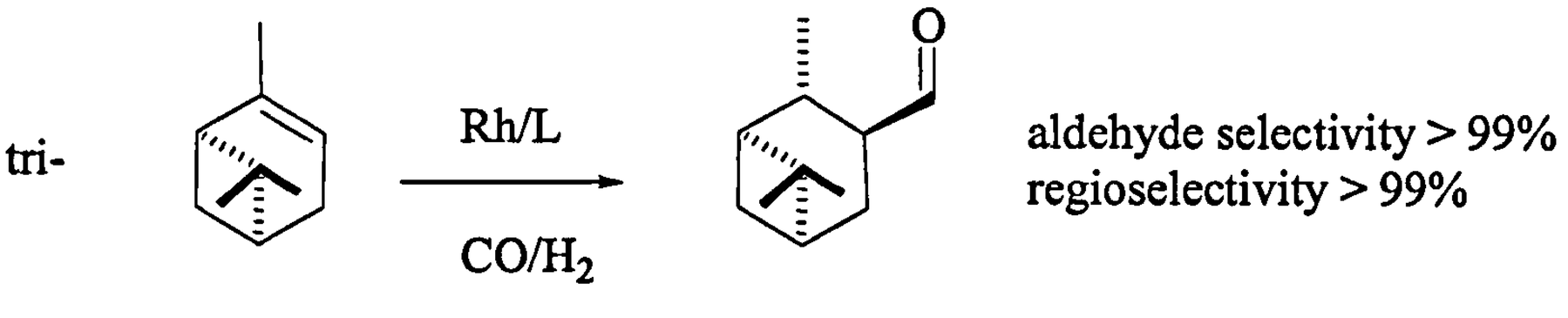

Equation 4.5

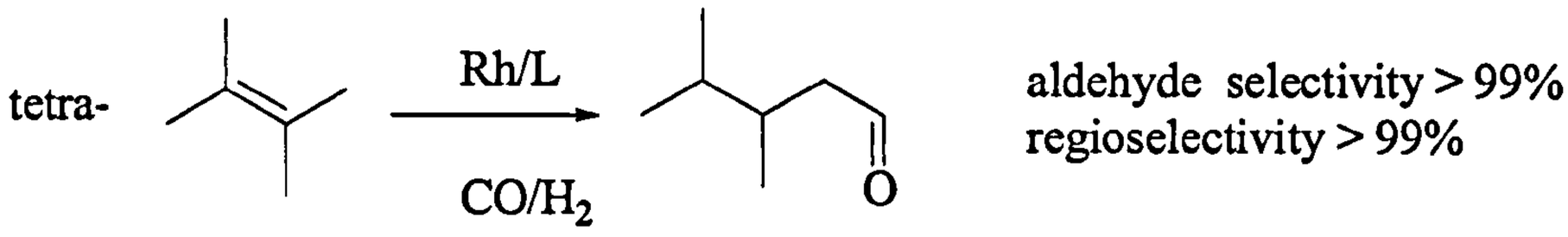

Equation 4.6

4.3.3 Hydroformylation of epoxides

The hydroformylation of epoxides provides an elegant and inexpensive pathway to β-hydroxyaldehydes that may easily be hydrogenated to 1,3-diols which have a wide variety of uses.[149] Recently, interest in 1,3-propanediol has grown for its potential application in industry as an intermediate in the production of polyester fibers and films.[149]

In the hydroformylation of epoxides (Equation 4.7), special attention in the design of the catalyst is needed to suppress side reactions such as isomerization and hydrogenation.[149] It has recently been reported that in the cobalt-catalyzed hydroformylation of ethylene oxide,[149] oxide chelating ligands e.g. bis(diphenylphosphino)methane oxide (dppmO) are superior in terms of higher selectivities and yields compared to their phosphine analogues, e.g. bis(diphenylphosphino)methane (dppm).

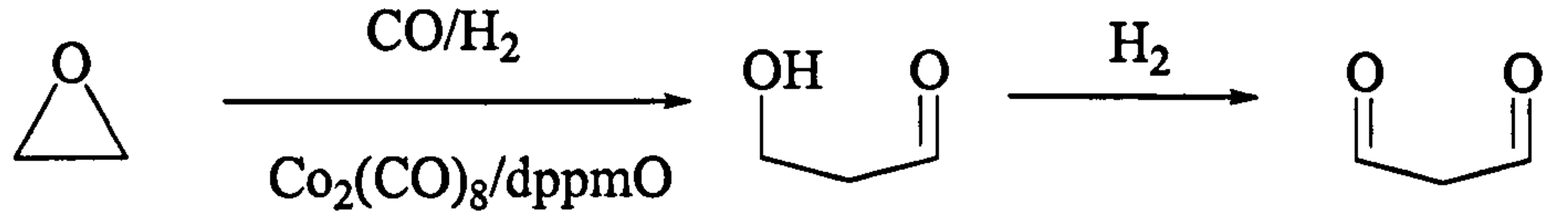

Equation 4.7

4.4 Bicyclic phosphines for hydroformylation

Trialkylphosphines such as tributylphosphine have been used as ligands for cobalt-catalyzed hydroformylation, but bicyclic phosphines have been preferred due to reduced volatility and catalyst stability.[90]

Sasol has reported[90] exceptionally good catalysts for the hydroformylation of 1-dodecene using a cobalt catalyst system with a family of bicyclic phosphines derived from (*R*)-(+)-limonene (Figure 4.5).

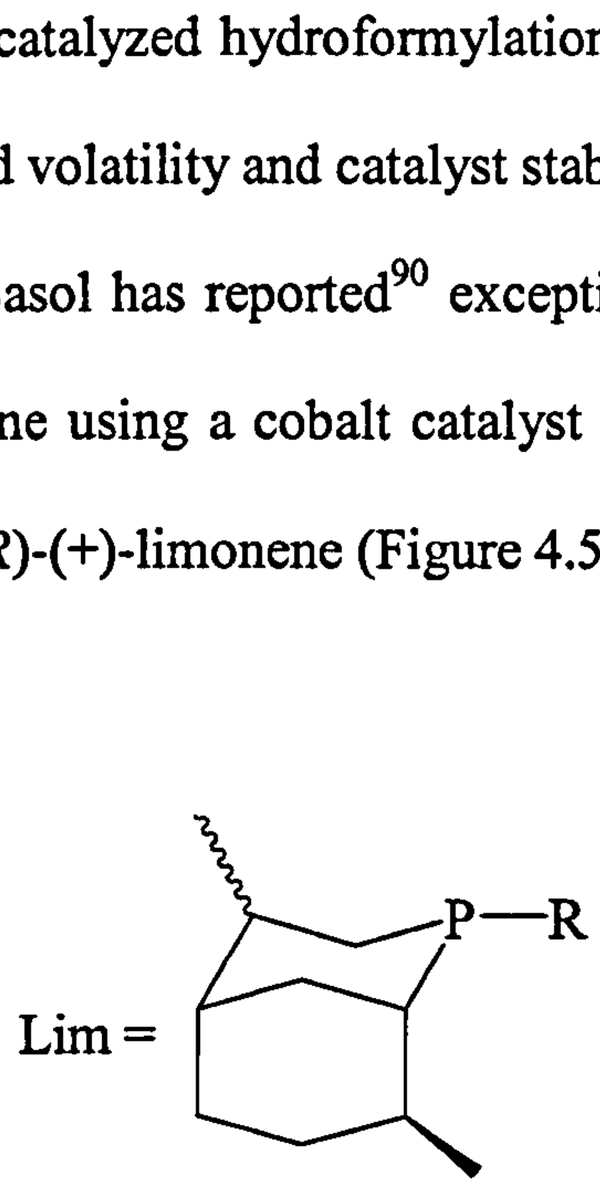

Compound Abbreviation	R
Lim-H	H
Lim-C18	$(CH_2)_{17}CH_3$
Lim-C10	$(CH_2)_9CH_3$
Lim-C5	$(CH_2)_4CH_3$
Lim-Aph	$(CH_2)_3C_6H_5$
Lim-ACN	$(CH_2)_2CN$
Lim-ABE	$(CH_2)_3OCH_2C_6H_5$
Lim-EVE	$(CH_2)_2OCH_2CH_3$

Figure 4.5

In 1992, the bicyclic water-soluble phosphine NORBOS-Na (**4.27**) was shown to be the most active catalyst in the hydroformylation of propene.[114]

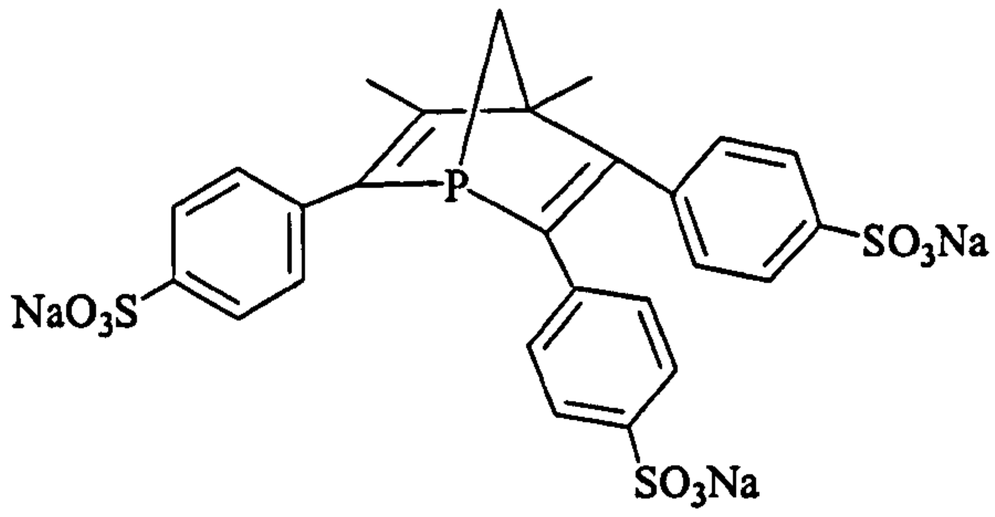

4.27

Historically the most important class of bicyclic phosphines for hydroformylation are derivatives of 9-phosphabicyclononanes. The parent compounds are also known as phobanes **(4.28)** and **(4.29)**. The mixture is synthesised by the hydrophosphination of 1,5-cyclooctadiene with PH_3 using a radical initiator to give the isomeric mixture **(4.28)** and **(4.29)** in quantitative yield in a ratio of approximately 2:1 (Equation 4.8).[150,151]

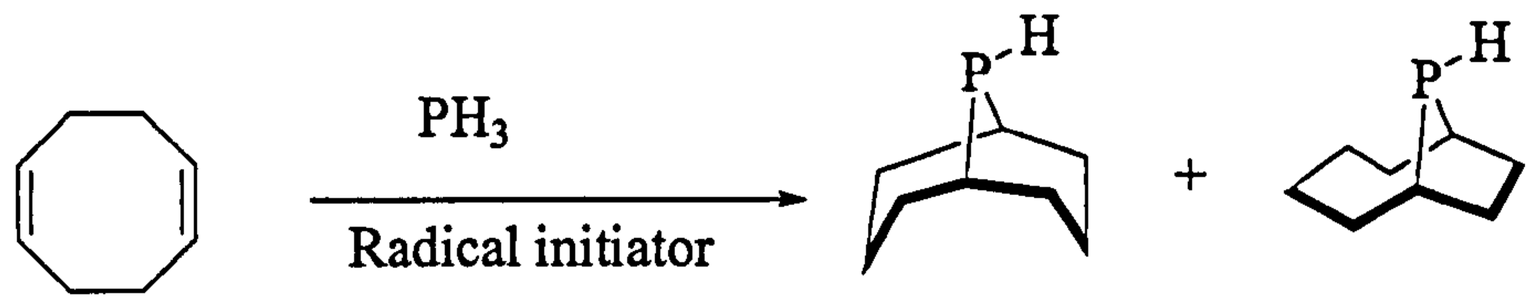

4.28 **4.29**

Equation 4.8

The synthesis of phobanes was first reported by Shell in 1966,[152-154] and this prompted the interest of other companies in these compounds. In 1977 Hoechst AG [155] and in 1980 Nippon Chemical Industrial Co.[156] patented the synthesis of **(4.28)** and **(4.29)**.

The catalytic activity of the phosphines **(4.30)** and **(4.31)** in cobalt-catalysed hydroformylation of higher alkenes was also reported[153,154,157] and these proved to be very active catalysts.

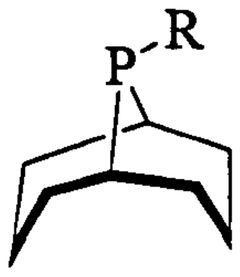

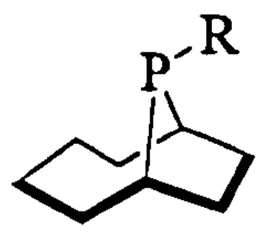

R = Ph
R = $(CH_2)_{19}CH_3$

4.30 **4.31**

Another compound in this family to show high activity in the cobalt-catalysed hydroformylation of alkenes was the bidentate ligand **(4.32)**.[158]

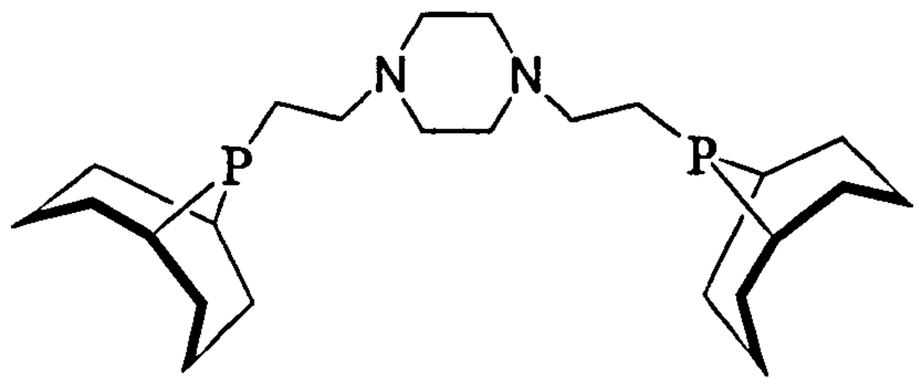

4.32

Diphosphine **(4.33)** below has been reported for the rhodium-catalyzed hydroformylation of 1-octene,[159] and in the hydroformylation of citronellene (Equation 4.9). This reaction is of industrial interest as the hydroformylation product is a useful raw material in the perfume industry. The ligand **(4.33)** was previously synthesised by Fawcett *et al.* in 1993.[160]

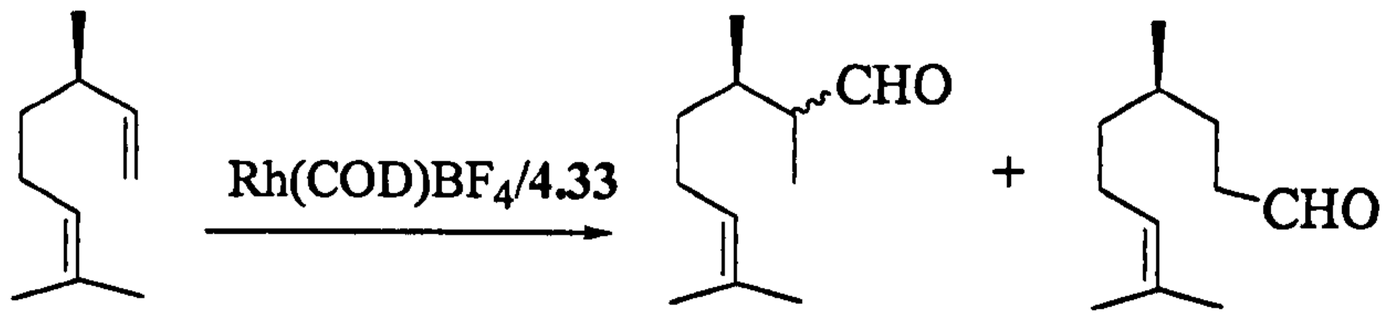

Equation 4.9

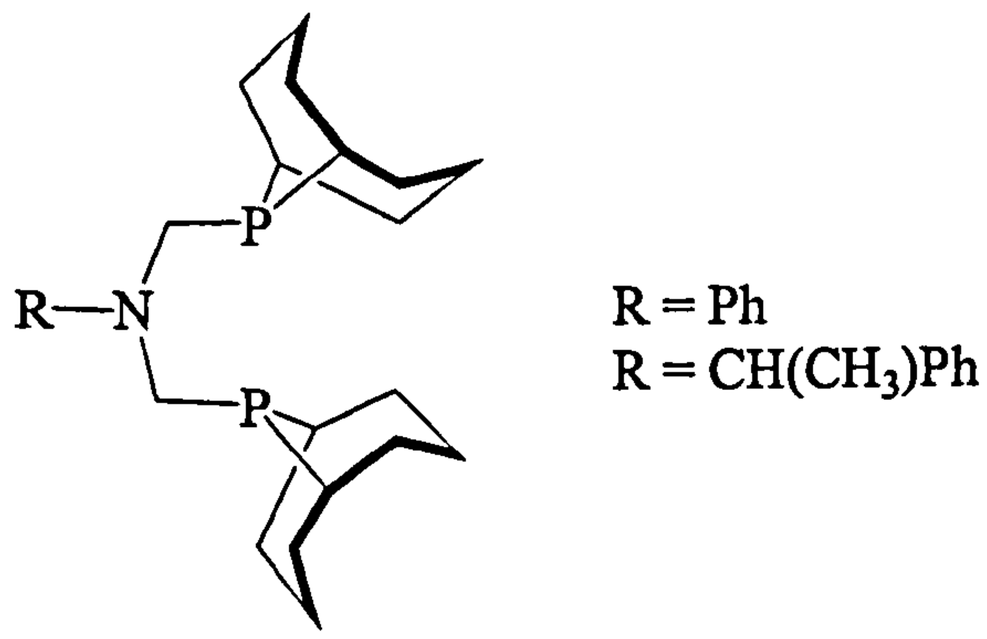

R = Ph
R = $CH(CH_3)Ph$

4.33

4.5 Bite angle effects in hydroformylation

Extensive research has been dedicated to fine tune stereoelectronic properties, pursuing higher activities and selectivities.[161]

Although there have been a wide variety of ligands studied for hydroformylation, consistent structure-activity relationships are still lacking.[161,162] The explanation for this is that a complex set of electronic and steric effects govern selectivity in hydroformylation.

The term "electronic effect" refers to the electronic properties of the ligand (basicity, π acceptor/donor capabilities) whereas steric effects describe ligand bulkiness. It has been said that diphosphine ligands generate two kinds of steric effects; those associated with ligand-ligand or ligand-substrate non-bonding interactions (non-bonding effects) and those directly related to the bite angle, which have been called orbital effects.[161]

The trigonal bipyramidal rhodium complexes containing two coordinated phosphine ligands can exist in two isomeric forms as an equilibrium as shown in Figure 4.6.[163] In these forms the phosphine ligands coordinate in a diequatorial (ee) or a equatorial-apical (ea) fashion.

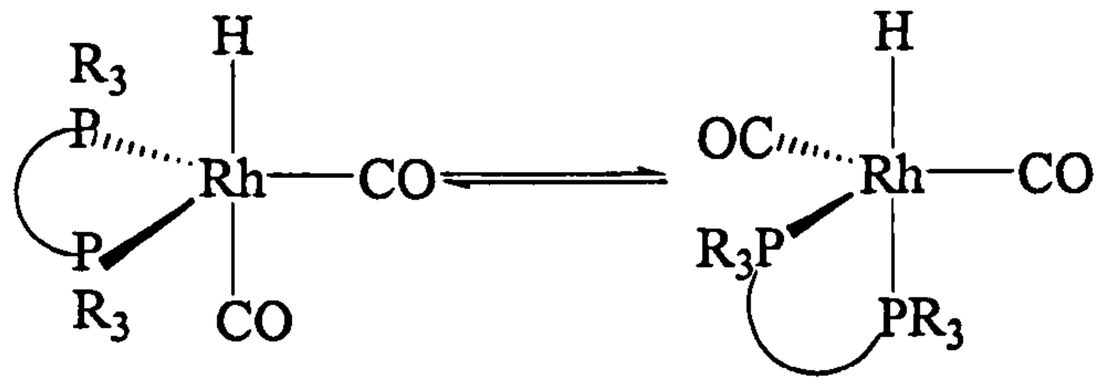

Figure 4.6 Equilibrium ee-ea

Bidentate ligands can have a preference for a specific geometry since the bite angle β (Figure 4.7) is strongly dependent on the bridge between the two bonding ligand atoms (see Section 1.3.2.2).

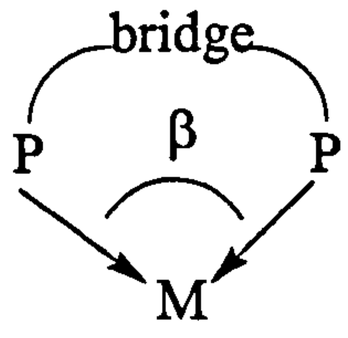

Figure 4.7 Bite angle β

Chelating ligands with β around 90°, will stabilize ea (Figure 4.6) coordination in trigonal-bipiramidal geometry.[164] Whereas a ligand with β of 120° could stabilize ee coordination. This is critically important in hydroformylation where the ee coordination species is involved in the formation of the linear product in the hydroformylation cycle (Scheme 4.1).[163]

In the search to explain the bite angle effect, a series of xantphos ligands (Figure 4.8) have been reported which were designed to ensure minimal variation in electronic properties and steric size. The bite angle (102-121°) was the only feature that was varied.[165] In the hydroformylation of 1-octene, an increase in activity and selectivity for linear aldehyde formation was observed with increasing natural bite angle. For styrene the same trend in selectivity for the linear aldehyde was found, although the selectivity was also found to be dependent on temperature and CO pressure.[165]

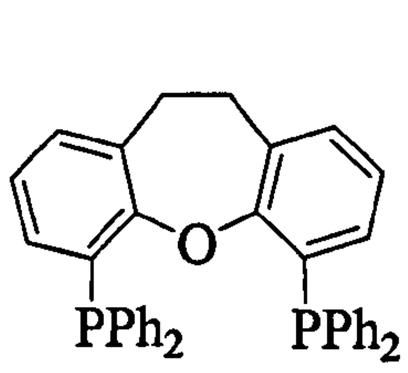

Homoxantphos

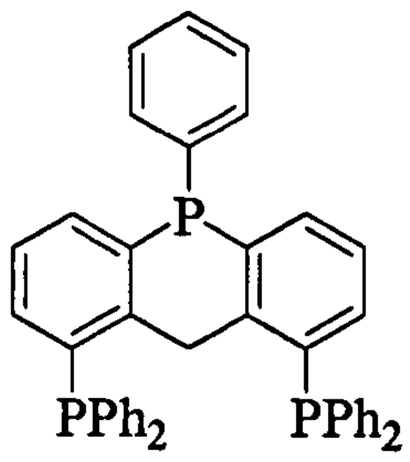

Phosxantphos

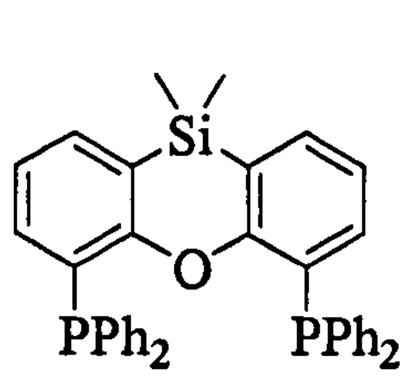

Sixantphos

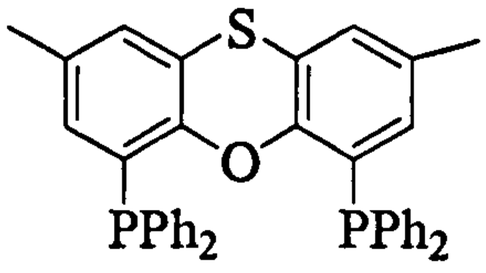

Thixantphos

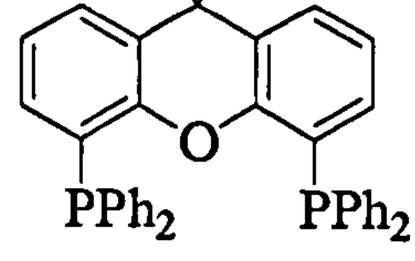

Xantphos

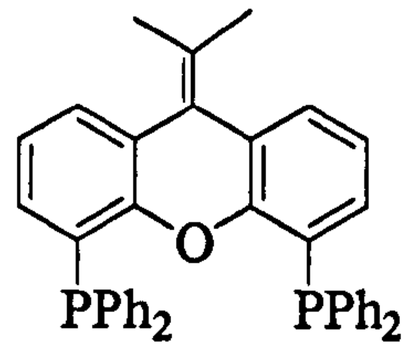

Isopropxantphos

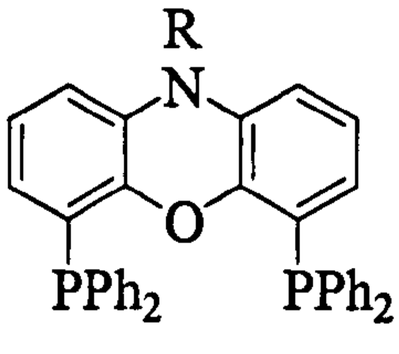

R = H, Nixantphos
R = Bn, Benzylnixantphos

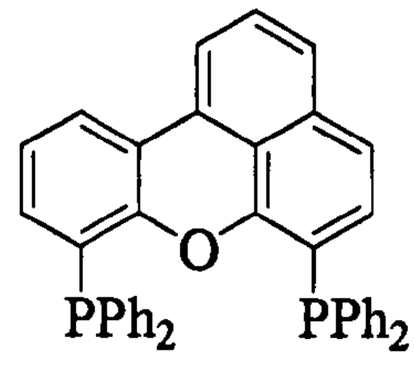

Benzoxantphos

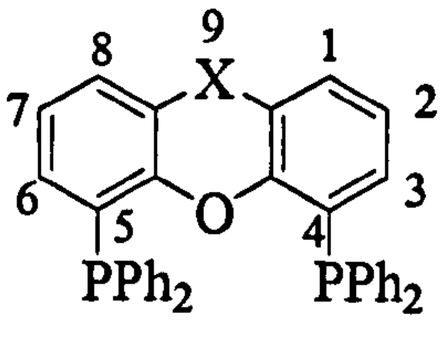

generic structure

Figure 4.8 Xantphos family of ligands

The bite angle effect has been explained by showing that as the natural bite angle increases, the congestion around the metal atom also increases, which favours the less sterically demanding transition state, and driving the reaction towards the formation of the linear product.[161] A theoretical study of rhodium systems containing xantphos type ligands has shown that correlation between natural bite angle and regioselectivity takes place at the transition state for alkene insertion.[161]

The effect of the bite angle in the rhodium-catalyzed hydroformylation of 1-octene and styrene was studied with a homologous series of bidentate phosphines (Figure 4.9) based on xanthene-like backbone ligands.[166] The series of ligands are based on rigid aromatic heterocycles. A comparison with BISBI shows that rigidity of the

ligand backbone is essential for obtaining high selectivity in hydroformylation reactions.[166]

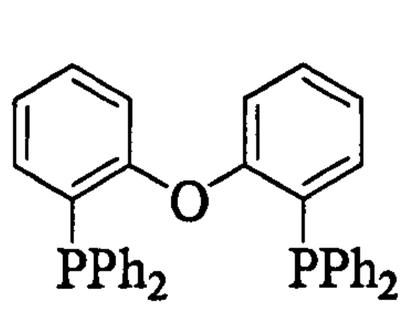

DPEphos

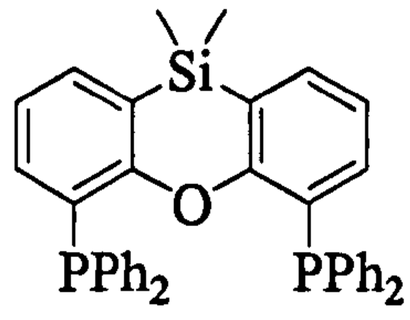

Sixantphos

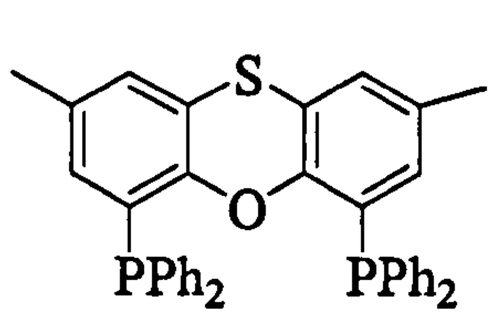

Thixantphos

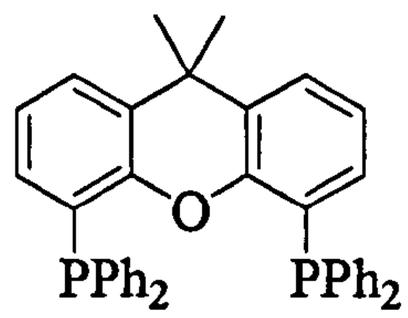

Xantphos

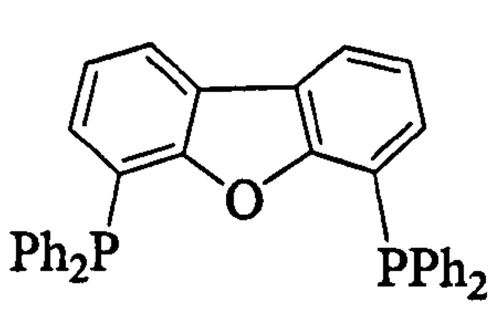

DBFphos

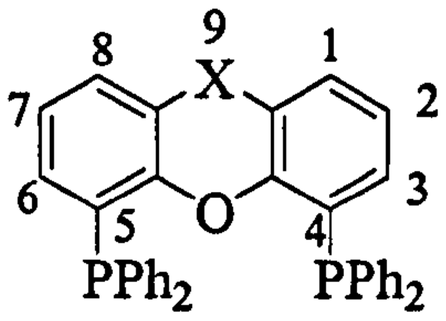

generic structure

Figure 4.9

In a systematic study, a series of phosphacyclic xantphos ligands (Figure 4.10) with bite angles ranging from 110° to 126° have shown high activities in the hydroformylation of internal octenes.[167] The high activity was connected to the synergy of the low phosphine basicity and the wide bite angles of the ligands. The low phosphine basicity leads to the required high isomerization (ee:ea) and hydroformylation activity, while the large bite angle induces the high selectivity for the linear aldehyde formation.

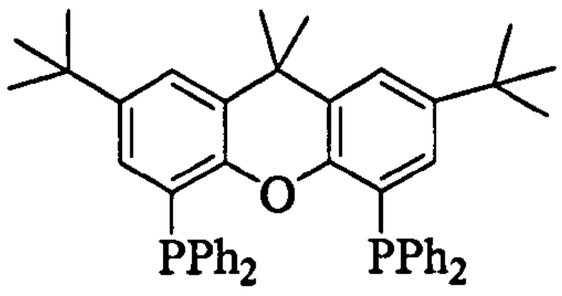

Xantphos

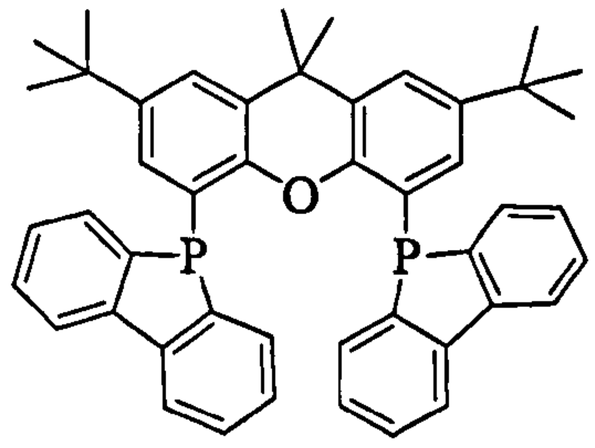

DPB-xantphos

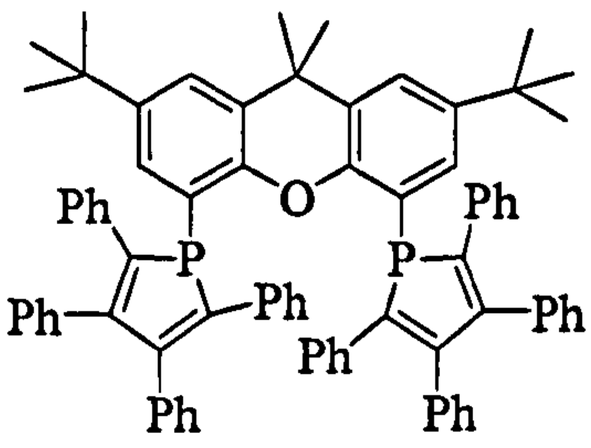

TPP-xantphos

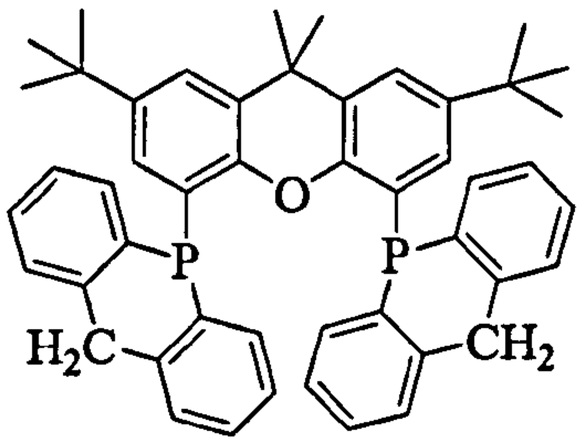

PCP-xantphos

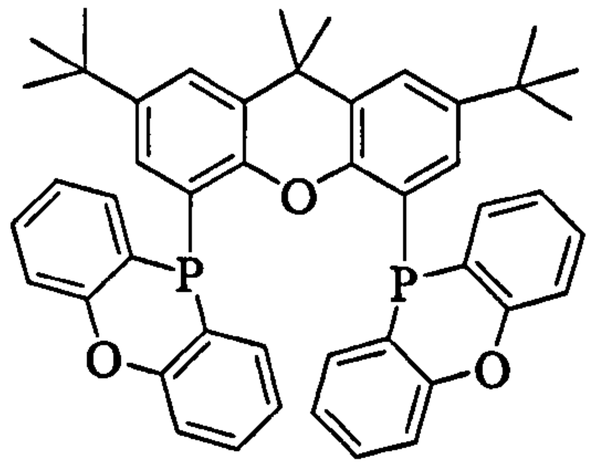

POP-xantphos

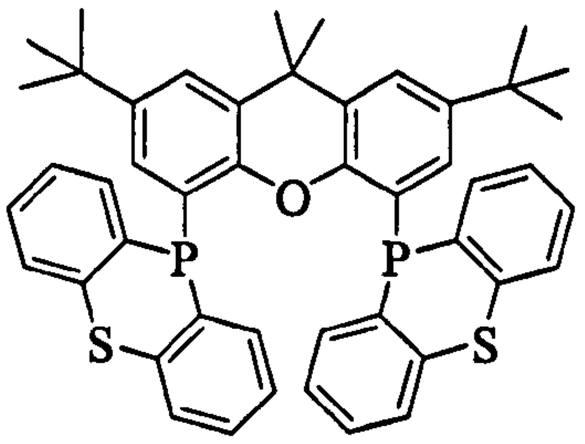

PSP-xantphos

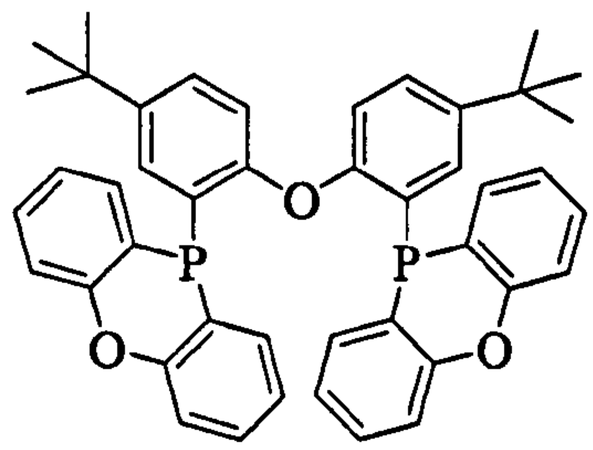

POP-DPEphos

Figure 4.10

4.6 Hydroformylation catalysis with monodentate adamantyl cages

The rhodium complexes of ligands **(4.34)** and **(4.35)** were tested as catalysts for the hydroformylation of hex-1-ene.

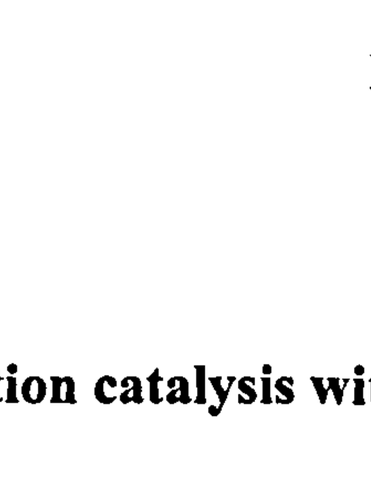

4.34

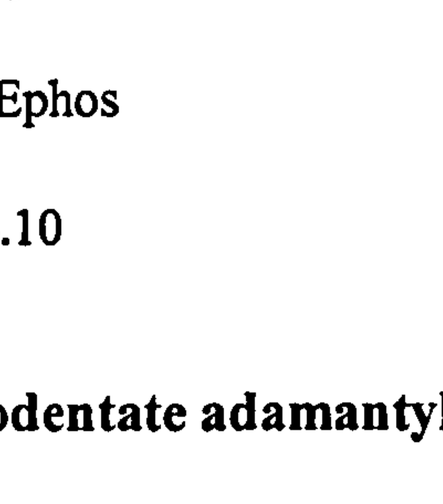

4.35

The hydroformylations were carried out in an autoclave. The catalyst was prepared *in situ* under N_2 by dissolving [Rh(acac)$(CO)_2$] and the ligand in THF. Biphenyl was added in stoichiometric amounts as the internal standard for the analysis of the products by GC. The autoclave was operated remotely from a control panel where the temperature, time, CO and H_2 pressure were set and monitored by a computer throughout the reaction period. The conditions were the same for each ligand. The data was analysed using a plot of syngas uptake versus time. The catalysis was also performed using PPh_3 for comparison.

The gas uptake for hydroformylation with PPh_3 and (**4.35**) are plotted in Figure 4.11. However due to problems with the autoclave the kinetic data for (**4.34**) is not suitable for plotting. The n:i ratio was measured by ^{1}H NMR and GC after 100% conversion and the kinetic data gathered was used to calculate an average turnover frequency value for 40% conversion.

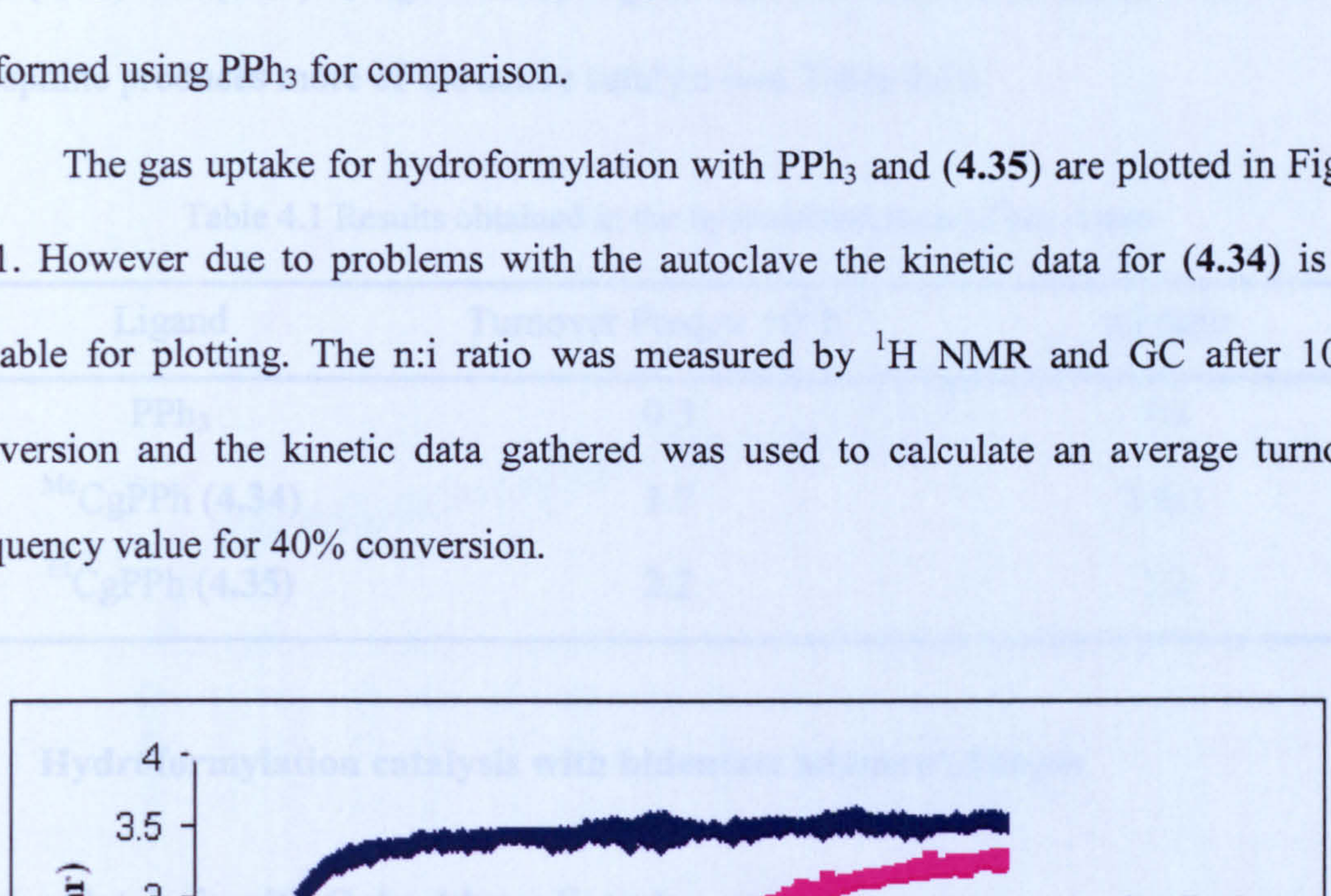

Figure 4.11 Gas uptake for hydroformylation of hex-1-ene

It can be seen in Figure 4.11 that the catalyst derived from ligand (**4.35**) is faster than PPh_3. With (**4.35**), *ca.* 97% of the total syngas was consumed in 30 min, compared to PPh_3 which used *ca.* 88% in almost 2 h. This result is very promising considering that $[Rh(acac)(CO)_2]/PPh_3$ is a commercial catalyst for the hydroformylation process. The n:i ratio with (**4.35**) is lower than for (**4.34**) (see Table 4.1) suggesting that increasing the bulkiness does not lead to an increase in selectivity. The average turnover frequency with (**4.34**) and (**4.35**) is significantly higher than for PPh_3 which means that the cage phosphine produces more of the active catalyst (see Table 4.1).

Table 4.1 Results obtained in the hydroformylation of hex-1-ene

Ligand	Turnover Freq./$\times 10^3\ h^{-1}$	n:i ratio
PPh_3	0.3	3:1
^{Me}CgPPh (**4.34**)	1.7	1.6:1
^{Et}CgPPh (**4.35**)	2.2	1:1

4.7 Hydroformylation catalysis with bidentate adamantyl cages

4.7.1 Catalysis with C_3 backbone ligands

The hydroformylation of hex-1-ene with catalysts derived from bidentate ligands was carried out and compared with the catalysis using 1,3-bis(diphenylphosphino)-propane (**4.4**).

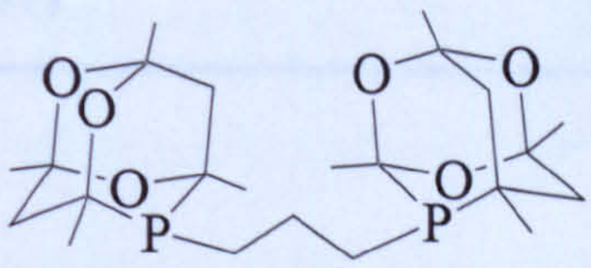

4.36

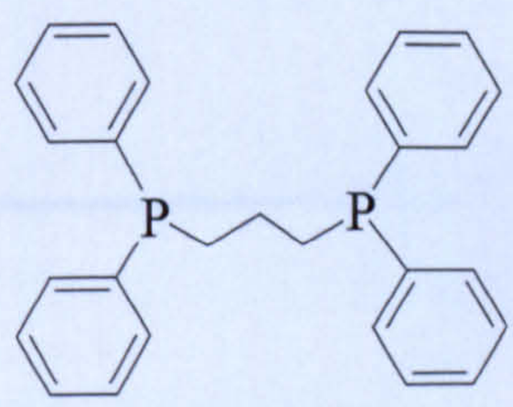

4.37

The results with (**4.36**) and (**4.37**) are given in Table 4.2 and plotted in Figure 4.12. It is clear that the catalyst with (**4.37**) is faster than with (**4.36**) and also the reaction with (**4.36**) did not go to completion. After 90 min with ligand (**4.37**), 83% of the syngas had been consumed whereas with ligand (**4.36**), even after 6 h, only 52% had been consumed.

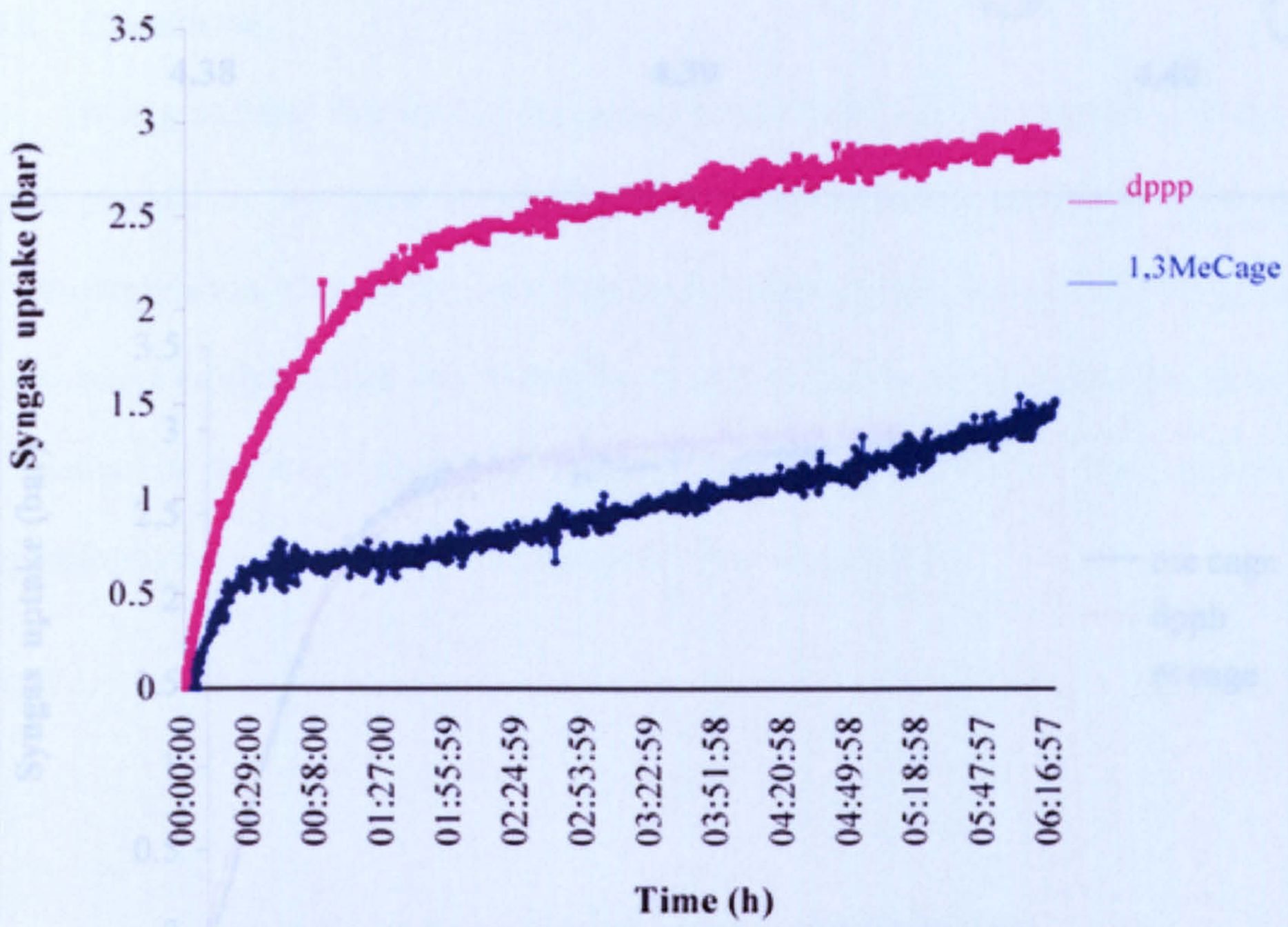

Figure 4.12 Syngas uptake for hydroformylation of hex-1-ene with C_3 bidentate ligands

Table 4.2 Results obtained in the hydroformylation of hex-1-ene with C_3 bidentate ligands

Ligand	% conversion	n:i ratio
1.3^{Me}Cg (**4.36**)	52	1.2
dppp (**4.37**)	92	1.4

4.7.2 Catalysis with C_4 backbone ligands

The ligands (**4.38-4.40**) were tested in the hydroformylation of hex-1-ene and the results plotted in Figure 4.13.

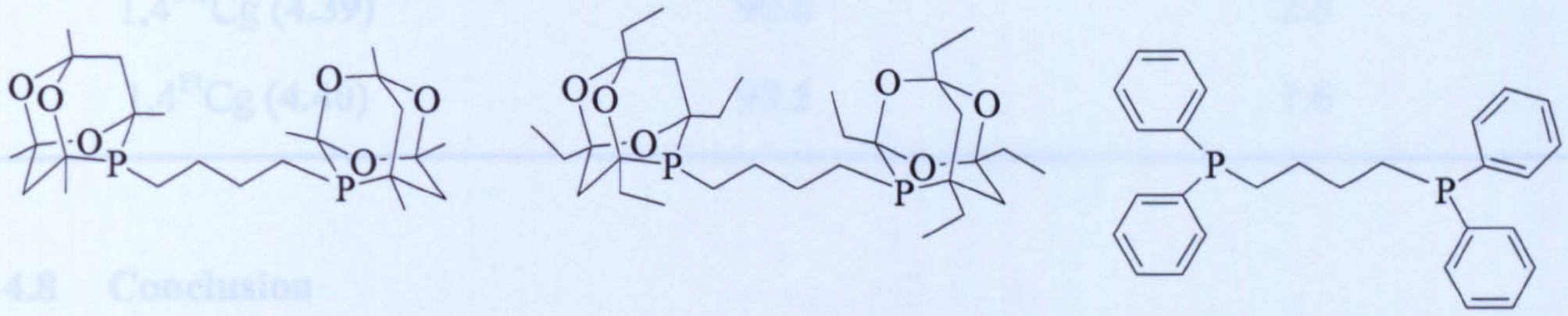

4.38 **4.39** **4.40**

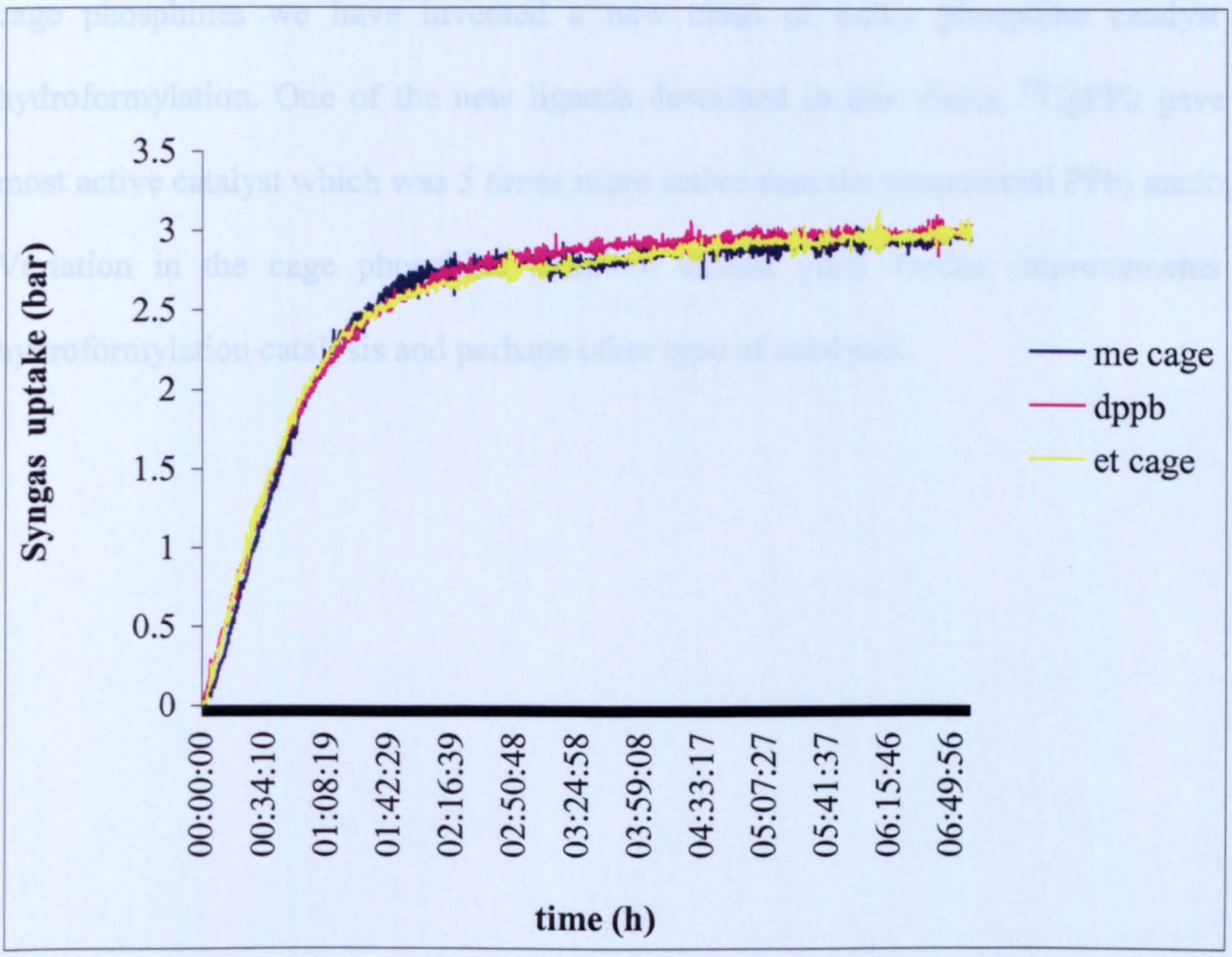

Figure 4.13 Kinetic data for the hydroformylation of hex-1-ene

This plot shows that the three ligands tested (**4.38**), (**4.39**) and (**4.40**) have almost identical behaviour in terms of rate but the n:i ratios are significantly different indicating that the ligand is participating in directing the selectivity.

Table 4.3 shows the conversion and n:i ratios. The bulkiest ligand (**4.39**) gave the highest conversion while the ligand (**4.38**) gave the highest n:i ratio.

Table 4.3 Results obtained in the hydroformylation of hex-1-ene with C_4 bidentate ligands

Ligand	Conversion	n:i ratio
dppb **(4.38)**	92.0	1.1
$1,4^{Me}$Cg **(4.39)**	90.6	2.5
$1,4^{Et}$Cg **(4.40)**	98.5	1.6

4.8 Conclusion

It is gratifying that during the course of investigating the chemistry of unusual cage phosphines we have invented a new class of bulky phosphine catalyst for hydroformylation. One of the new ligands described in this thesis, ^{Et}CgPPh gave the most active catalyst which was 5 times more active than the commercial PPh_3 analogue. Variation in the cage phosphine structure should yield further improvements for hydroformylation catalysis and perhaps other type of catalysis.

Chapter 5

Experimental

E.1 Experimental: General experimental details

Unless otherwise stated, all operations were carried out under a N_2 atmosphere by standard Schlenk line techniques. Solvents were purified using the purification system shown in Figure 5.1. This system consists of 2 columns connected in series. The first column contains activated alumina, which removes polar impurities such as water and peroxides. The second is a column of supported copper catalyst (Q-5), which removes traces of O_2 to the ppm levels. Diethyl ether, THF and acetonitrile were purified using only the first column due to undesirable reactivity with the second column. These solvents were deoxygenated by bubbling N_2 through them. Commercial reagents were used as supplied unless otherwise stated. Starting materials prepared by literature methods were $[PdCl_2(NCPh)_2]$,[169] and $[PtCl_2(cod)]$.[170]

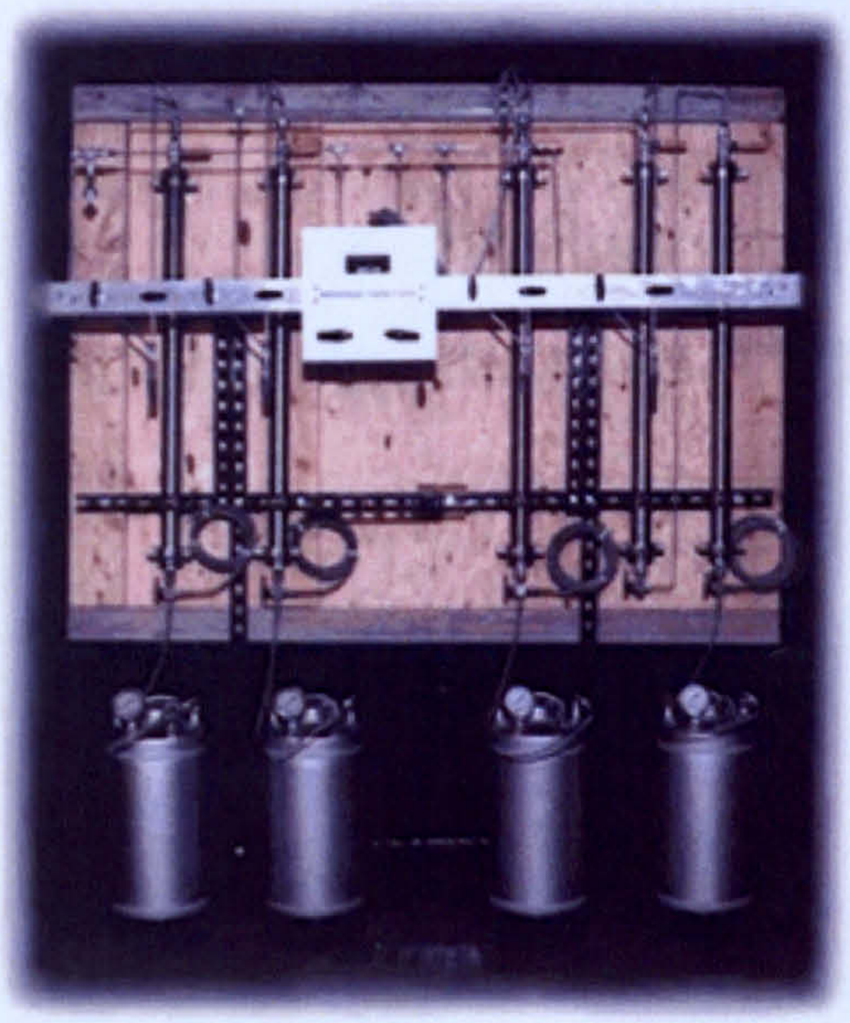

Figure 5.1

The Mass Spectrometry Service, University of Bristol, recorded electron Impact and Fast Atom Bombardment mass spectra on a MD800 and Auto spec.

The following NMR spectrometers were used:

$^{31}P\{^{1}H\}$ NMR spectra;	Jeol Λ300 (121.4 MHz) with chemical shifts relative to high frequency of 85% H_3PO_4 Jeol Λ400 (161.9 MHz) with chemical shifts relative to high frequency of 85% H_3PO_4
^{1}H NMR spectra;	Jeol Λ300 (300 MHz) with chemical shifts relative to tetramethylsilane Jeol Λ400 (400 MHz) with chemical shifts relative to tetramethylsilane
$^{13}C\{^{1}H\}$ NMR spectra;	Jeol Λ300 (75 MHz) with chemical shifts relative to tetramethylsilane Jeol Λ400 (100.6 MHz) with chemical shifts relative to tetramethylsilane
$^{19}F\{^{1}H\}$ NMR spectra;	Jeol Λ300 (282.6 MHz) with chemical shifts relative to high frequency of $CFCl_3$

Spectra were recorded using deoxygenated $CDCl_3$ unless otherwise stated.

E.2 Chapter 2: Bidentate tetramethyl-trioxa-phospha-adamantanes

E.2.1 Separation of *meso*- and *rac*-1,3-bis(^{Me}adamphosphino)propane

E.2.1.1 Recrystallisation of *meso/rac*-(2.54)

E.2.1.1.1 Recrystallisation from a mixture of CH_2Cl_2 and methanol

Following the procedure described by Pugh[73] a round-bottomed flask was connected to a condenser under N_2. *Meso/rac*-1,3-bis(^{Me}adamphosphino)propane **(2.54)** (0.500 g, 1.1 mmol) was dissolved in hot CH_2Cl_2 (2 cm^3), and then methanol (10 cm^3) was added dropwise until a turbid solution was observed. The mixture was allowed to cool to room temperature and then cooled in a refrigerator at 4 °C over 24 h to facilitate precipitation of *rac*-**(2.54)**. The *meso*-isomer remained in solution. The white solid was collected by filtration and recrystallized again by the same procedure. The $^{31}P\{^1H\}$ NMR spectrum of which showed two signals at –29.4 and –30.2 ppm corresponding to the two diastereoisomers in a ratio of *ca.* 3:97 (*meso*:*rac*) with 60% recovery.

E.2.1.1.2 Recrystallisation from ethanol

A mixture of *meso/rac*-**(2.54)** (0.501 g, 1.06 mmol), was placed in a 50 cm^3 round-bottomed flask and hot (60 °C) ethanol (9.5 cm^3) was slowly added. The flask was kept warm with a thermal mantle to reflux (80 °C) until the solid had dissolved. The resulting solution was allowed to cool to room temperature. After 24 h, a white precipitate was observed, the $^{31}P\{^1H\}$ NMR spectrum of which showed two signals at –29.4 and –30.2 ppm corresponding to the two diastereoisomers in a ratio of *ca.* 10:90 (*meso*:*rac*) with 76% recovery.

E.2.1.1.3 Recrystallisation from methanol

A mixture of *meso/rac*-(**2.54**) (0.100 g, 0.21 mmol), was dissolved by the slow addition in the minimum amount of boiling methanol (4 cm^3). The resulting solution was allowed to cool to room temperature. After 1 h, a white precipitate was observed, the $^{31}P\{^1H\}$ NMR spectrum showed two signals at –29.5 and –30.2 ppm corresponding to the two diastereoisomers in a ratio of *ca.* 5:95 (*meso:rac*) with 80% recovery.

E.2.1.2 Selective complexation of *meso/rac*-(2.54)

E.2.1.2.1 Complexation with nickel(II)

A mixture of *meso/rac*-(**2.54**) (0.560 g, 1.19 mmol) was added to a solution of $NiCl_2.6H_2O$ (0.026 g, 0.11 mmol) in ethanol (5 cm^3) and the resulting solution was stirred for 2 h to afford a purple precipitate. The nickel complex was filtered off and then added to an aqueous solution (5 cm^3) of KCN (0.230 g, 3.5 mmol). Diethyl ether (5 cm^3) was added to the solution to give two layers. The $^{31}P\{^1H\}$ NMR spectrum of the ethereal layer showed two signals at –29.5 and –30.5 ppm corresponding to the two diastereoisomers in a ratio of *ca* 1:1.

E.2.1.2.2 Complexation with platinum(II)

To a solution of $[PtCl_2(cod)]$ (0.098 g, 0.21 mmol) in CH_2Cl_2 (5 cm^3) was added dropwise *meso/rac*-(**2.54**) (0.195 g, 0.41 mmol) in CH_2Cl_2 (5 cm^3) and the resulting solution was stirred for 2 h to afford a pale yellow precipitate. The platinum complex was filtered off and then added to an aqueous solution (5 cm^3) of KCN (0.230 g, 3.5 mmol). Diethyl ether (5 cm^3) was added to the solution to give two layers. The $^{31}P\{^1H\}$ NMR spectrum of the ethereal layer showed two signals at –29.5 and –30.5 ppm corresponding to the two diastereoisomers in a ratio of *ca.* 3:1 (*meso:rac*).

E.2.1.2.3 Complexation with palladium(II)

A solution of $[PdCl_2(NCPh)_2]$ (0.025 g, 0.06 mmol) in CH_2Cl_2 (5 cm^3) was added to a solution of *meso/rac*-(**2.54**) (0.056 g, 0.12 mmol) in CH_2Cl_2 (10 cm^3) and the resulting mixture was stirred for 2 h to afford a yellow precipitate. The product was collected by filtration and then added to an aqueous solution (5 cm^3) of KCN (0.230 g, 3.5 mmol). Diethyl ether (5 cm^3) was added to the solution to give two layers. The $^{31}P\{^1H\}$ NMR spectrum of the ethereal layer showed two signals at –29.5 and –30.5 ppm corresponding to the two diastereoisomers in a ratio of *ca.* 5:1 (*meso*:*rac*).

E.2.1.3 Attempted resolution of *rac*-1,3-bis(^Meadamphosphino)propane

Following the literature procedure,[81] a solution of bis-(μ-chloro)-bis-[*R*-2-[1-(dimethylamino)ethyl]-naphthyl-*C*,*N*]dipalladium(II) (**2.61**) (0.080 g, 0.24 mmol) in methanol (10 cm^3) was added to a solution of *rac*-(**2.54**) (0.056 g, 0.12 mmol) in methanol (10 cm^3), and the mixture was stirred for 2 h under nitrogen. An excess of NH_4PF_6 (0.50 g) in water (10 cm^3) was then added, and the mixture was stirred until dissolution was complete. The $P\{^1H\}$ NMR of the resulting solution showed various peaks between +20 and +30 ppm.

E.2.2 Synthesis and coordination chemistry of bidentate tetramethyl-trioxa-phospha-adamantanes

E.2.2.1 Synthesis of *meso/rac*-1,4-bis(^Meadamphosphino)butane (2.64)

E.2.2.1.1 Synthesis of 1,4-bis(diethoxyphosphinyl)butane

Adapting the method described in the literature,[82] using a Perkin triangle distillation apparatus, a solution of 1,4-dibromobutane (50 cm^3, 90.4 g, 0.42 mol) and triethylphosphite (189 cm^3, 182.8 g, 1.10 mol) was stirred and heated to 160-170 °C at atmospheric pressure for 5 h. During this time, bromoethane (*ca.* 70 cm^3) was collected by continuous distillation. The reaction mixture was then allowed to cool to room

temperature and then volatile impurities were removed *in vacuo*. Lower boiling fractions were distilled from the product under reduced pressure (0.21 mmHg, 95-110 °C), leaving the 1,4-bis(diethoxyphosphinyl)butane as an air-stable, colourless, viscous oil (117.85 g, 85%), which crystallised slowly at 4 °C. The $^{31}P\{^{1}H\}$ NMR spectrum of the liquid showed a singlet at +32.6 ppm.

E.2.2.1.2 Synthesis of 1,4-diphosphinobutane

A 2 litre, 3-necked round-bottomed flask was fitted with a dropping funnel, mechanical stirrer and condenser. Adapting the method described in the literature,[83] 1,4-bis(diethoxyphosphinyl)butane (47.0 g, 0.14 mol) was dissolved in diethyl ether (140 cm^3). The solution was added cautiously, dropwise over 3 h (strongly exothermic reaction) to a stirred, cooled (0 °C) suspension of lithium aluminium hydride (16.3 g, 0.43 mol) in diethyl ether (350 cm^3). The mixture was allowed to warm to room temperature and stirring was continued for a further 96 h. The reaction mixture was then cooled again to 0 °C and water (25 cm^3) was added steadily over 1 h, (*note, evolution of H_2 gas*). N_2-saturated phosphoric acid (5M, 150 cm^3) was then added cautiously over 2 h, resulting in the formation of two layers. The upper organic layer was separated, the aqueous phase was washed with diethyl ether (3 x 80 cm^3), and the extracts combined and dried over anhydrous $MgSO_4$ overnight. A portion of this solution (*ca.*100 cm^3) was transferred to a 250 cm^3 flask fitted with a Vigreux column equipped for distillation and, as the diethyl ether was distilled, more solution was added. After the distillation was complete the remaining solvent was removed at reduced pressure (50 mmHg). The temperature of the distillation was between 152-154 °C, to afford 1,4-diphosphinobutane as a clear, colourless liquid with an unpleasant odour (12.1 g, 71%). The $^{31}P\{^{1}H\}$ NMR spectrum of the liquid showed a singlet at –135.4 ppm and the ^{31}P NMR spectrum showed a triplet at –135.2 (^{1}J(PH) 190 Hz).

E.2.2.1.3 Synthesis of meso/rac-1,4-bis(^{Me}adamphosphino)butane (2.64)

1,4-Diphosphinobutane (2.8 cm^3, 2.6 g, 0.023 mol) was added dropwise over 5 min to a solution of 2,4-pentanedione (10 cm^3, 9.5 g, 0.095 mol) in aqueous HCl (60 cm^3, 5 M). A white solid began to precipitate after *ca.* 1 h. The reaction mixture was stirred for a further 93 h, after which time the white solid product was filtered off in air, washed with water (3 x 20 cm^3) and dried *in vacuo* to afford *meso/rac*-(**2.64**) (8.8 g, 79%).

δ_P (121.4 MHz; $CDCl_3$)	-28.4 (s), -28.5 (s)
δ_H (300 MHz; $CDCl_3$)	1.50 - 1.92 (16 H, m, CH_2) 1.24 - 1.44 (24 H, m, CH_3)
δ_C (75 MHz; $CDCl_3$)	a 96.5 (s) b 95.7 (s) c 72.2 (s), 72.1 (s) d 72.0 (s), 71.7 (s) e 44.5 (d, ^1J(PC) 15.4) f 37.0 (s) g 28.0 (d, ^1J(PC) 23.06) h 27.9 (s), 27.7 (s) i 27.2, (d, ^4J(PC) 13.83) j 26.8, (d, ^4J(PC) 13.07) k 29.7-31.2 (m) l 20.7 (d, ^1J(PC) 23.06)
FAB mass spectrum: m/z	486 (70%) (M^+)
Elemental analysis (calc.)	C: 58.8 (59.2) H: 8.1 (8.3)

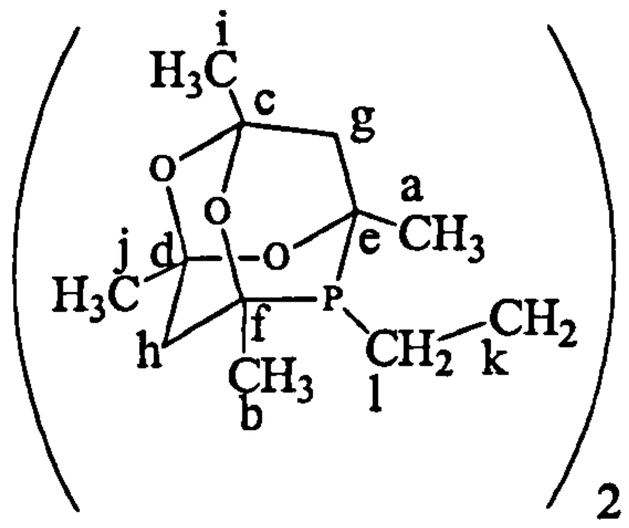

E.2.2.2 Synthesis of (2.64) from borane adduct

n-Butyl lithium (3.1 cm^3, 1.6 M, 4.96 mmol) was added dropwise to a cooled solution (–5 °C) of ^{Me}CgPH.BH_3 (**2.65**) (1.0 g, 4.35 mmol) in THF (8 cm^3). The mixture

was allowed to warm to room temperature, and stirring was continued for a further 2 h. The mixture was then cooled to –72 °C and a solution of 1,4-dibromobutane (0.26 cm^3, 0.47 g, 2.19 mmol) in THF (45 cm^3) was cautiously added dropwise over 5 min. Stirring was continued for a further 24 h to afford a colourless solution. The $^{31}P\{^1H\}$ NMR spectrum showed a broad signals at 12.5 ppm that correspond to the borane adduct of the product (**2.66**). To deprotect the product, SiO_2 (6.0 g) was added to the solution and stirred for 48 h. The solution was then filtered and the solvent removed *in vacuo* to afford the *meso/rac*-(**2.64**) in a ratio *ca* of 1:2 in 62% of recovery.

δ_P (121.4 MHz; $CDCl_3$)	-28.4 (s), -28.5 (s)
δ_H (300 MHz; $CDCl_3$)	1.50 - 1.92 (16 H, m, CH_2) 1.24 - 1.44 (24 H, m, CH_3)
δ_C (75 MHz; $CDCl_3$) 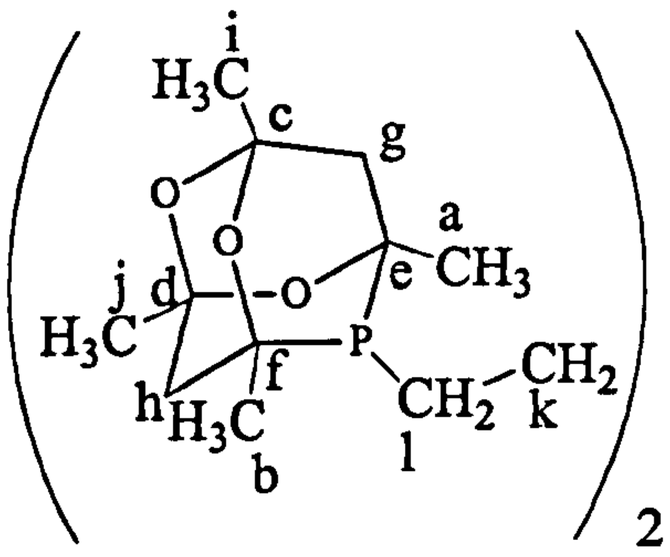	A 96.5 (s) b 95.7 (s) c 72.2 (s), 72.1 (s) d 72.0 (s), 71.7 (s) e 44.5 (d, ^1J(PC) 15.4) f 37.0 (s) g 28.0 (d, ^2J(PC) 23.06) h 27.9 (s), 27.7 (s) i 27.2, (d, ^4J(PC) 13.83) j 26.8, (d, ^4J(PC) 13.07) k 29.7-31.2 (m) l 20.7 (d, ^1J(PC) 23.06)
FAB mass spectrum: m/z	486 (80%) (M^+)
Elemental analysis (calc.)	C: 58.8 (59.2) H: 8.1 (8.3)

E.2.2.3 Dichloroplatinum(II) complex of (2.64)

A solution of $[PtCl_2(cod)]$ (33.6 mg, 0.09 mmol) in CH_2Cl_2 (5 cm^3) was added to a solution of *meso/rac*-(**2.64**) (45 mg, 0.09 mmol) in CH_2Cl_2 (5 cm^3). The resulting pale yellow solution was stirred for 4 h, after which time a pale yellow precipitate had formed. The $^{31}P\{^1H\}$ NMR spectrum of the solid showed a singlet at –4.9 ppm with platinum satellites (^1J(PtP) 3513 Hz) corresponding to the diastereoisomers *meso/rac*-**(2.67)**.

δ_P (121.4 MHz; $CDCl_3$)	-4.9 (s) (^1J(PtP) 3513 Hz)
FAB mass spectrum: m/z	717 (M^+-^{35}Cl) (99%)
Elemental analysis (calc)	C: 38.31 (38.73) H: 5.36 (5.04)

E.2.2.4 Dichloropalladium(II) complex of (2.64)

A solution of $[PdCl_2(NCPh)_2]$ (34.7 mg, 0.09 mmol) in CH_2Cl_2 (5 cm^3) was added to *meso/rac*-(**2.64**) (45 mg, 0.09 mmol) in CH_2Cl_2 (2 cm^3). The yellow-orange solution was stirred for 5 h. The $^{31}P\{^1H\}$ NMR spectrum showed different signals from 4 to 6 ppm and 8 to 12 ppm. The elemental analysis of the product does not correspond to $[PdCl_2$**(2.64)**$]_n$.

δ_P (121.4 MHz; $CDCl_3$)	4-5 (m), 7-12 (m)
FAB mass spectrum: m/z	627 (M^+ -^{35}Cl) (50%)
Elemental analysis (calc)	C: 47.52 (43.42) H: 5.43 (6.07)

E.2.2.5 Synthesis of *meso/rac*-1,4-bis(hexafluoro-adamphosphino)butane (2.69)

To a solution of 1,1,1-trifluoro-2,4-pentanedione (4.8 cm^3, 6.0 g, 40.5 mmol) in aqueous HCl (40 cm^3, 5 M, 200 mmol) was added 1,4-phosphinobutane (1 cm^3, 6.7 mmol) dropwise over 5 min. The solution was stirred for 48 h, during which time an

off-white solid formed which was then filtered in air and washed with water (2 x 20 cm^3) to give crude *meso/rac*-1,4-bis(hexafluoroadamphosphino)butane **(2.69)** (3.4 g, 72%). The $^{31}P\{^1H\}$ NMR spectrum of the solid showed two overlapping septets in a ratio of 1:1 corresponding to the diastereoisomers *meso/rac*-**(2.69)**. Recrystallization of the crude solid from methanol gave the pure white solid product *meso/rac*-**(2.69)** in *ca.* 60% recovery. in a ratio of 1:3 (*meso*:*rac*)

δ_P (121.4 MHz; $CDCl_3$)	-33.8 (septet), -33.9 (septet)
δ_H (300 MHz; $CDCl_3$)	1.90 – 2.40 (16 H, m, CH_2) 1.20 - 1.80 (12 H, m, CH_3)
δ_C (75 MHz; $CDCl_3$) 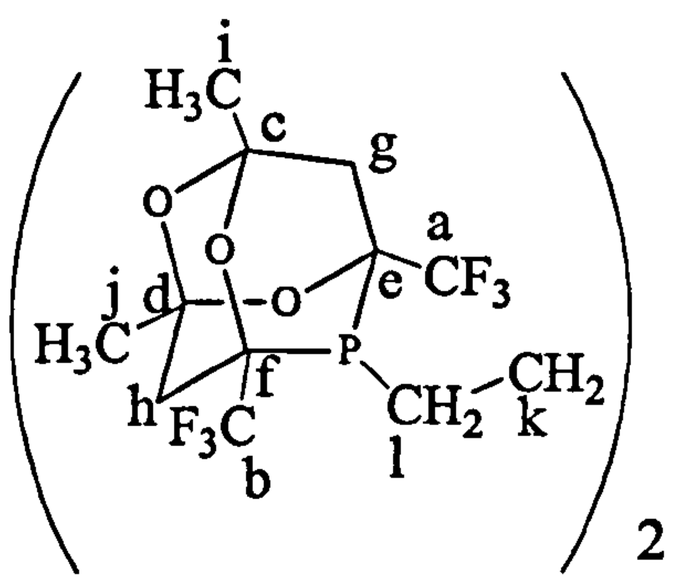	A 125 (qd, ^1J(FC) , ^2J(PC) 16.9) b 123 (qd, ^1J(FC) , ^2J(PC) 8.5) c 96.1 (s) d 96.8 (s) e 76.6 (d, ^1J(PC) 8.5), 76.5 (s) f 76.6 (d, ^1J(PC) 8.5), 76.5 (s) g 35.2 (d, ^2J(PC) 10.4) h 29.2 (s) i 27.4 (s) j 27.1 (s) k 25.8 – 26.3 (m) l 21.0 (d, ^1J(PC) 24.6)
δ_F (286.2 MHz; $CDCl_3$)	74.8 (d), 74.8 (d) ^3J (PF) 15, 16 75..1 (d), 75.2 (d) ^3J (PF) 15, 16
FAB mass spectrum: m/z	702 (34%) (M^+), 683 (10%) (M^+ - ^{19}F)
Elemental analysis (calc.)	C: 40.54 (41.04) H: 3.67 (4.02)

E.2.2.6 Attempted complexation of (2.69) with platinum(II) and palladium(II)

The reaction of *meso/rac*-(**2.69**) (0.07 mmol, 50.0 mg) with $[PtCl_2(cod)]$ (0.07 mmol, 26.2 mg) in CH_2Cl_2 (8 cm^3) gave a pale yellow solution. The solution was monitored by $^{31}P\{^1H\}$ NMR spectroscopy. After 2 h, the $^{31}P\{^1H\}$ NMR spectra showed two septets at -33.95 ppm, that corresponded to the free ligand. The solution was heated to reflux for 1 day, but no change in the $^{31}P\{^1H\}$ NMR was observed.

The reaction of *meso/rac*-(**2.69**) (0.07 mmol, 50.0 mg) with $[PdCl_2(NCPh)_2]$ (0.07 mmol, 27.3 mg) CH_2Cl_2 (8 cm^3) gave an orange solid. The $^{31}P\{^1H\}$ NMR spectrum of the solid in $CDCl_3$ showed various species had formed with broad signals at 8 ppm, 8.5 ppm and a broad singlet at 9.3 ppm; these species were assigned to polymers and oligomers formed in the solution.

E.2.2.7 Synthesis of *meso/rac*-1,5-bis(^{Me}adamphosphino)pentane (2.72)

E.2.2.7.1 Synthesis of 1,5-bis(diethoxyphosphinyl)pentane (2.70)

Adapting the literature,[82] using a Perkin triangle distillation apparatus, a solution of 1,5-dibromobutane (40 cm^3, 79.6 g, 0.4 mol) and triethylphosphite (171.5 cm^3, 166.2 g, 1.0 mol) was stirred and heated to 160-170 °C at atmospheric pressure for 5 h. During this time, bromoethane (*ca.* 60 cm^3) was collected by continuous distillation. The reaction mixture was then allowed to cool to room temperature and volatile impurities were removed *in vacuo*. Lower boiling fractions were distilled from the product under reduced pressure (0.21 mmHg, 100-120 °C), leaving the 1,5-bis(diethoxyphosphinyl)-pentane (**2.70**) as an air-stable, colourless, viscous oil (121.5 g, 88%). The $^{31}P\{^1H\}$ NMR spectrum of the liquid showed a singlet at 34.4 ppm.

E.2.2.7.2 Synthesis of 1,5-diphosphinopentane (2.71)

A 2 litre, 3-necked round-bottomed flask was fitted with a dropping funnel, mechanical stirrer and condenser. Adapting the method described in the literature,[83] 1,5-

bis(diethoxyphosphinyl)pentane (**2.70**) (60.0 g, 0.17 mol) was dissolved in diethyl ether (140 cm^3). The solution was added cautiously, dropwise over 3 h (strongly exothermic reaction) to a stirred, cooled (0 °C) suspension of lithium aluminium hydride (19.8 g, 0.50 mol) in diethyl ether (360 cm^3). The mixture was allowed to warm to room temperature and stirring was continued for a further 96 h. The reaction mixture was then cooled again to 0 °C and water (25 cm^3) was added steadily over 1 h, (*note, evolution of H_2 gas*). N_2-saturated hydrochloric acid (5M, 150 cm^3) was then added cautiously over 2 h, resulting in the formation of two layers. The upper organic layer was separated, the aqueous phase was washed with diethyl ether (3 x 80 cm^3), and the organic extracts combined and dried over anhydrous $MgSO_4$. A portion of this solution (*ca.* 100 cm^3) was transferred to a 250 cm^3 flask fitted with a Vigreux column equipped for distillation and, as the diethyl ether was distilled, more solution was added. The product was distilled at 92 °C. After the distillation was complete the remaining solvent was removed under reduced pressure (50 mmHg), to afford 1,5-diphosphinopentane (**2.71**) as a clear, colourless liquid with an unpleasant odour (18.9 g, 80%). The $^{31}P\{^1H\}$ NMR spectrum showed a singlet at –136.4 ppm and the ^{31}P NMR spectrum showed a triplet at -136.3 ppm (^1J(PH) 189.9 Hz).

E.2.2.7.3 Synthesis of meso/rac-1,5-bis(^{Me}adamphosphino)pentane (2.72)

The diprimary phosphine 1,5-diphosphinopentane (**2.70**) (1 cm^3, 0.90 g, 60 mmol) was added dropwise over 5 min to a solution of 2,4-pentanedione (3.6 cm^3, 3.6 g, 40 mmol) in aqueous HCl (30 cm^3, 5 M). A white solid began to precipitate after *ca.* 3 h. The reaction mixture was stirred for a further 4 d, after which time the white solid product was filtered in air, washed with water (3 x 20 cm^3) and dried *in vacuo* to afford *meso/rac*-1,5-bis(^{Me}adamphosphino)pentane (**2.72**) in a ratio of *ca.* 1:1.

δ_P (121.4 MHz; $CDCl_3$)	-28.31 (bs)
δ_H (300 MHz; $CDCl_3$)	1.40 – 2.20 (m, 18 H, CH_2) 1.12 – 1.34 (m, 24 H, CH_3)
δ_C (75 MHz; $CDCl_3$) 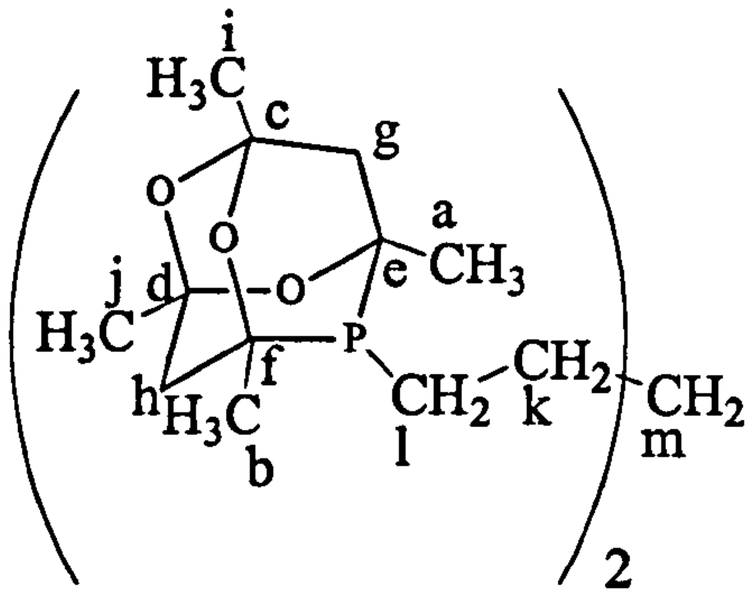	a 96.5 (s) b 95.7 (s) c 72.1 (s), 72.0 (s) d 71.8 (s) e 44.4 (d, ^1J(PC) 15.4) f 37.0 (s) g 28.0 (d, ^2J(PC) 10.7) h 27.9 (s), 27.8 (s) i = j = 26.8, (d, ^4J(PC) 13.07) k = m = 33.0 (m) l 20.7 (d, ^1J(PC) 21.53)
FAB mass spectrum: m/z	500 (2%) (M^+)
Elemental analysis (calc.)	C: 60.19 (59.97) H: 8.95 (8.46)

E.2.2.8 Dichloroplatinum(II) complex of (2.72)

A solution of $[PtCl_2(cod)]$ (33.6 mg, 0.090 mmol) in CH_2Cl_2 (5 cm^3) was added to a solution of *meso/rac*-1,5-bis(^{Me}adamphosphino)pentane (**2.72**) (45 mg, 0.090 mmol) in CH_2Cl_2 (5 cm^3). The resulting pale yellow solution was stirred for 4 h. The solvent was removed in *vacuo* and the $^{31}P\{^1H\}$ NMR spectrum showed a singlet at – 1.33 ppm with broad platinum satellites (^1J(PtP) 3513 Hz). Peaks at 0.9 ppm, 0.8 ppm and 0.5 ppm were also observed.

δ_P (121.4 MHz; $CDCl_3$)	-1.33 (s), 0.90 (s), 0.80 (s), 0.50 (s)
FAB mass spectrum: m/z	731 (M^+ -^{35}Cl) (30%)

E.2.2.9 Synthesis *meso/rac*-1,5-bis(hexafluoro-adamphosphino)pentane (2.73)

To a solution of 1,1,1-trifluoro-2,4-pentanedione (7.4 cm^3, 9.2 g, 59.5 mmol) in aqueous HCl (40 cm^3, 5 M, 200 mmol) was added 1,5-diphosphinopentane (**2.70**) (0.5 cm^3, 9.16 mmol) dropwise over 5 min. The solution was stirred for 96 h, during which time an off-white solid was produced. The off-white solid was filtered in air and washed with water (2 x 20 cm^3) to give crude *meso/rac*-1,5-bis(hexafluoro-adamphosphino)pentane (5.20 g, 73%). The $^{31}P\{^1H\}$ NMR spectrum of the solid showed two signals at –33.1 and –33.2 ppm in a ratio of 1:1 corresponding to the diastereoisomers *meso/rac*-1,5-bis(hexa-fluoroadamphosphino)pentane (**2.73**). Recrystallization of the crude solid from methanol gave pure white solid product *meso/rac*-(**2.73**) in *ca.* 70% recovery.

δ_P (121.4 MHz; $CDCl_3$)	-33.12 (sept), ^3J(PF) -33.18 (sept) ^3J(PF)
δ_H (300 MHz; $CDCl_3$)	1.40 – 2.20 (18 H, m, CH_2) 1.12 – 1.34 (12 H, m, CH_3)
δ_C (75 MHz; $CDCl_3$) 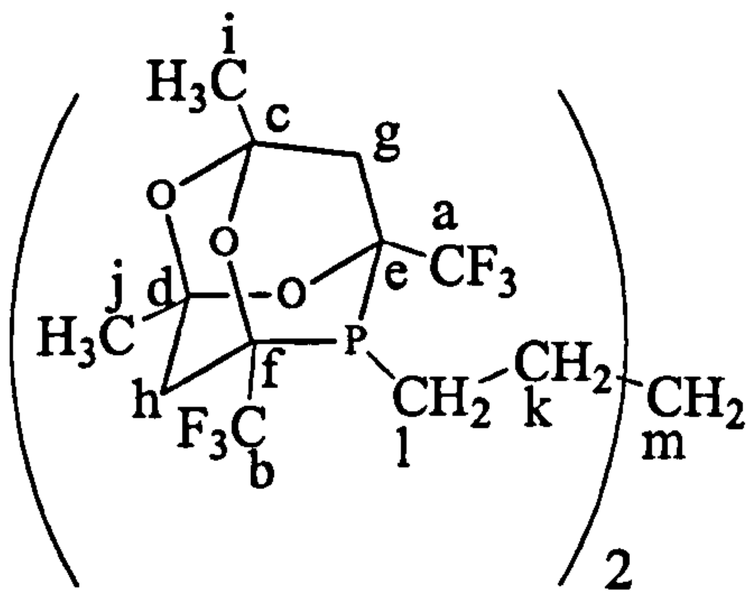	a 124.1 (qd, ^1JFC 280.6, ^2JPC 16.9) b 124.2 (qd, ^1JFC 280.6, ^2JPC 8.5) c 95.2 (s) d 95.1 (s) e 76.6 (d, ^1J(PC) 10.2), 76.5 (s) f 76.5 (d, ^1J(PC) 8.5), 76.4 (s) g 35.2 (d, ^2J(PC) 10.4) h 29.2 (s) i 27.4 (s) j 27.1 (s) k 25.8 – 26.3 (m) l 21.0 (d, ^1J(PC) 24.6) m 32.0 (t, ^3J(PC) 29.2)

FAB mass spectrum: m/z	681 (92%) (M^+ - ^{35}Cl)
δ_F (286.2 MHz; $CDCl_3$)	-77.0 (d), -77.0 (d) ^3J (PF) 15, 16 -78.6 (d), -78.7 (d) ^3J (PF) 15, 16
Elemental analysis (calc.)	C: 41.95 (42.01) H: 3.90 (4.20)

Chapter 3: Experimental

E.3 Chapter 3: Mono- and bidentate tetraethyl-trioxa-phospha-adamantanes

E.3.1 Synthesis of monodentate tetraethyl-trioxa-phospha-adamantanes

E.3.1.1 Synthesis of 1,3,5,7-tetraethyl-2,4,8-trioxa-6-phospha-adamantane (3.1)

A 250 cm^3, 3-necked round-bottomed flask was connected with one inlet, switchable to N_2 or phosphine gas, and an outlet to a bleach trap. A solution of 3,5-heptanedione (10 cm^3, 9.36 g, 73 mmol) in aqueous HCl (100 cm^3, 8 M) was stirred under N_2 overnight. The flask was cooled with an ethylene glycol / CO_2 bath to –12 °C. PH_3 gas was then bubbled through the solution for 6 h. After this time, the inlet was switched to N_2 and the solution was allowed to warm up to room temperature. N_2 was bubbled through the reaction mixture overnight to flush out the excess of phosphine gas remaining in the flask. A test with $AgNO_3$ solution on filter paper was carried out to check that the reaction mixture was free of phosphine gas. The solution was then cooled with an ice-salt bath and neutralized by the slow addition of N_2-saturated NaOH solution (160 cm^3, 5 M) until pH = 7. N_2-saturated diethyl ether (200 cm^3) was then added to the round-bottomed flask and two layers were formed. The ethereal layer was separated and the aqueous phase was washed with diethyl ether (3 x 20 cm^3). The organic extracts were combined and the solvent was removed *in vacuo* to afford (**3.1**). The ^{31}P NMR spectrum showed a doublet of multiplets at –57.9 ppm (^1J(PH) 164.68 Hz) corresponding to the secondary ethyl-cage phosphine in 75% recovery.

δ_P (121.4 MHz; $CDCl_3$)	-57.9 dm, ^1J(PH) 164.68
δ_H (300 MHz; $CDCl_3$)	1.40 – 2.20 (m, 18 H, CH_2) 0.8 – 1.34 (m, 12 H, CH_3)
δ_C (75 MHz; $CDCl_3$)	a 97.4 (s) b 97.1 (s) c 75.0 (s), 74.7 (s) d 73.6 (s), 73.5 (s) e 41.6 (d, ^1J(PC) 13.4) f 39.0 (d, ^1J(PC) 13.8) g 35.7 (s), 35.5(s) h 35.2 (s), 35.0 (s) i = j = 33.5 (d, ^4J(PC) 16.12) l = n = k = m = 6.9 - 6.0 (m)
FAB mass spectrum: m/z	272 (M^+)
Elemental analysis (calc.)	C: 61.31 (61.73) H: 8.90 (9.26)

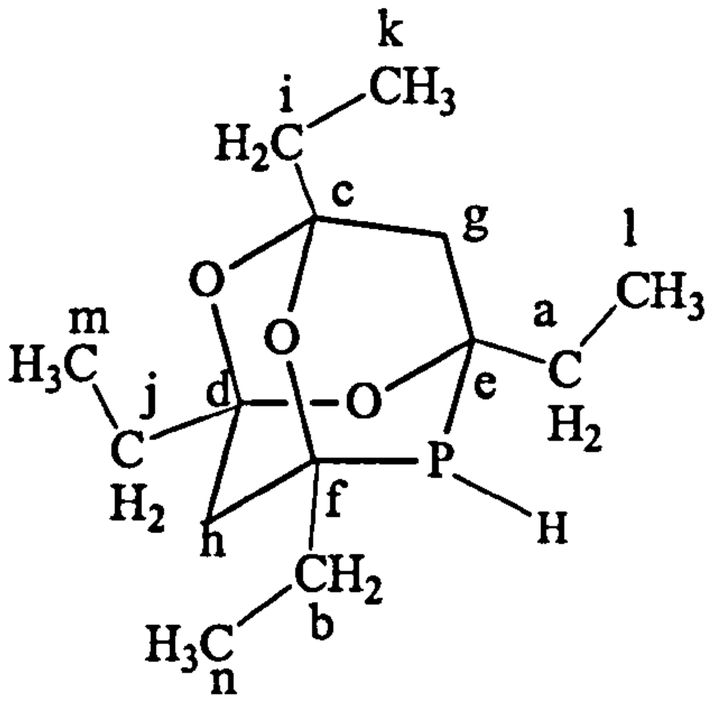

E.3.1.2 Dichloroplatinum(II) complex of (3.1)

To a solution of [$PtCl_2$(cod)] (16 mg, 0.040 mmol) in CH_2Cl_2 (5 cm^3) was added a solution of (**3.1**) (60.0 mg, 0.020 mmol) in CH_2Cl_2 (5 cm^3). The pale yellow solution which formed was stirred for 4 h, after which time a pale yellow precipitate of [$PtCl_2$(**3.1**)] formed, which was filtered off. $^{31}P\{^1H\}$ NMR spectrum of the solution yellow precipitate in $CDCl_3$ showed a signals at –1.4 and -1.7 ppm with platinum satellites (^1J(PtP)) 3308 and 3305 Hz) that correspond to the secondary ethyl-cage phosphine *meso/rac*-[$PtCl_2(^{Et}CgPH)_2$] (**3.2**).

δ_P (121.4 MHz; $CDCl_3$)	-1.4, (s) -1.7 (s) (^1J(PtP) 3308 and 3305)
FAB mass spectrum: m/z	794 (M^+ - ^{35}Cl)
Elemental analysis (calc.)	C: 40.1 (40.53) H: 5.9 (6.03)

E.3.1.3 Dichloropalladium(II) complex of (3.1)

To a solution of $[PdCl_2(NCPh)_2]$ (42.4 mg, 0.11 mmol) in CH_2Cl_2 (5 cm^3) was added a solution of **(3.1)** (59.8 mg, 0.22 mmol) in CH_2Cl_2 (5 cm^3). The yellow solution was stirred for 4 h, after which time a yellow precipitate of $[PtCl_2 (^{Et}CgPH)_2]$ formed, which was filtered off. $^{31}P\{^1H\}$ NMR spectrum of the yellow precipitate in $CDCl_3$ showed signals at –0.4 and -0.9 ppm that correspond to the secondary ethyl-cage phosphine *meso/rac*-$[PdCl_2(^{Et}CgPH)_2]$ **(3.3)**.

δ_P (121.4 MHz; $CDCl_3$)	-0.4 (s), -0.9 (s)
FAB mass spectrum: m/z	705 (M^+ - ^{35}Cl)
Elemental analysis (calc.)	C: 44.91 (45.40) H: 6.30 (6.75)

E.3.1.4 Synthesis of 1,3,5,7-tetraethyl-6-phenyl-2,4,8-trioxa-6-phospha-adamantane (^{Et}CgPPh) (3.4)

In collaboration with Mr. Andrew Ward, a solution of 3,5-heptanedione (2.6 cm^3, 1.5 g, 11.4 mmol) in N_2-saturated aqueous H_2SO_4 (10 cm^3, 12 M) was stirred for *ca.* 2 h. To this solution, phenylphosphine (0.5 cm^3, 460 mg, 4.6 mmol) was added dropwise over 5 min. The reaction mixture was stirred for 5 h, after which time yellow oil drops had formed. The solution was neutralized with N_2-saturated NaOH (80 cm^3, 2.5 M) until pH = 7 and then $CHCl_3$ (30 cm^3) was added to give two layers. The lower organic layer was separated and the aqueous phase was washed with $CHCl_3$ (3 x 20

cm^3), the extracts combined and the solvent was removed *in vacuo*. The crude product was passed through a (30 cm x 2 cm) silica column under N_2 using CH_2Cl_2 as eluent (250 cm^3), and the solvent was removed *in vacuo*. The product was collected to afford ^{Et}CgPPh (**3.4**) (1.5 g, 92%) as a viscous white oil.

δ_P (121.4 MHz; $CDCl_3$)	–30.7 (s)
δ_H (300 MHz; $CDCl_3$)	7.73 – 7.81 (m, 2H, ArH), 7.20 - 7.29 (m, 3H, ArH), 1.65 – 1.96 (m, 12H, CH_2) 0.8 – 1.05 (m, 12H, CH_3)
δ_C (75 MHz; $CDCl_3$)	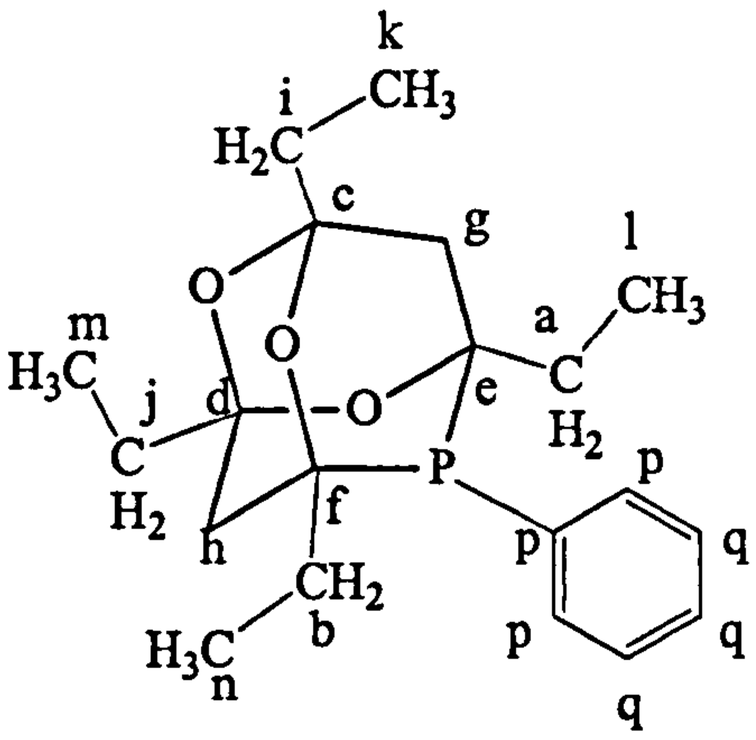 p 134.5 – 135.7 (m) q 128.1 – 129.4 (m) a = b = 97.9 (s), e = f = 97.0 (m), c = d = 77.0 (s) h 76.7 (s), i 75.7 (s) j 75.6 (s), l = n = 31.9 – 34.3 (m) k = m = 6.4 – 7.2 (m).
FAB mass spectrum: m/z	349 (M^+ + H)
Elemental analysis (calc.)	C: 68.50 (68.9) H: 7.9 (8.3)

E.3.1.5 Dichloropalladium(II) complex of (3.4)

To a solution of $[PdCl_2(NCPh)_2]$ (42.4 mg, 0.11 mmol) in CH_2Cl_2 (2 cm^3) was added a solution of ^{Et}CgPPh (75 mg, 0.216 mmol) in CH_2Cl_2 (2 cm^3). The pale yellow solution was stirred for 2 d, after which time a yellow precipitate was formed. The solvent was removed *in vacuo* leaving a yellow solid corresponding to $[PdCl_2(^{Et}CgPPh]$ (**3.5**) (65 mg, 0.075 mmol, 70%).

δ_P (121.4 MHz; $CDCl_3$)	9.81 (s), 9.57 (s)
IR υ(Pd—Cl)	359 cm^{-1}
FAB mass spectrum: m/z	837 (M^+ - ^{35}Cl), 802 (M^+ - 2 ^{35}Cl)
Elemental analysis (calc.)	C: 55.90 (54.96) H: 7.54 (6.69)

E.3.1.6 Preliminary studies of the dichloroplatinum(II) complex of ^{Et}CgPPh

A solution of [$PtCl_2$(cod)] (33.6 mg, 0.09 mmol) in CH_2Cl_2 (5 cm^3) was added to a solution of ^{Et}CgPPh (62.6 mg, 0.18 mmol) in CH_2Cl_2 (5 cm^3). The resulting pale yellow solution was stirred for 4 h. The $^{31}P\{^1H\}$ NMR spectrum showed a singlet at 4.2 ppm with platinum satellites (^1J(PtP) 2682 Hz)), assigned to the monomer (**3.6**) and 15.3 with platinum satellites (^1J(PtP) 4570 Hz) assigned to the dimer compound (**3.7**).

E.3.2 Synthesis of bidentate tetraethyl-trioxa-phospha-adamantanes

E.3.2.1 Attempted synthesis of 1,2-bis(^{Et}adamphosphino)ethane (3.9)

A solution of 3,5-heptanedione (5.5 cm^3, 5.33 g, 41.6 mmol) in N_2-saturated aqueous HCl (40 cm^3, 8 M) was stirred for *ca.* 3 h at room temperature. To this solution, 1,2-diphosphinoethane (1.3 cm^3, 1.02 g, 10.8 mmol) was added dropwise over 5 min. The reaction mixture was stirred for a further 4 d, after which time yellow oil drops had formed. The solution was neutralized with N_2-saturated NaOH (64 cm^3, 5 M) until pH = 7 and then $CHCl_3$ (50 cm^3) was added to form two layers. The lower organic layer was separated and the aqueous phase was washed with $CHCl_3$ (3 x 20 cm^3). The extracts were combined and the solvent removed *in vacuo* to afford the 1,2-diphospha-adamantyl cage (**3.9**) (2.9 g, 85%). The $^{31}P\{^1H\}$ NMR spectrum of the organic layer showed a singlet at –0.9 ppm.

δ_P (121.4 MHz; $CDCl_3$)	-0.9 (s)
δ_H (300 MHz; $CDCl_3$)	2.1 - 1.8 (m, 4 H, CH_2) 1.6 – 1.3 (m, 12H, CH) 0.8 – 1.00 (m, 12 H, CH_3)
δ_C (75 MHz; $CDCl_3$) 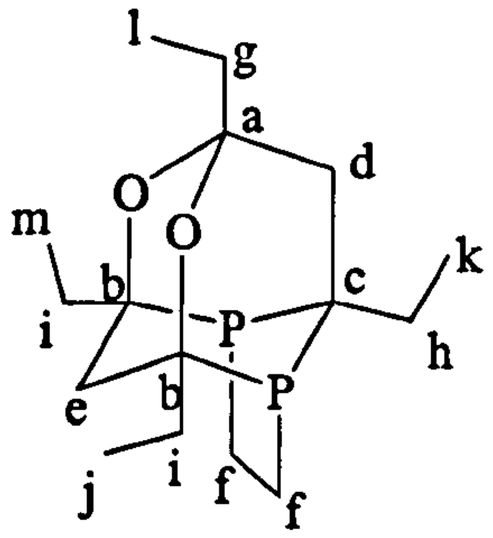 	a 97.3 (s) b 74.5 (m) c 40 (t, ^1J(PC) 39) d 36.5 (t, ^2J(PC) 30) e 35.7 (t, ^2J(PC) 10.4) g 34.6.0 (m) f 31.9 (t, ^1J(PC) 34,6) h = i = 26.5 (m) j = k = 8.2 (t, ^3J(PC) 25.4) l = m = 8.2 (m)
FAB mass spectrum: m/z	314 (M^+)
Elemental analysis (calc.)	C: 61.39 (61.14) H: 9.34 (8.98)

E.3.2.2 Synthesis of *meso/rac*-1,3-bis(^{Et}adamphosphino)propane (3.10)

A solution of 3,5-heptanedione (6.2 cm^3, 45.7 mmol) in N_2-saturated aqueous H_2SO_4 (25 cm^3, 8 M) was stirred for *ca.* 2 h at room temperature. To this solution, 1,3-diphosphinopropane (1.0 cm^3, 0.82 g, 7.6 mmol) was added dropwise over 5 min(preparation of the 1,3-diprimary phosphines was carried out in a similar way as the 1,4-diprimary phosphine section E.2.2.1.2). The reaction mixture was stirred for a further 10 d, after which time oil drops had formed. The solution was neutralized with N_2-saturated NaOH (80 cm^3, 5 M) until pH = 7 and then $CHCl_3$ (45 cm^3) was added to form two layers. The upper organic layer was separated and the aqueous phase was washed with $CHCl_3$ (4 x 10 cm^3). The organic extracts were then combined and the solvent was removed *in vacuo*. The product was dissolved in toluene (8 cm^3) and then

the solvent and unreacted diketone was removed *in vacuo*. The crude product was passed through a (30 x 2 cm) silica column with a mixture of $CHCl_3$/diethyl ether 70:30. The product was collected as a pale yellow fraction and the solvent was removed *in vacuo* to afford *meso/rac*-**(3.10)** (2.5 g, 57%).

δ_P (121.4 MHz; $CDCl_3$)	–38.4 (s)
δ_H (300 MHz; $CDCl_3$)	1.7 – 1.5 (m, 30 H, CH_2) 1.2 – 0.8 (m, 24 H, CH_3)
δ_C (75 MHz; $CDCl_3$)	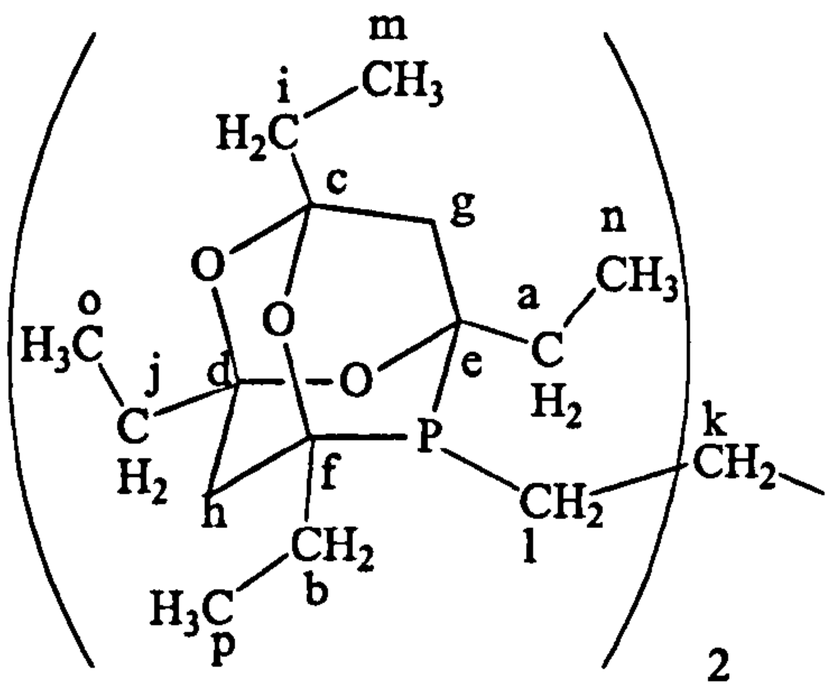 a 96.5 (s) b 95.7 (s) c 72.2 (s), 72.1 (s) d 72.0 (s), 71.7 (s) e 44.5 (d, ^1J(PC) 15.4) g 37.0 (s) f 28.0 (d, ^1J(PC) 23.06) h 27.9 (s), 27.7 (s) i 27.2, (d, ^4J(PC) 13.83) j 26.8, (d, ^4J(PC) 13.07) k 29.7-31.2 (m) l 20.7 (d, ^1J(PC) 23.06)
FAB mass spectrum: m/z	584 (M^+)
Elemental analysis	C: 43.34 (43.76) H: 6.6 (6.3)

E.3.2.3 Dichloroplatinum(II) of (3.10)

To a solution of [$PtCl_2$(cod)] (40 mg, 0.11 mmol) in CH_2Cl_2 (2 cm^3) was added a solution of *meso/rac*-1,3-bis(^{Et}adamphosphino)propane (64.2 mg, 0.11 mmol) in CH_2Cl_2 (2 cm^3). The pale yellow solution was stirred for 3 h, after which time a yellow

precipitate formed. The solvent was removed *in vacuo* leaving a yellow solid corresponding to [$PtCl_2$(**3.10**)].

δ_P (121.4 MHz; $CDCl_3$)	-15.7 (s) (^1J(PtP) 3388) -19.15 (s) (^1J(PtP) 3386)
FAB mass spectrum: m/z	815 (M^+ - ^{35}Cl)
Elemental analysis (calc.)	C: 41.01 (41.63) H: 5.80 (6.55)

E.3.2.4 Dichloropalladium (II) complex of (3.10)

To a solution of [$PdCl_2(NCPh)_2$] (42.4 mg, 0.11 mmol) in CH_2Cl_2 (2 cm^3) was added a solution of *meso/rac*-1,3-bis(^{Et}adamphosphino)propane (**3.10**) (126 mg, 0.216 mmol) in CH_2Cl_2 (2 cm^3). The pale yellow solution was stirred for 3 h, after which time a yellow precipitate formed. The solvent was removed *in vacuo* leaving a yellow solid. The $^{31}P\{^1H\}$ NMR spectrum showed that several products had formed, but two singlets at 0.4 and 2.7 ppm were assigned to the chelate products (**3.12**).

δ_P (121.4 MHz; $CDCl_3$)	0.4 (s), 2.7(s)
FAB mass spectrum: m/z	761 (M^+)

E.3.2.5 Synthesis of *meso/rac*-1,4-bis(^{Et}adamphosphino)butane (3.13)

A solution of 3,5-heptanedione (2.7 cm^3, 2.63 g, 20.2 mmol) in N_2-saturated aqueous H_2SO_4 (20 cm^3, 8 M) was stirred for *ca.* 2 h. To this solution, 1,4-diphosphinobutane (0.5 cm^3, 0.41 g, 3.4 mmol) was added dropwise over 5 min. The reaction mixture was then stirred for a further 10 d, after which time yellow oil drops had formed. The solution was neutralized with a N_2-saturated solution of NaOH (64 cm^3, 5M) until pH = 7 and then $CHCl_3$ (50 cm^3) was added to form two layers. The

lower organic layer was separated and the aqueous phase was washed with $CHCl_3$ (3 x 10 cm^3). The organic extracts were combined and the solvent removed *in vacuo*. The product was dissolved in toluene (8 cm^3) and then the solvent and unreacted diketone removed *in vacuo*. The crude product was passed through a 30 cm silica column with a mixture of $CHCl_3$/diethyl ether 70:30. The product was collected as a pale yellow fraction and the solvent was removed *in vacuo* to afford *meso/rac*-**(3.13)** (1.7 g, 85%).

δ_P (121.4 MHz; $CDCl_3$)	-36.5 (s), -36.4 (s)
δ_H (300 MHz; $CDCl_3$)	1.8 – 1.5 (m, 32 H, CH_2) 1.3 – 0.8 (m, 24 H, CH_3)
δ_C (75 MHz; $CDCl_3$) 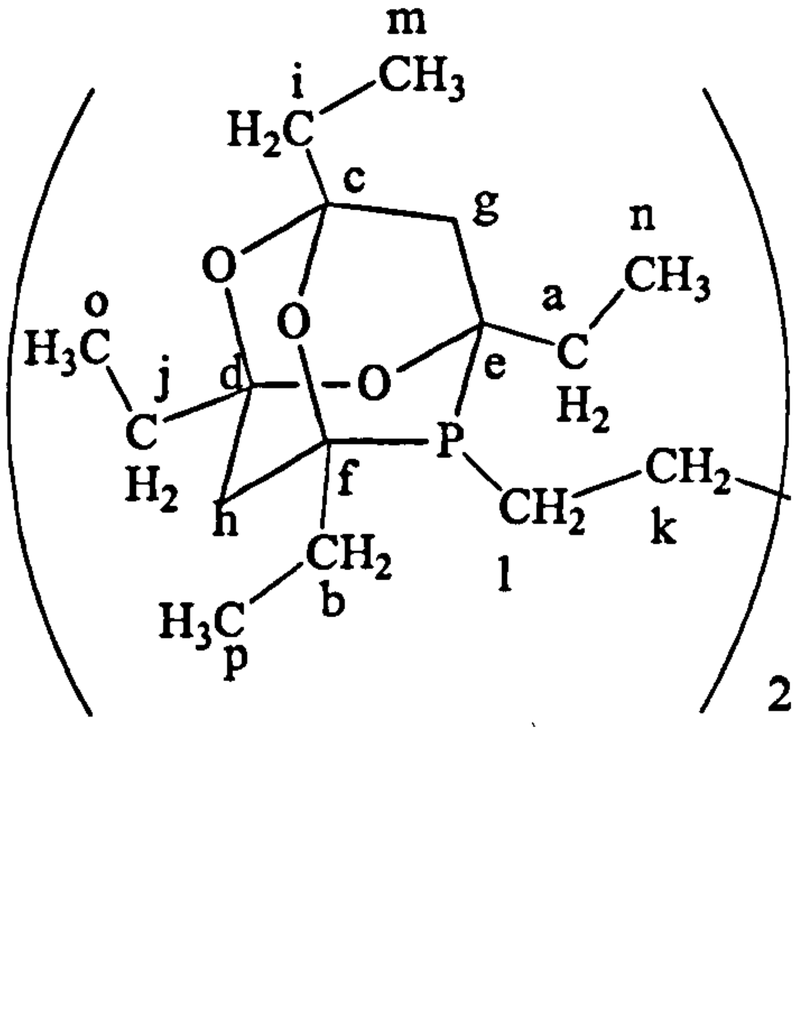	a 97.6 (s) b 96.6 (s) c 75.3 (s), 75.1 (s) d 74.5 (s), 74.4 (s) e 38.9 (d, ^1J(PC) 15.1) g 34.3 (s) f 33.7 (d, ^1J(PC) 22.6) h 31.9 (s), 31.8 (s) i 30.2, (d, ^4J(PC) 13.7) j 30.0, (d, ^4J(PC) 13.5) k 29.6 (m) l 20.4 (d, ^1J(PC) 23.3) n = p 15.2 (s) m 6.4 (s) o 6.2 (s)
FAB mass spectrum: m/z	596 (M^+).
Elemental analysis (calc.)	C: 64.36 (64.19) H: 9.78 (9.35)

E.3.2.6 Dichloroplatinum(II) complex of (3.13)

To a solution of $[PtCl_2(cod)]$ (63.6 mg, 0.17 mmol) in CH_2Cl_2 (2 cm^3) was added a solution of *meso/rac*-1,4-bis(^{Et}adamphosphino)butane (**3.12**) (100 mg, 0.17 mmol) in CH_2Cl_2 (2 cm^3). The pale yellow solution was stirred for 3 h, after which time a pale yellow precipitate had formed. The solvent was removed *in vacuo* leaving a yellow solid corresponding to $[PtCl_2$(**3.13**)$]$. The $^{31}P\{^1H\}$ NMR spectrum showed a signal at –3.9 with platinum satellites (^1J(PtP) 3420 Hz) corresponding to the *meso/rac*-diastereoisomers.

δ_P (121.4 MHz; $CDCl_3$)	–3.9 (s) (^1J(PtP) 3420 Hz)
FAB mass spectrum: m/z	846 (M^+- ^{35}Cl).
Elemental analysis (calc.)	C: 43.96 (43.58) H: 6.78 (6.35)

E.3.2.7 Synthesis of *meso/rac*-1,5-bis(^{Et}adamphosphino)pentane (3.15)

A solution of 3,5-heptanedione (3.9 cm^3, 3.8 g, 29.7 mmol) in N_2-saturated aqueous H_2SO_4 (25 cm^3, 8 M) was stirred for *ca.* 2 h. To this solution, 1,5-bis-(phosphino)pentane (1.0 cm^3, 0.82 g, 6.6 mmol) was added dropwise over 5 min. The reaction mixture was then stirred for a further 10 d, after which time yellow oil drops had formed. The solution was neutralized with N_2 saturated NaOH (80 cm^3, 5 M) until pH 7 and then $CHCl_3$ (45 cm^3) was added to form two layers. The lower organic layer was separated and the aqueous phase was washed with $CHCl_3$ (3 x 15 cm^3). The organic extracts were combined and the solvent removed *in vacuo*. The crude product was passed through a 30 cm silica column with a mixture of $CHCl_3$/diethyl ether 70:30, the product was collected as a pale yellow fraction and the solvent was removed *in vacuo* to afford *meso/rac*- (**2.4**) (3.2 g, 80%). The product was dissolved in toluene (8 cm^3) and then the solvent and unreacted diketone removed *in vacuo*. The $^{31}P\{^1H\}$ NMR spectrum

showed two signals at –36.7 and –36.6 ppm corresponding to the two diastereoisomers **(3.15)** in a ratio of *ca* 1:1.

δ_H (300 MHz; $CDCl_3$)	1.8 – 1.3(m, 34 H, CH_2) 1.3 – 0.7 (m, 24 H, CH_3)
δ_C (75 MHz; $CDCl_3$) 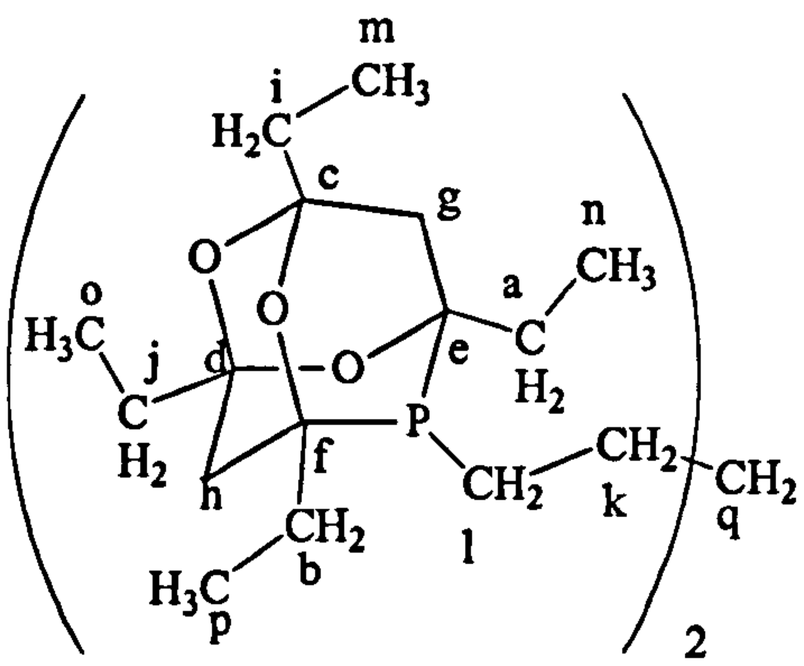	a 97.5 (s) b 96.5 (s) c 72.2 (s), 72.1 (s) d 72.0 (s), 71.7 (s) e 44.5 (d, ^1J(PC) 15.4) g 37.0 (s) f 28.0 (d, ^1J(PC) 23.06) h 27.9 (s), 27.7 (s) i 27.2 (d, ^4J(PC) 13.83) j 26.8 (d, ^4J(PC) 13.07) k 29.7-31.2 (m) l 20.7 (d, ^1J(PC) 23.06)
FAB mass spectrum: m/z	612 (M^+)
Elemental analysis (calc.)	C: 41.01 (41.63) H: 5.80 (6.55)

E.3.2.8 Dichloroplatinum(II) complex of (3.15)

To a solution of $[PtCl_2(cod)]$ (59.8 mg, 0.16 mmol) in CH_2Cl_2 (2 cm^3) was added a solution of *meso/rac*-1,5-bis(^{Et}adamphosphino)pentane **(3.15)** (100 mg, 0.16 mmol) in CH_2Cl_2 (2 cm^3). The pale yellow solution was stirred for 3 h, after which time a pale yellow precipitate was formed. The solvent was removed *in vacuo* leaving a pale yellow solid corresponding to $[PtCl_2$**(3.15)**$]$, The $^{31}P\{^1H\}$ NMR spectrum showed a signal at 1.5 ppm with platinum satellites (^1J(PtP) 2684 Hz) corresponding to the *meso/rac*-diastereoisomers **(3.16)**.

E.3.2.9 Dichloropalladium(II) complex (3.15)

To a solution of $[PdCl_2(NCPh)_2]$ (61.6 mg, 0.16 mmol) in CH_2Cl_2 (2 cm^3) was added a solution of 1,5-bis(^{Et}adamphosphino)pentane (100 mg, 0.16 mmol) in CH_2Cl_2 (2 cm^3). The yellow solution was stirred for 2 d, after which time the $^{31}P\{^1H\}$ NMR spectrum showed signals from 9 ppm to 11.5 ppm.

E.3.2.10 Attempted synthesis of 1,3-bis(^{Et}adamphosphino)propane (3.10) *via* BH_3 adduct

n-Butyl lithium (3.1 cm^3, 1.6 M, 4.96 mmol) was added dropwise to a cooled (–5 °C) solution of ^{Et}CgPH.BH_3 (**3.18**) (0.5 g, 1.84 mmol) in THF (8 cm^3). The mixture was allowed to warm to room temperature, and stirring was continued for a further 2 h. The $^{31}P\{^1H\}$ NMR spectrum showed a broad signals at –8.3 ppm that correspond to the borane adduct. The mixture was then cooled to –72 °C and a solution of 1,3-diiodopropane (0.54 g, 1.84 mmol) in THF (45 cm^3) was cautiously added dropwise over 5 min. Stirring was continued for a further 24 h at room temperature, the $^{31}P\{^1H\}$ NMR spectrum showed various peaks, one in 42% at –0.4 ppm, a peak corresponding to the free ligand ^{Et}CgPH (**3.1**) at –59 ppm in 6%, and a peak corresponding to the borane/lithium adduct in 21%.

Chapter 4: Experimental

E.4 Hydroformylation catalysis

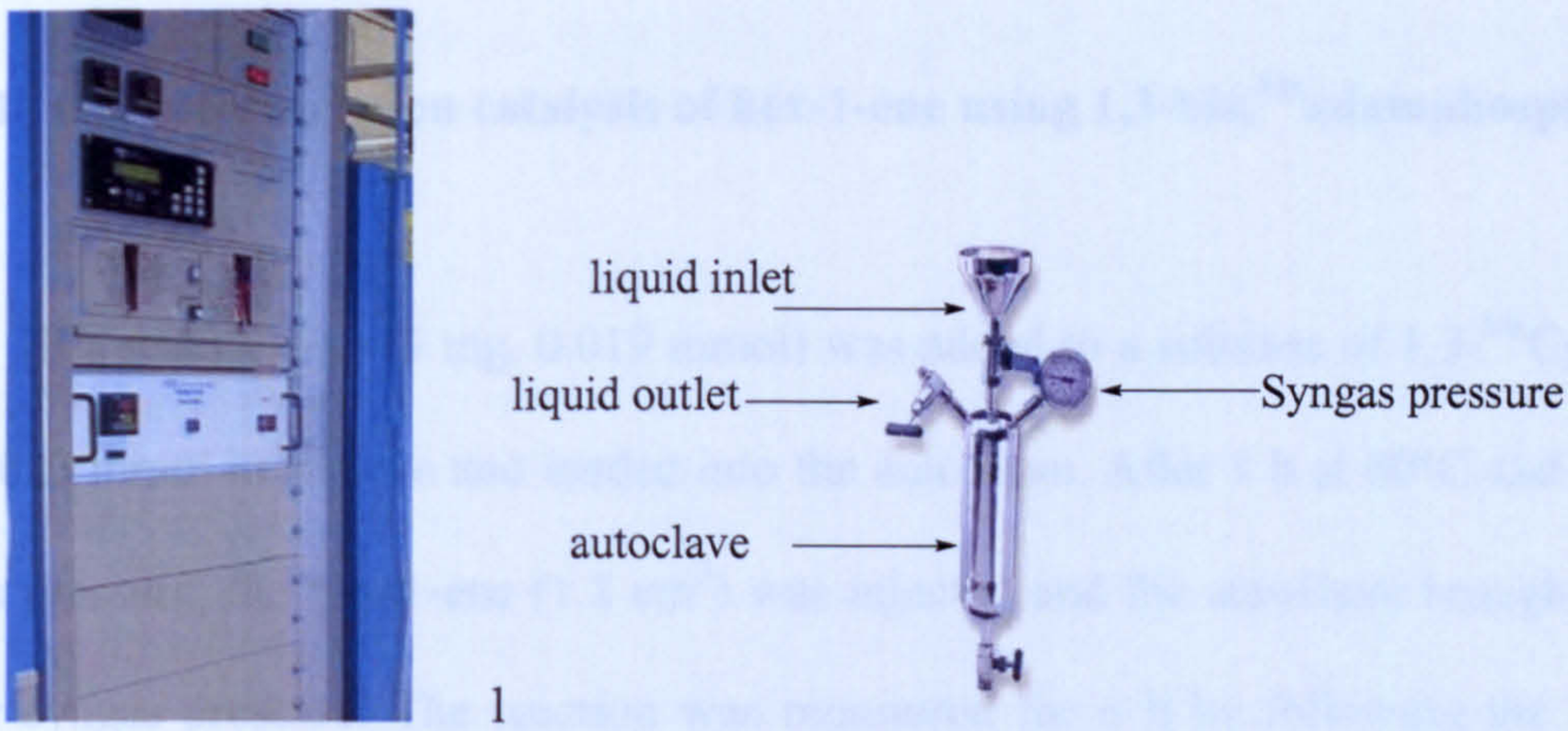

Figure 5.2

The autoclave consists of a high pressure SS-316 pot (designed for 100 kg/cm^2 pressure) with ports for N_2 gas, liquid inlet, liquid outlet and pressure gauge. The liquid to be charged is fed into the pot and pressurised with N_2 gas until its pressure is higher than the autoclave pressure and then the liquid is charged into the autoclave. For every ligand (0.086 mmol) the experiment was repeated exactly in the same way and the amount of ligand used was calculated relative to a fixed amount of [Rh(acac)(CO)$_2$] and hex-1-ene (1.2 cm^3).

E.4.1 Hydroformylation catalysis with monodentate trioxa-phospha-adamantanes

E.4.1.1 Hydroformylation catalysis of hex-1-ene using ^{Et}CgPPh (4.35)

[Rh(acac)(CO)$_2$] (5 mg, 0.019 mmol) was added to a solution of ^{Et}CgPPh (30 mg, 0.086 mmol) in toluene and loaded into the autoclave. After 1 h at 60°C and 10 bar syngas pressure, the hex-1-ene (1.2 cm^3) was injected and the autoclave brought up to 20 bar syngas pressure. The reaction was monitored for 2.5 h by following the syngas

uptake from the ballast vessel. The autoclave was then allowed to cool and the reaction solution analysed by ^{1}H NMR spectrum and GC.

E.4.2 Hydroformylation catalysis with bidentate trioxa-phospha-adamantanes

E.4.2.1 Hydroformylation catalysis of hex-1-ene using 1,3-bis(^{Me}adamphosphino) propane

$[Rh(acac)(CO)_2]$ (5 mg, 0.019 mmol) was added to a solution of 1,3-^{Me}Cg (10.9 mg, 0.023 mmol in toluene and loaded into the autoclave. After 1 h at 60°C and 10 bar syngas pressure, the hex-1-ene (1.2 cm^3) was injected and the autoclave brought up to 20 bar syngas pressure. The reaction was monitored for 6 h by following the syngas uptake from the ballast vessel. The autoclave was then allowed to cool and the reaction solution analysed by ^{1}H NMR spectrum and GC.

E.4.2.2 Hydroformylation catalysis of hex-1-ene using 1,3-bis(diphenylphosphino) propane

$[Rh(acac)(CO)_2]$ (5 mg, 0.019 mmol) was added to a solution of dppp (30 mg, 0.086 mmol) in toluene and loaded into the autoclave. After 1 h at 60 °C and 10 bar syngas pressure, the hex-1-ene (1.2 cm^3) was injected and the autoclave brought up to 20 bar syngas pressure. The reaction was monitored for 6 h by following the syngas uptake from the ballast vessel. The autoclave was then allowed to cool and the reaction solution analysed by ^{1}H NMR spectrum and GC.

E.4.2.3 Hydroformylation catalysis of hex-1-ene using 1,4-bis(^{Me}adamphosphino)butane

$[Rh(acac)(CO)_2]$ (5 mg, 0.019 mmol) was added to a solution of 1,4-^{Me}Cg (11.1 mg, 0.023 mmol) in toluene and loaded into the autoclave. After 1 h at 60 °C and 10 bar syngas pressure, the hex-1-ene (1.2 cm^3) was injected and the autoclave brought up to

20 bar syngas pressure. The reaction was monitored for 6.4 h by following the syngas uptake from the ballast vessel. The autoclave was then allowed to cool the reaction solution analysed by ^{1}H NMR spectrum and GC.

E.4.2.4 Hydroformylation catalysis of hex-1-ene using 1,4-bis(^{Et}adamphosphino) butane

[Rh(acac)(CO)$_2$] (5 mg, 0.019 mmol) was added to a solution of 1,4-^{Et}Cg (13.7 mg, 0.023 mmol) in toluene and loaded into the autoclave. After 1 h at 60 °C and 10 bar syngas pressure, the hex-1-ene (1.2 cm^3) was injected and the autoclave brought up to 20 bar syngas pressure. The reaction was monitored for 6.4 h by following the syngas uptake from the ballast vessel. The autoclave was then allowed to cool and the reaction solution analysed by ^{1}H NMR spectrum and GC.

E.4.2.5 Hydroformylation catalysis of hex-1-ene using 1,4-bis(diphenylphosphino) butane

[Rh(acac)(CO)$_2$] (5 mg, 0.019 mmol) was added to a solution of dppb (9.8 mg, 0.023 mmol) in toluene and loaded into the autoclave. After 1 h at 60 °C and 10 bar syngas pressure, the hex-1-ene (1.2 cm^3) was injected and the autoclave brought up to 20 bar syngas pressure. The reaction was monitored for 6.4 h by following the syngas uptake from the ballast vessel. The autoclave was then allowed to cool and the reaction solution analysed by ^{1}H NMR spectrum and GC.

Appendices

A.1 Crystal data and structure refinement for (2.58) nickel(II) complex of 1,3 bis(^{Me}adamphosphino)propane

Identification code	perth	
Empirical formula	$C_{23}H_{38}C_{12}NiO_6P_2$	
Formula weight	602.08	
Temperature	173(2) K	
Wavelength	0.71073 Å	
Crystal system	Orthorhombic	
Space group	Cmc2(1)	
Unit cell dimensions	a = 26.140(13) Å	α = 90°
	b = 7.537(7) Å	β = 90°
	c = 13.782(12) Å	γ = 90°
Volume	2715(4) Å^3	
Z	4	
Density (calculated)	1.473Mg/m^3	
Absorption coefficient	1.065mm^{-1}	
F(000)	1264	
Crystal size	0.1 x 0.1 x 0.05 mm	
θ range for data collection	1.56 to 27.54°	
Index ranges	-33<=h<=33, -3<=k<=9, -17<=l<=15	
Reflections collected	6990	
Independent reflections	3069 [R_{int} = 0.0897]	
Completeness to θ = 27.54°	99.1 %	
Absorption correction	Semi-empirical from equivalents	
Max. and min. transmission	0.927971 and 0.763450	
Refinement method	Full-matrix least-squares on F^2	
Data / restraints / parameters	3069 / 1 / 164	
Goodness-of-fit on F^2	S = 1.007	
R indices [for 2013reflections with I>2σ(I)]	R_1 = 0.0545, wR_2 = 0.0894	
R indices (for all 3069data)	R_1 = 0.1091, wR_2 = 0.1062	
Absolute structure (Flack) parameter	0.07(3)	
Largest diff. peak and hole	0.542 and -0.569 eÅ^{-3}	

A.2 Crystal data and structure refinement for (2.67) platinum(II) complex of 1,4-bis(^{Me}adamphosphino)butane

Identification code	Atlanta	
Empirical formula	$C_{26.50}H_{42.50}C_{19.50}O_6P_2Pt$ (disordered CH_2Cl_2)	
Formula weight	1050.91	
Temperature	173(2) K	
Wavelength	0.71073 Å	
Crystal system	Monoclinic	
Space group	$P2_1/c$	
Unit cell dimensions	a = 12.127(3) Å b = 21.224(6) Å c = 15.594(4) Å	α = 90° β = 95.605(7)° γ = 90°
Volume	3994.5(19) $Å^3$	
Z	4	
Density (calculated)	1.748 Mg/m^3	
Absorption coefficient	4.265 mm^{-1}	
F(000)	2076	
Crystal size	0.10 x 0.05 x 0.05 mm	
θ range for data collection	1.63 to 24.00°	
Index ranges	-9<=h<=13, -24<=k<=23, -17<=l<=17	
Reflections collected	19463	
Independent reflections	6262 [R_{int} = 0.1388]	
Completeness to θ = 24.00°	99.9 %	
Absorption correction	Multiscan	
Max. and min. transmission	0.745559 and 0.266728	
Refinement method	Full-matrix least-squares on F^2	
Data / restraints / parameters	6262 / 36 / 432	
Goodness-of-fit on F^2	S = 0.958	
R indices[for 3658 reflections with$I>2\sigma(I)$]	R_1 = 0.0673, wR_2 = 0.1494	
R indices (for all 6262 data)	R_1 = 0.1329, wR_2 = 0.1801	
Weighting scheme	$w^{-1} = \sigma^2(F_o^2) + (aP)^2 + (bP)$, where $P = [\max(F_o^2, 0) + 2F_c^2]/3$ a = 0.0935, b = 0	
Largest diff. peak and hole	2.882 and -2.497 $eÅ^{-3}$	

A.3 Crystal data and structure refinement for (2.69) 1,4-bis(hexafluoro-adamphosphino)butane

Identification code	bonn	
Empirical formula	$C_{24}H_{28}F_{12}O_6P_2$	
Formula weight	702.40	
Temperature	173(2) K	
Wavelength	0.71073 Å	
Crystal system	Monoclinic	
Space group	P2(1)/n	
Unit cell dimensions	a = 18.801(3) Å b = 8.0293(11) Å c = 19.220(3) Å	α = 90° β = 93.067(3)° γ = 90°
Volume	2897.3(7) $Å^3$	
Z	4	
Density (calculated)	1.610 Mg/m^3	
Absorption coefficient	0.266 mm^{-1}	
F(000)	1432	
Crystal size	0.10 x 0.05 x 0.05 mm	
θ range for data collection	1.56 to 27.50°	
Index ranges	-24<=h<=18, -9<=k<=10, -23<=l<=24	
Reflections collected	18266	
Independent reflections	6600 [R_{int} = 0.1197]	
Completeness to θ = 27.50°	99.1 %	
Absorption correction	None	
Refinement method	Full-matrix least-squares on F^2	
Data / restraints / parameters	6600 / 0 / 401	
Goodness-of-fit on F^2	S = 0.932	
R indices[for 2940 reflections with I>2σ(I)]	R_1 = 0.0622, wR_2 = 0.1118	
R indices (for all 6600 data)	R_1 = 0.1763, wR_2 = 0.1455	
Weighting scheme	$w^{-1} = \sigma^2(F_o^2) + (aP)^2 + (bP)$, where $P = [\max(F_o^2, 0) + 2F_c^2]/3$	
Largest diff. peak and hole	0.376 and -0.332 $eÅ^{-3}$	

A.4 Crystal data and structure refinement for (2.73) 1,5-bis(hexafluoro-adamphosphino)pentane (crystallographically twinned it was solved using the Windows NT program GEMINI. GEMINI Twinning Solution Program Suite, Version 1.0, 2000, Bruker Advanced X-ray Solutions Inc.)

Identification code	probe	
Empirical formula	$C_{25}H_{30}F_{12}O_6P_2$	
Formula weight	716.43	
Temperature	100(2) K	
Wavelength	1.54178 Å	
Crystal system	Monoclinic	
Space group	P2(1)/c	
Unit cell dimensions	a = 8.7850(3) Å b = 21.3936(7) Å c = 15.4860(5) Å	α = 90° β = 98.416(2)° γ = 90°
Volume	2879.14(16) $Å^3$	
Z	4	
Density (calculated)	1.653 Mg/m^3	
Absorption coefficient	2.477 mm^{-1}	
F(000)	1464	
Crystal size	0.25 x 0.02 x 0.02 mm	
θ range for data collection	3.55 to 70.21°	
Index ranges	-9<=h<=9, -25<=k<=25, -18<=l<=17	
Reflections collected	16998	
Independent reflections	17139 [R_{int} = 0.0000]	
Completeness to θ = 70.21°	85.7 %	
Absorption correction	None	
Refinement method	Full-matrix least-squares on F^2	
Data / restraints / parameters	17139 / 0 / 413	
Goodness-of-fit on F^2	S = 1.031	
R indices[for 12302 reflections with$I>2\sigma(I)$]	R_1 = 0.1151, wR_2 = 0.2782	
R indices (for all 17139 data)	R_1 = 0.1339, wR_2 = 0.2940	
Weighting scheme	$w^{-1} = \sigma^2(F_o^2) + (aP)^2$ where $P = [\max(F_o^2, 0) + 2F_c^2]/3$ a = 0.2000	
Largest diff. peak and hole	1.433 and -0.860 $eÅ^{-3}$	

A.5 Crystal data and structure refinement for (3.5) EtCgPPh

Identification code	kirke
Empirical formula	$C_{40}H_{28}ClO_6PPd$
Formula weight	421.93
Temperature	293(2) K
Wavelength	0.71073 Å
Crystal system	Triclinic
Space group	P-1
Unit cell dimensions	a = 8.6852(13) Å, α = 96.531(2)° b = 9.8884(14) Å, β = 98.137(2)° c = 11.9403(17) Å, γ = 94.415(2)°
Volume	1004.0(3) $Å^3$
Z	1
Density (calculated)	1.396 Mg/m^3
Absorption coefficient	0.718 mm^{-1}
F(000)	426
Crystal size	0.025 x 0.1 x 0.15 mm
θ range for data collection	1.74 to 27.50°
Index ranges	-11<=h<=11, -12<=k<=12, -15<=l<=15
Reflections collected	10673
Independent reflections	4576 [R_{int} = 0.0353]
Completeness to θ = 27.50°	99.1 %
Absorption correction	None
Refinement method	Full-matrix least-squares on F^2
Data / restraints / parameters	4576 / 0 / 288
Goodness-of-fit on F^2	S = 1.063
R indices[for 3544 reflections withI>2σ(I)]	R_1 = 0.0437, wR_2 = 0.1199
R indices (for all 4576 data)	R_1 = 0.0621, wR_2 = 0.1319
Weighting scheme	$w^{-1} = \sigma^2(F_o^2) + (aP)^2 + (bP)$, where $P = [\max(F_o^2, 0) + 2F_c^2]/3$
Largest diff. peak and hole	0.945 and -1.450 $eÅ^{-3}$

A.6 Crystal data and structure refinement for palladium (3.12) complex(II) of 1,3-bis(^{Et}adamphosphino)propane

Identification code	hwin	
Empirical formula	$C_{31}H_{54}C_{l2}O_6P_2Pd$	
Formula weight	761.98	
Temperature	173(2) K	
Wavelength	0.71073 Å	
Crystal system	monoclinic	
Space group	P2(1)/m	
Unit cell dimensions	a = 7.420(3) Å	α = 90°
	b = 28.332(13) Å	β = 93.495(10)°
	c = 8.223(4) Å	γ = 90°
Volume	1725.4(13) Å^3	
Z	2	
Density (calculated)	1.467 Mg/m^3	
Absorption coefficient	0.825 mm^{-1}	
F(000)	796	
Crystal size	0.1 x 0.05 x 025 mm	
θ range for data collection	1.44 to 20.01°	
Index ranges	-6<=h<=7, -27<=k<=23, -7<=l<=6	
Reflections collected	5245	
Independent reflections	1642 [R_{int} = 0.2389]	
Completeness to θ = 20.01°	99.5 %	
Refinement method	Full-matrix least-squares on F^2	
Data / restraints / parameters	1642 / 0 / 148	
Goodness-of-fit on F^2	S = 2.197	
R indices [for 1101 reflections withI>2σ(I)]	R_1 = 0.1572, wR_2 = 0.3935	
R indices (for all 1642 data)	R_1 = 0.2049, wR_2 = 0.4145	
Weighting scheme	$w^{-1} = \sigma^2(F_o^2) + (aP)^2 + (bP)$, where $P = [\max(F_o^2, 0) + 2F_c^2]/3$	
Largest diff. peak and hole	5.719 and -2.016 eÅ^{-3}	

A.7 Crystal data and structure refinement for (3.13) 1,4-bis(^{Et}adamphosphino)butane

Identification code	diggory
Empirical formula	$C_{30}H_{30}O_3P_2$
Formula weight	500.48
Temperature	100(2) K
Wavelength	0.71073 Å
Crystal system	Triclinic
Space group	P-1
Unit cell dimensions	a = 8.8569(18) Å α = 106.10(3)° b = 8.9903(18) Å β = 92.88(3)° c = 12.127(2) Å γ = 114.96(3)°
Volume	825.5(3) $Å^3$
Z	1
Density (calculated)	1.007 Mg/m^3
Absorption coefficient	0.155 mm^{-1}
F(000)	264
Crystal size	0.10 x 0.05 x 0.025 mm
θ range for data collection	1.78 to 27.48°
Index ranges	-11<=h<=11, -11<=k<=11, -15<=l<=15
Reflections collected	9531
Independent reflections	3773 [R_{int} = 0.0644]
Completeness to θ = 27.48°	99.7 %
Absorption correction	None
Refinement method	Full-matrix least-squares on F^2
Data / restraints / parameters	3773 / 0 / 167
Goodness-of-fit on F^2	S = 1.178
R indices[for 2136 reflections withI>2σ(I)]	R_1 = 0.1256, wR_2 = 0.3481
R indices (for all 3773 data)	R_1 = 0.1784, wR_2 = 0.3869
Weighting scheme	$w^{-1} = \sigma^2(F_o^2) + (aP)^2 + (bP)$, where $P = [\max(F_o^2, 0) + 2F_c^2]/3$
Largest diff. peak and hole	2.625 and -0.664 $eÅ^{-3}$

References

References

1. E. Drent and P.H.M. Budzelaar, *J. Organomet. Chem.*, 2000, **593-594**, 211.
2. A.M. Trzeciak and J.J. Ziólkowski, *Coord. Chem. Rev.*, 1999, **190-192**, 883.
3. B. Cornils, W.A. Herrmann and M. Rasch, *Angew. Chem. Int. Ed. Engl.*, 1994, **33**, 2144.
4. V.W. Reppe, *Liebigs Ann.*, 1953, **582**, 1.
5. G. Kiss, *Chem. Rev.*, 2001, **101**, 3345.
6. J.A. Osborn and G. Wilkinson, *Inorg. Synth.*, 1967, **10**, 68.
7. C.K. Brown and G. Wilkinson, *J. Chem. Soc. A.*, 1970, **27**, 53.
8. L.D. Quin *A Guide to Organophosphorus chemistry*, ed. L. D. Quin, New York, 2000.
9. F.A. Cotton, G. Wilkinson, C.A. Murillo and M. Bochmann, *Advanced Inorg. Chem.*, ed. F. Albert Cotton, Wiley-Interscience, New York, 1999.
10. A.G. Orpen and N.G. Connelly, *J. Chem. Soc., Chem Comm*, 1985, 1310.
11. C.A. Tolman, *Chem. Rev.*, 1977, **77**, 33.
12. C.A. Tolman, *Inorg. Chem.*, 1972, **11**, 3128.
13. J.D. Druliner, D. Jesson, J.P. Meakin and C.A. Tolman, *J. Am. Chem. Soc.*, 1976, **98**, 2156.
14. C.P. Casey, E.L. Paulsen, E.W. Beuttenmueller, B.R. Proft, C.M. Petrovich, B.A. Matter and D.R. Powell, *J. Am. Chem. Soc.*, 1999, **121**, 63.
15. L.A. Van der Veen, P.H. Keeven, G.C. Schoemaker, N.H.J. Reek, P.C.J. Kamer, P.W.N.M. Van Leeuwen, M. Lutz and L.A. Spek, *Organometallics*, 2000, **19**, 872.
16. B.L. Shaw, *J. Organomet. Chem.*, 1980, **200**, 307.
17. C.J. Moulton and B.L. Shaw, *J. Chem. Soc., Chem. Commun.*, 1976, 365.
18. K.B. Renkema, J.C. Huffman and K.G. Caulton, *Polyhedron*, 1999, **18**, 2575.
19. K.B. Renkema, M. Ogasawara, W.E. Streib, J.C. Huffman and K.G. Caulton, *Inorg. Chim. Acta*, 1999, **317**, 226.
20. J.T. Poulton, K. Folting, W.E. Streib and K.G. Caulton, *Inorg. Chem.*, 1992, **31**, 3190.
21. T. Gottschalk-Gaudig, K. Folting and K.G. Caulton, *Inorg. Chem.*, 1999, **38**, 5241.
22. B. Chaudret, A. Duteil and X. Dong He, *J. Organomet. Chem.*, 1990, **391**, C45.
23. S.T Nguyen and R.H. Grubbs, *J. Am. Chem. Soc*, 1993, **115**, 3, 9858.

24. P.A. van der Schaaf, R. Kolly and A. Hafner, *J. Chem. Soc., Chem. Commun.*, 2000, 1045.
25. P.A. van der Schaaf, R. Kolly, H.J. Kirner, F. Rime, A. Muhlebach and A. Hafner, *J. Organomet. Chem.*, 2000, **606**, 65.
26. D. Huang, J.C. Huffman, J.C. Bollinger, O. Eisenstein and K.G. Caulton, *J. Am. Chem. Soc.*, 1997, **119**, 7398.
27. Z. Guan and W.J. Marshall, *Organometallics*, 2002, **21**, 3580.
28. D.L. Reger, Y. Ding, D.G. Garza and L. Lebioda, *J. Organomet. Chem.*, 1993, **452**, 263.
29. J.N. Coalter, J.C. Huffman and K.G. Caulton, *Organometallics*, 2000, **19**, 3569.
30. R. Mason, K.M. Thomas, D.F. Gill and B.L. Shaw, *Organometallics*, 1973, 311.
31. V.V. Dunina, O.N. Gorunova, M.V. Livantsov, Y.K. Grishin, L.G. Kuz'mina, N.A. Kataeva and A.V. Churakov, *Tetrahedron: Asymm.*, 2000, **11**, 3967.
32. M.E. van der Boom, S.Y. Liou, Y. Ben-David, A. Vigalok and D. Milstein, *Angew. Chem. Int. Ed. Engl.*, 1997, **36**, 625.
33. D.E. Bergbreiter, P.L. Osburn and Y.S. Liu, *J. Am. Chem. Soc.*, 1999, **121**, 9531.
34. D.E. Bergbreiter, P.L. Osburn, Y.S. Liu, A. Wilson and E.M. Sink, *J. Am. Chem. Soc.*, 2000, **122**, 9058.
35. A. Sudermann, O. Uzan and J.M.L. Martin, *Organometallics*, 2001, **20**, 1783.
36. M.E. van der Boom, S.Y. Liou, Y. Ben-David, L.J.W. Shimon and D. Milstein, *J. Am. Chem. Soc.*, 1998, **120**, 6531.
37. C. Perthuisot and W.D. Jones, *Organometallics*, 1994, **116**, 3647.
38. N. Carr, B.J. Dunne, A.G. Orpen and J.L. Spencer, *J. Chem. Soc., Chem. Commun.*, 1988, 926.
39. N. Carr, B.J. Dunne, L. Mole, A.G. Orpen and J.L. Spencer, *J. Chem. Soc., Dalton Trans.*, 1991, 863.
40. F.M. Conroy Lewis, L. Mole, A.D. Redhouse, S.A. Litster and J.L. Spencer, *J. Chem. Soc., Chem Commun*, 1991, 1601.
41. L. Mole, J.L. Spencer, N. Carr and A.G. Orpen, *Organometallics*, 1991, **10**, 49.
42. N. Carr, B.J. Dunne, L. Mole, A.G. Orpen, J.L. Spencer, *J. Chem. Soc. Dalton Trans.*, 1992, 2653.
43. J.L. Spencer and G.S. Mhinzi, *J. Chem. Soc., Dalton Trans.*, 1995, 3819.
44. M. Brokhart, D.M. Lincoln, M.A. Bennett and S. Pelling, *J. Am. Chem. Soc.*, 1990, **112**, 2691.
45. D. Foster and T.W. Dekleva, *J. Chem. Educ.*, 1986, **63**, 204.

46. E. Drent, *Pure Appl. Chem.*, 1990, **62**, 661.

47. E. Drent and P.H.M. Budzelar, *Chem Rev.*, 1996, **96**, 663.

48. W. Clegg, G.R. Eastham, M.R.J. Elsegood, R.P. Tooze, X. Lan Wang and K. Whiston, *Chem. Commun.*, 1999, 1877.

49. G.R. Eastham, B.T. Heaton, J.A. Iggo, R.P. Tooze, R. Whyman and S. Zacchini, *Chem Commun.*, 2000, 609.

50. W. Clegg, G.R. Eastham, M.R.J. Elsegood, B.T. Heaton, J.A. Iggo, R.P. Tooze, R. Whyman and S. Zacchini, *Organometallics*, 2002, **21**, 1832.

51. T.M. Conroy-Lewis, L. Mole, A.D. Redhouse, S.A. Listen and J.L. Spencer, *J. Chem. Soc., Chem Commun.*, 1991, 1601.

52. R.I. Pugh, E. Drent and P.G. Pringle, *Chem Commun.*, 2001, 1476.

53. V. Gee, A.G. Orpen, H. Phetmung, P.G. Pringle and R.I. Pugh, *Chem. Commun.*, 1999, 901.

54. E. Drent and E. Kragtwijk, *Eur. Pat.* EP 495 548, (1992) to Shell.

55. R.I. Pugh and E. Drent, *Adv. Synth. Catal.*, 2002, **344**, 837.

56. M.E. van der Boom and D. Milstein, *Chem. Rev.*, 2003, **103**, 1759.

57. D. Krogh-Jespersen, M. Czerw, N. Summa, K.B. Renkema, P.A. Archod and A.S. Goldman, *J. Am. Chem. Soc.*, 2002, **124**, 11404.

58. P. Dani, T. Karlen, R.A. Gossage, S. Gladiali and G. van Koten, *Angew. Chem. Int. Ed. Engl.*, 2000, **39**, 743.

59. R.B. Bedford, S.M. Draper, P.N. Scully and S.L. Welch, *New. J. Chem.*, 2000, **24**, 745.

60. M. Ohff, M.E. van der Boom and D. Milstein, *J. Am. Chem. Soc.*, 1997, **119**, 11687.

61. I.P. Beletskaya, A.V. Chuchurjukin, H.P. Dijkstra, G.P.M. van Klink and G. van Koten, *Tetrahedron*, 2000, **41**, 1075.

62. H.P. Dijkstra, M. Albrecht and G. van Koten, *Chem Commun.*, 2002, 126.

63. N. Kataoka, Q. Shelby, J.P. Stambuli and J.F Hartwig, *J. Org. Chem.*, 2002, **67**, 5553.

64. A.H. Roy and J.F. Hartwig, *J. Am. Chem. Soc.*, 2003, **125**, 8704.

65. D.A. Culkin and J.F. Hartwig, *Acc. Chem. Res.*, 2003, **36**, 234.

66. E.J. Hennessy and S.L. Buchwald, *J. Am. Chem. Soc.*, 2003, **125**, 12084.

67. H.N. Nguyen, X. Huang and S.L. Buchwald, *J. Am. Chem. Soc.*, 2003, **125**, 11818.

68. R.H. Grubbs and S. Chang, *Tetrahedron*, 1998, **54**, 4413.

69. B. Alcaide and P. Almendros, *Chem. Eur. J.*, 2003, **9**, 1258.

70. D.F. Taber, K.J. Frankowski, *J. Org. Chem*, 2003, **68**, 6047.

71. M. Epstein and S.A. Buckler, *J. Am. Chem. Soc.*, 1961, **83**, 3279.

72. M. Epstein and S.A. Buckler, *U.S. Pat.* 3 050 531 (1962)

73. R.I. Pugh, PhD thesis, University of Bristol, 2000.

74. J.H. Downing, PhD thesis, University of Bristol, 1992.

75. V. Gee, PhD thesis, University of Bristol, 1997.

76. P.H.M. Budzelaar, E. Drent and P.G. Pringle, *Eur Pat.* 97 302 079 (1996) to Shell Oil Co.

77. J.C.L. Suykerbuyk, E. Drent and P.G. Pringle, *World Pat. 42* 717, 1997, to Shell

78. G. Adjabeng, T. Brenstrum, J. Wilson, C. Frampton, A. Robertson, J. Hillhouse, J. McNulty and A. Capretta, *Org. Lett.*, 2003, **5**, 953.

79. S.B. Wild, D.G. Allen, G.M. McLaughlin, G.B. Robertson, W.L. Steffen and G. Salem., *Inorg. Chem.*, 1982, 1007.

80. S.B. Wild, J.W.L. Martin and J.A.L. Palmer, *Inorg. Chem.*, 1984, 2664.

81. D.C.R. Hockless, P.A. Gugger, P.A. Gugger, P.H. Leung, R.C. Mayadunne, M. Pabel and S.B. Wild, *Tetrahedron*, 1997, **53**, 4083.

82. K. Moedritzer and R.R. Irani, *J. Inorg. Nucl. Chem.*, 1961, **22**, 297.

83. L. Maier, *Helv. Chim. Acta*, 1966, **49**, 842.

84. A. Marr and P.G. Pringle, 'Unpublished results', Bristol, 2001.

85. A. Ward and P.G. Pringle, 'Unpubished results', 2002.

86. Chemische Verwertungsgesellschft mbH, Oberhausen (O. Roelen), DE 849.548 (1938/1952).

87. C.D. Frohing and C.W. Kohlpaintner *Applied Homogeneous Catlysis with Organometallic Compound*, VCH publishers, New York, 1996.

88. L.A. van der Veen, P.C.J. Kamer and P.W.N.M. van Leeuwen, *Cat. Tech*, 2002, **6**, 116.

89. D.F Shriver, P. Atkins and Cooper H. Langford, *'Inorganic Chemistry'*, Oxford Univeristy, 1994.

90. C. Crause, L. Bennie, L. Damoense, C.L. Dwyer, C. Grove, N. Grimmer, W.J. van Rensburg, M.M. Kirk, K.M. Mokheseng, S. Otto and P.J. Steynberg, *J. Chem. Soc., Dalton Trans*, 2003, 2036.

91. L.H. Slaugh and R.D. Mullineaux, *J. Organomet. Chem.*, 1968, **13**, 469.

92. F.A. Cotton and G. Wilkinson, *Advanced Inorganic Chemistry*, ed. 5th edition, Wiley Interscience, New York, 1988.

93. R.L. Pruett, *U.S. Pat. 3,499,932* (1967).

94. B. Breit and W. Seiche, *Synthesis*, 2001, 1.

95. D. Evans, J.A. Osborn and G. Wilkinson, *J. Am. Chem. Soc.*, 1968, 3133.

96. M. F. Sellin, I. Bach, J.M. Webster, F. Montilla, V. Rosa, T. Aviles, M. Poliakoff and D.J. Cole-Hamilton, *J. Chem. Soc., Dalton Trans.*, 2002, 4569.

97. B. Breit, R. Winde, T. Mackewitz, R. Paciello and K. Harms, *Chem. Eur. J.*, 2001, **7**, 3106.

98. B. Heil and L. Markó, *Chem. Ber.*, 1969, **102**, 2238.

99. B. Cornils in *New Synthesis with Carbon Monoxide*, Ed. J. Falbe, Springer, Berlin,1980, p. 577.

100. A. Aghmiz, A. Orejon, M. Dieguez, M.D. Miquel-Serrano, C. Claver, A.M. Masdeu-Bulto, D. Sinou and G. Laurenczy, *J. Mol. Cat. A.*, 2003, **195**, 113.

101. A.M.B. Osuna, W. Chen, E.G. Hope, R.D.W. Kemmitt, D.R. Paige, A.M. Stuart, J. Xiao and L. Xu, *J. Che. Soc. Dalton Trans*, 2000, 4052.

102. W.P. Chen, L.J. Xu and J.L. Xiao, *Chem. Commun.*, 2000, 839.

103. E. de Wolf, G van Koten and B.J. Deelman, *Chem. Soc. Rev.*, 1999, **28**, 37.

104. I.T. Horvath, G. kiss, R.A. Cook, J.E. Bond, P.A. Stevens,J. Rabai and E.J. Mozeleski, *J. Am. Chem. Soc.*, 1998, **120**, 3133.

105. D.F. Foster, D.J. Adams, D. Gudmunsen, A.M. Stuart, E.G. Hope and D.J. Cole-Hamilton, *Chem. Commun.*, 2002, 916.

106. W. Chen, L. Xu, Y. Hu, A.M. B.Osuna and J. Xiao, *Tetrahedron*, 2002, **58**, 3889.

107. J. Andrade, J.J. Garcia, H. Torrens, F. del Rio, C. Claver and N. Ruiz, *Inorg. Chim. Acta*, 1997, **255**, 389.

108. H. Klein, R. Jackstell, K.D. Wiese, C. Borgmann and M. Beller, *Angew. Chem. Int. Ed. Engl.*, 2001, **40**, 3408.

109. I.T. Horvath and I. Rabai, *Science*, 1994, **266**, 72.

110. I.T. Horvath and I. Rabai, *U.S. Pat.* 5 463 082, (1995), toExxon.

111. D.F. Foster, D.J. Adams, D. Gudmunsen, A.M. Stuart, E.G. Hope, D.J. Cole-Hamilton, G.P. Schwarz and P. Pogorzelec, *Tetrahedron*, 2002, **58**, 3901.

112. F. Favre, H. Olivier-Bourbigou, D. Commereuc and L. Saussine, *Chem Commun.*, 2001, 1360.

113. S. Shirakawa, S. Shimizu and Y. Sasaki, *New J. Chem.*, 2001, **25**, 777.

114. H. Bahrmann, H Bach, C.D. Frohning, H.J. Kleiner, P. Lappe, D. Peters, D. Regnat and W.A. Herrmann, *J. Mol. Catal.*, 1997, **116**, 49.

115. G. Fremy, Y. Castanet, R. Grysbek, E. Mortreux, A.M. Trzeciak and J.J. Ziolkowski, *J. Organomet. Chem.*, 1995, **505**, 11.

116. E. Mieczynska, A.M. Trzeciak, J.J. Ziolkowski and R. Grzybek, *J. Mol. Cat. A.*, 1998, **132**, 203.

117. E. Mieczynska, A.M. Trzeciak, J.J. Ziolkowski and R. Grzybek, *J. Mol. Catal. A.*, 1999, **148**, 59.

118. B. Breit and W. Seiche, *J. Am. Chem. Soc.*, 2003, **125**, 6608.

119. A. Solsona, J. Suades and R. Mathieu, *J. Organomet. Chem.*, 2003, **669**, 172.

120. Y. Wang, J. Jiang, X. Wu, F. Cheng and Z. Jin, *Catal. Lett.*, 2001, **79**, 55.

121. Y. Wang, J. Jiang, Q. Miao, X. Wu, F. Cheng and Z. Jin, *Catal. Today*, 2002, **74**, 85.

122. X.L. Zheng, J.Y. Jiang, X.Z. Liu and Z.L. Jin, *Catal. Today*, 1998, **44**, 175.

123. S. Haji and C. Erkey, *Tetrahedron*, 2002, **58**, 3929.

124. M.F. Sellin, D.J. Cole-Hamilton, *J. Chem. Soc., Dalton Trans.* 2000, 1681.

125. T. Davis and C. Erkey, *Indust. Eng. Chem. Res.*, 2000, **39**, 3671.

126. Y. Hu, W. Chen, L. Xu, L.J. Xiao, *Organometallics*, 2001, **20**, 3206.

127. D.R. Paolo and C. Erkey, *Organometallics*, 2000, **19**, 81.

128. Y. Hu, W. Chen, A.M.B. Osuna, J.A. Iggo and J. Xiao, *Chem. Commun*, 2002, 788.

129. E. Lindner, T. Schneller, F. Auer and H.A. Mayer, *Angew. Chem. Int. Ed. Engl.*, 1999, **38**, 2155.

130. P. Jessop and R. Noyori, *Chem. Rev.*, 1999, **99**, 475.

131. R.J. Klinger and J.W. Rathke, *J. Am. Chem. Soc.*, 1994, **116**, 4772.

132. F. Shin-ichiro, S. Fujisawa, B.M. Bhanage, Y. Ikushima and M. Arai., *New J. Chem.*, 2002, **26**, 1479.

133. C.R. Yonker and J.C. Linehan, *J. Organomet. Chem.*, 2002, **650**, 249.

134. R.J. Sowden, M.F. Sellin, N. De Blasio and D.J. Cole-Hamilton, *Chem. Commun*, 1999, 2511.

135. M.F. Sellin, P.B. Webb, D.J. Cole-Hamilton, *Chem. Commun*, 2001, 781.

136. S. Dharmidhikari and M. Abraham, *J. Supercrit. Fluids*, 2000, 4569.

137. G.E. Oterom, S. Steffens, J.N.H. Reek, P.C.J. Kamer and P.W.N.M. van Leeuwen, *Topics in Catalysis*, 2002, **19**, 61.

138. L. Ropartz, R.E. Morris, D.F. Foster and D.J. Cole-Hamilton, *J. Mol. Catal. A*, 2002, **182-183**, 99.

139. L. Ropartz, R.E. Morris, D.F. Foster, D.J. Cole-Hamilton, K.J. Haxton and A.M.Z. Slawin, *J. Chem. Soc., Dalton Trans*, 2002, 4323.

140. P.W.N.M. van Leewen and C.F. Roobeek, *J. Org. Chem*, 1983, **258**, 343.

141. L.A. van der Veen, P.C.J. Kamer and P.W.N.M. van Leeuwen, *Organometallics*, 1999, **18**, 4765.

142. B. Breit, *Chem. Commun*, 1996, 2071.

143. For a review on phosphabenzene coordination chemistry see G. Märkl, *'Multiple Bonds and Low Coordination in Phosphorus Chemistry'*, ed. M. Regitz and O.J. Scherer, Thieme, Stuttgart, 1990, pp 247-249.

144. G. Märkl, *Angew. Chem. Int. Ed. Engl.*, 1966, **5**, 846.

145. E.F. DiMauro, and M.C. Kozlowski, *J. Chem. Soc., Perkin Trans.*, 2001, **1**, 439.

146. P. Le Floch and F. Mathey, *Coord. Chem. Rev.*, 1998, **179-180**, 771.

147. H. Kanter and K. Dimroth, *Tetrahedron Lett.*, 1975, 541.

148. C. Elschenbroich, M. Nowotony, B. Metz, W. Massa, J. Graulich, K. Biehler and W. Sauer., *Angew. Chem. Int. Ed. Engl.*, 1991, **30**, 547.

149. R. Weber, W. Keim, M. Mothrath, U. Englert and B. Ganter, *Chem. Commun.*, 2000, 1419.

150. J.H. Downing, V. Gee and P.G. Pringle, *Chem. Commun.*, 1997, **16**, 1527.

151. M. Eberhard, PhD Thesis, University of Bristol, 2002.

152. J.P. Mulders, *Neth. Pat.* 6 604 094 (1966) to Shell.

153. J. P. Mulders, *Chem. Abstr.*, 1967, **66**, 65101r.

154. R.F. Mason, J.L.V. Winkle, *U.S. Pat* 3 400 163 (1968).

155. G. Elsner, G. Heymer and H.W. Stephan, *Chem. Abstr.*, 1978, **89**, 180154x.

156. K., Torii, *Chem. Abstr.*, 1981, **95**, 43338v.

157. J.L.V. Winkle, R.C. Morris and R.F. Mason, *Chem. Abstr.*, 1970, **72**, 3033k.

158. Y. Okago, Y. Yanagi, M. Yoshihira and M. Takeda, *Chem. Abstr.*, 1991, **115**, 279424c.

159. M.T. Reetz, *Heterocycles*, 2000, **52**, 935.

160. J. Fawcett, P.A.T. Hoye, R.D.W. Kemmitt, D.J. Law and D.R. Russell, *J. Chem. Soc., Dalton Trans.*, 1993, 2563.

161. J.J. Carbo, F. Maseras, C. Bo and P.W.N.M. van Leeuwen, *J. Am. Chem. Soc.*, 2001, **123**, 7630.

162. Z. Freixa, P.W.N.M. van Leeuwen, *J. Chem. Soc., Dalton Trans*, 2003, 1890.

163. J.M. Brown and A.G. Kent, *J. Chem. Soc., Perkin Trans.*, 1987, **2**, 1597.

164. P.W.N.M. van Leeuwen, P.C.J. Kamer and J.N.H. Reek, *Pure Appl. Chem.* 1999, **71**, 1443.

165. L.A. van der Veen, P.H. Keeven, G.C. Schoemaker, J.N.H. Reek, P.C.J. Kamer, P.W.N.M. van Leeuwen, M. Lutz and A.L. Spek, *Organometallics*, 2000, **19**, 872.

166. M. Kranenburg, Y.E.M. van der Burgt, P.C.J. Kamer and P.W.N.M. van Leeuwen, *Organometallics*, 1995, **14**, 3081.

167. L.A. van der Veen, P.C.J. Kamer and P.W.N.M. van Leeuwen, *Angew. Chem. Int. Ed. Engl.*, 1999, **38**, 336.

168. A.B. Pangborn, M.A. Giardello, R.H. Grubbs, R.K. Rosen and F.J. Timmers, *Organometallics*, 1996, **15**, 1518.

169. M.S. Kharasch, R.C, Seyler and F.R. Mayo, *J. Am. Chem. Soc.*, 1938, **60**, 882.

170. J.X. Dermott, J.F. White and G.M. Whitesides, *J. Am. Chem. Soc.*, 1976, **98**, 6521.